



University  
of Glasgow

Nash, Besma (2010) *The dual role of astrocytes in myelination*. PhD thesis.

<http://theses.gla.ac.uk/2378/>

Copyright and moral rights for this thesis are retained by the Author

A copy can be downloaded for personal non-commercial research or study, without prior permission or charge

This thesis cannot be reproduced or quoted extensively from without first obtaining permission in writing from the Author

The content must not be changed in any way or sold commercially in any format or medium without the formal permission of the Author

When referring to this work, full bibliographic details including the author, title, awarding institution and date of the thesis must be given

# **The Dual Role of Astrocytes in Myelination**

Besma Nash BSc (Hons)

A thesis submitted in fulfilment of the requirements of the University of Glasgow for the degree of Doctor of Philosophy

College of Medical, Veterinary and Life Sciences  
Institute of Infection, Immunity and Inflammation  
University of Glasgow

December 2010



*"My Lord! Increase me in knowledge."*

*(Holy Quran, 20:114)*

*I dedicate this thesis to my mum – for everything*

## Acknowledgments

---

I am extremely grateful to everyone who has helped me during my time in Glasgow. I would especially like to thank Professor Sue Barnett for giving me the opportunity to work in her lab and for all her advice, direction and encouragement. I have genuinely enjoyed working with you and hope to continue doing so sometime in the future. I would also like to thank past and present members of the Glial Biology Lab including Susan, Jen, Rebecca, Peter, Calliope, Stephanie, Ale and Mercedes. You guys are magnificent and have truly made my time in Glasgow. A special thanks to Dr Martin McBride and Dr John McClure for all their technical and statistical support with the microarray study. I would also like to thank Professor Hugh Willison, Professor Chris Linington and Dr Tomoko Iwata for support and feedback throughout my PhD.

I am extremely grateful to my family for their enthusiasm and support throughout my entire life. Thank you to my Mum and Dad for always believing in me. A special thank you goes to my little sisterino, Raya; I cannot thank you enough for all the times you made me laugh about my 'cells'. You were always there when I needed you. A huge thank you to my fiancé, Thomas, for your love, support, patience and for putting up with me! I am eternally grateful to you all and I would have never gotten this far without you.

# Table of Contents

---

Acknowledgments	i
Dedication	ii
Tables of Contents	iii
List of Figures	ix
List of Tables	xiii
List of Abbreviations	xiv
Abstract	xvi
Author's Declaration	xviii

## Chapter 1

<b>Introduction</b>	1
1.1 Glial Cells in the Central Nervous System	2
1.1.1 Oligodendrocytes	2
1.1.2 Microglia	9
1.1.3 Astrocytes	10
1.2 Functions of Astrocytes in Health and Disease	13
1.2.1 The Blood Brain Barrier	13
1.2.2 Neurotransmitter Control and Synaptogenesis	14
1.2.3 Water, Ion and pH Balance	15
1.2.4 Gap Junctions	15
1.2.5 Energy and Metabolism	16
1.2.6 Neuronal Support	16
1.2.7 Other Astrocytic Functions	17
1.3 Astrocytes and their Role in Multiple Sclerosis	18
1.3.1 Multiple Sclerosis (MS)	18
1.3.2 The Pathophysiology of MS	18
1.3.3 Astrocytes and Myelination	19
1.3.4 Astrocytes and Models of Demyelination	22
1.4 Astrocytes and their Phenotypes	23
1.4.1 Mild Gliosis (Activated Astrocytes)	24
1.4.2 Factors Secreted by Activated Astrocytes	24
1.4.3 Severe Gliosis (Reactive Astrocytes)	27
1.4.4 The Glial Scar	27

1.4.5	Factors Secreted by Reactive Astrocytes	28
1.4.6	Astrocyte Phenotype and Environment	31
1.5	Conclusions	32
1.6	Aims	34

## Chapter 2

<b>Materials and Methods</b>		<b>36</b>
2.1	Tissue Culture	37
2.1.1	Astrocyte Culture	37
2.1.2	Olfactory Ensheathing cells (OECs)	38
2.1.3	Myelinating Cultures	38
2.1.4	Conditioning of E15.5 Spinal Cord Cultures	39
2.2	Western Blotting	40
2.3	Enzyme-Linked Immunoabsorbent Assay (ELISA)	41
2.4	Bromodeoxyuridine Assay	42
2.5	Immunohistochemistry	42
2.5.1	General Immunohistochemistry	42
2.5.2	BrdU Immunohistochemistry	43
2.5.3	External Markers	43
2.5.4	Internal Markers	43
2.6	RNA extraction	43
2.7	cDNA Synthesis	44
2.8	Polymerase Chain Reaction	46
2.8.1	Primer Design	46
2.8.2	PCR Reaction	48
2.8.3	Agarose Gel Preparation	49
2.8.4	Running and Visualising the Gel	49
2.9	Quantitative Real Time PCR (qRT-PCR)	49
2.9.1	Plate Preparation	50
2.9.2	Reaction Conditions	50
2.9.3	Data Quantification	51
2.10	Microarray	52
2.10.1	RNA Integrity	52
2.10.2	RNA Amplification and Biotinylation	52
2.10.3	Direct Hybridisation Assay	56

2.10.4	Analysis of BeadChip Data	57
2.11	Microscopy and Image Analysis	57
2.11.1	Neurite Density	59
2.11.2	Myelin Quantification	59
2.11.3	Quantification of Cell Number	60
2.11.4	Cell Proliferation	61
2.11.5	Neurite Diameter	61
2.11.6	GFAP and Nestin Immunoreactivity	61
2.12	Statistical Analysis	62
<b>Chapter 3</b>		<b>63</b>
<b>Characterisation of the Myelinating Culture System</b>		<b>63</b>
3.1	Introduction	64
3.1.1	Background	64
3.1.2	Aims	66
3.2	Results	67
3.2.1	Establishment of the Myelinating Culture System	67
3.2.2	Astrocytes, Microglia, and Oligodendrocytes at Different Maturation Stages	69
3.2.3	Neurite Density Increases and OPC Numbers Fall during the Culture Period	69
3.2.4	Myelination Increases over Time in the Myelinating Culture System	71
3.2.5	Underlying Monolayer of Astrocytes contains O4+ Oligodendrocytes	71
3.2.6	Growth Factors can Promote Myelination	74
3.3	Discussion	76
<b>Chapter 4</b>		
<b>The Effect of Ciliary Neurotrophic Factor on Myelination</b>		<b>81</b>
4.1	Introduction	82
4.1.1	Background	82
4.1.2	Aims	84
4.2	Results	84

4.2.1	Expression of O4 in Myelinating Cultures after CNTF Treatment . . . . .	84
4.2.2	Concentration-Dependent Effect of CNTF . . . . .	85
4.2.3	CNTF does not have a Promyelinating Effect when Cultures are plated on a Monolayer of OECs . . . . .	85
4.2.4	CNTF does not Induce Oligodendrocyte Proliferation . . . . .	88
4.2.5	CNTF and Oligodendrocyte Differentiation . . . . .	88
4.2.6	CNTF and Microglial Activation . . . . .	91
4.2.7	Effect of CNTF on Neurite Diameter . . . . .	93
4.2.8	Effect of CNTF on Astrocyte Reactivity . . . . .	93
4.2.9	Effect of CNTF Treatment on Astrocytic Expression of Nestin . . . . .	96
4.3	Discussion . . . . .	99

## **Chapter 5**

	<b>Understanding the role CNTF and its Receptor . . . . .</b>	<b>102</b>
5.1	Introduction . . . . .	103
5.1.1	Background . . . . .	103
5.1.2	Aims . . . . .	107
5.2	Results . . . . .	107
5.2.1	Neutralising Antibodies to CNTF Lead to an Increase in Myelination . . . . .	107
5.2.2	Increase in Myelination with Neutralising Antibodies is only Observed at 4 µg/ml . . . . .	108
5.2.3	There is a Slight Reduction in CNTF Concentration after Antibody Treatment . . . . .	108
5.2.4	CNTF and anti-CNTF May Act via Different Pathways . . . . .	111
5.2.5	Neutralising Antibodies and Oligodendrocyte Differentiation . . . . .	111
5.2.6	Antibodies to CNTF do not lead to an Increase in Proliferation . . . . .	114
5.2.7	Neutralisation of CNTF may lead to a Slight Increase in Microglial Activation . . . . .	117
5.2.8	LIF and anti-LIF Increase Myelination . . . . .	117
5.3	Discussion . . . . .	120

## Chapter 6

### Changing the Phenotype of the Astrocyte and its

<b>Effect on Myelination</b> .....	125
6.1 Introduction .....	126
6.1.1 Background .....	126
6.1.2 Aims .....	128
6.2 Results .....	128
6.2.1 Myelination is Reduced on TnC-Astrocytes .....	128
6.2.2 Astrocytes on PLL and TnC Show Similar Cellular Characteristics. ....	128
6.2.3 Astrocytes on PLL Resemble the ‘Activated’ Phenotype .....	130
6.2.4 TnC-Astrocytes as a Substrate for Myelinating Cultures; Can TnC Directly Influence Oligodendrocyte Differentiation? .....	132
6.2.5 Expression of TnC is Comparable on PLL-Astrocytes and TnC-Astrocytes .....	132
6.2.6 Quiescent Astrocyte Phenotype can be Overcome by Activated Astrocyte Conditioned Media or CNTF .....	136
6.3 Discussion .....	136

## Chapter 7

### Identification of Molecules Secreted by Activated and Quiescent Astrocytes .....

7.1 Introduction .....	143
7.1.1 Background .....	143
7.1.2 Aims .....	144
7.2 Results .....	144
7.2.1 Schematic of Experimental Design and Analysis of Microarray .....	144
7.2.2 Gene Expression Changes over time in Untreated and CNTF Treated PLL-Astrocytes .....	145
7.2.3 Very few genes are changed in Untreated PLL-astrocytes compared to those Treated with CNTF .....	152
7.2.4 Numerous Genes are identified when TnC-astrocytes were compared to untreated and CNTF-Treated PLL-Astrocytes at 4 hours and 24 hours .....	155
7.2.5 Validation of CXCL10 by qRT-PCR in TnC-Astrocytes .....	157

7.2.6	CXCL10 Antibodies Increase Myelination in TnC-Astrocyte Cultures .....	167
7.2.7	CNTF may Regulate the Expression of CXCL10 .....	168
7.3	Discussion .....	168

## **Chapter 8**

<b>General Discussion</b> .....	179	
8.1	Cross-talk Between Astrocytes and Neurons .....	180
8.2	Mechanisms of Action .....	181
8.3	Astrocyte Phenotype and Control of Myelination .....	181
8.4	Astrocyte Heterogeneity .....	182
8.5	Astrocytes Phenotypes <i>In Vivo</i> .....	183
8.6	Cytokines and Models of Multiple Sclerosis .....	184
8.7	Future Experiments .....	184
8.8	Conclusions of Thesis .....	186

<b>References</b> .....	188
-------------------------	-----

<b>Appendix</b> .....	220
-----------------------	-----

# List of Figures

---

## Chapter 1

Figure 1.1	Nodes of Ranvier, Location and Structure . . . . .	3
Figure 1.2	Summary of Oligodendrocyte Differentiation . . . . .	7
Figure 1.3	Schematic Representations that Summarise Various Astrocytic Functions in the Healthy CNS . . . . .	20
Figure 1.4	MS Course and Subtypes . . . . .	21
Figure 1.5	Summary of Astrocyte Phenotypes and Key Molecules used to Identify them . . . . .	25
Figure 1.6	The Glial Scar . . . . .	30
Figure 1.7	Schematic Representation of Astrocytes in Activated and Reactive States . . . . .	33
Figure 1.8	Summary of How Astrocyte Phenotype can Influence Myelination . . . . .	35

## Chapter 2

Figure 2.1	RNA Integrity . . . . .	55
Figure 2.2	BeadChip Hybridization Chamber . . . . .	58
Figure 2.3	Loading Bay of BeadChip . . . . .	58
Figure 2.4	Measurement of Neurite Density . . . . .	59
Figure 2.5	Myelin Quantification . . . . .	60

## Chapter 3

Figure 3.1	Methodology of Generating a Myelinating Culture System . . . . .	68
Figure 3.2	Astrocytes, Microglia, and Oligodendrocytes at Different Maturation Stages . . . . .	70
Figure 3.3	Neurite Density Increases and OPC Numbers Fall during the Culture Period . . . . .	72
Figure 3.4	Myelination Increases over Time in the Myelinating Culture System . . . . .	73

Figure 3.5	Underlying Monolayer of Astrocytes contains O4+ Oligodendrocytes . . . . .	75
Figure 3.6	Growth Factors can Promote Myelination . . . . .	77
Figure 3.7	Excess Oligodendrocytes, Ensheathment and Myelination Issues . . . . .	80

## Chapter 4

Figure 4.1	CNTF Addition Increases Expression of the O4 Ligand . . . . .	86
Figure 4.2	Titration of CNTF Produced Variable Effects on Myelination . . . . .	87
Figure 4.3	CNTF does not have a Promyelinating Effect when Cultures are plated on a Monolayer of OECs . . . . .	89
Figure 4.4	CNTF Treatment does not lead to an Increase in OPC Proliferation . . . . .	90
Figure 4.5	Addition of CNTF does not lead to an Increase in O4+ Oligodendrocytes . . . . .	92
Figure 4.6	anti-CNTF Slightly Increases the Number of Activated Microglia . . . . .	94
Figure 4.7	Addition of CNTF does not Increase Neurite Diameter . . . . .	95
Figure 4.8	Addition of CNTF and Astrocyte Reactivity. . . . .	97
Figure 4.9	Addition of CNTF and Nestin Reactivity . . . . .	98

## Chapter 5

Figure 5.1	An Illustration of CNTF Binding and Signalling . . . . .	104
Figure 5.2	CNTFR $\alpha$ can be Soluble or Membrane Bound . . . . .	105
Figure 5.3	Receptor Complexes of the IL-6 Cytokines . . . . .	106
Figure 5.4	Neutralising CNTF leads to an Increase in Myelination . . . . .	109
Figure 5.5	Myelination is only increased at 4 $\mu$ g/ml . . . . .	110
Figure 5.6	Antibody Treatment Leads to a Slight Reduction in CNTF in Media from Cultures . . . . .	112
Figure 5.7	Addition of CNTF and anti-CNTF at Different Time Points Suggests that there may be Two Different Mechanisms for Their actions . . . . .	113
Figure 5.8	Addition of anti-CNTF does not lead to an Increase in O4+ Oligodendrocytes . . . . .	115

Figure 5.9	Addition of anti-CNTF does not lead to the Proliferation of O4+ Cells . . . . .	116
Figure 5.10	anti-CNTF does not Increase the Number of Activated Microglia . . . . .	118
Figure 5.11	anti-LIF addition leads to an Increase in Myelination . . . . .	119
Figure 5.12	Illustration of the Possible Biphasic Effect of CNTF . . . . .	123
Figure 5.13	Illustration of the Possible Competition between IL-6 Cytokines . . . . .	124

## Chapter 6

Figure 6.1	Myelination was Reduced on Astrocytes plated on TnC . . . . .	129
Figure 6.2	Cellular Characteristics of Astrocytes on PLL and TnC are Similar . . . . .	131
Figure 6.3	Astrocyte plated on PLL Exhibit an ‘Activated’ Phenotype whilst those on TnC Exhibit a ‘Quiescent’ Phenotype . . . . .	133
Figure 6.4	Confluency is achieved when Astrocytes are plated on PLL and TnC . . . . .	134
Figure 6.5	Plating Astrocytes on a TnC Substrate Does Not Affect Neurite Extension or Expression of TnC on Astrocytic Surface . . . . .	135
Figure 6.6	Myelinating Cultures Conditioned with Astrocytes Pre-treated with CNTF Increased Myelination and this effect was Dominant to the Reduction in Myelination by Quiescent Astrocytes. . . . .	137

## Chapter 7

Figure 7.1	Schematic Diagram Representing the Experimental Plan and Step Wise Process of a Microarray Study . . . . .	146
Figure 7.2	Venn diagram Representing Transcript Distribution over time in PLL-astrocytes with and without CNTF Treatment. . . . .	147
Figure 7.3	Venn diagram Representing Transcript Distribution between PLL-astrocytes Untreated and Treated with CNTF after 4 hours and 24 hours . . . . .	153
Figure 7.4	Venn diagram Representing Transcript Distribution between TnC-astrocytes compared to PLL-astrocytes untreated and treated with CNTF after 4 hours . . . . .	158
Figure 7.5	Venn diagram Representing Transcript Distribution between TnC-astrocytes at 4 hours compared to PLL-astrocytes untreated and treated with CNTF at 24 hours . . . . .	161
Figure 7.6	Validation of CXCL10 in TnC-Astrocytes . . . . .	166

Figure 7.7	CXCL10 Neutralising Antibodies Increase Myelination in TnC-Astrocytes .....	169
Figure 7.8	CXCL10 Neutralising Antibodies Increase Myelination in TnC-Astrocytes with No Effect on Neurite Density .....	170
Figure 7.9	The Addition of CXCL10 to Myelinating Cultures on PLL-Astrocytes Resulted in a Decrease in Myelination .....	171
Figure 7.10	The Addition of CXCL10 to Myelinating Cultures on TnC-Astrocytes does not Affect Myelination .....	172
Figure 7.11	CXCL10 is Slightly Reduced in Myelinating Cultures plated on TnC-Astrocytes Treated with CNTF as Measured by qRT-PCR .....	173

## Chapter 8

Figure 8.1	NF- $\kappa$ B Activation and its effects on Oligodendrocyte Precursor Cells .....	189
------------	--	-----

## List of Tables

---

### Chapter 2

Table 2.1	Primary Antibody List . . . . .	45
Table 2.2	Secondary Antibody List . . . . .	45

### Chapter 7

Table 7.1	Genes Identified by Microarray Expression Profiling between PLL-Astrocytes at 4 and 24 hours (Section A of Figure 7.2) . . . . .	148
Table 7.2	Genes Identified by Microarray Expression Profiling between PLL-Astrocytes Treated with CNTF at 4 and 24 hours (Section B of Figure 7.2) . . . . .	149
Table 7.3	Genes Identified by Microarray Expression Profiling between PLL-Astrocytes Untreated and Treated with CNTF after 4 and 24 hours (Section AB of Figure 7.2) . . . . .	151
Table 7.4	Genes Identified by Microarray Expression Profiling between PLL-Astrocytes Untreated and Treated with CNTF after 24 hours (Figure 7.3) . . . . .	154
Table 7.5	Genes identified by Microarray Expression Profiling between TnC-Astrocytes and PLL-Astrocytes untreated (A) and treated with CNTF (B) after 4 hours (Figure 7.4, A and B). . . . .	159
Table 7.6	Genes identified by Microarray Expression Profiling between TnC-Astrocytes and both PLL-Astrocytes untreated and treated with CNTF at 4 hours (Figure 7.4, Section AB). . . . .	160
Table 7.7	Genes identified by Microarray Expression Profiling between TnC-Astrocytes at 4 hours and PLL-Astrocytes at 24 hours (Figure 7.5, Section A). . . . .	162
Table 7.8	Genes Identified by Microarray Expression Profiling between TnC-Astrocytes after 4 hours and PLL-Astrocytes Treated with CNTF after 24 hours (Figure 7.5, Section B) . . . . .	163
Table 7.9	Genes Identified by Microarray Expression Profiling between TnC-Astrocytes after 4 hours and PLL-Astrocytes Untreated and Treated with CNTF after 24 hours (Figure 7.5, Section AB) . . . . .	164

## List of Abbreviations

---

-/-	knockout
3D	three dimensional
A $\beta$	Amyloid beta
ACM	astrocyte conditioned medium
AQ4	aquaporin-4
ATP	adenosine triphosphate
BBB	blood brain barrier
BDNF	brain derived neurotrophic factor
BMP	bone morphogenetic protein
BrdU	5-bromo-2'-deoxyuridine
Caspr	contactin associated protein
cDNA	cellular deoxyribonucleic acid
CNP	2',3'-cyclic nucleotide 3'-phosphohydrolase
CNS	central nervous system
CNTF	ciliary neurotrophic factor
CNTFR $\alpha$	CNTF R alpha
CO <sub>2</sub>	carbon dioxide
CSF	cerebrospinal fluid
CSPGs	chondroitin sulphate proteoglycans
CTGF	connective tissue growth factor
Cx-	Connexin
CXCL10	C-X-C motif chemokine 10
DAPI	4'-6-diamidino-2-phenylindole
DIV	days <i>in vitro</i>
DMEM	Dulbecco's Modified Eagle Medium
dNTP	Deoxyribonucleotide triphosphate
DRG	dorsal root ganglion
E	embryonic day
EAE	experimental autoimmune encephalitis
ECM	extracellular matrix
EGF	epidermal growth factor
EGFR	epidermal growth factor receptor
E-NCAM	embryonic form of polysialic acid containing N-CAM
FBS	foetal bovine serum
FCS	foetal calf serum
FDR	false discovery rate
FGF	fibroblast growth factor
FGFR	fibroblast growth factor receptor
GalC	galactocerebroside
GDF15	growth differentiation factor 15
GFAP	glial fibrillary acidic protein
GPI	glycosylphosphatidylinositol
IGF	insulin-like growth factors
IL-	Interleukin-
IP <sub>3</sub>	Inositol trisphosphate
Kv	voltage-gated potassium channels
KO	knockout
L-15	Leibovitz medium
LIF	leukaemia inhibitory factor
LIFR $\beta$	leukaemia inhibitory factor receptor beta
LPS	Lipopolysaccharides

μM	micromoles
MAG	myelin associated glycoprotein
MBP	myelin basic protein
min	minute(s)
MOG	Myelin oligodendrocyte glycoprotein
mRNA	mitochondrial ribonucleic acid
MS	multiple sclerosis
Nav	voltage-gated sodium channels
N-CAM	neural cell adhesion molecule
Nf155	155kDa isoform of neurofascin
Nf186	186kDa isoform of neurofascin
Nrg	neuregulin
NSC	neural stem cell
OEC	olfactory ensheathing cells
OPCs	oligodendrocyte progenitor cells
OSM	oncostatin M
p75NTR	low affinity neurotrophin receptor p75
PBS	phosphate buffered saline
PCR	polymerase chain reaction
PDGF	platelet-derived growth factor
PLL	poly-L-lysine
PLP	proteolipid protein
PNS	peripheral nervous system
PTN	pleitrophin
qRT-PCR	quantitive real time polymerase chain reaction
rpm	revolutions per minute
RT	room temperature
T12.5	12.5 cm <sup>3</sup> tissue culture flask
T25	25 cm <sup>3</sup> tissue culture flask
TGF-β1	Transforming growth factor beta
THBS4	thrombospondin-4
TnC	Tenascin-C
TNFα	Tumour necrosis factor-alpha
TNR	Tenascin-R
WMD	white matter disease

## Abstract

---

Astrocytes are the most abundant cell within the central nervous system (CNS) and yet despite this, the true extent of their role in health and disease has not been fully elucidated. In the undamaged CNS, they are termed quiescent, where they maintain homeostasis. However, after injury or disease astrocytes become reactive where they are described as a physical and molecular barrier to regeneration. Emerging literature has suggested the existence of an additional phenotype of astrocyte, termed the activated astrocyte. These astrocytes are thought to enhance regeneration by creating a more growth-permissive environment for repair. In addition, it has also been reported that astrocytes may play a role in regulating myelination; however, it is unclear how the phenotype of the astrocytes may affect this process. Therefore, this thesis will focus on the variable phenotypic state of astrocytes and subsequently how this relates to their ability to support myelination.

Using an *in vitro* myelinating culture, where dissociated spinal cord cells were plated on a monolayer of astrocytes, myelination can be followed over time. Since it is hypothesised that astrocytes can affect myelination we used two protocols known to affect the reactive status of the astrocyte, i) activate the astrocytes by treating with ciliary neurotrophic factor (CNTF) or ii) induce a quiescent astrocyte state by plating them on Tenascin C (TnC).

It is hypothesised that CNTF changes the activation state of the astrocyte therefore making it more supportive to myelination. The addition of the astrocyte derived factor ciliary neurotrophic factor (CNTF) was shown to enhance myelination. My results demonstrate that CNTF addition does not lead to an increase in oligodendrocyte or microglia cell numbers or an increase in the diameter of the neurites, thus suggesting that this CNTF-induced increase in myelination is mediated via the astrocyte.

Conversely, culturing astrocytes on the extracellular matrix molecule Tenascin-C (TnC), a method to make the astrocytes quiescent (Holley et al., 2005), resulted in a reduction in myelination. Astrocytes cultured on TnC were shown have decreased expression of nestin, which is typically a marker for reactivity. A microarray gene study comparing gene expression of the various astrocyte phenotypes identified CXCL10 to be upregulated in astrocytes on TnC. Furthermore, the addition of CXCL10 into the myelination cultures resulted in a decrease in myelination. Conversely, the addition of anti-CXCL10 to myelinating cultures on quiescent astrocytes increased myelination.

Taken together, these data indicate that the astrocyte phenotype has considerable influence on myelination; where activated astrocytes support myelination whilst quiescent astrocytes do not. The identification of factors which may modify astrocyte phenotypes could lead to potential therapeutic strategies for CNS pathologies.

## Author's Declaration

---

I declare that, except where explicit reference is made to the contribution of others, that this dissertation is the result of my own work and has not been submitted for any other degree at the University of Glasgow or any other institution.

Signature \_\_\_\_\_

Printed name \_\_\_\_\_

# **Chapter 1**

## **Introduction**

# Introduction

---

## 1.1 Glial Cells in the Central Nervous System

The central nervous system (CNS) comprises the brain and spinal cord and its primary function is to conduct sensory information from the peripheral nervous system (PNS) to the brain as well as conducting motor information from the brain to various effectors, such as muscles. The two major types of cells in the CNS are neurons and glia, which can be further divided into two groups: microglia and macroglia. In the CNS, macroglia consist of oligodendrocytes, the myelin forming cells, and astrocytes which are the major 'house-keeping' cells of the CNS. Resident macrophages in the CNS are the microglia which react quickly following an immune response to restore homeostasis. In order for these primary functions to take place, the microenvironment has to be highly controlled. Each of these cells types will be explored in turn, with special emphasis on astrocytes and their functions in myelination.

### 1.1.1.1 Oligodendrocytes

Oligodendrocytes are the myelin forming glial cells of the CNS. Myelin is the fatty proteolipid membrane that ensheaths axons by a process known as myelination. In order to myelinate axons, an oligodendrocyte extends its processes and wraps myelin in segments, known as internodes, around axons. The organisation of the myelin sheaths consists of functional domains which include the Node of Ranvier and paranode and juxtaparanode areas (Salzer, 2003). Each of these areas consists of a unique compilation of cell adhesion molecules and voltage regulated ion channels (Fig 1.1). One of these molecules is Caspr (Peles et al., 1997), a transmembrane protein located at the paranode. Neurofascin 155 (Nf155), a member of the L1 family of cell adhesion molecules, is expressed solely by oligodendrocytes and is found at the myelin paranodal loops (Tait et al., 2000). Together, these molecules form a complex with the main aim of anchoring the myelin to the axon.

In the exposed region of the node, clusters of the voltage dependent sodium channels (Nav) can be found. These are responsible for the propagation of action potentials down an axon (Rasband and Trimmer, 2001). Neurofascin 186 (Nf186), another isoform of neurofascin, is also located at the node (Fig 1.1). Recently, the role of Neurofascin autoimmune antibodies has been described in Multiple Sclerosis (MS, Mathey et al., 2007; Defruss et

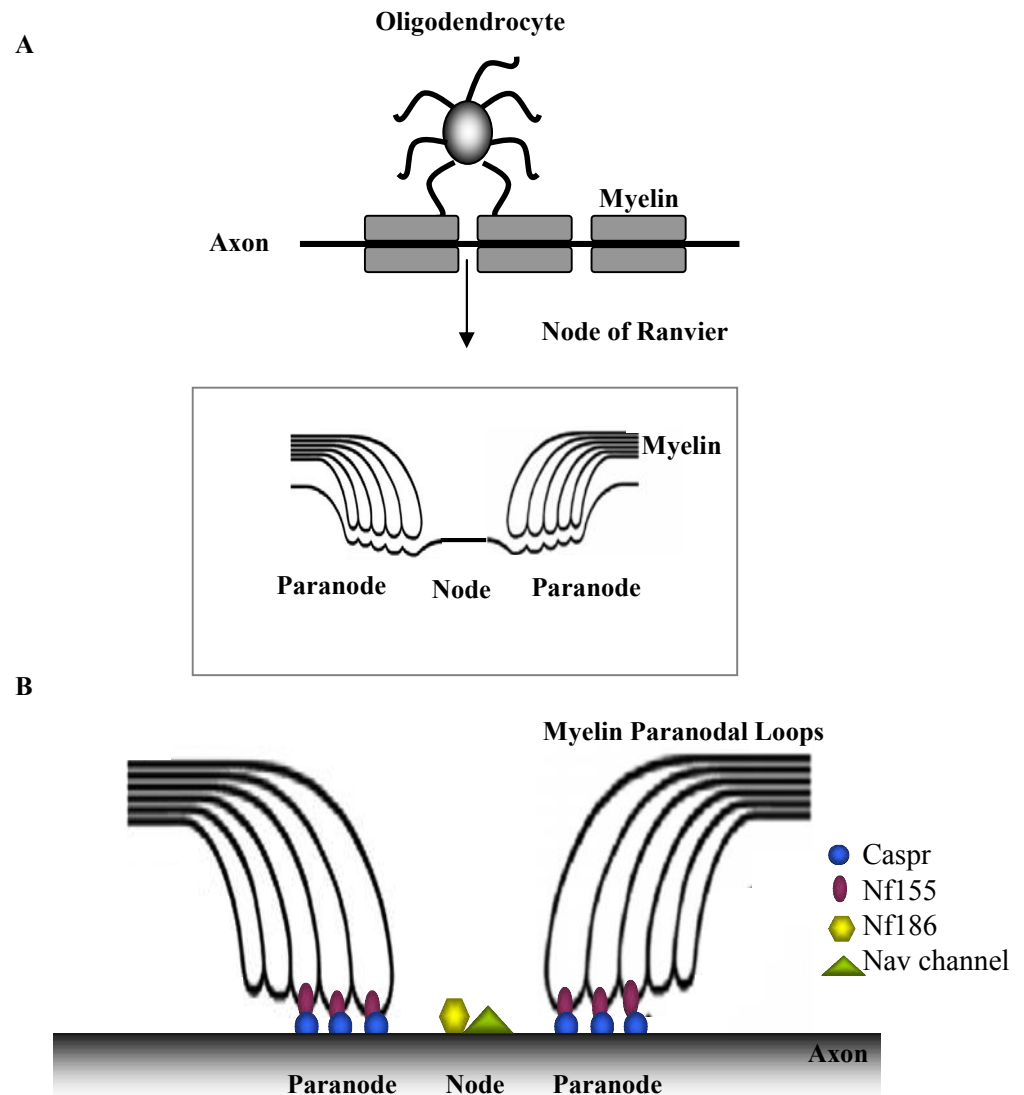


**Figure 1.1 Nodes of Ranvier Location and Structure.** The illustration represents a myelinated axon, where myelin sheaths from the oligodendrocytes are wrapped around the axon exposing the Nodes of Ranvier (A). The subdomains of the Nodes of Ranvier are the paranodes and juxtaparanodes (not shown), which are on either side of the node (box). Some of the cell adhesion molecules and voltage regulated ion channels are shown in B. Myelin associated Neurofascin155 (Nfasc155) is located at the myelin paranodal loops and Caspr the paranode. At the node, sodium channel and axonal neurofascin (Nfasc 186) are present. Figure adapted from Sherman and Brophy (2005) and Suzuki and Rasband (2008).

al., 2010). MS is an auto-immune attack on myelin sheaths leading to demyelination, glial scar formation and related axonal pathology. These researchers use an animal model of MS, known as experimental autoimmune encephalomyelitis (EAE), where they show that the transfer of anti-neurofascin antibodies (pan, recognising both Nf155 and Nf186) into these animals results in the exacerbation of disease severity. The authors show that neurofascin antibodies selectively bind to Nf186 where they mediate axonal damage, which is interesting as it is now thought that neuronal loss is a chief contributor to disability in MS (Ferguson et al., 1997).

The assembly of the Nodes of Ranvier and internodes of myelin is required for the fast propagation of action potentials. This method of rapid conduction allows communication between neurons over relatively long distances. The presence of the myelin sheath and the assembly of the nodes of Ranvier allow action potentials to ‘jump’ from node to node by a process known as saltatory conduction. The importance of myelin and saltatory conduction is highlighted when considering MS. The loss of myelin and axonal damage disables saltatory conduction. The features of MS will be discussed in further detail in Section 1.3.1. Briefly, the loss of myelin sheaths and axonal damage leads to interruption in signal propagation and leads to disability.

### **1.1.1.2 Oligodendrocyte Development**

Oligodendrocyte precursor cells (OPCs) are the precursors to the myelin forming cells in the CNS. They arise from a progenitor population in the ventral region of the ventricular zone (Sun et al., 1998; Rowitch, 2004). A subpopulation of OPCs also originates from developing brain homeobox 1 (Dbx-) expressing domain of the dorsal spinal cord (Fogarty et al., 2005). From the location of origin, OPCs then migrate down the spinal cord populating their final areas of maturation. The process of migration is tightly controlled and not yet fully understood but it is thought to be highly dependent on environmental cues, including secreted and extracellular matrix molecules (Bradll and Lassmann, 2010). One of these is the carbohydrate polymer,  $\alpha$  2-8 linked polysialic acid on neural cell adhesion molecule (PSA-NCAM). The cleavage of PSA from NCAM, which is located on the surface of OPCs, lead to a blockade of cells spreading from an explant model for cell motility, where the explant was the source of OPCs (Wang et al., 1994). This suggests that the expression of this molecule during development may contribute to guiding progenitor cells to where they are required and presumably its downregulation may confine cells to those specific areas.

OPCs are the progenitor cells that give rise to mature oligodendrocytes. It has also been suggested that OPCs have stem cell-like properties as they have the ability to give rise to astrocytes and neurons (Kondo and Raff, 2000). The authors showed that in the presence of platelet derived growth factor (PDGF) purified OPCs remained immature and the majority of them expressed A2B5+, a marker for early OPCs. In the presence of PDGF and Fetal Calf Serum (FCS), many OPCs also expressed glial fibrillary acidic protein (GFAP), an intermediate filament of astrocytes. In the presence of basic fibroblast growth factor (bFGF), FCS and bone morphogenetic proteins (BMPs) OPCs expressed microtubule-associated protein 2 (MAP2) and low and high molecular weight neurofilament (NF-L and NF-H, respectively), which are markers used to identify neurons *in vitro*. Furthermore, culturing OPCs with PDGF, FCS and FGF2 in non-coated culture dishes resulted in floating neurospheres, similar to stem cells in the CNS. Therefore, the study described the ability of OPCs to revert back to neurosphere stem cells as well as showing their ability to differentiate into astrocytes and neurons.

OPCs also exist in the adult CNS, where they remain undifferentiated (Wolswijk and Noble, 1989; Reynolds and Hardy, 1997; Dawson et al., 2003). These have been found to express the chondroitin sulfate proteoglycan, NG2 and were found in all areas of the CNS, including the cerebral cortex, hippocampus and corpus striatum (Dawson et al., 2003). It is hypothesised that the main function of these OPCs is to proliferate and repopulate areas devoid of oligodendrocytes (Dawson et al. 2003). For instance, in a model of antibody-induced demyelination, where antibodies are directed to myelin proteins leading to a loss of myelin sheaths from myelinated axons, the number of NG2+ cells increased by 72% over 3 days (Keirstead et al., 1998). Whether or not this increase was due to the inflammatory environment surrounding these cells was addressed by Cenci di Bello et al. (1999). The authors showed an increase in the NG2+ OPC population as a result of EAE demyelination. When the authors used non-specific mouse immunoglobulins to induce an inflammatory response without demyelination, no increase in NG2+ OPCs was observed. These data clearly indicate that the NG2+ OPC population in the adult CNS is highly active in demyelinating conditions.

### **1.1.1.3 Oligodendrocyte Differentiation and Myelination**

In order for oligodendrocytes to accomplish their primary role as myelinating cells, correct differentiation of OPCs must take place. OPCs are bipolar cells and can be identified by their expression of A2B5 and PDGFR $\alpha$  and as they differentiate they progressively

become more branched and begin to express markers such as O4 and NG2 (Zhang, 2001; Figure 1.2). Their processes extend and retract until they find suitable axons to myelinate (Pfeiffer et al., 1993; Kirby et al., 2006). It has been reported that oligodendrocytes have a short time frame (12-72 hours) in which the selection of axons and the initial ensheathment begins (Barres et al., 1992; Barres, 2010), thus forming a stable cell-to-cell contact between the two cells. Axonal selection, contact, initiation of ensheathment, control of myelin thickness and the extension of myelin sheaths along with neural growth are finely tuned processes that are in need of further understanding (Sherman and Brophy, 2005). Myelin is composed of 70% lipid and 30% protein and can be identified using a panel of markers including, proteolipid protein (PLP), myelin basic protein (MBP) and myelin-associated glycoprotein (MAG) (Dubois-Dalcq, et al., 1986, Fig 1.2).

Oligodendrocytes which fail to make contact with axons have been shown to undergo apoptosis (Trapp et al., 1997). It has been suggested that the overproduction of oligodendrocytes during development ensures that all axons which require myelination are myelinated (Trapp et al., 1997). In fact, around half of oligodendrocytes fail to reach maturity and subsequently die, partly due to competition for axonally-derived survival factors and contact (Barres et al., 1992; Trapp et al., 1997). The role of axons in mediating oligodendroglial differentiation has been described previously, where it was suggested that axons have recognition signals which attract oligodendrocyte processes, thus initiating myelination (Lubetzki et al., 1997). However, Rosenberg et al. (2008) demonstrated that seeding OPCs on top of fixed dorsal root ganglion neurons (DRG) resulted in the differentiation of OPCs to mature oligodendrocytes and they were able to myelinate fixed neurons. Interestingly, the authors also showed that OPCs did not myelinate axons when plated at low densities, but do when artificial beads with a similar diameter to OPCs were bound to the axonal surface. Therefore, the study suggests that OPCs differentiate and myelinate due to space constraints. However, it must be noted that DRG neurons are of peripheral origin and whether OPCs will behave in the same manner in the presence of CNS neurons has not been established.

The environment surrounding OPCs, including growth factors and extracellular matrix molecules, have been reported to affect their differentiation. Without any exogenous addition of growth factors *in vitro*, oligodendrocytes differentiate after dropping out of several division cycles (Raff et al., 1988). A group of proteins which has been implicated in oligodendrocyte differentiation are the neuregulins which exist as soluble and

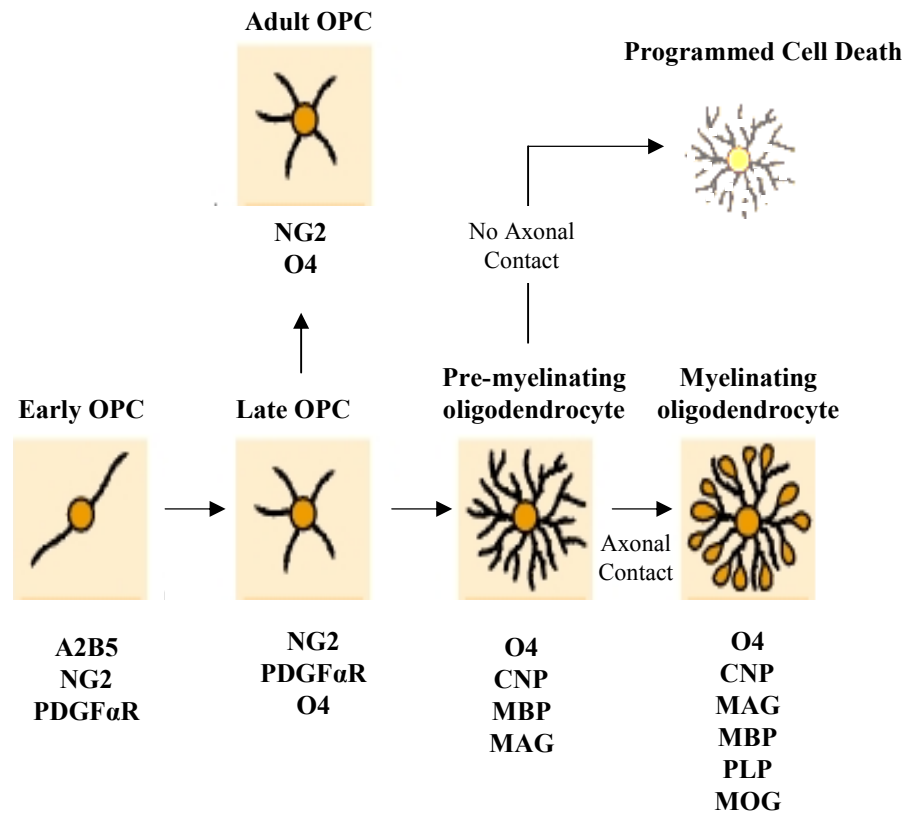


**Figure 1.2 Summary of Oligodendrocyte Differentiation.** The illustration represents the differentiation of oligodendrocytes and the markers used to identify them at each stage. Bipolar early oligodendrocyte precursor cells (OPCs) give rise to late OPCs which are more branched. These give rise to pre-myelinating oligodendrocytes. Upon axonal contact, they become myelinating oligodendrocytes expressing mature myelin markers. Otherwise, they undergo programmed cell death. Adult OPCs can also be found in the adult. Figure adapted from Trapp et al. (1997) and Siegel et al. (1999)

transmembrane proteins of the epidermal growth factor family. Neuregulins activate the ErbB family of tyrosine kinase receptors, which include ErbB1, ErbB2, ErbB3 and ErbB4. The activation of the ErbB4 receptor by neuregulin is associated with a signaling cascade that leads to the maturation of oligodendrocytes, possibly via the activation of  $\gamma$  secretase and the translocation of ErbB4 intracellular domain to the nucleus (Lai and Fang, 2004). Neuregulins are necessary for the formation of oligodendrocytes, as *in vitro* spinal cord explants from neuregulin null mice (Nrg<sup>-/-</sup>) fail to differentiate (Vartanian et al., 1999). They are also potent mitogens for OPCs, but inhibit their differentiation into MBP<sup>+</sup> myelinating oligodendrocytes (Canoll et al., 1996). Conversely, Park et al. (2001) showed that spinal cord explants from ErbB2<sup>-/-</sup> mice had significantly reduced numbers of mature oligodendrocytes, whilst those that did mature failed to ensheath axons. Myelinated axons have been reported to have a higher expression of neuregulin than unmyelinated fibres, suggesting an instructive signal from axons to initiate myelination (Taveggia et al. 2005). Although neuregulin is not essential for myelination in the CNS, it has a significant effect in myelin sheath formation *in vivo* (Taveggia et al., 2008). The study showed that myelinated segments in neuregulin null mice (Nrg<sup>-/-</sup>) were reduced significantly (70%) compared to wildtype controls. However, this study also showed that oligodendrocyte differentiation was similar in both types of mice, thus suggesting that neuregulin's importance in the process of myelination is exerted via the formation of myelin, rather than the integrity of the oligodendrocytes. Addition of neuregulin to DRG neurons and OPCs led to a dose dependent increase in myelination, whilst a blocking antibody showed a significant reduction in myelination in the absence of any exogenous neuregulin (Wang et al., 2007). The effect of neuregulins on oligodendrocyte differentiation and myelination differ depending on the age of the oligodendrocyte. These data provide evidence to show that oligodendrocytes are highly influenced by surrounding soluble factors.

The precise mechanism by which an oligodendrocyte wraps its processes around axons is still unknown. It has been suggested that whilst an oligodendrocyte wraps its processes around several axons, its cell body remaining stationary (Bauer et al., 2009). Two models have been proposed to describe the wrapping mechanism (Pedraza et al., 2001; Bauer et al., 2009). One model involves the oligodendrocyte processes wrapping the axons in non-overlapping spirals which then extend out laterally forming overlapping sheets of myelin. The second model involves wrapping axons in a sheet-like manner and then extending by longitudinal movements.

### **1.1.2.1 Microglia**

Microglia are the brain's resident macrophages and are the most common immune cells in the CNS. The origin of microglia is a highly contested issue in neuroscience with three main possible origins: mesodermal, nectodermal or possibly monocytic, although this has been widely disputed (Kaur et al., 2001; Guillemin and Brew, 2004). In the normal, healthy brain, microglia are described as resting, where their function is mainly to monitor the environment for potential pathogens, however, other functions remain to be fully elucidated (Gehrmann et al., 1995). As microglia are extremely sensitive to their surrounding environment, they are the first cells to respond following disease or injury to the CNS (Liberto et al., 2004). Thus, the majority of literature describes microglia post activation and how this in turn changes the milieu for other cells.

### **1.1.2.2 Activated Microglia**

Microglia become activated after injury or infection of the CNS, as well as in demyelinating diseases such as MS (Skaper, 2007). This activation may lead to direct or indirect production of cytokines which then contribute to the inflammatory environment. IL-1 $\beta$ , a member of the interleukin-1 cytokine family, is produced by microglia and has been described as the dominant signal after injury (Liberto et al., 2004; Auro, 1998). Indeed, Herx et al. (2000) have demonstrated that mice lacking IL-1 $\beta$  signal have a delayed astroglial reaction following acute CNS trauma in mice. Thus, the quick response shown by microglia is required for the initiation of a more widespread reaction from other cell types, such as astrocytes.

As MS is an immune-mediated disease, there is no doubt that a microglial reaction is involved. However, the extent of its involvement, and whether there is a direct or indirect cause for demyelination, still remains under investigation. Defaux et al. (2010) used three models of *in vitro* demyelination; lysophosphatidylcholine (LPC), interferon- $\gamma$  combined with lipopolysaccharide (IFN- $\gamma$ +LPS) and anti-MOG antibodies plus complement, using embryonic rat brain aggregates which grew within a 26 day period. Demyelination (the loss of myelin from myelinated axons) was assessed by the loss of MBP and MOG expression as measured by qRT-PCR. The authors used this model to not only demonstrate the extent of myelination, but also to demonstrate an increase in microglial numbers as a result of demyelination. Interestingly, they found that specific genes were upregulated by specific treatments, for instance, CXCL2, a chemokine of the CXC family, was

upregulated only by LPC treatment whereas IL-1 $\beta$  and IL-14 only by IFN- $\gamma$ +LPS. This study is of great interest as not only does it strengthen the link between microglial activation and demyelination but it also suggests that there are different patterns of demyelination depending on the cause of inflammation. This observation may shed light on the different subtypes of MS to provide more specific treatments.

### **1.1.3.1 Astrocytes**

Astrocytes are a type of macroglial cell representing 50% of the total cellular volume of the CNS (Roessmann and Gambetti, 1986). They are defined by their stellate morphology and expression of glial fibrillary acidic protein (GFAP, Eng et al., 1971). They have been termed 'support cells' and in the normal adult brain are thought to have a relatively passive role in the CNS. However, astrocytes are emerging as key players in many aspects of CNS diseases and injury. Their diverse roles extend from energy metabolism, neurotransmitter homeostasis, myelination, axonal outgrowth, maintenance of the blood brain barrier (BBB) and synaptogenesis (Liberto et al., 2004; Silver and Miller, 2004; Ullian et al., 2004; Pellerin, 2005; Nair et al., 2008, Sørensen et al., 2008; Watkins et al., 2008). The following sections will expand on these properties.

### **1.1.3.2 Astrocyte Development**

Astrocytes are categorised as fibrous, mainly found in the white matter; or protoplasmic, found in the grey matter (Peters et al., 1976; Wilkin et al., 1990). Morphologically they differ as fibrous astrocytes have numerous long processes, whilst protoplasmic astrocytes have fewer and shorter processes (Peters et al., 1976). The heterogeneity of astrocytes allows them to respond appropriately in each specific environment. Two subsets of astrocytes have been described *in vitro*, Type-1 and Type-2, corresponding to *in vivo* location, proliferative ability and morphology (Raff et al., 1983 a+b; Wilkin et al., 1990). Type-1 astrocytes are flat and have a fibroblast-like morphology and divide in response to FCS and epidermal growth factor (EGF, Raff et al., 1983a). Type-2 astrocytes, on the other hand, have more processes (Raff et al., 1983a) and divide less frequently. Furthermore, type-2 astrocytes are only found in developing white matter, whereas Type-1 astrocytes are found in both white and gray matter (Raff et al., 1983a). It is thought that Type-2 astrocytes and oligodendrocytes arise from a common progenitor (Raff et al., 1983b). The marker A2B5 is also used to discriminate between these two types of astrocytes; Type 1 astrocytes do not express A2B5, whereas Type-2 astrocytes do (Raff et al., 1983a). On the basis of

immunohistochemistry with the A2B5 antibody and frozen sections of developing and adult rat brain, Miller and Raff (1984) have suggested that Type-1 astrocytes represent protoplasmic astrocytes whereas Type-2 astrocytes represent fibrous astrocytes. Interestingly, the presence of these two subtypes has also been demonstrated *in vivo* (Miller et al., 1985). The authors show that in the rat Type-1 astrocytes first appear at E16 whilst Type-2 astrocytes appear much later between P7 and P10. However, others have opposed this view by suggesting only one type of astrocyte exists *in vivo*, raising the possibility that Type-1 astrocytes are an *in vitro* artifact (Skoff, 1990). The study suggests that only one wave of astrocytes is generated in the first 2 post natal weeks, which then proliferate to give rise to more astrocytes postnatally. Furthermore, others have suggested that as the A2B5 marker recognises an external ganglioside epitope, and the staining of frozen sections show A2B5 to be internal, the reliability of these studies has been questioned (Williams and Price, 1992). In terms of other classifications of astrocyte heterogeneity, 9 variants have been described in the normal CNS (Matyash and Kettenmann, 2010). These variants are characterised based on their morphology, with significant overlap in their localization.

Precursors of astrocytes originate in the subventricular zone (SVZ) where they migrate along the medial ventrodorsal pathway and give rise to astrocytes (Marshall and Goldman, 2002). Astrocytes originate from the common neural stem cells (NSC) which are non-committed progenitors and are able to give rise to glial restricted precursors (GRP), astrocyte restricted precursors (ARP) and neuron restricted precursors (NRP, Liu and Rao, 2004; Dietrich et al., 2007). ARPs, although not yet identified, give rise to astrocytes whilst GRPs give rise to both oligodendrocytes and astrocytes (Liu and Rao, 2004; Dietrich et al., 2007). Neurospheres generated from neonatal rat striatum have the ability to differentiate into astrocytes in the presence of FCS (Thomson et al., 2006; Thomson et al., 2008; Sørensen et al., 2008). Similar neurosphere preparations have been shown to differentiate into other cell types, including neurons, oligodendrocytes and astrocytes (Maciaczyk et al., 2009; Darsalia et al., 2010), suggesting their possible use for regeneration in neurodegenerative disorders.

Interestingly, astrocytes have emerged to have stem-cell like properties and their potential in regeneration has been considered. For instance, Pillai et al., (2006) cultured human fetal astrocytes for 4 weeks in a cocktail of proteases and FGF-1, after which they changed morphology and began expressing neuronal makers. However, these newly differentiated

neuron-like cells had no electrophysiological properties, suggesting incomplete differentiation. Nonetheless, this study demonstrates that astrocytes have stem-cell like properties and under the yet undefined appropriate conditions they may have the ability to change cell type. Furthermore, Buffo et al. (2008) demonstrated the potential of astrocytes using a stab injury model. They showed that astrocytes isolated from the lesioned cortex, unlike the unlesioned cortex, formed neurospheres which could be further differentiated into neurons and oligodendrocytes. In an earlier study, Doetsch et al. (1999) used an *in vitro* scratch-wound model to test the multipotential ability of astrocytes. They showed that astrocytes generated neurospheres, proliferated and differentiated into neurons and oligodendrocytes under specific conditions. The data above demonstrated that astrocytes in the adult CNS have stem cell like properties under the correct guidance cues, usually observed in injury conditions. The pronounced response from astrocytes in most CNS injuries has been generally described as an obstacle to repair (Silver and Miller, 2004; to be discussed in detail in Section 1.4.4). The fact that astrocytes have such potential is extremely appealing as this can be further developed and manipulated in CNS injuries in order to create a favourable environment for regeneration and repair.

The age of the astrocyte has been implicated in the effectiveness of the support which astrocytes provide other cells. It has been suggested that the severity of CNS damage in neonatal animals is much less severe than that of adult animals (Barrett et al., 1984; Fujimoto et al., 2006; Filous et al., 2010). Barrett et al. (1984) performed spinal transection at T5 on neonatal and adult rats and examined GFAP immunohistochemistry of sections of cervical, thoracic and lumbar spinal cord to determine the extent of the glial reaction. Increase in GFAP reactivity is associated with a more pronounced glial reaction. They found that in neonatal rats, a mild GFAP reaction was present, which was mainly restricted to the lesion site. However, in the adult rats, not only was GFAP intensity greater, but it also spread further anatomically. Similarly, Fujimoto et al. (2006) demonstrated a comparable observation using fetal spinal cord. They transected fetal rats at T8-10 and then returned them to the uterus for delivery, and compared this group to adult rat spinal cord which had been transected. The authors report increased tissue scar formation and persistent glial reaction 5 weeks after surgery in the adult group. In the fetal group, scar formation was limited and the glial reaction was restored during the same time period. The authors discuss that the degree of astrocytic involvement in injury may be different for mature and immature tissues and the roles of astrocytes may change at different stages of maturity.

## 1.2 Functions of Astrocytes in Health and Disease

### 1.2.1 The Blood Brain Barrier

The blood brain barrier (BBB) is a physical barrier to restrict the entrance of harmful chemicals from the blood into the brain parenchyma and also to control the cellular transport of lipid soluble molecules using tight junctions. Water soluble molecules, such as potassium and sodium ions, require the use of carrier mediated transport, such as the sodium/potassium exchanger. The BBB is composed of specialised endothelial cells, which usually line the interior surface of blood vessels, as well as pericytes and their basal lamina. The main aim of the BBB is to supply the CNS with the required nutrients by controlling the permeability of blood vessels, thus regulating homeostasis of the CNS (Abbot et al., 2006; Fig 1.3). Astrocytes form ‘end-feet’ processes which surround blood capillaries and are thought to play a role in maintaining the integrity of the BBB. Janzer and Raff show direct *in vivo* evidence that astrocytes induce endothelial cells of non-CNS origin to form capillary endothelial cells which form the BBB. Furthermore, co-culture of astrocytes and endothelial cells increased the number and length of tight junctions (Tao-Cheng et al., 1987). Thus, astrocytes play a major role in controlling and maintaining the BBB via their direct actions on endothelial cells. In pathological conditions such as MS, AD and PD, the integrity of the BBB is compromised and how astrocytes contribute to this is not well understood. In MS, where there is an auto-immune attack on myelin sheaths leading to demyelination, loss of axons, and glial scar formation, the exposure of pro-inflammatory cytokines, which may be produced by astrocytes, enhances the migration of monocytes and promotes shedding of endothelial microparticles, thus contributing to the BBB disruption (Minagar et al., 2001; Minagar and Alexander, 2003). Voskuhl et al. (2009) used Experimental Autoimmune Encephalomyelitis (EAE), a rodent model of MS, where mice were exposed to the myelin protein MOG resulting in an auto-immune attack on the host’s myelin sheaths, resembling the occurrence in MS. Conversely, they showed that activated astrocytes around the BBB formed barriers to stop the infiltration of leukocytes and protect CNS function (Voskuhl et al., 2009). Furthermore, patients with neuromyelitis optica, an acquired demyelinating autoimmune disease similar to MS, have antibodies to aquaporin-4; a molecule which is highly expressed at contact junctions between astrocytes and the BBB (Lennon et al., 2005; Satoh et al., 2007). It is clear that the contact between astrocyte ‘end-feet’ and the BBB serve a regulatory mechanism in the normal brain and its role in CNS pathologies is yet to be further clarified.

## 1.2.2 Neurotransmitter Control and Synaptogenesis

Astrocytes are emerging as key players in the regulation of synaptic activity throughout the brain. It has been demonstrated that astrocytes become activated by an increase in intracellular calcium from presynaptic neurons and in turn release glutamate and ATP, which have been shown to directly stimulate postsynaptic neurons (Parpura et al., 1994; Hassinger et al., 1995; Newman, 2003). This increase in intracellular calcium has been termed calcium-waves and can be mediated to neighbouring astrocytes via the diffusion of inositol triphosphate (IP<sub>3</sub>, Finkbeiner, 1992). Experiments using cultures as well as intact tissue have demonstrated many other examples of communication between neurons and astrocytes in order to regulate synaptic activity and function (reviewed in Newman, 2003).

Synaptogenesis is the formation of new synapses between neurons and is an essential process during development as well as throughout life (Eckenhoff and Rakic, 1991). Although it is a matter involving neurons, recent evidence suggests that the correct formation of these synapses is highly dependent on the presence of astrocytes (Slezak and Pfriege, 2003). Neurons cultured without astrocytes showed that although synapses formed between neurons in the absence of astrocytes, they had little spontaneous synaptic activity (Pfriege and Barres, 1997; Nagler et al., 2001). However, culturing neurons with astrocytes not only increased the number of synapses but also increased spontaneous synaptic activity. Interestingly, Nagler et al. (2001) have also found that conditioned media from glial cells resulted in an increase in spontaneous neuronal activity, suggesting glial derived factor(s) may induce this neuronal activity. Although no specific astrocyte-derived factor for synaptogenesis has been identified, the literature above suggests that astrocytes play a dynamic role in controlling such a significant process in the CNS.

Communication of pre- and post-synaptic neurons with astrocytes is a new concept known as the tripartite synapse, where the location of the astrocyte allows it to be in close association with to both terminals. Amongst other neurotransmitter receptors, astrocytes also possess G protein coupled receptors where upon activation, they lead to the formation of IP<sub>3</sub>, which in turn leads to an increase in intracellular calcium concentration through the release from IP<sub>3</sub>-sensitive calcium internal stores (Araque et al., 2002). This in turn, causes the release of gliotransmitters from astrocytes, which has modulatory effects on neurons (Halassa et al., 2007). Furthermore, astrocytes remove extracellular glutamate via

glutamate transporters in order to clear excess glutamate from the synaptic cleft, therefore modulating synaptic transmission (Bergles et al., 1999).

The concept of glial activation and intracellular calcium stores impact in pathological conditions such as epilepsy. Epilepsy is a neurological disorder in which brain function is disrupted as a consequence of intensive bursts of activity from groups of neurons. A biological model was presented by Halassa et al. (2007) where hyperactive astrocytes (as well as hypoactive astrocytes) may contribute to pathological states by increasing or decreasing calcium oscillation frequency and gliotransmission. In support of this, many epileptic drugs block calcium signalling in astrocytes (Tian et al., 2005), suggesting a key pathological role played by astrocytes in epilepsy.

### **1.2.3 Water, Ion and pH Balance**

Astrocytes respond to external stimulation as they express a wide range of receptors and specialised transporters and because of this they are able to control fluid, ion and pH balance in the CNS (Simard and Nedergaard, 2004; Fig 1.3). For instance, astrocytes express the water-channel receptor aquaporin-4 (AQP4; Nielsen et al., 1997), a member of the aquaporin family of integral membrane proteins. In an interesting study using RNA interference (RNAi) to inhibit AQP4, Badaut et al. (2010) demonstrated a significant loss in water mobility in the rat brain as shown by the reduction in apparent diffusion coefficient (as measured by diffusion weighted imaging). Furthermore, astrocytes have numerous carriers of ions and other metabolites, including sodium/hydrogen exchanger, sodium/potassium/chloride co-transporter and bicarbonate transporters (Obara et al., 2008; Jayakumar and Norenberg, 2010; Sofroniew and Vinters, 2010) which all contribute to regulating the internal milieu.

### **1.2.4 Gap Junctions**

Gap junctions between astrocytes serve as a great means of communication, allowing for direct chemical or electrical communication between cells and preventing leakage into extracellular space. Astrocytes communicate to each other as well as with oligodendrocytes via gap junctions forming what is known as a 'glial syncytium' (Nagy and Rash, 2003; Fig 1.3). The cellular components of gap junctions are connexons (group of connexins) and these differ depending on the cell type and location. In the cuprizone model of experimental demyelination, where mice are fed with the copper chelator cuprizone,

leading to oligodendrocyte death and a subsequent reversible demyelination, astrocytes were shown to infiltrate the area and begin the *de novo* expression of connexin Cx-47, normally expressed by oligodendrocytes (Parenti et al., 2010). The expression of Cx-47 then shifted back to oligodendrocytes which repopulated demyelinated areas. Although the authors do not fully describe the primary function of Cx-47, the fact that astrocytes express a foreign connexin in a disease condition reflects their capabilities to control and maintain homeostasis. Further evidence for astrocytes providing support for oligodendrocytes was shown by Lutz et al. (2009), as they have demonstrated that the global loss of Cx-30 and astrocyte specific loss of Cx-43 in mice lead to loss of oligodendrocytes as well as a reduction of myelin basic protein, as measured by Western blotting. Furthermore, the double knock-out mice performed poorly in sensorimotor and spatial memory tasks. Thus, the communication of astrocytes to other astrocytes and oligodendrocytes serves as a crucial function in development and the maintenance of other cell types.

### **1.2.5 Energy and Metabolism**

Astrocytes also play an active role in energy and metabolism. For instance, astrocytes store glycogen, which can be used as a source of energy when glucose levels plunge (Cataldo and Broadwell, 1986). The main purpose of glycogen storage in astrocytes is to supply surrounding neurons with energy during times of large activity utilization or during hypoglycaemia (Brown and Ransom, 2007). Recently, the role of astrocytes and their coping mechanism with Amyloid  $\beta$  ( $A\beta$ ) was investigated (Allaman et al., 2010).  $A\beta$  is the main constituent of fibrous protein aggregates associated with Alzheimer's Disease, a neurodegenerative disease causing dementia due to loss of neurons. As astrocytes are the major homeostatic cells in the CNS, the authors' aim was to investigate how  $A\beta$  affected glucose metabolism in cultured astrocytes. Astrocytes exposed to  $A\beta$  increased their uptake of glucose as well as glycolysis. Furthermore, the authors used a co-culture model with astrocytes to demonstrate that  $A\beta$  treatment of astrocytes reduced neuronal viability. These observations strongly suggest that astrocytes are key players in energy and metabolism.

### **1.2.6 Neuronal Support**

The presence of astrocytes was originally thought to be for the sole purpose of neuronal support. Although much more is now known about key roles that astrocytes perform, their support for neurons remains important, physically by providing structural support and chemically by modulating the environment via the secretion of growth factors and

cytokines (Svendsen, 2002). *In vitro*, astrocytes have been shown to induce neural stem cells (NSC), which can differentiate into glial or neuronal progenitors, to a neuronal fate by promoting their proliferation (Song et al., 2002). The authors demonstrated this observation by culturing NSC with astrocytes, fibroblasts or neurons. Whereas the NSC cultured with neurons or fibroblasts did not change fate, those cultured with astrocytes increased the rate of neurogenesis by 8-fold. However, the role of astrocytes in the damaged CNS is disputed. Original work by Aguayo and colleagues suggests that the adult CNS environment is inhibitory to neuronal growth (Bray et al., 1991), possibly due to the environment created by astrocytes. Indeed, a study by Kinouchi et al. (2003) used transgenic mice that lack GFAP and vimentin expression to demonstrate this point. The authors transplanted donor cells engineered to express green fluorescent protein (GFP) and tracked these cells in wild type and transgenic mice. Transplanted cells in wild type animals failed to survive and integrate whereas those in the transgenic mice integrated successfully and had a significant increase in neurite length and extension. Both GFAP and vimentin are intermediate filaments which have been reported to be upregulated in glial scar formation, where astrocytes clump together forming an inhibitory physical barrier to repair (Fawcett and Asher, 1999). However, exactly how GFAP and vimentin contribute the ability of neurites to integrate is not understood. Emsley et al. (2004) argued that i) astrocytes from GFAP and vimentin null mice may be different developmentally and less able to form scars, ii) astrocytes from transgenic mice may have an altered secretory profile which creates a more favourable environment for transplanted cells, or iii) transgenic mice have altered expression of other molecules which may contribute to the effects observed and that GFAP and vimentin may not be the sole effectors. The contribution of the glial scar to regeneration post injury is further discussed in Section 1.4.1.

### **1.2.7 Other Astrocytic Functions**

Some of the functions that astrocytes perform in the normal CNS are summarised in Figure 1.3. The functions of astrocytes are diverse and complex and are beyond the scope of this thesis. Other astrocytic functions include angiogenesis, synaptic network formation, clearance of excess neurotransmitters, detoxification of free radicals and many more (Stein et al., 1995; Krum and Rosenstein, 1998; Ransom et al., 2003; Sofroniew and Vinters, 2010). It is clear that with the diversity of functions astrocytes carry out throughout the CNS, that they must play a vital role in injury and disease.

## **1.3 Astrocytes and Their Role in Multiple Sclerosis**

### **1.3.1 Multiple Sclerosis**

Multiple sclerosis (MS) is an acquired autoimmune disease with usual onset of the disease occurring in early adulthood, making MS the most common CNS disorder to cause disability in young people (Noseworthy et al., 2000). Scotland has the highest incidence of MS cases in the world, with a higher incidence in females than males (Swingler and Compston, 1986; Ramagopalan et al., 2010). Although disease etiology is not yet fully understood, it is generally accepted that MS is acquired as a result of a combination of genetic susceptibility and environmental factors (Compston and Coles, 2008; Ramagopalan et al., 2010). MS was originally described by Charcot (1868) where the main observation was the presence of demyelinated plaques. MS has 4 subtypes, namely: primary progressive, secondary progressive, progressive relapsing and relapsing-remitting (Fig 1.4). Primary progressive tends to show the most disability, where there are no periods of remission. Secondary progressive initially begins with episodes of disability followed by continuous decline without periods of remission. Progressive relapsing MS is characterised by individuals having a steady decline in disability but with defined attacks throughout. Finally, relapsing-remitting MS is a subtype where spontaneous episodes take place followed by long periods of remission. The disability that MS causes depends on where the demyelinating plaques are located, for instance, reduced visual acuity if demyelination is at the optic nerve (Compston and Coles, 2008). Generally, however, most MS patients suffer from fatigue, muscle weakness and change in sensation amongst others (Compston and Coles, 2008).

### **1.3.2 The Pathophysiology of MS**

It is generally accepted that MS is an autoimmune disease, where there is a penetration of the BBB allowing the access of auto-lymphocytes, namely T cells, into the CNS (Steinman, 1996). This leads to destruction of the myelin sheaths that surround myelinated axons (demyelination). There is also an associated axonal pathology, where the progressive element of MS is mainly due to the degeneration of axons (Anderson et al., 2008; Compston and Coles, 2008). A characteristic feature of MS are the plaques, where astrocytes are the main constituent. They become hypertrophic and show increased GFAP expression and stellation (Fedoroff et al., 1984; Wu and Raine, 1992; Dagainakatte et al.,

2008). The role of astrocytes in MS is a highly debatable issue in neuroscience, where some believe that they have a pro-regenerative role via the secretion of growth factors and maintaining homeostasis for the benefit of the host whilst others believe that they are completely debilitating by contributing to demyelination and the failure of OPCs to differentiate (Rudge and Silver, 1990; Eddleston and Mucke, 1993; Silver and Miller 2004; Williams et al., 2007; Sofroniew and Vinters, 2010). The role of the glial scar in terms of remyelination will be further discussed in Section 1.4.4.

### **1.3.3 Astrocytes and Myelination**

In order to understand the role of astrocytes in MS, the importance of astrocytes in myelination in general needs to be discussed. A key indication of their role comes from a study of mutations in astrocyte specific genes. GFAP, which is upregulated when the astrocyte becomes activated, was mutated in a series of experiments by Liedtke et al. (1996). The authors showed that a defective GFAP gene resulted in a loss of integrity of CNS white matter architecture and long-term maintenance of myelination. Furthermore, there is a strong association of GFAP mutations with Alexander disease (Brenner et al., 2001; Li et al., 2002), a neurodegenerative disease classified as a leukodystrophy with loss of myelin, oligodendrocytes and neuronal degeneration (Alexander, 1949). Mutations in eukaryotic translation initiation factor 2B5, EIF2B5, causes childhood ataxia with CNS hypomyelination (CACH) also known as vanishing white matter disease (VWM). This mutation was found in neural progenitor cells, preventing their differentiation into astrocytes, suggesting that a lack of astrocytic development in the brain may contribute to VWM (Dietich et al., 2005). Additional evidence that astrocytes are important for CNS repair came from elegant transgenic mice experiments in which dividing, and therefore reactive, astrocytes were selectively ablated after induction of spinal cord injury. Resulting injury was far worse in groups where astrocytes were removed with a failure of blood-brain barrier repair, leukocyte infiltration, local tissue disruption, severe demyelination, neuronal and oligodendrocyte death, and pronounced motor function loss (Faulkner et al., 2004). These data clearly indicate that the presence of astrocytes is crucial for myelination.

It has been known for many years that astrocytes secrete promyelinating factors that directly affect the oligodendrocyte lineage. Astrocyte conditioned medium (ACM) is the media collected, usually overnight, from confluent astrocyte cultures and contains soluble factors produced by them. ACM has been shown to increase the survival of neurons after insults and that ACM from different regions of the brain demonstrate varying extents of

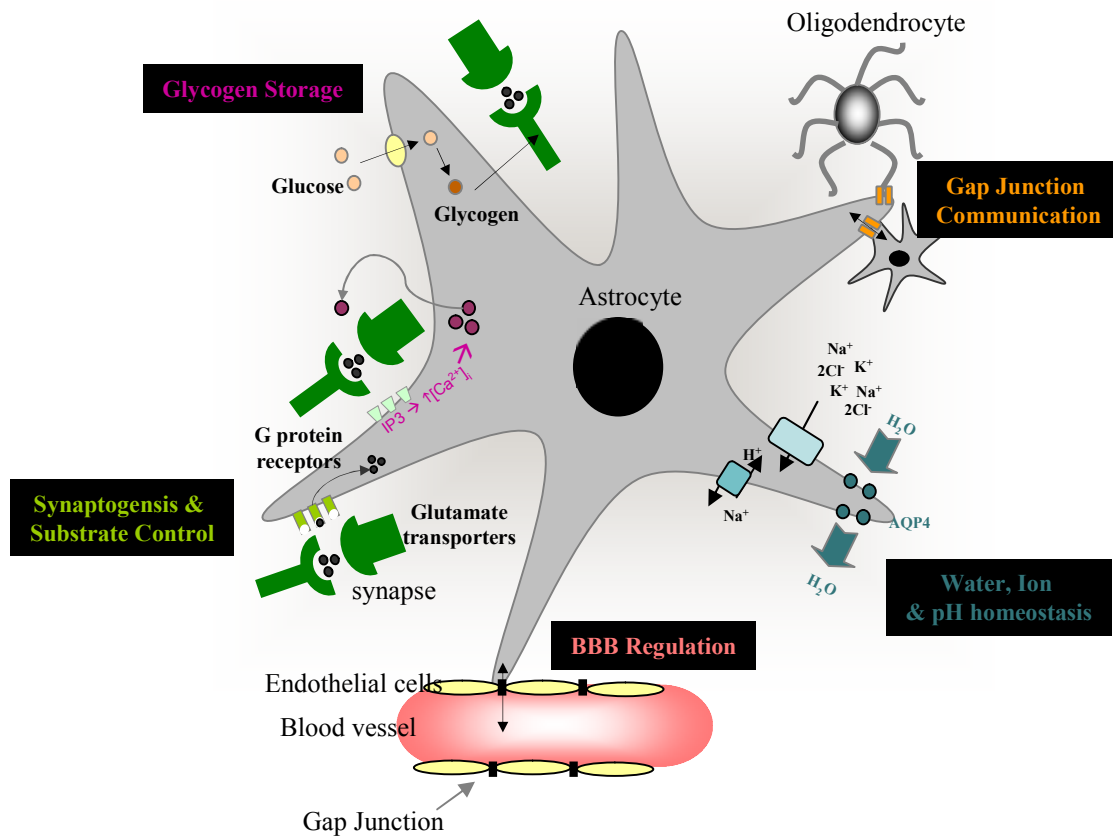


**Figure 1.3 Schematic Representations that Summarise Various Astrocytic Functions in the Healthy CNS.** Astrocytes are capable of performing many roles in the CNS including the regulation of Blood Brain Barrier (BBB), water, ion and pH homeostasis, gap junction communication with other astrocytes or oligodendrocytes, glycogen storage as well as roles in synaptogenesis and substrate control. *BBB* blood brain barrier,  $Na^+$  Sodium,  $Cl^-$  calcium,  $K^+$  potassium,  $H^+$  hydrogen, AQP4 Aquaporin 4, IP3 Inositol trisphosphate.

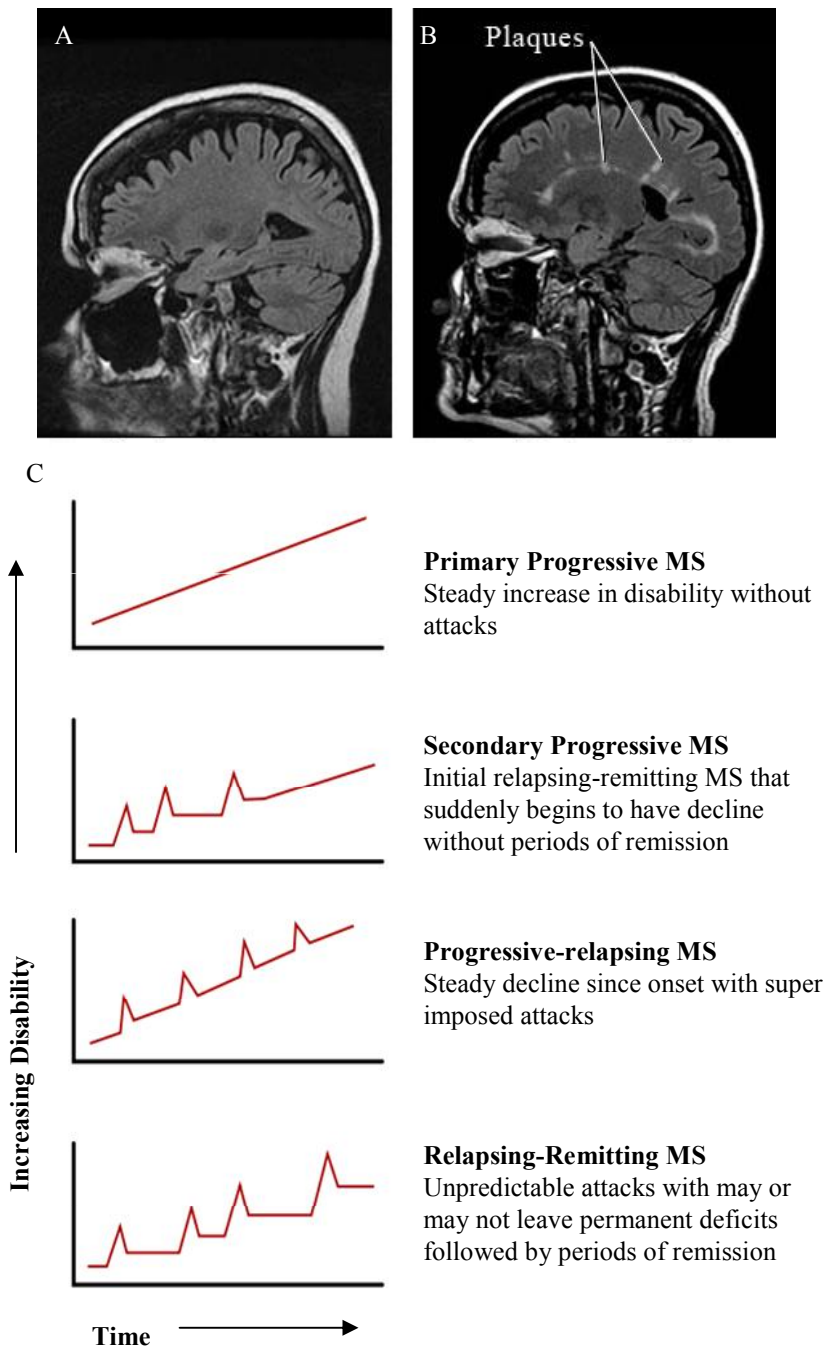


**Figure 1.4 MS Course and Subtypes.** A sagittal view of Magnetic Resonance Imaging (MRI) scans of a healthy brain (A) and one with MS (B). Plaques (as indicated in B) reveal areas where there is absence of myelin. MS subtypes with their clinical course and disability scale. Section A and B taken from health.com and adapted. Section C taken from Wikipedia.com and adapted.

neuroprotection (Yoshida et al., 1995; Yamamuro et al., 2003; Zhu et al., 2006). ACM has also been used as mitogen for OPCs (Noble and Murray, 1984). Recently it has been shown that the presence of astrocytes allowed faster and more thorough ensheathment of axons by oligodendrocytes in an *in vitro* co-culture system (Watkins et al., 2008). The addition of astrocytes on top a monolayer of reaggregated neurons and OPCs enhanced the rate and degree of wrapping compared to cultures without astrocytes. Although the above studies do not specify the mechanisms by which astrocytes affect myelination, it is clear that they do have a major influence on oligodendrocyte function. Recently, a study by Arai and Lo (2010) demonstrated that ACM molecules are able to protect oligodendrocytes against H<sub>2</sub>O<sub>2</sub>-induced oxidative stress, starvation, and oxygen-glucose deprivation. They show that ACM protection is partly via the upregulation of phospho-ERK levels and phospho-Akt in OPCs, pro-survival signaling pathways in oligodendrocytes (Stariha and Kim, 2001; Cui and Almazan, 2007). The data above indicate that ACM is rich in factors which induce pro-differentiation and pro-survival pathways in oligodendrocytes. Although some molecules have been identified (discussed in Section 1.4.2), many still need to be recognised. The recognition of these molecules may contribute potential therapies in demyelinating diseases, where there is a failure in OPC differentiation.

In terms of myelination and astrocytes in development, immunohistochemical studies of the developing rat spinal cord show that a temporary increase in GFAP positive cells correlated with an increase in immunoreactivity with the late myelin marker, myelin basic protein (MBP) suggesting that this increase of GFAP positive cells accompanying myelination is necessary for normal myelin development (Dziewulska et al., 1999).

A link has been demonstrated between astrocytes, myelination and electrical activity in axons (Ishibashi et al., 2006). In this study it was shown that astrocytes secrete leukaemia inhibitory factor (LIF) in response to ATP being liberated from axons firing, which in turn increased the number of myelinated fibres. Thus, LIF-secretion by electrically stimulated astrocytes results in enhanced oligodendrocyte differentiation. Therefore, secreted factors by astrocytes help create an accommodating and permissive environment for oligodendrocytes to mature into successful myelin-producing cells.

#### **1.3.4 Astrocytes and Models of Demyelination**

Experimental models of demyelination have also been used to demonstrate an important role for astrocytes in subsequent remyelination. These use the glial toxin ethidium bromide

(ED) to create a focal area of demyelination in the CNS (Graça and Blakemore, 1986). It has been shown that oligodendrocytes favour the remyelination of axons in areas where astrocytes were localised (Talbot et al., 2005). The authors show that proliferating NG2+ cells (OPCs) infiltrate demyelinated areas, and that astrocytes are localised within the perimeter of the lesion and not within it. Interestingly, they find mature oligodendrocytes and remyelination taking place in the region where astrocytes were localised. Likewise, transplantation of astrocytes into these experimentally-created demyelinated lesions enhanced remyelination by host oligodendrocytes (Franklin et al., 1991). These observations strongly suggest that the presence of astrocytes is essential for the remyelination process. The failure of OPCs to differentiate into mature myelinating oligodendrocytes in astrocyte-free areas can be either due to the absence of astrocyte-derived signaling enhancing terminal differentiation or that astrocyte-free areas have a negative dominant signal on OPC differentiation (Talbot et al., 2005). Another suggestion could be that both types of signals compete for the promotion of myelination.

The evidence above suggests that the presence of astrocytes has an influential effect on the cells within the surrounding environment, including a direct functional effect on oligodendrocytes. Astrocytes seem to have a dual role in myelination, where their presence is crucial but they are also the main component of the glial scar, impeding regeneration and remyelination. Further elucidating the panel of factors secreted by astrocytes in different conditions will expand our understanding of astrocyte biology and in turn their role in disease. It is therefore crucial that phenotypes of astrocytes are classified, where their morphological, antigenic and physiological properties are characterised. Astrocyte phenotypes can then be related to their biological relevance in health and disease.

## **1.4 Astrocytes and their Phenotype**

In the normal CNS, astrocytes are often described as resting or quiescent (Eddleston and Mucke, 1993; Holley et al., 2005) but it is more likely that they are actively regulating normal brain function as described in Section 1.2. In response to damage, astrocytes within the CNS tissue acquire a change in phenotype known as astrocytosis, where their morphology, size and secretory profile changes from that of a resting/quiescent astrocyte to one that is reactive, also known as anisomorphic astrocytosis. It has also been suggested that there is an intermediate phenotype in which the astrocytes are activated, known as isomorphic astrocytosis (Liberto et al., 2004). These categories are not completely exclusive but instead show a graded progression from one to the other, with possible

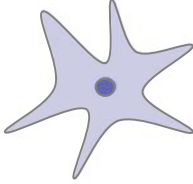
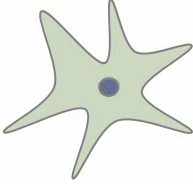
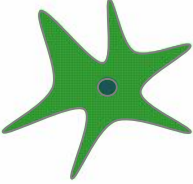
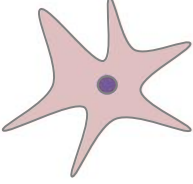
phenotypes in between (Sofroniew and Vinters 2010, Fig 1.5). The remyelinating capacity of oligodendrocytes in the vicinity of astrocytes in injury appears to depend on the severity of this astrocytic response, whether activated (mild gliosis) or reactive (severe gliosis). In this section, the aim is to further elucidate the various astrocyte phenotypes and their characteristics and secretory profiles with emphasis on those that appear to play a role in influencing myelination.

### **1.4.1 Mild Gliosis (Activated Astrocytes)**

Mild astrogliosis is also often described as isomorphic astrogliosis or astrocyte activation. This phenotype usually refers to astrocytes which have slightly upregulated levels of GFAP expression, show some degree of proliferation, and secrete anti-inflammatory cytokines (John et al., 2003; Liberto et al., 2004). There is currently a general view that mild astrogliosis is beneficial to axonal regeneration and remyelination in injured CNS tissue (White and Jakeman, 2008; Sofroniew and Vinters 2010). Cytokine-treated astrocytes are thought to be activated and have previously been shown to promote angiogenesis, restore the BBB, neuronal survival and synaptogenesis (Krum and Rosenstein, 1998; Gozes et al., 1999; Marz et al., 1999; Blondel et al., 2000; Herx and Yong, 2001; Mason et al., 2001). A great deal of research has been undertaken to identify the secretory profile of cytokine-treated astrocytes with emphasis on their effect on OPCs differentiation (Meeuwsen et al., 2003; John et al., 2003, 2005).

### **1.4.2 Factors Secreted by Activated Astrocytes**

Many factors have been reported to be secreted by astrocytes. For example, the treatment of mouse spinal cord astrocytes with CNTF resulted in an increase in FGF-2 mRNA (Albrecht et al., 2003). FGF-2 is a growth factor known to be secreted by astrocytes but thought to act on oligodendrocytes as they express the FGF receptor (Woodward et al., 1992; Redwine et al., 1998). In a viral-induced model of spinal cord demyelination, FGF-2 mRNA peaked 30 days post infection, the early remyelination stage of disease progression showing a correlation of FGF-2 expression and myelination (Messersmith et al., 2000). This study suggests that CNTF induces astrocytes to secrete FGF-2 which then acts on oligodendrocytes. Since OPCs are present within a demyelinated lesion but are unable to differentiate, it is suggested that astrocyte-derived FGF-2 acts directly on OPCs to induce their differentiation and subsequently promote myelination to take place.

			
Quiescent	Activated		Reactive
Normal	Mild gliosis		Severe gliosis
Resting	Isomorphic astrogliosis		Anisomorphic astrogliosis
Key Molecules Used Regularly for the Identification of Astrocyte Phenotype			
Low GFAP	↑ GFAP		↑↑ GFAP
No Vimentin	↑ Vimentin *		↑↑ Vimentin
No Nestin	↑ Nestin *		↑↑ Nestin
↑ S100β	↑ S100β		↑↑ S100β

**Figure 1.5 Summary of Astrocyte Phenotypes and Key Molecules used to identify them.** The astrocyte can be termed quiescent in normal adult resting CNS tissue. They can become activated by various mechanisms that result in mild/isomorphic astrogliosis, with a mild increase in cytoskeleton markers. Activated astrocytes are also more distal to the injury site. The most severe phenotype is the reactive/anisomorphic astrocyte that forms at the gliotic scar. This phenotype is characterised by a high increase in cytoskeletal molecules. Based on reviews from Liberto et al., 2004; Ridet et al., 1997; and Sofroniew and Vinters, 2010. Asterisks represent predicted information. Arrows indicate direction of expression and intensity.

Another example of astrocytes affecting the repair process in models of MS is seen by their interactions with vasoactive intestinal peptide (VIP). VIP is a polypeptide produced in part by cholinergic and sensory nerves (Goetzl et al., 2001). Astrocytes are responsive to VIP as functional receptors have been shown to be present on astrocytes *in vitro* (Magistretti et al., 1983). The treatment of MOG-induced EAE mice with VIP resulted in inhibition of the Th1 response and the down regulation of inflammatory cytokines such as RANTES (Li et al., 2006). It is considered that EAE disease suppression and thus the beneficial clinical outcome is consequential to VIP acting on astrocytes to release neuroprotective factors. Indeed, Brenneman et al. (1987) show evidence that conditioned medium from VIP-treated astrocyte cultures prevented neuronal death in neuronal cultures treated with tetrodotoxin. VIP was shown to elevate cAMP (a regulator of oligodendrocyte development) levels within oligodendrocytes *in vitro* (Wiemelt et al., 2001). The data above demonstrates that VIP treatment of astrocytes leads to the secondary secretion of neuroprotective agents which protect neurons, accelerate the rate of oligodendrocyte maturation as well as overall disease amelioration in EAE.

Astrocytes have been reported to secrete leukemia inhibitory factor (LIF), a member of the IL-6 family of cytokines (Aloisi et al., 1994; Ishibashi et al., 2006). LIF has also been shown to promote differentiation of oligodendrocytes and its absence in transgenic mice (null) reveals a reduction of the mature myelin protein, MBP (Mayer et al., 1994; Bugga et al., 1998). Furthermore, Khan and De Vellis (1994) show that the addition of LIF to immature (O4+) and mature (MBP+) oligodendrocytes resulted in a significant increase in cell survival compared to untreated cultures. Thus, astrocyte-derived LIF has the ability to potentiate the survival and differentiation of oligodendrocytes. These observations suggest that LIF may be implicated in inflammatory conditions. To investigate this, Aloisi et al. (1994) stimulated astrocytes with Interleukin-1 $\beta$  (IL-1 $\beta$ ), tumour necrosis factor- $\alpha$  (TNF- $\alpha$ ), and transforming growth factor- $\beta$ 1 (TGF- $\beta$ 1), cytokines known to be increased in MS and other inflammatory conditions (Selmaj et al., 1988; Barazini et al., 2000; Mirshafiey and Mohsenzadegan, 2009; Uzawa et al., 2010;). They show that inflammatory cytokines lead to the increased production of LIF from cultured astrocytes, strongly suggesting that LIF may play a regenerative role in disease. Indeed, the administration LIF to an EAE mouse model of MS resulted in decrease of EAE severity (Butzkueven et al., 2002). The authors show an increase in STAT-3 signaling, which can induce transcription of the anti-apoptotic proteins Bcl-2 and Bcl-xl (Bowman et al., 2000). Oligodendrocytes also upregulate LIFR $\beta$ , part of the receptor for LIF, and this therefore allows an increased

response to LIF. These data suggest that LIF secreted from astrocytes generally has a positive effect on oligodendrocytes during inflammatory conditions.

Mild astrogliosis usually occurs in areas where there is a much less disrupted environment usually distal from the injury site. The establishment of such astrocytes in these remote areas may be due to i) the release and widespread diffusion of cytokines from the injury site, ii) migration of reactive astrocytes from the injured area to distant sites, iii) neuronal degeneration at the site of injury leading to anterograde and retrograde fibre degeneration which affects the astrocyte at the projection territory or iv) direct astrocyte injury leading to reduced gap junction activity which then propagated via the astrocyte syncytial network to distant astrocytes (Malhotra and Shnitka, 2002). Thus, cytokine-activated distal astrocytes play a role in the re-establishment of the injured CNS. The presence of these astrocytes contributes to the regeneration capacity of the tissue, partly via the secretion of promyelinating factors.

### **1.4.3 Severe Gliosis (Reactive Astrocytes)**

The most extreme form of the astrocyte response, severe astrogliosis, also known as anisomorphic astrogliosis or astrocyte reactivity, results in a much higher increase in GFAP expression, elevated proliferation rates, and secretion of pro-inflammatory cytokines (Fedoroff et al., 1984; Eddleston and Mucke 1993; Dagainakatte et al. 2008; Sofroniew and Vinters, 2010). This astrocytic phenotype is frequently associated with the glial scar and can occur after any major damage to CNS tissue, for example after spinal cord injury and in MS. The environment is generally inhibitory to regeneration due to the presence of inflammatory cytokines, residual tissue damage products and immune cells, which is why the glial scar is often described as an impediment for axonal regeneration (Fawcett and Asher 1999; Fitch and Silver, 2008). Reactive astrocytes are mainly associated with the secretion of pro-inflammatory cytokines. In the next sections, the glial scar will be described in more detail and pro-inflammatory cytokines are identified and discussed in terms of their effects on myelination.

### **1.4.4 The Glial Scar**

The glial reaction is a hallmark of many CNS pathologies including multiple sclerosis (MS), spinal cord injury and Alzheimer's disease (Eng, 1985; Ridet et al., 1997; Nair et al., 2008; Vekhratsky and Parpura, 2010). A severe glial reaction usually forms the glial scar,

typical of CNS injury. The glial scar is a characteristic feature in MS, where it forms around areas of demyelination and in spinal cord injury where it forms around the penetrated cavity and injured axons (Fig 1.6). CNS injuries trigger a widespread response which is initiated with the infiltration of microglia (resident macrophages in the CNS) as well as ones from the BBB (Fawcett and Asher, 1999). Indeed, the greater the BBB disruption the higher the number of macrophages found within the glial scar (Silver and Miller, 2004). Macrophages in CNS injuries become activated and their main role is to clear away debris via phagocytosis (Brück et al., 1995). Recently, however, the roles of macrophages are emerging to be much more complex. For instance, Neumann et al. (2009) discuss the dual role the microglia can play in inflammatory diseases, where a blockade of the macrophage receptor TREM2 during the EAE resulted in disease exacerbation whereas its overproduction by transplanted cells improved disease severity (Piccio et al., 2007; Takahashi et al., 2007). Proliferating OPCs then move into the glial scar area, but fail to differentiate into myelin forming cells (Levine and Reynolds, 1991; Redwine et al., 1998; Fawcett and Asher, 1999; Talbot et al., 2005). Astrocytes are the main constituent of the glial scar. The intermediate filaments GFAP, nestin and vimentin are upregulated, there is cell hypertrophy and upregulation of extracellular molecules (Eddleston and Mucke, 1993; Fawcett and Asher, 1999; Dagainakatte et al., 2008; Sofroniew and Vinters, 2010). The glial scar forms a physical barrier for regenerating axons. However, the main aim of the glial scar is to form a barrier that secludes necrotic tissue and prevent widespread tissue damage (Faulkner et al., 2004; Silver and Miller, 2004). Furthermore, the evolutionary conservation of the glial scar (Larner et al., 1995) suggests that it must serve some kind of functional role and its absence may be more detrimental than its presence (Faulkner et al., 2004).

#### **1.4.5 Factors Secreted by Reactive Astrocytes**

As the glial scar is composed mainly of reactive astrocytes, it is necessary to examine their molecular and secretory changes. Chondroitin sulphate proteoglycans (CSPGs) are a group of extracellular molecules which have been associated and are thought to play a part in the regeneration failure in demyelinated regions (Canning et al., 1996; Filious et al., 2010). The CSPGs include neurocan, brevican, phosphacan and versican. It has recently been shown that astrocytes treated with chondroitinase ABC (enzyme digesting chondroitin sulphate chains) and then transplanted into a minimal brain lesion, lead to axonal regeneration when compared to untreated astrocytes (Filious et al., 2010). Further, Hunanyan and colleagues (2010) found that the administration of chondroitinase ABC

prevented the reduction in conduction which is usually observed after chronic unilateral hemisection in the rat. It is speculated that the presence of CSPG-presenting reactive astrocytes after injury hinder axonal regeneration and subsequently re-myelination.

The deleterious effects of secreted factors of reactive astrocytes have been well documented. The most striking is a cytokine from the tumour necrosis factor (TNF) family, TNF $\alpha$ , which is secreted at low levels by astrocytes in culture but strongly amplified when induced by pro-inflammatory agents, such as Interferon- $\gamma$  (IFN- $\gamma$ ) and Interleukin-1 $\beta$  (IL-1 $\beta$ ) (Chung and Benveniste, 1990). TNF $\alpha$  levels increase in EAE (Villarroya et al., 1996) as well as in the cerebrospinal fluid of MS patients (Tsukada et al., 1991). TNF $\alpha$  has been reported to induce myelin and oligodendrocyte damage *in vitro* (Selmaj and Raine, 1991) and its expression in MS plaques from patients is positively correlated with the extent of demyelination (Bitsch et al., 2000). Furthermore, it has been shown that the major target for TNF $\alpha$  is the maturation of oligodendrocytes (Cammer and Zhang, 1999) and thus supports evidence that OPCs are locally present in lesion sites but are unable to differentiate. These data demonstrate that the secretion of TNF $\alpha$  from astrocytes contributes to the damaging and inflammatory environment in MS. However, macrophage colony stimulating factor (M-CSF) derived from amoeboid microglial cells promoted TNF $\alpha$  from astrocytes which resulted in axonal degeneration and myelin sheath disturbance in hypoxic rats (Deng et al., 2010). This suggests that although the astrocyte may be producing the inflammatory cytokines, it is the presence of the activated macrophages that initiates anti-regenerative environment.

A range of molecules which are upregulated in MS are known to produce severe gliosis in experimental models of MS and in cultures *in vitro*. One of these molecules interferon- $\gamma$  (INF- $\gamma$ ) and it is known be expressed by astrocytes and be present in MS plaques (Traugott and Lebon, 1988; Meeuwssen et al., 2003). High levels of this cytokine are found in preterm infants with the leukodystrophy White Matter Disease (WMD; Hansen-Pupp et al., 2005). Yong et al. (1991) aimed to find the effect of INF- $\gamma$  on the glial reaction after corticectomy, where a region of the cortex was removed. They then packed an absorbable Gelfoam soaked with either INF- $\gamma$  or saline (control). After 7 days, they investigated the spread and intensity of GFAP using paraffin-embedded sections. They found that INF- $\gamma$  significantly enhanced the extent of reactive gliosis and increased its spread when compare to controls. Furthermore, Lin et al. (2006) use two models of experimental MS, cuprizone-induced demyelination and EAE, and transgenic mice in which INF- $\gamma$  transgene expression

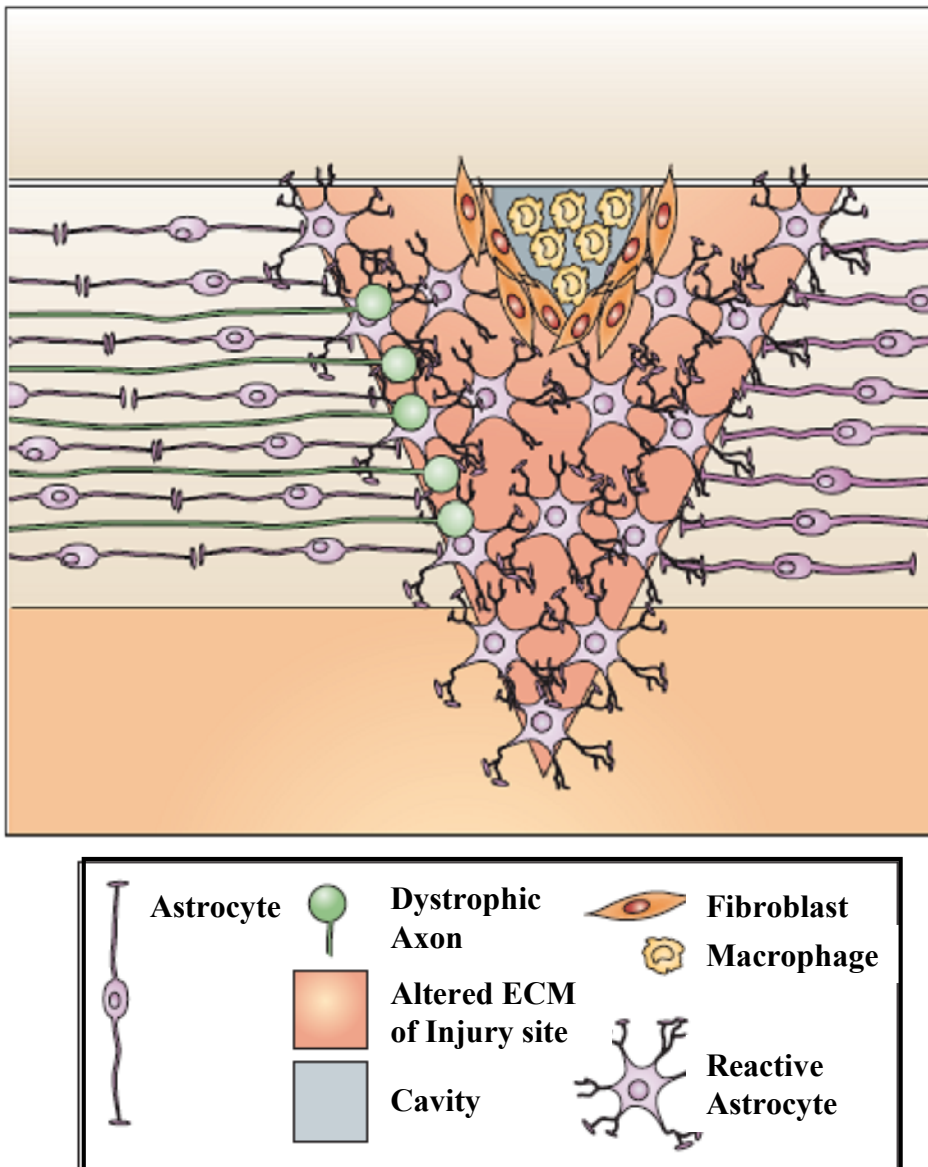


**Figure 1.6 The Glial Scar.** Schematic representation of a glial scar. Fibroblasts and macrophages infiltrate the area. Astrocyte proliferate and undergo hypertrophy, forming a dense network of interwoven cells. Astrocytes within the injury site are termed reactive. The extracellular matrix of astrocytes is altered, where there is an increase in chondroitin sulphate proteoglycans, amongst other molecules. The glial scar forms a physical barrier to regenerating axons. Astrocytes outside the injury site are 'activated' and respond by secreting anti-inflammatory molecules. Taken from Silver and Miller (2004).

was selectively targeted to astrocytes. Their results show that IFN- $\gamma$  was an impediment to remyelination in the cuprizone model and it also increase disease severity in EAE. They attribute these effects to endoplasmic reticulum stress in oligodendrocytes. In addition, a study by LaFerla et al. (2000) used similar mice strains and showed regional hypomyelination as well as death before maturity. Therefore, not only is IFN- $\gamma$  an activator of astrocytes, it is also secreted by astrocytes. These results strongly indicate that proinflammatory cytokines produced by astrocytes can have a direct functional effect on oligodendrocytes.

The data presented here highlights the dual role played by astrocytes in disease (summarised in Fig 1.7); where astrocytes become activated and aid regeneration, or become reactive and impede it. The factors that lead to the creation of reactive astrocytes as opposed to activated astrocytes require further investigation. Understanding these factors may provide avenues for the possible reversal of reactive astrogliosis and may therefore be of vast therapeutic potential for CNS diseases and injuries. Generally, however, a reactive astrocyte is regarded as a barrier for regeneration, partly via the secretion of factors that halt the survival and maturation of OPCs.

#### **1.4.6 Astrocyte Phenotype and Environment**

The ability of astrocytes to present a graded response to the intensity of injury highlights the versatility and adaptability of these cells. Although severe astrogliosis is correlated with well documented studies regarding them as an obstacle to regeneration, it must be noted that other cell types, such as microglia (Liberto et al., 2004) are much more responsive and can override any beneficial effects of the astrocytes. Apart from the vast array of growth factors and cytokines secreted by astrocytes, the physical barrier they form may be more protective than inhibitory. The evolutionary conservation of the glial scar (Larner et al., 1995) suggests that it must serve some kind of functional role and its absence may be more detrimental than its presence (Faulkner et al, 2004). The cytokine activation of astrocytes is clearly favourable for OPC proliferation, maturation and myelination. Dissecting out how cytokine activated astrocytes influence oligodendrocyte differentiation may provide clues into devising a therapy for demyelinating diseases

The phenotypic state of astrocytes and their ability to support myelination depends on many factors including the age of the astrocytes, the proximity to injury site and the state of activation (Fig 1.8). As previously described in Section 1.1.3.2, the age of the astrocyte

determines its ability to support other cells in injury conditions. This observation is likely to relate to the activation state of the astrocyte. For instance, astrocytes in neonatal animals may be more activated compared to the quiescent astrocytes in the adult. If astrocyte phenotype is considered as a spectrum of reactivity intensity, it can be argued that the closer the astrocyte is to being in an 'activated' state, the better it responds to injury and subsequently its ability to support (re)myelination. Thus, the neonatal astrocyte is more equipped to deal with insults than that of an adult. This observation highlights why many researchers generate neural cultures from neonatal rather than adult tissue. Astrocytes *in vitro* are usually grown as a monolayer, which is very different to their 3D environment in tissue. In fact, the process of dissection and enzymatic dissociation of tissue for generation of cells in culture may induce an activated state. Indeed, the expression of reactivity markers, GFAP, vimentin and AQP4, were reduced in astrocytes grown on a 3D collagen gel system compared to astrocytes grown in a monolayer (East et al., 2009). Furthermore, astrocytes *in vitro* are usually exposed to foetal bovine serum whereas those in the normal brain are not. Serum contains many factors including Bone Morphogenetic Protein-like factors which can induce astrocyte differentiation (Obayashi et al., 2009). Therefore, the artificial culture conditions to grow and maintain astrocytes may lead to a higher state of activation than at their tissue source. As astrocytes in culture have been shown to be supportive for myelination (Ishibashi et al., 2006; Sørensen et al., 2008; Watkins et al., 2008) it can be argued that the greater the level of activation, the more supportive an astrocyte is for myelination (Fig 1.8).

## 1.5 Conclusions

It is generally accepted that astrocytes within the glial scar inhibit regeneration and can have negative effects on remyelination (Rudge and Silver, 1990; Silver and Miller, 2004). Conversely, the emerging view is that astrocytes can also be essential for repair and subsequently myelination (Williams et al., 2007; White and Jakeman 2008; Sofroniew and Vinters, 2010). However, it is thought that these astrocytes are generally at more distal sites and probably respond to molecules emerging from the damaged area (Ridet et al., 1997). In fact, astrocytes more distal to injury contribute a great extent to regeneration via the secretion of growth factors and cytokines (Ridet et al., 1997; Williams et al., 2007; Nair et al., 2007; Sofroniew and Vinters, 2010). Consistency in the terminology and classification of astrocytes will be highly valuable for understanding their specific roles in CNS pathology.

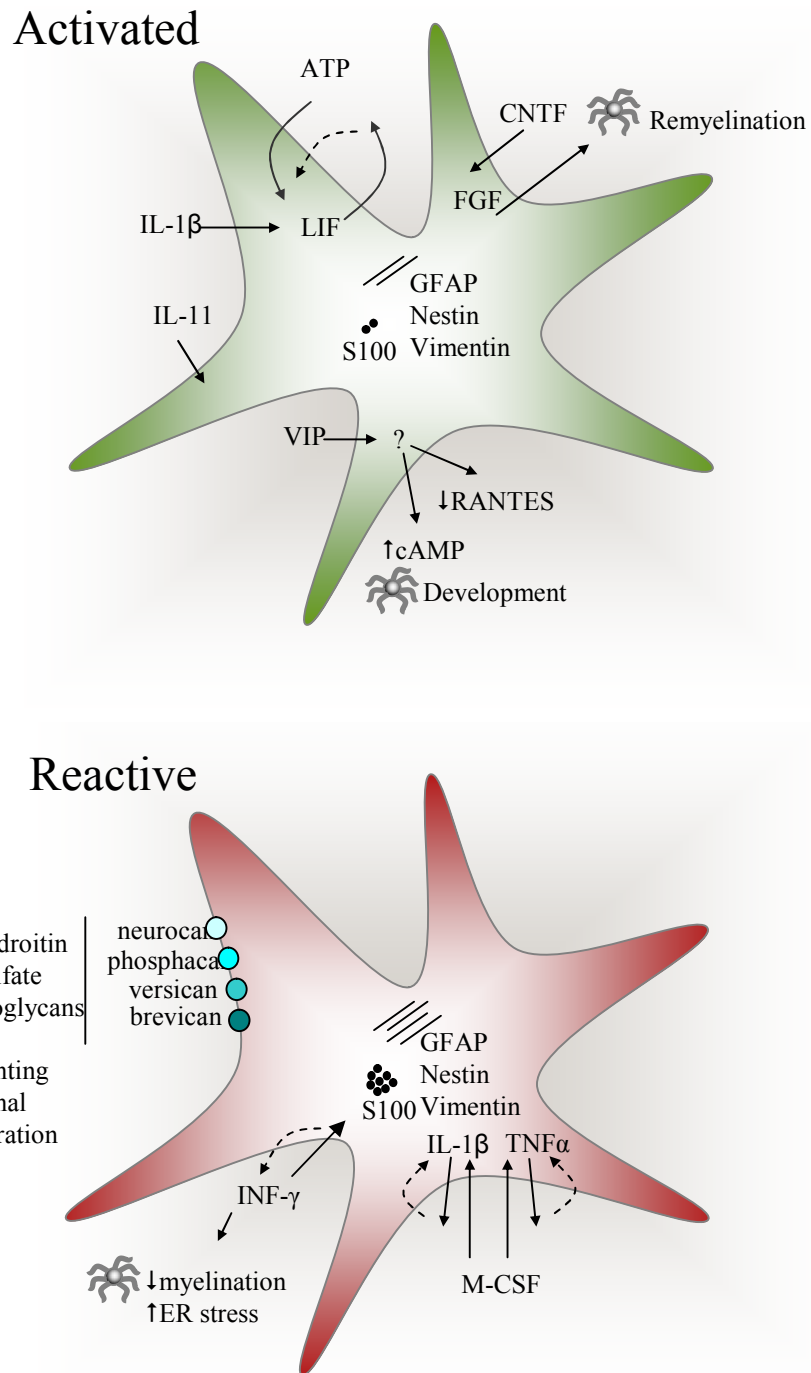


**Figure 1.7 Schematic Representation of Astrocytes in Activated and Reactive States.** A) An astrocyte can be activated by a number of cytokines which lead to a mild increase in cytoskeletal molecules and the secretion of factors which aid oligodendrocyte remyelination and development. B) An astrocyte in reactive state upregulates chondroitin sulphate proteoglycans and secretes molecules which reduce the ability of oligodendrocytes to remyelinate.

Research into astrocyte phenotypes looks at a ‘snapshot’ of a very active and constantly changing environment that is highly dependent on environmental cues. It is important for future strategies in CNS repair to identify the molecular and cellular changes in these polarised astrocyte phenotypes. Furthermore, it should be acknowledged that the environment around CNS damage and demyelinated areas contain very heterogeneous cell populations and relatively small changes in this responsive milieu may have an impact on other areas within the CNS. Therefore, results observed are very likely to be due to an indirect activation of complex cell-cell interactions. It is probable that the dynamic nature of astrocytes allows them to effectively respond to minute changes in the microenvironment mainly for the benefit of the host.

## 1.6 Aims

Data from animal models and *in vitro* studies suggest that astrocytes in injury and disease can be protective as well as destructive to regeneration. The phenotype of astrocytes, which is likely to be modulated by surrounding cytokines, is likely to play a big role as to whether or not an astrocyte is considered supportive.

In our laboratory, we have developed a myelinating culture system where embryonic mixed spinal cord cells are plated on top of a monolayer of confluent astrocytes (Thomson et al., 2008, Sørensen et al., 2008). The cultures develop over 26-28 days and allow the study of neuronal survival and neurite outgrowth, followed by oligodendrocyte precursor proliferation and extension of their processes to axons, and eventually progressing to ensheathment of axons and formation of myelin internodes. Using these myelinating cultures, we have shown that astrocytes have a direct role in promoting myelination (Sørensen et al., 2008). In fact myelination was poor on monolayers of other supporting glia such as olfactory ensheathing cells or Schwann cells, suggesting that astrocytes promote myelination either by releasing a soluble factor or via cell-cell contact.

The main aim of this thesis is to establish if there is a dual role for astrocytes in myelination. This will be carried out as follows:

- i) Establish culture conditions for astrocytes which could promote or inhibit myelination.
- ii) Define and characterise these astrocyte phenotypes and the cells within the myelinating cultures under conditions identified in i)
- iii) Identify the astrocyte-derived molecules that affect myelination using a microarray approach.

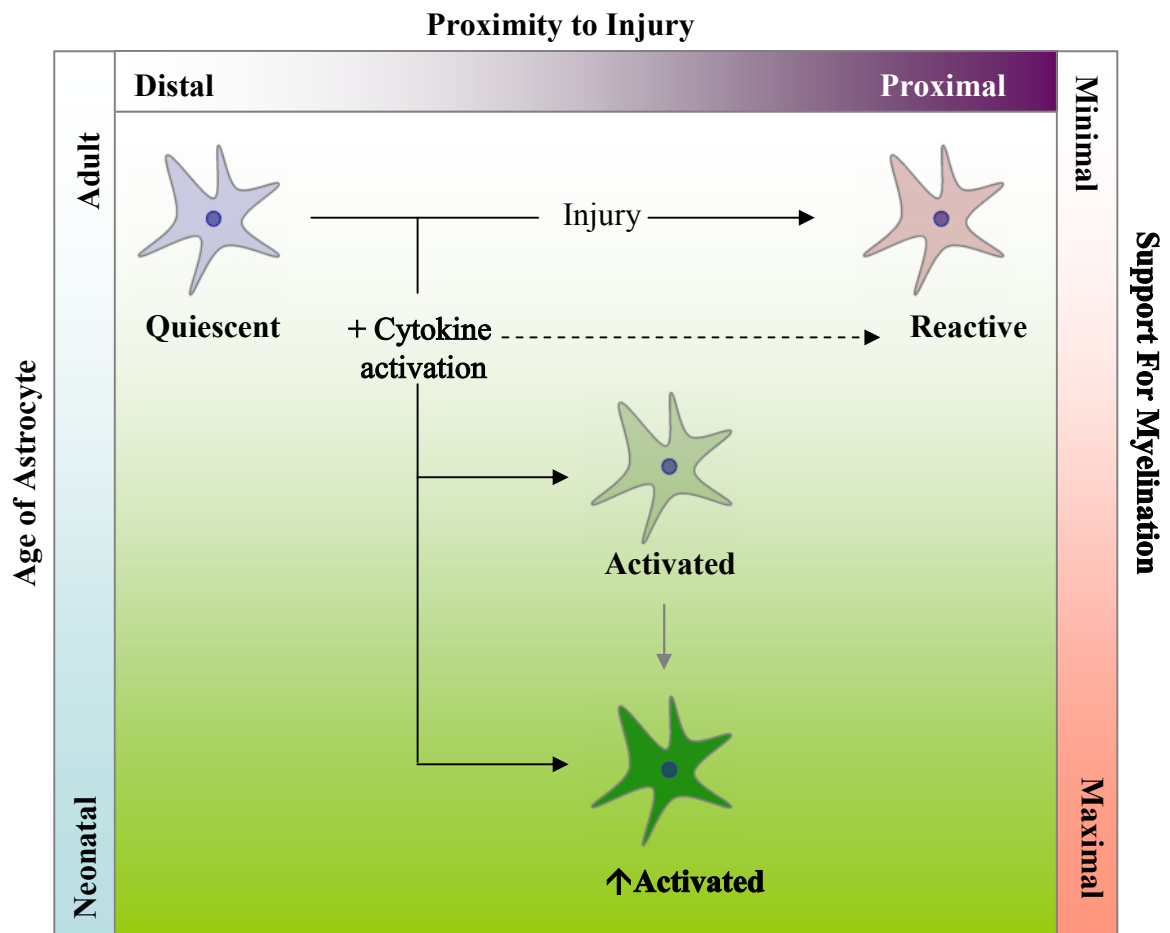


**Figure 1.8 Summary of How Astrocyte Phenotype can Influence Myelination.** Astrocyte phenotype can be affected by age and location. Astrocytes in close proximity to the site of injury are typically described as reactive and their support for myelination is poor. Astrocytes more distal to the site of injury receive ‘injury’ signals in the form of cytokines and increase their state of activation, ultimately increasing their support for oligodendrocytes via the secretion of trophic factors. Astrocyte in the neonatal animals respond better to injury possibly due to the reactivation state of the astrocytes and are therefore more equipped to support myelination than in the adult. Green represents a more positive effect on myelination.

## **Chapter 2**

### **Materials and Methods**

# Materials and Methods

---

## 2.1 Tissue Culture

Primary cell culture of astrocytes, olfactory ensheathing cells (OECs) and dissociated spinal cord cultures were cultured as described below. Neurospheres were cultured in an uncoated T75cm<sup>2</sup> flask whilst astrocytes and OECs were grown on glass coverslips (13 mm diameter, VWR International, Leicestershire, UK) placed in a 24-well culture plate. Coverslips were coated with poly-L-Lysine solution (PLL, 13.3 µg/ml in distilled water, Sigma), for 30 minutes (min) at 37°C, washed in distilled water (dH<sub>2</sub>O) and left air dry in tissue culture hood before use. Other coverslips were coated with Tenascin-C substrate (TnC, 5 µg/ml, Millipore) for 30 min at 37°C. TnC was then removed and coverslips left to air dry. Myelinating cultures on coverslips were grown in 35 mm culture dishes.

All cultures were maintained in a humidified incubator maintained at 37°C with 7% carbon dioxide. Cultures were fed every other day by removing half the media and replacing it with fresh media. All media and reagents were filtered through a 0.22 µm filter.

### 2.1.1 Astrocyte Culture

Neurospheres were generated from both striata of Sprague Dawley (SD) rats aged less than 36 hours (based on methods from Reynolds and Weiss, 1996; Zhang et al., 1998). The tissue was placed in 1 ml of L-15 (Invitrogen, Paisley, UK) and mechanically dissociated using a 21G needle. The suspension was centrifuged at 800 rpm (136 RCF) for 5 min and the pellet resuspended in 20 ml neurosphere media consisting of DMEM/F12 (1:1, DMEM containing 4,500 mg/L glucose), supplemented with 0.105% NaHCO<sub>3</sub>, 2 mM glutamine, 5,000 IU/ml penicillin, 5 µg/ml streptomycin, 5.0 mM HEPES, 0.0001% bovine serum albumin, (all from Invitrogen), 25 µg/ml insulin, 100 µg/ml apotransferrin, 60 µM putrescine, 20 nM progesterone, and 30 nM sodium selenite (all from Sigma). The suspension was then placed into a 75 cm<sup>3</sup> tissue culture flask (Greiner, Gloucestershire, UK) and supplemented with 20 ng/ml mouse submaxillary gland epidermal growth factor (EGF, R&D systems). Every 2-3 days, 5 ml NSM and 4 µl EGF (20ng/ml) was added into the flask. When the spheres are large enough, they were spun them down (800 rpm for 5 min) and triturated with 1 ml of fresh media to produce smaller spheres/cell clusters. The cell suspension was then plated into a flask with 10 ml of original media and 10 ml fresh

media and supplemented with 4  $\mu$ l EGF for a further 24 hours. The spheres were then differentiated into astrocytes as described in Thomson et al., (2006). Briefly, the spheres were plated onto coverslips (13 mm diameter, VWR International, Leicestershire, UK) in low glucose DMEM supplement with 10% foetal bovine serum (DMEM-FBS10%) and 2mM L-glutamine (both from Sigma) for 7-10 days until a confluent monolayer is formed. Astrocytes were either plated on PLL- coated coverslips (13  $\mu$ g/ml, Sigma) for making the standard monolayer support for myelination or TnC coated coverslips (5  $\mu$ g/ml, Millipore) for generating a quiescent astrocyte phenotype.

### **2.1.2 Olfactory Ensheathing Cells (OECs)**

Olfactory ensheathing cells (OECs) were isolated from the olfactory bulb of 7 day old SD pups and purified using magnetic beads (Higginson and Barnett, 2010; STEMCELL technologies, UK) and the p75<sup>NTR</sup> antibody (Abcam, Cambridge, UK). The cells were grown in low glucose DMEM (1000 mg/ml glucose) with 5% FBS and further supplemented with fibroblast growth factor 2 (FGF2, 500 ng/ml, Peprotech, London UK), heregulin  $\beta$ -1 (50 ng/ml, R&D Systems, Oxon, UK), forskolin ( $5 \times 10^{-7}$  M Sigma) and astrocyte conditioned media (ACM, 1:5, fresh serum free-media taken after incubation with a confluent astrocyte monolayer for 48 hours, see Noble and Murray, 1984; Alexander et al., 2002). The cells were grown on PLL-coated coverslips and either used as supporting monolayers or to condition spinal cord myelination cultures.

### **2.1.3 Myelinating Cultures**

The method of generating myelinating spinal cord cultures is based on that developed for mice (Thomson et al., 2008) and rats (Sørensen et al., 2008), with some modifications. SD rats were time mated and embryos used on E15.5 (day of plugging is embryonic day 0.5). The pregnant female was killed by carbon dioxide overdose followed by cervical dislocation. The abdomen was sterilised using 70% ethanol. Using sterile scissors, a cut was made to expose the muscle tissue, which was also cut. This exposed the female's uterus and the embryos were removed, released of the embryonic sack and decapitated about 3 mm rostra to the cervical flexure and the umbilical cord cut. The bodies of the embryos were placed in a dish containing L-15 and the skin and tissue were gently removed, until the spinal cord was uncovered. The meninges were then stripped and the bare cords were placed in a bijou containing L-15 on ice.

The spinal cords (5-6) were then minced with a scalpel blade and enzymatically dissociated with trypsin (100  $\mu$ l of 2.5%, Invitrogen, Paisley, Scotland) and collagenase (100  $\mu$ l of 1.33%, ICN Pharmaceuticals, UK). Enzymatic activity was stopped by adding 1 ml of a solution containing 0.52 mg/ml soybean trypsin inhibitor, 3.0 mg/ml bovine serum albumin and 0.04 mg/ml DNase (Sigma, Poole, Dorset, UK) to prevent cell clumping. The cells were triturated through a 21G needle and spun at 800 rpm (136 RCF) for 5 min. The cell pellet was resuspended in plating medium (PM, 50% DMEM, 25% Horse Serum, 25% HBSS). The cells were then plated on to a confluent monolayers of astrocytes or olfactory ensheathing cells (OECs) at a density of 150,000 cells per 100  $\mu$ l. Astrocytes were either directly plated on coverslips coated with either Poly-L-Lysine (13  $\mu$ g/ml, Sigma, Dorset UK) or tenascin-C (Tnc 5  $\mu$ g/ml, Millipore, Durham, UK) to generate quiescent astrocytes (TnC-astrocytes, Holley et al., 2005). The coverslips are placed in a 35-mm Petri dish and left in the incubator to attach for 2 hours. A combination of 300  $\mu$ L of PM and 500  $\mu$ l of differentiation medium (DM) (Thomson et al., 2006) which contained DMEM 4,500 mg/ml glucose, 10 ng/ml biotin, 0.5% hormone mixture (1 mg/ml apotransferrin, 20 mM putrescine, 4  $\mu$ M progesterone, and 6  $\mu$ M selenium (formulation based on N2 mix of Bottenstein and Sato, 1979), 50 nM hydrocortisone, and 0.5 mg/ml insulin (all reagents from Sigma) was added. After 12 days in culture, the insulin was removed from the DM. Cultures were fed every 2 days by removing 500  $\mu$ l of media and replacing it with fresh DM media.

In some cases on day 12 cultures received designated treatments; CNTF (Peprotech, London, UK) at varying concentrations of 0.02 pg/ml – 20 ng/ml, CNTF ligand neutralising antibody at 0.5  $\mu$ g/ml – 32  $\mu$ g/ml (anti-CNTF) and CNTF alpha subunit neutralising antibody at 0.2  $\mu$ g/ml (both R&D Systems, Abingdon, UK), LIF at 2 ng/ml (Millipore, Watford, UK), LIF neutralising antibody at 0.2  $\mu$ g/ml, CXCL10 neutralising antibody at 0.2  $\mu$ g/ml – 2.0  $\mu$ g/ml, Neuregulin at 10 ng/ml (all from R&D Systems, Abingdon, UK), CXCL10 at 10 ng, BDNF at 1 ng/ml (both from Peprotech, UK), IgG1 myeloma protein (0.2  $\mu$ g/ml, Sigma) and IgG2a myeloma protein (4  $\mu$ g/ml, Sigma). The cultures were then cultured for a total of 26-28. For some experiments, the addition of CNTF or its neutralising antibody was started at day 12, 18 or 24 and every 2 days thereafter until fixation.

#### **2.1.4 Conditioning of E15.5 Spinal Cord Cultures**

To determine the effects of OEC conditioned media on the myelination of the mixed spinal cord cells grown on astrocytes, two coverslips containing confluent monolayers of OECs

were placed in the same 35-mm Petri dish as the spinal cord cells. This meant that the OEC were continuously secreting soluble factors for these cultures and alleviates problems of adding the correct concentration of factors. As controls, 2 confluent astrocyte monolayers were also placed in the same dish as a coverslip containing spinal cord cells plated on OECs (results shown in Sørensen et al., 2008). Some dishes were further supplemented with CNTF (2 ng/ml) on day 12 onwards.

To determine the effects of quiescent astrocytes (TnC-astrocytes) on myelination, astrocytes grown on a TnC substrate, were placed in the same dish as myelinating cultures plated on astrocytes on PLL (PLL-astrocytes) to continually condition them. In addition, confluent PLL-astrocytes were placed in the same dish as myelinating cultures plated on quiescent astrocytes (TnC-astrocytes). Some PLL-astrocytes were also pre-conditioned with CNTF. In these experiments, the PLL-astrocytes were treated with 2 ng/ml of CNTF for 24-48 hours, washed three times in PBS and placed in the same dish as myelinating cultures plated on PLL-astrocytes or TnC-astrocytes. PLL-astrocytes pre-treated with CNTF were continually made so that they could be changed in the Petri dish with every feed.

## **2.2 Western Blotting**

Astrocyte monolayers were washed 3x with PBS and lysed using CellLytic M Cell Lysis Reagent (Sigma, Dorset, UK) for 15 min at room temperature (RT). The cells were then scraped off the coverslip and spun down to remove debris. Protein concentrations were measured using the Nanodrop (under Protein setting) and equal concentrations of 5-10 µg total protein for each condition was loaded into a NuPage 4-12% Bis-Tris Gel (Invitrogen, Paisley, UK) with rainbow molecular-weight markers (Amersham International, Little Chalfont, UK). The gel was run for 45 min in Running Buffer (Invitrogen), with a constant voltage of 200V. The gel was transferred using the iBlot (Invitrogen, Paisley UK) and the membrane blocked with 5% dried milk (Marvel) in PBS and 0.1% Tween (PBST). Membranes were incubated with either polyclonal rabbit tenascin antibody (1:1000, kind gift from Andreas Faissner), mouse monoclonal nestin antibody (1:1000; Chemicon Europe Ltd, UK), polyclonal rabbit GFAP (1:100000, Dako, Glostrup, Denmark) or mouse monoclonal GAPDH (1:1000, Abcam, UK) in 5% milk in PBST for 1 hour at RT. The membrane was then washed with PBST three times for 15 min each and then incubated with the appropriate horseradish peroxidase (HRP)-conjugated secondary antibody for 1 hour at RT in 5% powdered milk in PBST (anti rabbit, 1:10000, Santa Cruz; anti mouse

IgG1, 1:10000, Amersham). Following a further 3 washes, the membrane was developed using enhanced chemiluminescence (Amersham) and visualised using Konica Minolta SRX101A imaging system (Tokyo, Japan). Densitometry was carried out on the bands using Image J. For statistical analysis, a paired 2 sample t-test was used on the densitometry arbitrary values, comparing band intensity of treatment group to control group for both test protein and GAPDH.

## **2.3 Enzyme-Linked Immunoabsorbent Assay (ELISA)**

RayBio® Rat CNTF DuoSet ELISA Kit (Catalog No: DY557) was purchased from RayBiotech, Inc. (Insight Biotechnology, Middlesex, UK). CNTF levels were measured using enzyme-linked immunosorbent assay (ELISA). Media assayed was collected from astrocytes and myelinating cultures at different time points throughout the culture period before and after treatment with CNTF and frozen until use. All antibodies and reagents were diluted according to the manufacturer's protocol. A 96-well well plate (flat bottom) was coated with capture antibody overnight at room temperature. The plate was then washed three times with PSB-Tween 0.05% (PBST 0.05%) using a squirt bottle. After the last wash, the plate was inverted and blotted against clean paper towels. This ensures that the complete removal of liquid which is essential for good performance. The plate was then blocked using 1% BSA in PBS (pH 7.2 - 7.4) for a minimum of 1 hour at room temperature. The plate was then washed three times with PBST 0.05%. Protein standards were diluted in media which corresponds to the media in which the samples are in. For instance, astrocytes media samples are in DMEM-FBS 10% whereas DM was used for cultures. The same media was also used to dilute the standards. The concentration of standards ranged from a low concentration of 32.5 pg/ml to a high concentration of 2000 pg/ml, and blank wells containing media only were also included. The standards and samples were added to the wells in duplicate and left at room temperature for 2 hours. The plate was washed again and detection antibody added for 2 hours. Following another wash, Streptavidin-HRP was added to each well and left for 20 min. The plate was placed away from direct light as Streptavidin-HRP is a light sensitive solution. The plate was washed once again and substrate solution (1:1 mixture of Colour Reagent A (H<sub>2</sub>O<sub>2</sub>) and Colour Reagent B Tetramethylbenzidine) was added and left for 20 min (R&D Systems Catalog # DY999) away from direct light. Stop solution (2N H<sub>2</sub>SO<sub>4</sub>) was added and the plate was gently tapped to ensure thorough mixing. The plate was then directly read to determine the optical density of each well. The reader was set to 450 nm, with wavelength correction set

to 570 nm. Readings from the standards were used to create a standard curve, off which sample readings were read.

## **2.4 Bromodeoxyuridine Assay**

Bromodeoxyuridine (5-bromo-2-deoxyuridine, BrdU) is an analogue of thymidine. It is used as a marker of cell proliferation as it becomes incorporated into the DNA as the cell divides (S-phase of the cell cycle).

Astrocytes were cultured onto glass coverslips which were previously coated with either PLL (13.3  $\mu\text{g/ml}$ ) or TnC (5  $\mu\text{g/ml}$ ) and grown in DMEM-FBS 10% until confluency, usually 7-10 days. BrdU (10  $\mu\text{M}$ ) was added into the medium and left for 18-24 hours. The cells were then fixed and immunolabelled for anti-BrdU, as described in Section 2.5.2.

To assess whether the treatment with CNTF or its neutralising antibody (anti-CNTF) results in an increase in oligodendrocyte proliferation, E15.5 mixed spinal cord cells were plated on a confluent monolayer of astrocytes (PLL-astrocytes) and on day 12, treated with CNTF (2 ng/ml) or anti CNTF (4  $\mu\text{g/ml}$ ) and BrdU (10  $\mu\text{M}$ ) and left for 24 hours. The cells were then fixed and immunolabelled for anti-BrdU and O4 (oligodendrocyte marker, Sections 2.5.2 and 2.5.3)

## **2.5 Immunohistochemistry**

### **2.5.1 General Immunohistochemistry**

Cells plated on coverslips were taken out of 24-well plate or 35 mm dish and excess media was blotted against clean tissue paper. Primary and secondary antibodies are listed in Tables 2.1 and 2.2 respectively. For external markers, antibodies were diluted in cells own media. For internal marker, antibodies were diluted in blocking buffer (0.1% Triton-X-100 and 0.2% gelatine in PBS). Between all steps, the cells were washed three times in PBS and remaining media blotted onto tissue paper. Primary and secondary antibodies were added at 50  $\mu\text{l}$  volume per coverslip. External markers were stained live (before fixation and permeabilisation). Internal markers were fixed, permeabilised and blocked before addition of antibodies. After the final wash, the coverslips were mounted in Vectashield containing DAPI. However, if a blue secondary antibody was used Vectashield without DAPI was used.

## **2.5.2 BrdU Immunohistochemistry**

Ice-cold methanol was used to fix and permeabilise the cells. The cells were left at  $-20^{\circ}\text{C}$  for 10 min, washed in PBST 0.05%, and further fixed using 0.2% paraformaldehyde for 1 min at room temperature. They were washed in PBST 0.5% and 0.07 M sodium hydroxide was used added for 10 min at room temperature. The cells were washed again and anti-BrdU (1:20) was added for 45 min at room temperature. After another washing step, anti-mouse IgG1-TRITC (1:100) was added for 30 min at room temperature. The coverslips were then mounted in Vectashield with DAPI.

## **2.5.3 External Markers**

Coverslips of cells were blotted gently against a clean tissue paper. Primary antibody was diluted cell's own media and added to the coverslip and left for 20 min at room temperature. The appropriate secondary antibody was also diluted in the cells own media and left for 20 min. The cells were then fixed in 4% paraformaldehyde for 15 min. If markers of interest were external only, the cells were then mounted in Vectashield with DAPI. If markers of interest included internal markers, the protocol described below is then followed (Section 2.5.4).

## **2.5.4 Internal Markers**

Coverslips of cells are fixed with 4% paraformaldehyde for 15 min and permeabilised using 0.5% Triton-X 100. For GFAP, fixation and permeabilisation was achieved by addition ice cold methanol for 15 min at  $-20^{\circ}\text{C}$ . Cells were blocked using blocking buffer (0.1% Triton-X-100 and 0.2% gelatine in PBS) for 15 min at room temperature. Primary antibody was diluted in blocking buffer and added for 1 hour at room temperature. Secondary antibody, diluted in blocking buffer, was added for 45 min at room temperature. Cells were then mounted in Vectashield with DAPI, unless a blue secondary antibody is used.

## **2.6 RNA Extraction**

RNA extraction was prepared using Qiagen Kit. Astrocytes, which were grown in a monolayer, were washed three times in PBS. Buffer RLT Plus is the kit's lysis buffer and it was added in 380  $\mu\text{l}$  volume to each coverslip and the cells scrapped off gently using a pipette tip and placed in a sterile eppendorf. The cell lysate was triturated using a sterile

0.9 mm needle (20 gauge). Cell lysates can be frozen at this point and used at a later time point. However, RNA can degrade in as little as 24 hours, so it is recommended to extract RNA immediately. The lysates were then transferred into a gDNA column and spun for 30 sec at 10,000 rpm. All spinning steps in this section are at this speed. The gDNA column eliminates genomic DNA which will be trapped in the membrane and total RNA will be in the flow through. A volume of 350  $\mu$ l of 80% ethanol was then added to the flow-through, mixed well and transferred into an RNAeasy MinElute column in a 2 ml collection tube and spun for 15 seconds (sec). The flow through was discarded and total RNA was bound to the membrane. A volume of 700  $\mu$ l of RW1 Buffer was added to the membrane and spun for 15 sec and the flow-through discarded. Another buffer, Buffer RPE, was added and the membrane spun for a further 15 sec and flow through discarded. The buffer steps are to wash the membrane which contains total RNA. The column was then placed in a new 2 ml collection tube and the lid was left open and spun for 5 min to dry the membrane. The column was then placed in 1.5 ml collection tube and 14  $\mu$ l of RNA-free water was added directly onto the membrane and spun for 1 min. The elute contained the total RNA. The sample concentrations were then measured using Nanodrop under the Nucleic Acids RNA-40 setting. RNA was extracted for qRT-PCR and Microarray (Sections 2.9 and 2.10, respectively).

## 2.7 cDNA Synthesis

cDNA synthesis was carried out for polymerise chain reaction (PCR). RNA was extracted as described in Section 2.6. Invitrogen Superscript First-Strand Synthesis System was used for cDNA synthesis and manufacture's guidelines were followed. All ingredients of the kit and RNA samples were thawed on ice before use. The kit recommends using up to 5  $\mu$ g total RNA. The RNA was made up in 10  $\mu$ l volume consisting of 1  $\mu$ l of Random Hexamers and dNTP mix (10 mM). The maximum volume of RNA (8  $\mu$ l) was added, as long as it did not exceed 5  $\mu$ g limit. Otherwise, 10  $\mu$ l was made up using RNA-free water. The master mix was made up as follows for a 1x reaction:

	1x ( $\mu$ l)
10 RT Buffer	2
25mM MgCl <sub>2</sub>	4
0.1M DTT	2
RNase OUT	1
Superscript III	1

**Table 1.1 Primary Antibody List**

<b>Antigen</b>	<b>Raised in</b>	<b>Isotype</b>	<b>Dilution</b>	<b>Fixation method</b>	<b>Internal/ External</b>	<b>Source</b>
A2B5 (oligodendrocyte progenitor)	Mouse	IgM	1:1	n/a	External	Hybridoma
AA3 (PLP, mature myelin)	Rat	IgG	1:100	4% Para	Internal	Hybridoma
BrdU	Mouse	IgG1	1:20	Ice cold methanol	Internal	DAKO
ED1	Mouse	IgG1	1:100	n/a	External	Abcam
GFAP	Rabbit	IgG	1:500	Ice cold methanol	Internal	DAKO
Nestin	Mouse	IgG1	1:200	Ice cold methanol	Internal	Abcam
NG2	Rabbit	IgG	1:200	n/a	External	Chemicon
O4 (pre-myelinating oligodendrocyte)	Mouse	IgM	1:1	n/a	External	Hybridoma
SMI31 (phosphorylated neurofilament)	Mouse	IgG1	1:1500	4% Para	Internal	Covance
Tenascin C	Rabbit	IgG	1:100	n/a	External	Gift from Andreas Faissner

**Table 2.2 Secondary Antibody List**

<b>Antibody</b>	<b>Conjugate</b>	<b>Dilution</b>	<b>Source</b>
Goat anti-mouse IgG1	FITC, TRITC	1:100	Southern Biotech
Goat anti-mouse IgG1	Alexa Fluor: 350, 488, 555	1:600	Molecular Probes
Goat anti-mouse IgM	FITC, TRITC	1:100	Southern Biotech
Goat anti-rat IgG	FITC, TRITC	1:100	Southern Biotech
Goat anti-rabbit IgG	FITC, TRITC	1:100	Southern Biotech

Superscript III is the enzyme which reverse transcribes the RNA to cDNA. The master mix was made up according to the number of samples there were and took into account pipetting error. The magnesium ions and the buffer, which create a neutral pH, create a favourable environment for reverse transcription. The DTT reduces disulfide bonds and therefore used as a stabiliser for the reaction.

Using a heating block (Biometra T3 Thermocycler) the program below was selected:

	Temp (°C)	Time (hh:mm)	
1.	65	00:05	
2.	4	pause	pause to add master mix
3.	25	00:10	
4.	50	00:50	
5.	85	00:05	
6.	4	pause	pause to add RNase H
7.	37	00:20	
8.	37	pause	

The mixture with the RNA was placed into the heating block for 5 min. This allows the random hexamers to anneal to RNA. A volume of 10 µl of the master mix is added to each RNA sample and left for a total of 65 min at varying temperatures, optimal for SuperScript III. The enzyme reverse transcribes RNA to make copies of cDNA. A volume of 1 µl of RNase H is added to the mixture and left for a further 20 min at 37°C, the optimal working temperature for the enzyme. This step eliminates template RNA via degradation. The concentration of resulting cDNA samples is measured using the Nanodrop under Nucleic Acids ssDNA 30 setting.

## **2.8 Polymerase Chain Reaction (PCR)**

The aim of using PCR is to test whether designed primers work effectively and to acknowledge the presence of genes of interest in samples.

### **2.8.1 Primer Design**

The full genomic sequence the gene of interest was searched for in a genome informatics website (<http://genome.ucsc.edu/cgi-bin/hgGateway>). This sequence was transferred into a

primer design website (Primer 3, <http://frodo.wi.mit.edu/primer3/>) and the introns were manually removed, leaving behind coding DNA only.

For instance:

Genomic Sequence

TCTTGAGGAAGATCCATGAGGAGgtgaggccagggagggggagggaaggg  
 ccttacgagaaactgcaggtgatagacagagacgctcacagagggaaacggagaaaccaattca  
 ggaagaaaacaaaacgagagaaagagtgaagactttactttttgacaggatcactgtgtag  
 ccttggtggcctgtataaatggcagacagaggcgtgagctctgggagagtgcagcctaggccccc  
 AGTTCGAGAACTCCAGGAGCAGCTGGCCCAGCAGCAGGTCCA  
 GTGGAGATGGATGTGGCCAAGCCAGACCTCACAGCGGCTCTG  
 AGAGAGAT

Coding DNA (exons)  
 Non Coding DNA  
 (introns)

Genomic Sequence after intron removal

TCTTGAGGAAGATCCATGAGGAG  
 AGTTCGAGAACTCCAGGAGCAGCTGGCCCAGCAGCAGGTCCA  
 GTGGAGATGGATGTGGCCAAGCCAGACCTCACAGCGGCTCTG  
 AGAGAGAT

Coding DNA (exons)  
 Non Coding DNA  
 (introns)

Between the last two nucleotides of the first coding region, a left square bracket is added. And between the first two nucleotides of the second coding region, a right square bracket is added. This aids the program to identify the beginning and ends of region. This is shown below:

↓

TCTTGAGGAAGATCCATGAGGA|G

↓

A|GTTTCGAGAACTCCAGGAGCAGCTGGCCCAGCAGCAGGTCCA  
 GTGGAGATGGATGTGGCCAAGCCAGACCTCACAGCGGCTCTG  
 AGAGAGAT

Coding DNA (exons)  
 None Coding DNA  
 (introns)

The above sequences go from 5' to 3'. The product size is selected to be between 100 and 150 bases long. Primer melting temperatures were set to an optimum of 60°C (min 57°C, max 63°C). Primer 3 designs 5 primer pairs per gene.

Primer 3 selects primers for the gene of interest which fit the criteria above. These primers were then entered into the Sigma Specialty Primers E@sy Oligo® website ([http://www.sigmaaldrich.com/configurator/servlet/DesignTool?prod\\_type=E@SYOLIGO](http://www.sigmaaldrich.com/configurator/servlet/DesignTool?prod_type=E@SYOLIGO)). This service will construct the primers to a concentration of 100 µM. It also predicts the likelihood of a secondary structure, i.e. the possibility of the primer folding over itself rendering it inactive. If the likelihood is high, another primer pair was selected. Upon arrival, a working concentration of 10 µM was made up with RNA-free water.

## 2.8.2 PCR Reaction

Deoxiribonucleotides (dATP, dCTP, dGTP and dTTP) were used at a working concentration of 10 µM. The reactions were made up in snap-cap PCR tubes in 25 µl volume for 1x reaction. The amount required was calculated depending on sample number and took into account pipetting error.

Reaction (25 µl reaction)

	1x (µl)
Taq Buffer Green	5
Forward Primer	2.5
Reverse Primer	2.5
dNTPs	0.5
Taq (DNA Polymerase)	0.25
ddH <sub>2</sub> O	13.25
cDNA template	1

The cDNA template and enzyme (DNA Polymerase) were added last. Reaction tubes were then placed in a thermocycler (echne Touchgene Gradients) set to the conditions below:

Program:

	Time	Temp (°C)
Initial denaturation	00:02:00	95
Number of Cycles: 35		
Seg Max	00:00:30	95
Seg Max	00:00:30	55
Seg Max	00:00:30	72
Final extension	00:05:00	72
Final hold		4

### **2.8.3 Agarose Gel Preparation**

Agarose was made up in TAE buffer which is comprised of Tris(hydroxymethyl)aminomethane (Tris), acetate and ethylenediaminetetraacetic acid (EDTA). The combination provides optimum pH required for DNA migration down the gel. EDTA is used due to its scavenging metal ions property therefore suppressing damage to DNA. A 2% agarose gel was made up and heated in a microwave for 1 min. It was then taken out and swirled. If the powder was not dissolved completely, it was returned to the microwave for a further 10 sec. This step was repeated until powder has completely dissolved. It was then left to cool, but not solidify. Ethidium bromide, a fluorescent dye used to visualise DNA in Ultra Violet light, was added (final concentration 0.5 µg/ml) and the bottle given a gentle swirl. The gel is then poured into a casting tray with a comb, for the desired number of wells. The gel is set when it turns into an opaque colour.

### **2.8.4 Running and Visualising the Gel**

When the gel set, the comb was carefully removed and along with the plastic tray underneath, the gel was fully submerged into EDTA in the electrophoresis chamber. DNA samples were loaded into the wells, alongside a 1kb DNA ladder. The power leads were connected and the voltage applied 80 V and current variable for 1 hour. This procedure separates molecules on the basis on their rate of movement through a gel under the influence of an electrical field. As DNA is negatively charged, when placed electrical field, it will migrate towards the positive pole. Thus, the gel is used to control the movement of these molecules depending on their size. The gel is then visualised under a gel documentation system (Alpha Innotech). An image of the gel is then acquired and printed. Based on the DNA ladder and migration of the DNA, the presence of genes in sample was checked for the tested primers. This procedure is done as it is inexpensive to ensure working order of primers before embarking on Real-Time PCR (Section 2.9).

## **2.9 Quantitative Real-Time PCR (qRT-PCR)**

Real-time PCR offers a method of measuring the extent of gene expression compared to a sample group, using the delta delta Threshold Cycle (CT, Section 2.9.3) as an end-point measurement.

The RNA of TnC-astrocytes and PLL-astrocytes with or without treatment with CNTF (2 ng/ml) was extracted at 4 hours and 24 hours, post-treatment as described in Section 2.6 and the cDNA synthesised as described in Section 2.7.

### 2.9.1 Plate Preparation

A semi-skirted 96-well plate was used for the reaction. Triplicates of each sample were used. SYBR Green® contains a synthetic fluorescent dye which binds non-covalently to DNA. As it binds to DNA, it emits light (522 nm), which can be measured. By comparing the fluorescence emission between sample groups, the relative amount of DNA can be quantified. SYBR Green® also contains AmpliTaq Gold® DNA polymerase, the enzyme catalyzing the polymerisation of deoxyribonucleotides into a DNA strand. The mixture also contains all dNTPs (dATP, dCTP, dGTP and dTTP) with dUTP, the enzyme which removes dUTP from the enzyme pool reducing the probably of dUTP being incorporated into the DNA. The master mix was calculated for each gene (number of samples x number of wells per sample). The master mix for a 1x reaction is as follows:

Reaction (20 µl)	1x (µl)
SYBR Green®	10
Forward Primer	2
Reverse Primer	2
ddH <sub>2</sub> O	4
cDNA template	2

The cDNA template was added directly into the well and not incorporated into the master mix. This was to avoid making a master mix for each gene for each condition and also to prevent reaction taking place whilst other master mixes were being made up.

### 2.9.2 Reaction Conditions

A 7900HT Fast Real-Time PCR System with SDS 2.3 software was used for the reaction. The software was set up to the conditions of the plate, setting GAPDH as an endogenous control gene.

The plate was inserted into the machine and the following program was performed:

	Temperature (°C)	Time (mm:ss)
Stage 1	95	10:00
Stage 2 (x40 cycles)	95	00:15
	60	01:00
Stage 3	95	00:15
	60	00:15
Stage 4 (dissociation)	95	00:15

In stage 1, the temperature is raised so that dissociation of the double-stranded DNA occurs. In stage 2, the temperature is lowered to allow primers to anneal. Stage 3 follows with a raise in temperature, which is optimal of the DNA polymerase to synthesise new DNA. As noted above, stage 2 also consists of a raised temperature phase and is repeated 40 times. This is to denature double-stranded DNA and allow the exponential growth of DNA product. The dissociation step is to confirm the presence of one gene in the sample tested (i.e. one peak equals one gene).

### 2.9.3 Data Quantification

The data output is in cycle threshold (CT) in triplicate values for each condition and each gene. The CT value is the number of cycles required for the fluorescence to cross the threshold level (background level). These values are inversely proportional to the amount of target nucleic acid in the sample. Thus, the higher the CT value, the more cycles were required to cross this threshold and the fewer amount product initially there.

The values are assessed and any outliers removed. The mean of each CT for each gene and each condition is calculated. Relative gene expression is the chosen quantification method, as opposed to absolute quantification. When using the relative quantification method data is represented relative to a housekeeping gene, such as GAPDH. The comparative CT method, known as the  $2^{-\Delta\Delta CT}$  (Livak and Schmittgen, 2001), was used as it describes data in terms of fold change. This method was used to analyse the data output and is described below:

$$2^{-\Delta\Delta CT} = \frac{(\text{CT gene of interest} - \text{CT internal control}) \text{ Treatment Sample}}{(\text{CT gene of interest} - \text{CT internal control}) \text{ Control Sample}}$$

By performing this calculation, the expression of the Treatment Sample is expressed in relative terms to the Control sample. The  $2^{-\Delta\Delta CT}$  of treatment condition is normalised to that of the control, presenting data as relative quantification (RQ) for straightforwardness.

## **2.10 Microarray**

A microarray is a method of measuring the expression value of thousands of known genes in samples.

The RNA of astrocytes plated on PLL or TnC, some PLL-astrocytes treated with CNTF (2 ng/ml) was extracted at 4 hours and 24 hours post-treatment as described in Section 2.6.

### **2.10.1 RNA Integrity**

In order for successful hybridisation to take place, excellent RNA integrity is crucial. To assess this, each sample was assessed using 2100 bioanalyzer. A volume of 2  $\mu$ l of each sample was placed on an RNA 6000 Nano LabChip platform, a platform to measure RNA concentration and quality.

RNA integrity is a measure of the proportion of RNA that is full-length and thus exhibits a ratio of 2:1 of the 28S and 18S rRNA bands. Partial degradation of RNA may translate to incomplete cDNA which lacks the coding region required. The software takes into account the entire electrophoretic trace of the sample, which includes degradation products, and gives an RNA Integrity Number (RIN). A sample read out is presented in Figure 2.1.

### **2.10.2 RNA Amplification and Biotinylation**

The amplification and biotinylation of RNA is a required step for DNA hybridization. An Illumina® TotalPrep RNA Amplification kit was used for this procedure and manufacturer's guidelines were followed.

Reverse transcription to synthesize first-strand cDNA was performed using a thermal cycler with a heat-adjustable lid.

RNA (250 ng) was placed in a 0.5 ml RNA-free tube and made up with Nuclease-free water if required, to make up a total volume of 11  $\mu$ l.

Reverse-transcriptase master mix was prepared as follows:

1x Reaction (20 $\mu$ l)	( $\mu$ l)
T7 Oligo(dT) Primer	1
10X First Strand Buffer	2
dNTP Mix	4
RNase Inhibitor	1
Array Script	1

A volume of 9 $\mu$ l of the master mix was added to each RNA sample (11  $\mu$ l). The samples were then placed in a thermal cycler and set to the following program:

Temperature ( $^{\circ}$ C)	Time (hh:mm)	Cycles
42 (50 lid)	02:00	1
4	hold	

The temperature and reagents are optimal for the Oligo Primers to anneal. Second strand cDNA master mix was prepared.

1x Reaction (100 $\mu$ l)	( $\mu$ l)
Nuclease-free Water	63
10X Second Strand Buffer	10
dNTP Mix	4
DNA Polymerase	2
RNase H	1

Second Strand master mix (80  $\mu$ l) was added to each sample (total 100 $\mu$ l) and placed back into a thermal cycler at the following settings:

Temperature ( $^{\circ}$ C)	Time (hh:mm)	Cycles
16 (disabled lid)	02:00	1
4	hold	

The temperature and reagents are optimal for DNA polymerase to bind and reverse transcribes the first-strand whilst RNase H removes any template RNA.

cDNA binding buffer was then added and mixed by gently pipetting. The whole mixture is then placed in cDNA Filter cartridge and spun for 1 min at 10,000 rpm. This step ‘cleans’ the amplified cDNA and traps it in the membrane. The flow-through is discarded. Wash buffer is added to the filter cartridge and spun for another 1 min at 10,000 rpm. The flow-through was discarded and the filter cartridge transferred to a cDNA elution tube. Pre-heated (50°C) Nuclease-free water (20 µl) was added to filter cartridge, left at room temperature of 2 min then spun for 1 min at 10,000 rpm. The elute contained the double-stranded cDNA samples were then transferred to PCR-tubes.

In vitro transcription (IVT) is a method of producing cRNA from cDNA. The reaction takes place in the presence of biotinylated NTPs. The master mix also contains buffers and enzymes to create biotinylated-single stranded cRNA.

1x Master mix for IVT (25 µl)

	(µl)
T7 10X Reaction Buffer	2.5
T7 Enzyme Mix	2.5
Biotin-NTP Mix	2.5

A volume of 7.5 µl of the above master mix was added to each cDNA sample and mixed thoroughly by pipetting. The mix was then placed in a thermal cycler under the following settings:

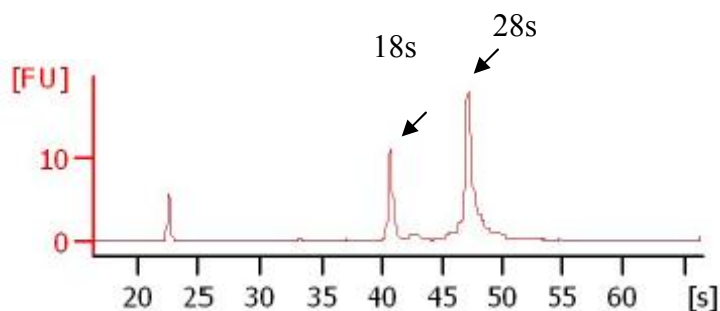
Temperature (°C)	Time (hh:mm)	Cycles
37 (lid 100-105)	04:00 – 14:00	1
4	hold	

To stop the reaction, 75 µl was added to each sample. The end product is cRNA – complementary RNA from cDNA.

The cRNA purification step removes any enzymes, salts and unincorporated nucleotides. To each sample, 350 µl of Binding Buffer was added followed by 250 µl of 100% ethanol and mixed by pipetting up and down. Each sample was placed in cRNA Filter cartridge

and centrifuged for 1 min at 10,000 rpm and the flow-through discarded. cRNA filter cartridge was then placed in a collection tube and 650  $\mu$ l of wash buffer added to each sample and spun for 1 min and flow-through discarded. The filter cartridge was then moved into a new collection tube and 200  $\mu$ l of pre-warmed (50°C) directly onto the filter and placed in heat block for 10 min at 55°C. The samples were spun for 2 min. The purified cRNA is collected in the elute of about 200  $\mu$ l.

Sample A



Sample B

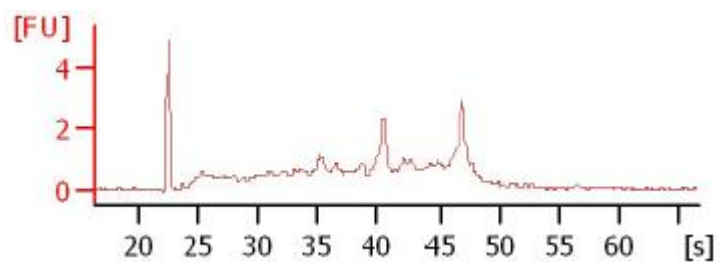


**Figure 2.1 RNA Integrity.** Sample A shows intact rRNA, with the two ribosomal peaks clearly observed at a 2:1 ratio. Sample B has degradation of rRNA and shows a shift towards shorter fragment sizes.

### 2.10.3 Direct Hybridisation Assay

Two Illumina RatRef-12 Expression BeadChip microarrays were used to assess the gene expression of the 15 samples. These samples came from RNA generated from astrocytes plated in 5 different conditions: PLL-astrocytes for 4 hr and 24 hr, PLL-astrocytes with CNTF for 4 and 24 hours and TnC-astrocytes for 4 hr (n=3 / group; astrocytes were derived from different groups of pups, each from a different outbred female). The Beadchip was hybridized at 58°C overnight.

cRNA was made up to 750 ng and 5 µl of RNase-free water was added into each sample.

*Setting Up the BeadChip Hybridization Chamber* - Humidity Control Buffer (HCB) and Hybridization Buffer (HYB) are buffers used for the reaction and were pre-heated in a 58°C oven for 10 min to dissolve any precipitated salts. BeadChip Chamber, gasket, and inserts were assembled as directed by manufacturer's instructions. A volume of 200 µl of HCB was loaded into each reservoir (Fig 2.2) of the chambers to be used.

*Preparation of Beadchip for Hybridization* - All samples were preheated to 65°C for 10 min and allowed to cool at room temperature. Samples (15 µl of each) were loaded into the loading points (Fig 2.3). Wells without samples had HYB. The BeadChip was then placed into the chamber. The chamber was securely fastened and placed into 58°C oven for 16 hours.

*Washing Steps* - The chamber was removed from the oven and disassembled. The BeadChip was removed and submerged into a beaker containing 1 L of diluted Wash E1BC buffer (provided with the kit). Whilst still submerged, the cover-seal of the BeadChip was removed. The BeadChip was transferred into a slide rack and staining dish also containing wash buffer and then placed into a Hybex Waterbath containing High-Temp Wash Buffer for 10 min.

*Washing Steps* - After the 10 min incubation, the BeadChip was returned to the staining dish with wash buffer and plunged in and out for several times and then shook on an orbital shaker for 10 min. This step was followed by a 100% ethanol wash for 10 min. BeadChip was again submerged in fresh wash buffer and washed for 2 min.

*Block* - BeadChip was then placed in a wash tray with 4 ml of blocking buffer and it was shook for 10 min at room temperature.

*Signal Detection* - BeadChip was placed in a new wash tray containing Streptavidin-Cy3 in block buffer and left on a shaker for 10 min. This step was followed with another wash step in wash buffer on the shaker for 5 min.

*Drying the BeadChip*- BeadChip was centrifuged for 4 min at 275 rcf at 25°C.

*Reading the BeadChip*- The Illumina BeadArray Reader (Illumina, San Diego, CA) was used to measure bead fluorescence using a 2-channel 0.8 µm resolution confocal laser scanner.

#### **2.10.4 Analysis of BeadChip Data**

Data was quantile normalised in BeadStudio (Illumina, San Diego, CA) and Rank Products (RP) (Breitling et al., 2005) was used to assess the statistical significance of pairwise intergroup differences. Significance was determined using the False Discovery Rates (FDR) multiple testing correction method (Benjamini and Hochberg, 1995), with a FDR cut-off of 5%. Venn diagrams were used to look for consistent differences between TnC-astrocytes and PLL-astrocytes, with and without CNTF. Differences between PLL-astrocytes with or without CNTF treatment at 4 and 24 hrs were also investigated.

#### **2.11 Microscopy and Image Analysis**

Cells were imaged using Olympus BX51 fluorescent microscope and Image-Pro software. For myelinating cultures, the SMI31-positive axons are usually immunostained with TRITC-red whilst the PLP-positive myelin sheaths with FITC-green. Images were taken according to these colours by taking an image of each channel individually and then merging them to create a composite image and saved as a TIFF file.



**Figure 2.2 BeadChip Hybridization Chamber.** The image shows the hybridization chamber, its lid, the gasket and the reservoirs were buffers are added. Image taken from Illumina Whole Genome Gene Expression Direct Hybridization Assay Guide (page 20) and slightly modified.

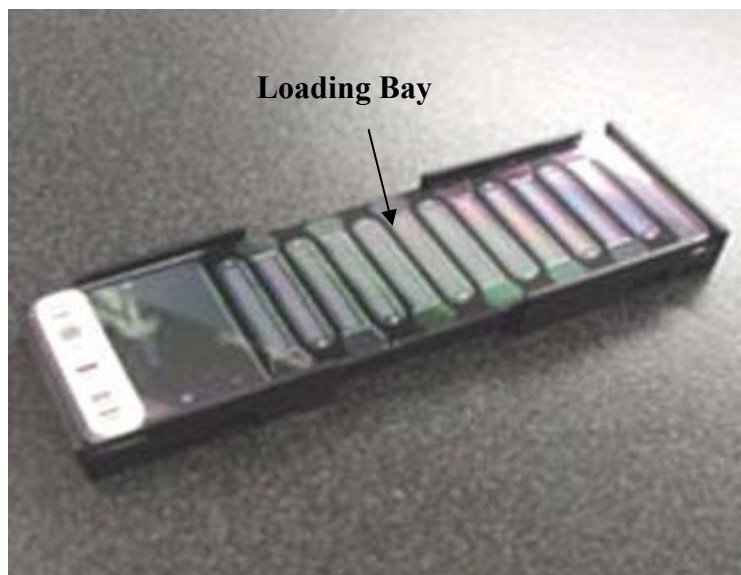


**Figure 2.3 Loading Bay of the BeadChip.** The images represents a BeadChip and the arrow indicates where loading bays are. Image from Illumina Whole Genome Gene Expression Direct Hybridization Assay Guide (page 22).

### 2.11.1 Neurite Density

For quantitative analysis of neurite density and myelination, 10 images from each coverslip were taken at random at 10x magnification. Images were taken randomly to avoid experimental bias. Each condition for each experiment was performed in duplicate, therefore, 20 images were taken per condition per experiments, and experiments were performed in triplicates. Thus, a total of 60 images for each condition were used for quantification and analysis.

Axonal density was measured using Image J software (NIH systems, version 1.45). The pixel value of the SMI31 reactivity (neurites) was measured as a percentage of the total pixel value in one image (total area) and therefore the 'neurite density'. The image was opened in Image J and split into the 3 colour channels (red, green and blue). The empty blue window and the green myelin sheaths window were both closed down, leaving the red channel showing the neurites open (Fig 2.4). The number of black and white pixels was obtained from the histogram selection and the percentage of black pixels was calculated ( $\text{black pixels} \div \text{total pixels [black and white pixels]} \times 100 = \% \text{ black pixels}$ ) for each image in Microsoft Excel.

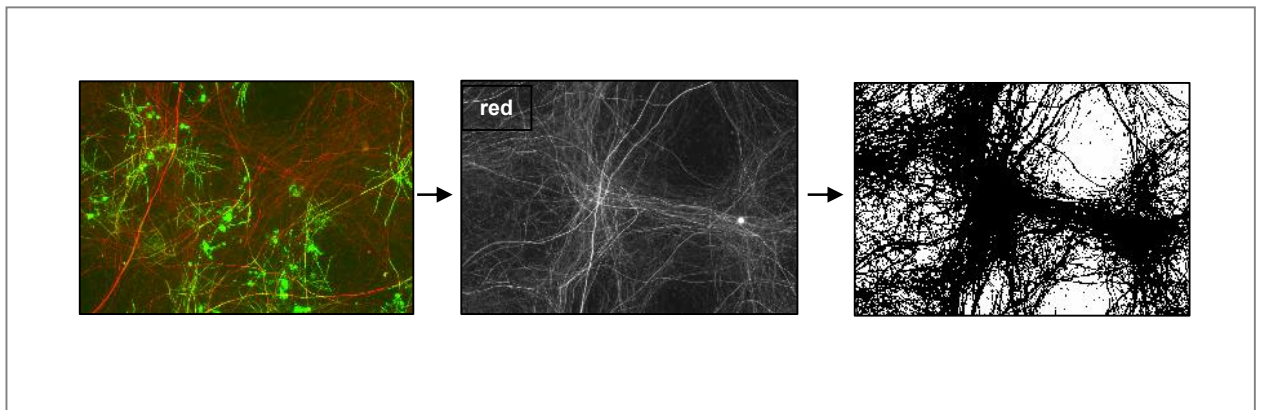


**Figure 2.4 Measurement of Neurite Density.** Composite image consisting of both SMI31 (red) neurites and PLP (green) myelin sheaths and oligodendrocytes was split into the 3 colour channels (red, green and blue) in Image J. The red channel was converted into black and white pixels and black pixels were measured as percentage of total.

### 2.11.2 Myelin Quantification

The AA3 antibody recognises both myelin sheaths and oligodendrocyte cell bodies therefore making it difficult to look at PLP immunoreactivity alone for the calculation of myelinated axons. It was therefore essential to manually identify and draw along the

myelinated sheaths using Adobe Photoshop (Elements 7.0) and brush shape size 9 using a pure blue colour (Blue:255, Red:0, Green:0). Whilst manually drawing on the myelin sheaths, the PLP-positive oligodendrocyte cell bodies were avoided (Figure 2.5, white arrows). The myelin is drawn on 20 images for one condition in one experiment and 3-4 representative images are opened in Image J. The colour channels are split, this time keeping the green channel open. The threshold of the average of the green channel is noted for each condition. A micro was programmed (Myelin Micro, see appendix) to calculate the amount of green and blue overlap, the pixel number representing the amount of myelinated axons. The micro calculated the value for all images within that condition. These values are then exported into Microsoft Excel, where they are expressed as a percentage of the total red pixel value (SMI31 reactivity, see Section 2.11.1) and therefore representation of the percentage of myelinated axons. Each green/blue image pixel value will correspond to its own red axonal density value.

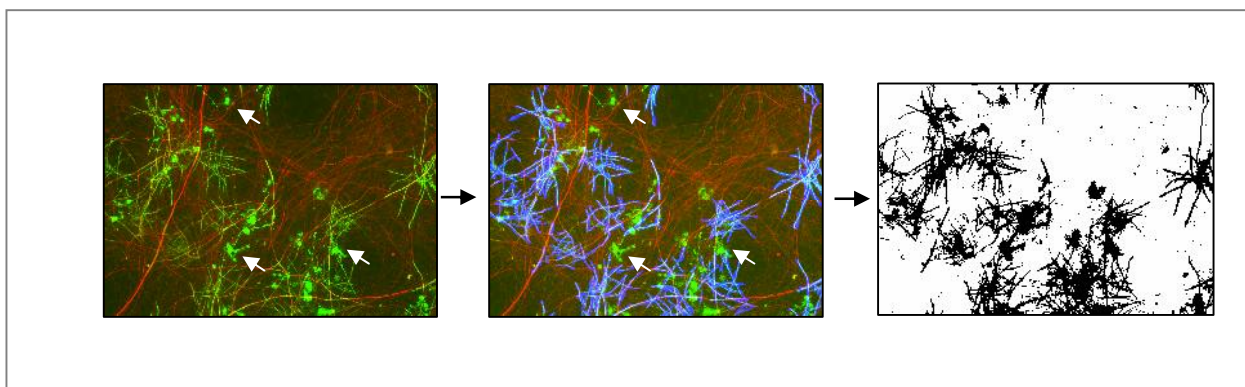


**Figure 2.4 Myelin Quantification.** Composite image consisting of both SMI31 (red) neurites and PLP (green) myelin sheaths and oligodendrocytes was opened in Adobe Photoshop and myelin sheaths were marked manually using a blue colour. Using a micro in Image J, the blue and green overlap in pixel was measured and expressed as percentage of total SMI31 reactivity for the particular image.

### 2.11.3 Quantification of Cell Number

In order to assess the number and type of oligodendrocyte lineage cells present, ten images were taken per coverslip (i.e. condition) per experiment, totalling up to 30 images per condition for three experimental repeats. Myelinating cultures were cultured as described in Section 2.1.4 and fixed and stained at 24 hours, 6 days and 12 days post treatment (treatment begins on day 12). The images were taken at x40 magnification and opened in Image J. For any of the markers, all positive cells which contained a nucleus were

manually counted using the Image J Cell Counter function. Further, all the nuclei was counted. Positive-cells for a particular marker are then expressed as percentage of the total number of cells for that image or the mean number of positive cells per view.

#### **2.11.4 Cell Proliferation**

To assess whether there was an increase in oligodendrocyte differentiation following treatment, myelinating cultures were fixed and stained 24 hours post treatment (treatment begins on day 12). Markers used were O4 (pre-myelinating oligodendrocyte marker), BrdU (cells in S-phase) and DAPI (nuclei). Ten images were taken per time-point, per condition, totalling in 15 images for 3 experimental repeats. The images were opened in Image J and the Cell Counter feature was used to manually count marker-positive cells. The number of O4-positive cells, which were also BrdU-positive were presented as mean number of proliferating oligodendrocytes per view. The same calculation was used to compare proliferation rates between PLL-astrocytes and TnC-astrocytes using GFAP, BrdU and DAPI.

#### **2.11.5 Neurite Diameter**

In order to assess whether there was an increase neurite diameter with CNTF treatment, 10 images of each condition were taken at 10x magnification of myelinating cultures at day 26. Each image was opened in Image J and a representative area was zoomed into 6 times (6 clicks). Using the Straight Line selection, a line was drawn across the diameter of the SMI31 positive neurite and these measurements recorded. Within the area, the axons were chosen randomly. It was also noted whether the axon was myelinated or not. The arbitrary measurements were converted to  $\mu\text{m}$  using the scale bar in the image. A total of 50 images were taken for each condition in each experiment. Experiments were done in triplicate.

#### **2.11.6 GFAP and Nestin Immunoreactivity**

In order to calculate GFAP and nestin reactivity, images within one experiment were taken at the same threshold for all conditions. Ten images per condition for each experiment were taken. Using Image J software, the colour channels were split separating GFAP (red channel) and nestin (green channel). For each split channel, a freehand selection was made around each cell for and integrated density and size were measured. The integrated intensity was measured as ratio of the cell size.

## 2.12 Statistical Analysis

For comparison of values between groups of conditions, data was analysed using paired Student's T-test in Microsoft Excel. All values were expressed as means  $\pm$  the standard error of the mean (SEM). Significance was represented using p-values where values below 0.05 were considered significant and were indicated by the presence of an asterisk.

For myelinating cultures, the percentage of myelinated neurites was expressed as a ratio of the value in the untreated group. Data was analysed using one sample Student's T-test, using 1 as the null hypothesis mean. When different substrates were used, i.e. astrocytes and OECs, the data was not logged and 0 was used as the null hypothesis of the mean.

## **Chapter 3**

# **Characterisation of the Myelinating Culture System**

# Characterisation of the Myelinating Culture System

---

## 3.1 Introduction

### 3.1.1 Background

Myelination is the process by which an axon becomes insulated by a proteolipid membrane known as myelin. Oligodendrocytes, the myelin forming glial cells of the CNS extend their processes and wrap myelin in segments (known as internodes) around axons. This process is necessary for axons to propagate electrical signals via salutatory conduction. Although research has unveiled many aspects of this dynamic process, there is still more required to fully understand it. Furthermore, myelin-related acquired diseases, such as multiple sclerosis (MS), as well as hereditary metabolic diseases such as the leukodystrophies, are still not understood and are treated only on a symptomatic basis. This raises the demand for laboratory investigations to reveal the exact causes behind myelin-disorders and in turn expose ways which they can be treated. This demand has given rise to a number of *in vitro* models for myelination which will be discussed and evaluated here.

The main culture systems used to study myelination are categorised as either organotypic (slice cultures), dissociated or co-culture. Organotypic models require a tissue fragment from the host's CNS, usually a segment of the spinal cord. Dissociated cultures involve the enzymatic digestion of a CNS region to a single-cell suspension and maintaining it until it forms a CNS-like environment. Co-cultures involve culturing purified cells, such as neurons and oligodendrocyte precursor cells (OPCs), then culturing them together to generate a more defined system.

The organotypic model uses CNS tissue grown in defined conditions and it has been widely used to observe neurite outgrowth and myelination (Bunge and Wood, 1973; Gähwiler et al., 1997; Thomson et al., 2006). These cultures are usually generated from neonatal tissue and one advantage is that the cytoarchitecture, the cell composition and their arrangement in the tissue, is well established. A disadvantage is that myelination tends to take place in the main mass of the explant and makes visualisation at a single cell level difficult with conventional light microscopy (Thompson et al., 2006). Furthermore, the process is also time-consuming (period 2-4 weeks). Organotypic cultures which are

sliced into thin sections (300-400  $\mu\text{m}$ ) have also been developed as they allow the ease of biochemical manipulation, for example using antibodies (Seal, 1977; Notterpek et al., 1993).

Another myelinating culture system is the co-culture method, where the purified neuronal cells can first be established followed by the later addition of OPCs, which over time ensheath the axons. Chan et al. (2004) used a system where dorsal root ganglion (DRG) neurons are dissected and purified from the embryonic rat (E14). OPCs (from P7-8 pups) are also purified and added on top of already established DRG neurons. Myelination can be observed after 14-15 days; where OPCs have differentiated in mature oligodendrocytes and ensheathed axons. It must be noted, however, that DRG neurons are part of the peripheral nervous system (PNS) and that axonal signals that prompt ensheathment differ from the CNS (Michailov et al., 2004; Brinkmann et al., 2008). Watkins et al. (2008) used retinal ganglion cells as the neuronal source and OPCs from a cortical origin. They demonstrated that the co-culture of these leads to fully myelinated fibres after 3 days *in vitro*. The co-culture system provides a defined system where the addition of biochemical or other cell types, such as astrocytes, is feasible. This system allows the identification of the effect of particular biochemical agents to a particular cell type. However, whether it is a true representation of the CNS environment is questionable. Furthermore, another main drawback is the lack of other relevant cell types in the culture such as astrocytes and microglia, therefore reducing the validation of the system.

The dissociated spinal cord culture system has been previously described in rat (Sørensen et al., 2008) and mouse (Thomson et al., 2008). These cultures require the use of intact CNS tissue which is then enzymatically digested and plated on a coverslip, or in the case of rat cultures, on a monolayer of neurosphere-derived astrocytes. The cultures develop over a period of 4 weeks, where neuronal growth, OPC proliferation and differentiation take place and ensheathment of surrounding neuronal processes. Although the cultures are plated on coverslip, they grow dense enough to create a 3D environment. The cultures also allow for easy immunolabelling, visualisation as well as protein and RNA extraction. However, the culture's main drawback is the presence of so many cell types makes it difficult to pinpoint the exact cell type(s) affected by a particular treatment. However, this can be overcome with markers to identify particular cell types and/or receptors, to some extent. Ironically, this is also an advantage, as the heterogeneous cell population more closely resembles the intact CNS.

The spheroid model is another type of a dissociated culture system. It comprises of dissociated embryonic rodent CNS cells, and by constant rotation, sphere-like cultures form (Vereyken et al., 2009). The authors argue that this model creates a 3D environment, more closely resembling the CNS *in situ*. They were able to demonstrate that lysophosphatidyl choline (LPC) results in a loss of myelin basic protein (MBP) expression and thus mature myelinating oligodendrocytes, whilst neurons, astrocytes and microglia were unaffected. Furthermore, using this model, the authors were able to identify Vitamin E as an alleviator of LPC damage demonstrating that this model can be used for testing potential therapeutics. However, the cause of LPC damage is unknown and thus alleviating the damage it causes does not answer key questions about the process of demyelination. The main drawback of the system is the difficulty encountered when visualising individual cells. As this model has been shown to work in rat and mouse cells, the authors argue that in combination with transgenic animals, this model offers researchers the ability to test potential therapeutics on specific cells types and therefore answering key questions about drug mechanisms.

Science benefits from having a diverse range of models in which myelination can be closely investigated. Although the benefits of the models are often highlighted, the drawbacks are often overlooked.

### **3.1.2 Aims**

Although the myelinating culture system has previously been validated (Sørensen et al., 2008; Thomson et al., 2008), it has not been fully characterised and its potential has not been investigated. Therefore, the aim of this chapter is to further characterise the myelinating culture system used in our laboratory with a more detailed identification of other cell types within the culture. Neurite growth and oligodendrocyte differentiation over the time frame of the culture period will also be investigated. Furthermore, because it was shown previously that astrocytes secrete a factor that promotes myelination I aim to use a candidate growth factor approach as a first screen to identify the astrocyte-secreted factor.

## **3.2 Results**

### **3.2.1 Establishment of the Myelinating Culture System**

The myelinating cultures used throughout this thesis comprises of dissociated rat embryonic day 15.5 (E15.5) spinal cord cells which are plated on a confluent monolayer of neurosphere-derived astrocytes on PLL-coated coverslips (PLL-astrocytes). The cultures are grown for a period of 26-28 days which leads to a reasonable amount of myelination for assessment (Fig 3.1). Although the cultures can be kept longer (up to 50 days, data not shown) and reach higher levels of myelination, it was decided to stop the culture system at 26-28 days before reaching full saturation. Although myelination of all axons is not likely due to their size (Friede, 1972), the time point was chosen to all allow the system to respond to changes before axons which are likely to be myelinated become myelinated. In this system, a monolayer of astrocytes was used as Poly-L-Lysine (PLL) alone does not support the long term development of dissociated spinal cord cultures (Sørensen et al., 2008). Although this system is already established (Thomson et al., 2008; Sørensen et al., 2008), a closer look was taken for the purpose of this thesis. Figure 3.1 demonstrates the methods used to produce these myelinating cultures (also described in Methods section 2.1.3). Briefly, astrocytes derived from striatum-derived neurospheres were differentiated and grown to confluency in media containing serum (Fig 3.1 A). The spinal cord of E15.5 embryo is dissected (top 2-3 mm rostral to the cervical flexure, and approximately 8–10 mm of spinal cord) cleared of meninges, minced and enzymatically (Trypsin and collagenase) digested to form a single-cell suspension of mixed CNS cells which are then plated on a confluent monolayer of PLL-astrocytes (Fig 3.1 B). The culture is then maintained in defined media, allowing neuronal survival and neurite outgrowth followed by myelination by resident oligodendrocytes (Fig 3.1 C). Therefore, these myelinating cultures provide a simple and straightforward system to study all aspects of myelination. The main complexity of these cultures is preparing the variety of appropriate media (Section 2.1).

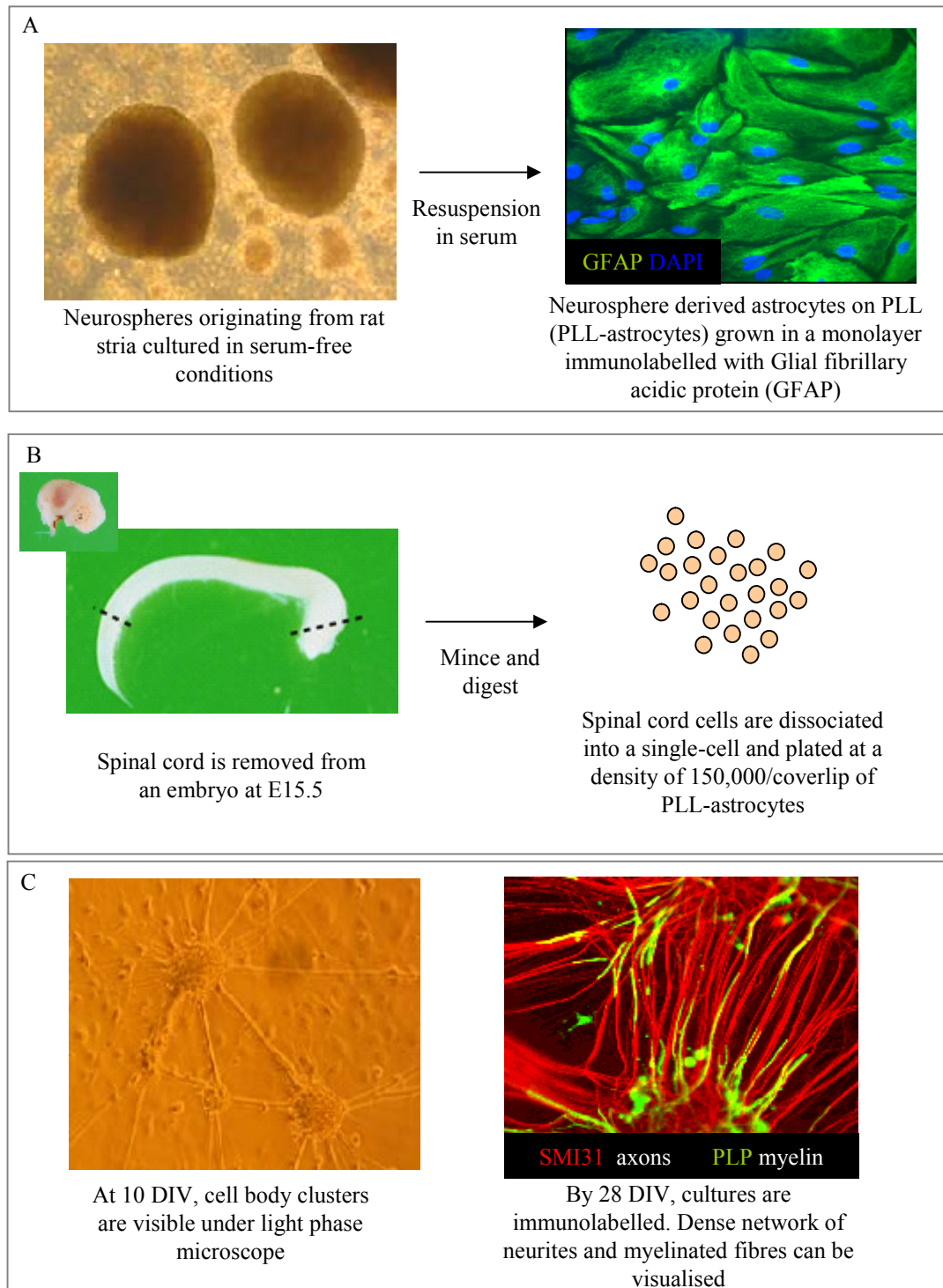


**Figure 3.1 Methodology of Generating a Myelinating Culture System.** A) Neurospheres originating from rat striata are cultured in serum-free media. The spheres are resuspended in media containing serum and plated on Poly-L-Lysine (PLL) coated coverslips. The spheres differentiate into a confluent layer of neurosphere-derived astrocytes plated on PLL (PLL-astrocytes), which can be labelled with the intermediate filament glial fibrillary acidic protein (GFAP). B) Spinal cords taken from embryos at E15.5 are removed, minced and enzymatically digested. The mixed spinal cord cells are dissociated into a single-cell population and plated at a density of 150,000 cells per confluent coverslip of PLL-astrocytes. C) At 10 days *in vitro* (DIV) cell body clusters with connecting neurites are visible under light phase microscope and by day 28 DIV cultures can be immunolabelled to show dense networks of neurites and myelinated axons.

### **3.2.2 Astrocytes, Microglia, and Oligodendrocytes at Different Maturation Stages**

The main cell types which reside in the CNS include neurons, oligodendrocytes, astrocytes and microglia. If the myelinating culture system is to resemble, as closely as possible, the intact CNS, then these main cell types must be present. Myelinating cultures were grown for 26-28 and immunolabelled with various cell type markers (Fig 3.2). Astrocytes were visualised using GFAP, and not only the cells as a monolayer but also other GFAP positive cells, were present in abundance throughout the culture, covering the entire expanse of the coverslip (Fig 3.2 A). Activated microglia, visualised using ED1, were also present throughout the culture (Fig 3.2 B), but at a much lower amount than astrocytes. Bipolar A2B5+ OPCs (Fig 3.2 C) were present suggesting that not all OPCs had differentiated into myelin-forming oligodendrocytes. O4+ pre-oligodendrocytes were visualised extending out processes (Fig 3.2 D), presumably to myelinate axons. Indeed, oligodendrocytes with numerous branches appearing to search for axons have been previously demonstrated by *in vitro* time-lapse in a co-culture system (Watkins et al., 2008). Mature oligodendrocytes were visualised using antibody to the mature myelin marker proteolipid protein (PLP). Oligodendrocytes can make many internodes of myelin from a single primary process (Fig 3.2 E, one asterisk) and sometimes from a secondary process (Fig 3.2 E, two asterisks). The culture system allows the visualisation of axo-glial interactions using antibodies to different cell types. Also, the process of myelination can be further dissected in terms of morphological changes of oligodendrocytes, time course of the process, axonal selection and initiation of myelination.

### **3.2.3 Neurite Density Increases and OPC Numbers Fall during the Culture Period**

For the purpose of characterising the cellular events taking place over time in culture, myelinating cultures were set up, fixed and immunolabelled on day 9, 18 and 27 with antibodies SMI31 for axons, NG2 for OPCs and O4 for pre-oligodendrocytes (Fig 3.3). Neurites become thicker and denser throughout the coverslip (Fig 3.3 A-C, J). NG2+ OPCs reduce in number throughout the culture period (Fig 3.3 D-F, K) suggesting either differentiation into myelin-forming oligodendrocytes or cell death due to competition for the enormous growth factor demand of mature oligodendrocytes in the culture (Barres et al., 1992). O4+ oligodendrocyte numbers remain relatively stable throughout the culture

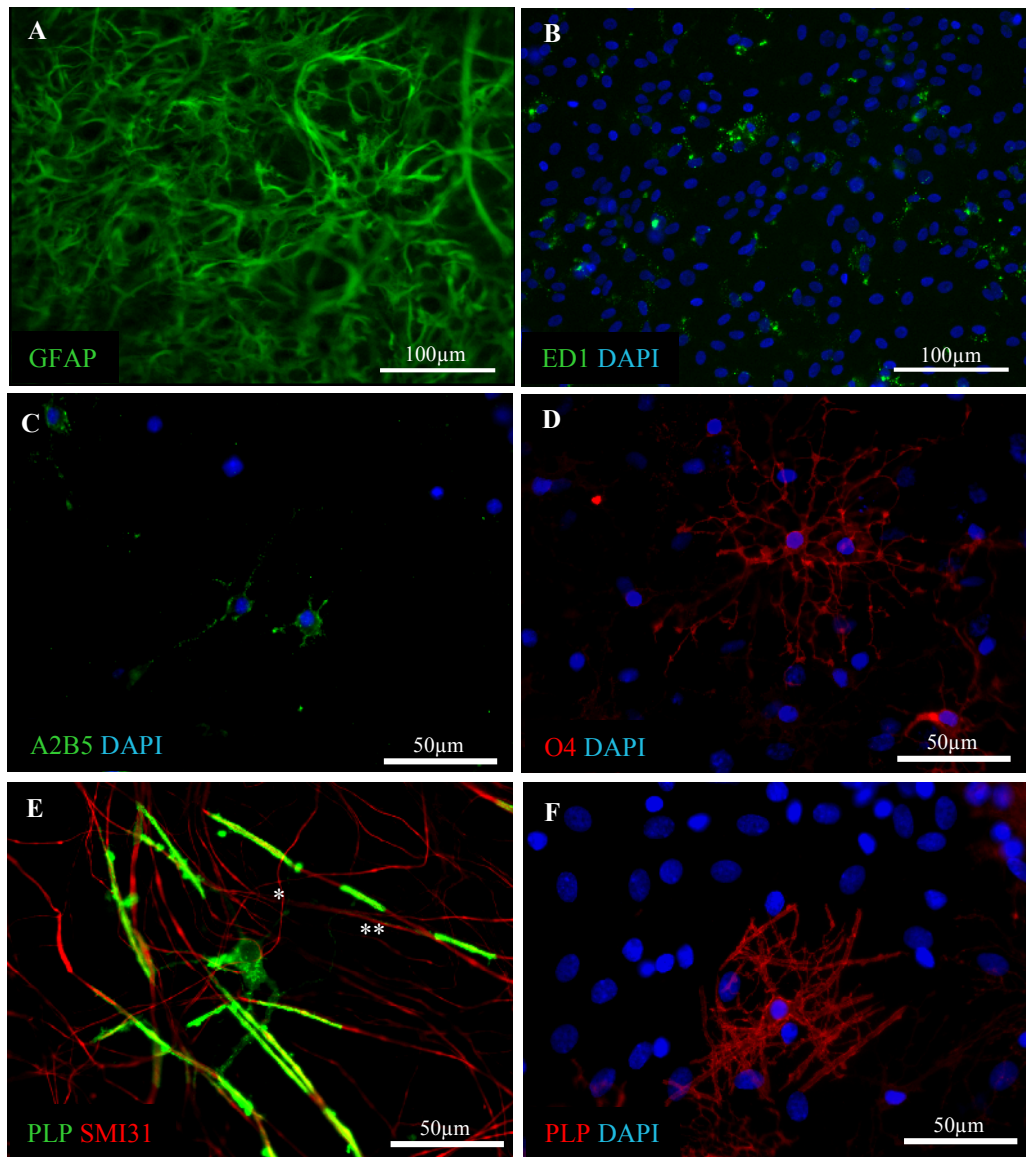


**Figure 3.2 Astrocytes, Microglia, and Oligodendrocytes at Different Maturation Stages.** E15.5 mixed spinal cord cultures were plated onto a confluent monolayer of astrocytes and cultured for 26-28 days. On Day 12, the insulin was removed to allow oligodendrocyte to differentiate. The cultures were immunolabelled with GFAP for astrocytes (A), ED1 for microglia (B), A2B5 for OPCs (C), O4 for immature oligodendrocytes (D) and PLP for mature myelin (E and F). Astrocytes in the culture covered the entire expanse of the coverslip (A) whilst there was a relatively small population of microglia (B). Oligodendrocytes were present at all different maturation stages, including bipolar OPCs (C) and branched O4+ pre-myelinating oligodendrocytes (D). Oligodendrocytes labeled with the mature myelin marker PLP can make many internodes of myelin from a single primary process (E, one asterisk) and sometimes from a secondary process (E, two asterisks). Scale bar 100  $\mu\text{m}$  for A and B, 50  $\mu\text{m}$  for C-F. GFAP, *glial fibrillary acidic protein*, PLP, *proteolipid protein*.

period, although at day 9, oligodendrocytes had simple processes and at day 18 they contained more membrane-like processes. By day 27, oligodendrocytes with myelin sheaths were visible (Fig 3.3 G-I, K). The myelinating culture system is a versatile and clear-cut system which allows the tracking of neurite outgrowth and oligodendrocyte differentiation.

### **3.2.4 Myelination Increases over Time in the Myelinating Culture System**

In order to assess the time frame suitable for the addition of pharmacological or biochemical agents, which can influence myelination, myelinating cultures were set up, fixed and immunolabelled with PLP and SMI31 at a range of time points (Fig 3.4). On day 13-15 thin myelin segment can be observed in close contact with neurites (Fig 3.4 A, B). From day 21 to 24, oligodendrocyte take on a more typical shape, where many processes are in contact with many neurites, and thicker myelin sheaths can be seen (Fig 3.4 C, D). By day 27, numerous oligodendrocytes can be seen myelinating surrounding axons with thick and relatively lengthier myelin sheaths (Fig 3.4 E). Myelination was measured (as described in Section 2.11.2) and an exponential increase in myelination was observed from day 15 to day 21 (Fig 3.4 F). Insulin was withdrawn at day 12 to allow oligodendrocyte differentiation as it has been reported that its presence promotes excessive OPC numbers (Thomson et al., 2008). It was concluded that the best time frame for the addition of biochemical agents that may influence myelination is when insulin is removed at day 12 which coincides with the start of oligodendrocyte precursor differentiation.

### **3.2.5 Underlying Monolayer of Astrocytes contains O4+ Oligodendrocytes**

As embryonic spinal cord cells are plated on top a monolayer of PLL-astrocytes to create the myelinating cultures, it was essential to identify the purity of these cells. PLL-astrocytes after differentiation were maintained in media containing serum until confluency (7-10 days, see Methods Section 2.1.1). The monolayers were fixed and immunolabelled with anti GFAP for astrocytes and the O4 antibody for oligodendrocytes (Fig 3.5). The O4 antibody was used as a marker as it typically allows the visualisation of simple early progenitors as well as more mature phenotypes (Fig 3.2). The number of GFAP+ astrocytes and O4+ oligodendrocytes were counted (Fig 3.5 C). Astrocytes made up the vast majority of cells present within the monolayer, with  $78.95 \pm 2.4\%$  of positive cells per

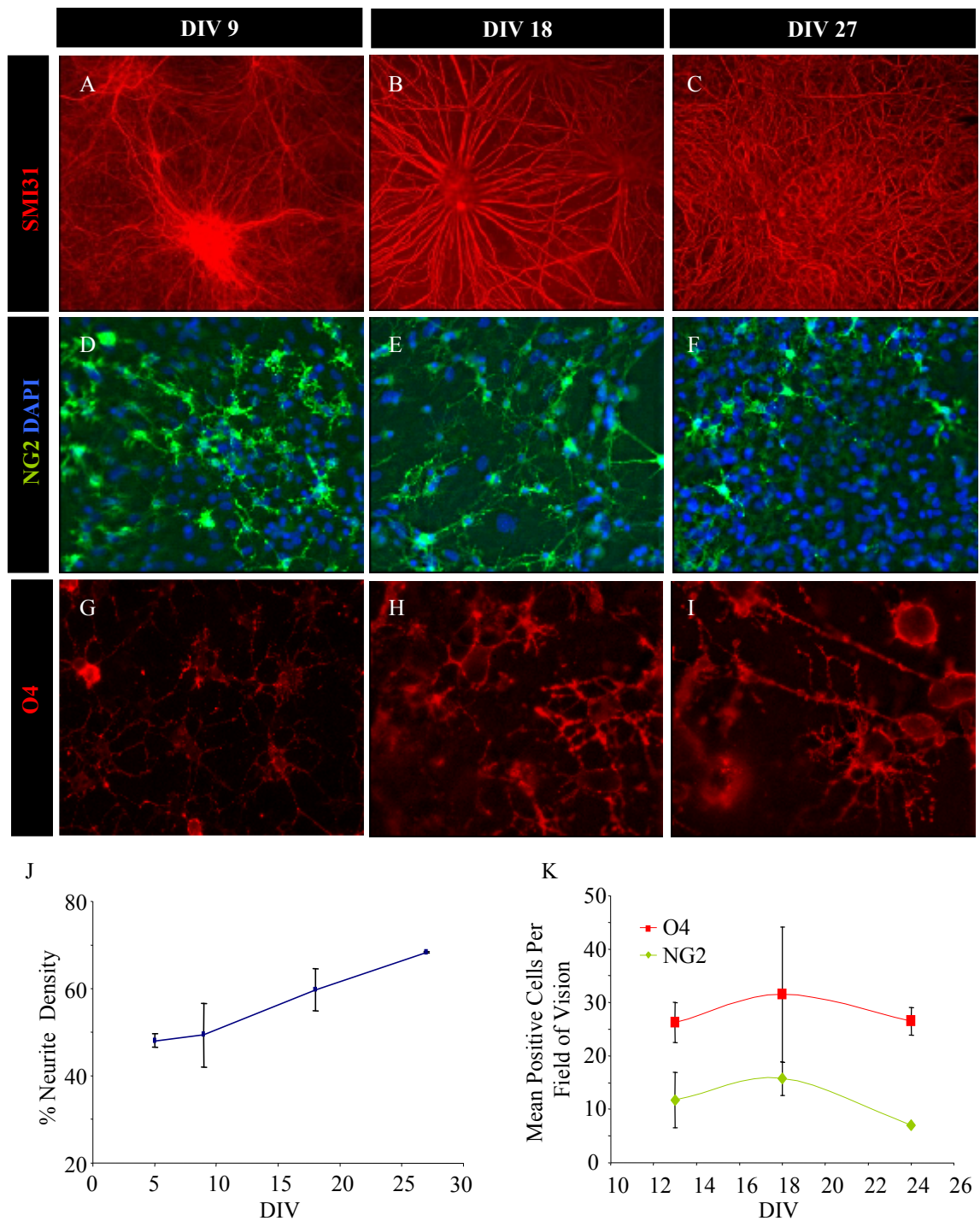


**Figure 3.3 Neurite density Increases and OPC Numbers Fall during the Culture Period.** E15.5 mixed spinal cord cultures were plated onto a confluent monolayer of astrocytes and cultured for 9 days (A,D,G) 18 days (B,E,H) or 27 days (C,E,I). The cultures were immunolabelled with SMI-31 for neurites (A-C), NG2 for OPCs (D-F) and O4 for pre-myelinating oligodendrocytes (G-I). There is a gradual increase in neurite density throughout the culture period (J). The number of NG2 cells decreases in the culture over time whilst O4 cell numbers remain relatively similar (K). Scale bar 100  $\mu$ m for A-F, 25  $\mu$ m for G-I. Errors bars indicate standard errors of the mean. Experiments were carried out in triplicate.

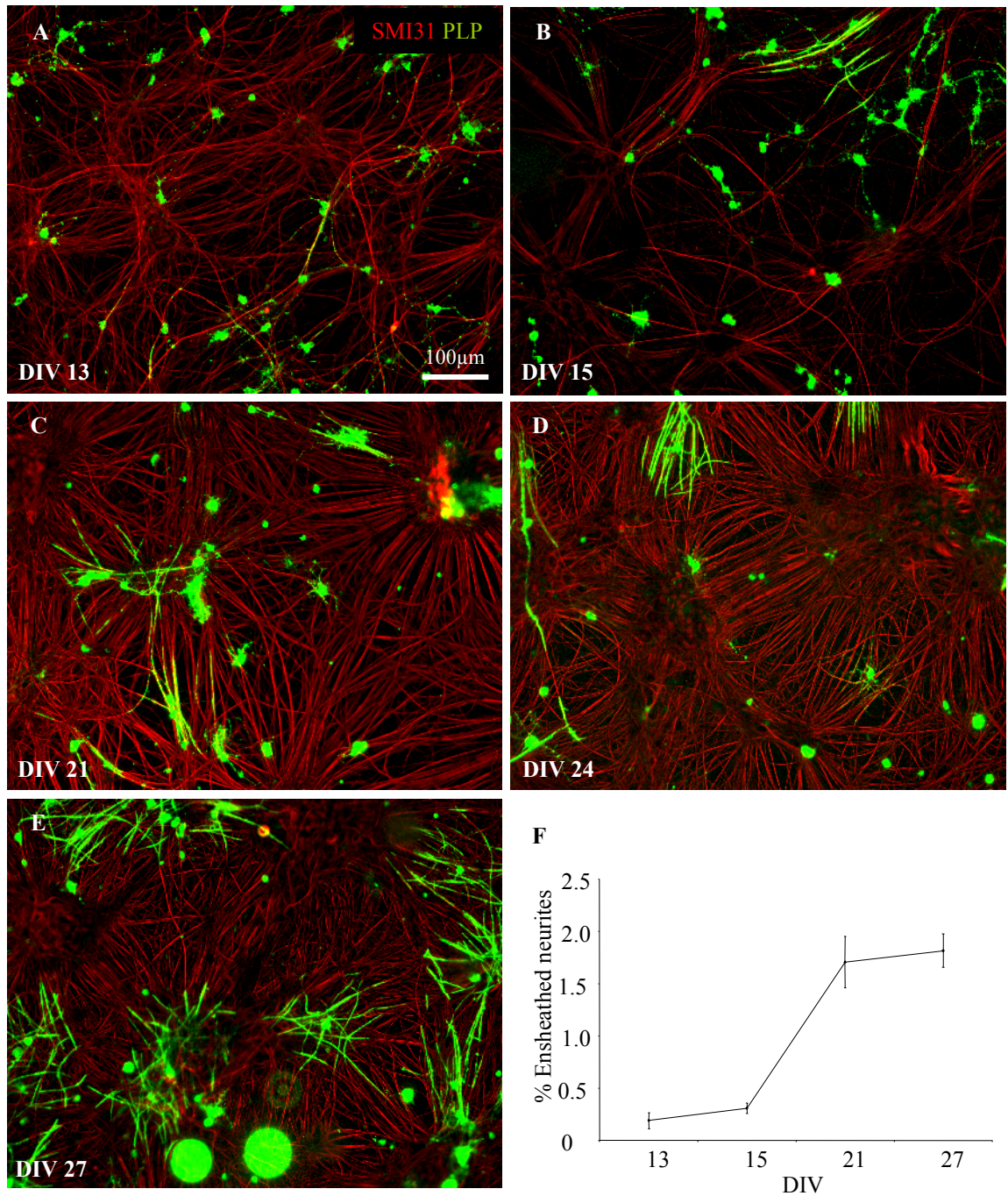


**Figure 3.4 Myelination Increases over Time in the Myelinating Culture System.** E15.5 mixed spinal cord cultures were plated onto a confluent monolayer of astrocytes and cultured for 13 (A), 15 (B), 21 (C), 24 (D) and 27 (E) days *in vitro* (DIV). At each time point, the cultures were fixed and immunolabelled with SMI31 for neurites and PLP for mature myelin. There is an increase in myelination over time, which gradually plateaus (F). Scale bar 100 μm. Errors bars indicate standard errors of the mean. Experiments were carried out in triplicate.

field of view. O4+ oligodendrocytes made up  $7.17 \pm 2.59\%$  of positive cells per field of view. DAPI+ nuclei with no marker made up the remaining  $13.88 \pm 2\%$  of cells. The cell bodies of these cells seem to cluster together and are likely to be neuronal in origin (further elucidated in Chapter 6, Fig 6.2). Although the purity of these astrocyte monolayers is lower than average, it must be noted that they are of neurosphere origin. Therefore, the likelihood of cells differentiating into other cell types is higher than astrocytes derived from a cortical origin, where the majority of cells have already differentiated into astrocytes. However, a direct comparison between PLL-astrocytes and astrocytes of cortical origin was not made. Nonetheless, the astrocyte monolayer provides a particularly exceptional substrate in which the myelinating culture can grow and myelination can be studied, possibly because in the intact CNS, astrocytes are in close contact with neurites and oligodendrocytes.

### **3.2.6 Growth Factors can Promote Myelination**

The intention of this thesis is to understand the role astrocytes play in the process of myelination. In order to assess whether the myelinating culture system can be influenced by exogenous factors known to be secreted by astrocytes, three candidates were chosen and added to the myelinating cultures. Brain derived neurotrophic factor (BDNF) was chosen as it is secreted by reactive astrocytes (Dougherty et al., 2000; Yoo et al., 2003). It is also able to induce neurogenesis and myelin formation in the injured adult spinal cord due to direct or indirect action on the proliferation of oligodendrocytes (McTigue et al., 1998). Ciliary neurotrophic factor (CNTF) is a cytokine of the interleukin-6 family and is known to be released by astrocytes (Rudge et al., 1994). It is also known to act on oligodendrocytes to induce their survival and proliferation (Albrecht et al., 2007). Neuregululin (Nrg) is a protein of the epidermal growth factor family, which are implicated in growth and developmental signalling and known to be secreted by astrocytes (Francis et al., 1999). Neuregulins have been reported to induce the proliferation and survival of oligodendrocytes precursor cells (Canoll et al., 1996). Myelinating cultures were set up and on day 12, treated with BDNF (1 ng/ml), CNTF (2 ng/ml) or Nrg (10 ng/ml) continuously until the end of the culture period. The concentrations chosen were based on a combination of information provided by suppliers as well as previously published articles (Rao et al., 1992; Stankoff et al., 2002; Ritch et al., 2005; Li et al., 2006). Cultures were fixed and immunolabelled and neurite density and myelination measured for all conditions (Fig 3.6). BDNF treatment resulted in a slight increase in myelination compared to untreated control (Fig 3.6 A, B, E). CNTF and Nrg promoted myelination, where more myelinated fibres

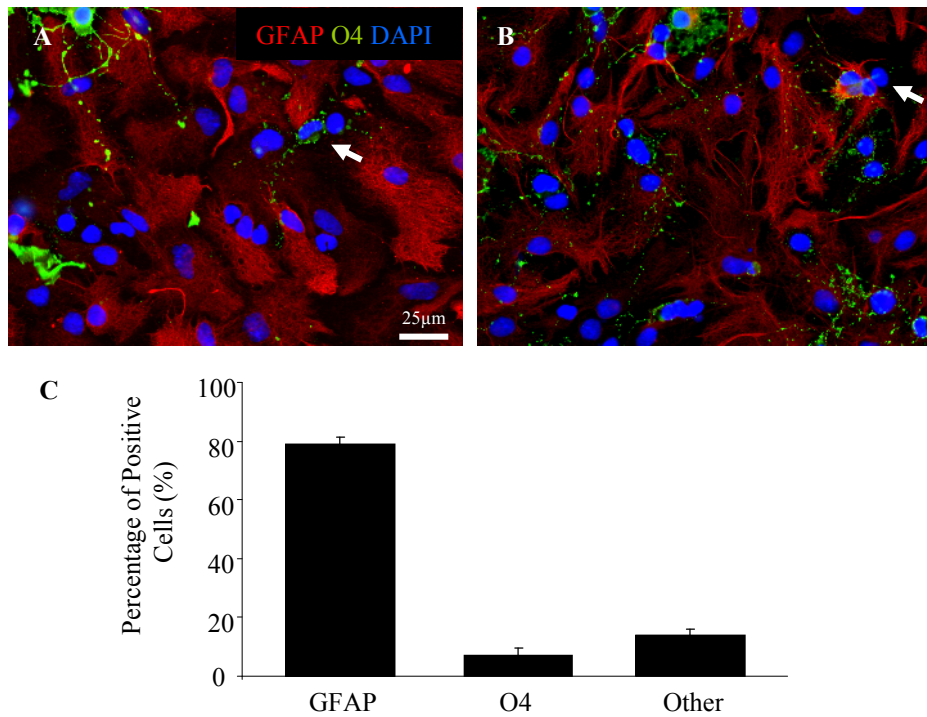


**Figure 3.5 Underlying Monolayer of Astrocytes contains O4+ Oligodendrocytes.** PLL-astrocytes were grown in media containing serum. On day 7, the cultures were fixed and immunolabelled with GFAP for astrocytes and O4 for immature oligodendrocytes (A, B). Both cells types were counted expressed as a percentage of the total using DAPI as a nuclear marker for cells (C). The majority of cells were GFAP-positive with a small population of O4-positive immature oligodendrocytes (A, arrow). GFAP and O4-negative cells (B, arrow) are counted as other in C. These cells are likely to be of a neuronal progenitor origin. Scale bar 25  $\mu$ m. Errors bars indicate standard error of the mean. Experiments were carried out in triplicate.

were observed compared to untreated controls (Fig 3.6 C-E,  $p < 0.05$ ). Neurite density was similar in all conditions (Fig 3.6 F) indicating that the treatments did not affect neuronal survival and allowed a sound comparison of each factor for myelination. Whether these growth factors act directly on the oligodendrocyte or indirectly via another cell type is not yet known and will be further investigated in this thesis.

### **3.3 Discussion**

These myelinating cultures provide a flexible and simple method for the visualisation and the quantification of different cell types over a time frame in which myelinated fibers form. These cultures were found to contain all four major cell types found in the CNS, show the correct assembly of nodal proteins in the nodes of Ranvier (Sørensen et al., 2008) and most importantly, the system is able to respond to the addition of growth factors, with a measurable increase the amount of fibres myelinated.

The myelinating cultures allow accurate measurement of myelinated fibres and distinguish them from differentiated oligodendrocytes that have not wrapped a myelin sheath. The type of myelin measurement described here is more advantageous than using other methods, such as Western blot, as measuring levels of myelin-related proteins may be misleading. For instance, PLP is expressed both in the cell bodies of oligodendrocytes and the myelin sheaths enwrapping an axon. Thus, an increase in oligodendrocyte differentiation could lead to an increase in PLP protein levels on a Western blot or even mRNA using qRT-PCR, and may therefore be misinterpreted as an increase in myelination. Therefore, an increase in myelin proteins and/or message does not necessary reflect as an increase in oligodendrocyte ensheathment of axons. This is usually offset with the use of another system for myelin measurement such as morphometric analysis or an enzymatic assay which measures the activation of myelination genes (Stankoff et al., 2002; Karim et al., 2007). In our myelinating cultures, manually drawing myelin around axons was necessary, as frequently, oligodendrocytes were present in the field of view but were not wrapping axons with a myelin sheath (Fig 3.7 A). When measuring myelination, the myelinating cultures therefore focus solely on myelinated fibres.

The myelinating culture system also has its flaws. Manual selection of myelinated neurites is a subjective process. However, as long as the assessment of myelination is consistent analysis is reproducible. Furthermore, there is no distinction between ensheathment, the

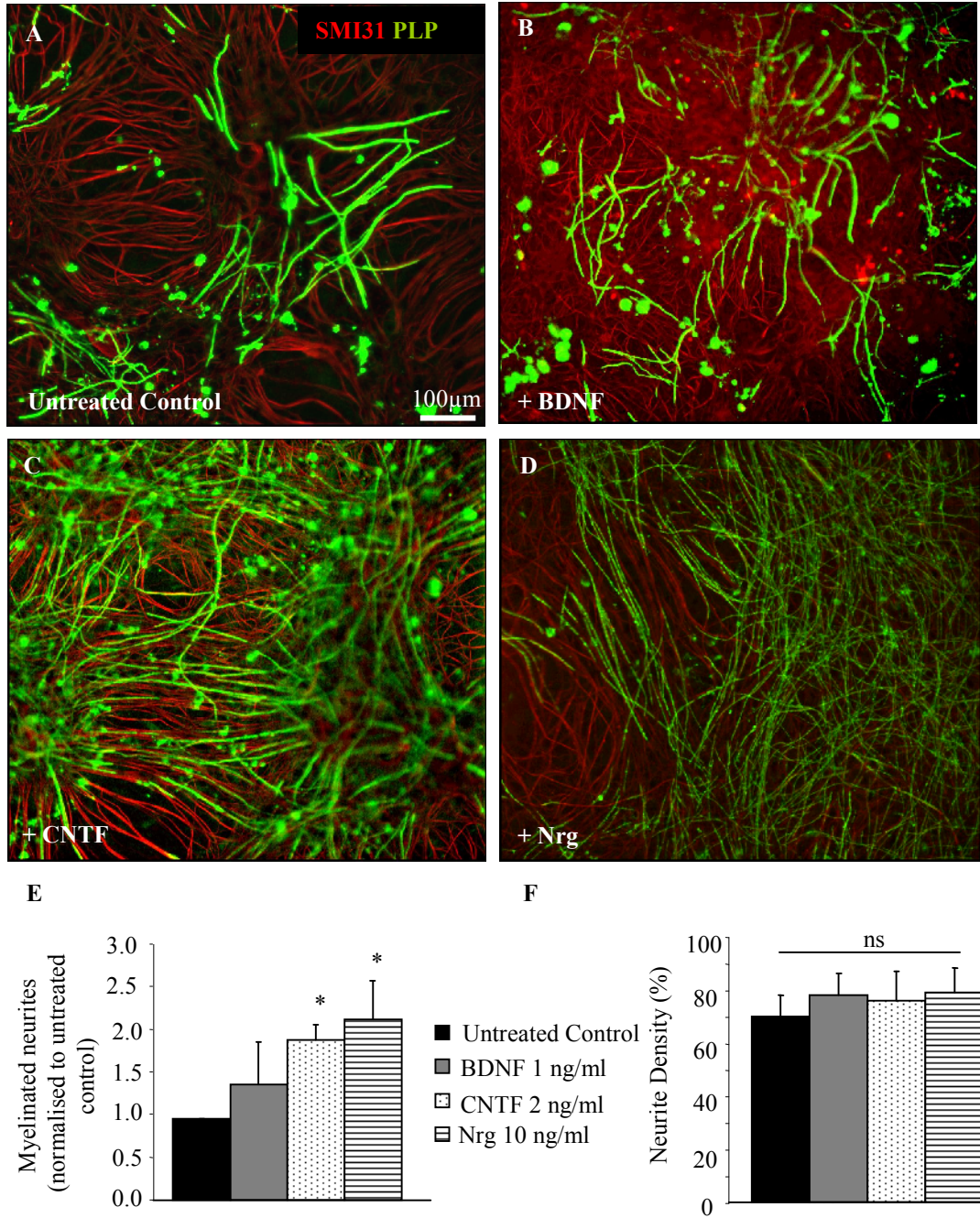


**Figure 3.6 Growth Factors can Promote Myelination.** E15.5 mixed spinal cord cultures were plated onto a confluent monolayer of astrocytes and cultured for 26-28 days. On day 12, some cultures left untreated (A), treated with brain-derived neurotrophic factor (BDNF, 1 ng/ml), ciliary neurotrophic factor (CNTF, 2 ng/ml) and neuregulin (Nrg, 10 ng/ml). The cultures were fixed and immunolabelled with SMI31 for axons and PLP for mature myelin. Myelination was increased significantly in all conditions, except BDNF (E,  $p < 0.05$ ). The neurite density was comparable across all treatments (F). Scale bar 100  $\mu\text{m}$ . Error bars indicate standard error of the mean. Experiments were carried out in triplicate.

initial contact and wrapping on an oligodendrocyte process around a neurite, and myelination, the formation of thick segments of myelin separated by Nodes of Ranvier. However, some images show what looks like ensheathment, but with the presence of the nodes (Figure 3.7 B). Therefore, this makes the myelinating culture system a relatively subjective method of myelin analysis. To improve this, a more specific marker for oligodendrocytic myelin sheath, such as MOG, should have been used.

For the purpose of studying diseases such as multiple sclerosis (MS), a reliable model of myelination with axonal wrapping is required. It can be argued that *in vivo* models of demyelination are a more accurate representation of the CNS as well as producing possible therapeutic approaches to demyelinating diseases. Models of demyelination *in vivo* can be mediated by an immune reaction, the exposure of the animal to auto-antibodies, or via cytokine/viral-induction (Bradl and Linington, 1996). All models either directly target oligodendrocytes and/or the myelin sheath or change the microenvironment inducing an inflammatory response. Although these models shed light on the events proceeding demyelination, they do not contribute to the understanding of myelination as a process. The models all lead to extensive demyelination via different methods, adding to the complexity and efforts to dissect out the cause of demyelination and the subsequent failure of remyelination. Although demyelination is present, it must be noted that the models create an artificial scenario of demyelination and thus the response from all cells may also be artificial and contribute to the outcome of any attempts to reverse it. Another major drawback of the animal model is the requirement of a large number of animals to produce statistically sound data. Furthermore, in the animal, it is difficult to study different variables, due to the complexity of whole tissues and organs and may all contribute to the end-result.

The myelinating culture system was able to respond to exogenous addition of growth factors (Fig 3.6). This is a very powerful observation as it suggests that the myelinating culture system can be used to test an unrestricted number of biochemical agents. As the cultures contain most cell types present in the CNS, it provides a testing ground not only for myelination, but for axonal-glia interactions, proliferation, apoptosis and differentiation of numerous cell types. This greatly expands the use of this myelinating culture system in the field of neuroscience.

Although the myelinating culture system has not been used for the study of demyelination/remyelination, it is still a valuable tool for the study of axo-glia interactions and how the 'normal' system can be manipulated to further the understanding of

myelination. This model is currently being used as a model for spinal cord injury (Boomkamp et al., 2010, in preparation). The model here is by no means perfect, but nonetheless, it provides a good platform on which myelination can be studied.

The exogenous addition of factors known to be secreted by astrocytes has led to an increase in myelination in the myelinating cultures. Although the supportive roles of astrocytes have been described in terms of neuronal support, maintenance of homeostasis, synaptogenesis and many more (Section 1.2), their role in myelination remains widely disputed due to the conflicting evidence the literature presents of their secretory molecules. It is the intention of the next sections of this thesis to investigate how exogenous molecules can modulate the state of the astrocyte in order to promote an environment which is supportive to myelination.

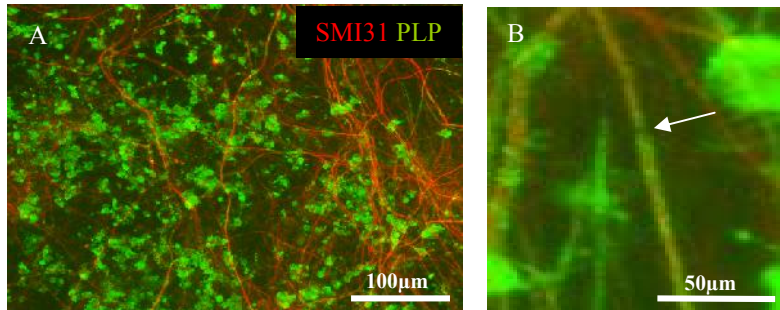


**Figure 3.7 Excess Oligodendrocytes, Ensheathment and Myelination Issues.** E15.5 mixed spinal cord were plated on a confluent monolayer of astrocytes and cultured for 26-28 days and immunolabelled with SMI31 for axons and PLP for mature myelin. Occasionally, there is an excess of PLP+ oligodendrocytes but no sign of myelination (A) which may lead to misleading interpretation of data if other methods, such as Western blot, were used. Some axons are ensheathed by oligodendrocytes, but not myelinated, despite having what appears to look like a Node of Ranvier (B, white arrow). Scale bar 100  $\mu\text{m}$  for A and 50  $\mu\text{m}$  for B.

## **Chapter 4**

# **The Effect of Ciliary Neurotrophic Factor on Myelination**

# The Effect of Ciliary Neurotrophic Factor on Myelination

---

## 4.1. Introduction

### 4.1.1 Background

It has previously been shown that a glial substrate generated from neurosphere-derived astrocytes was supportive for neuronal survival as well as myelination (Sørensen et al., 2008). Furthermore, it was shown that astrocytes secrete a factor that promoted myelination. To try and identify this factor, a candidate approach was taken and CNTF was chosen as a potential candidate (Fig 3.6). More interestingly, CNTF has been proposed as a molecule to activate astrocytes (Liberto et al., 2004) and for this reason this protocol was used to assess how activated astrocytes affect myelination.

Ciliary Neurotrophic Factor (CNTF) is a cytokine and member of the IL-6 family of cytokines, including IL-6, IL-11, IL-27, leukaemia inhibitory factor (LIF), oncostatin M (OSM), cardiotrophin-1 (CT-1), cardiotrophin-like cytokine (CLC) and neuropoietin (NPN) (Stahl and Yancopoulos, 1994). The 24kD protein was identified based on its ability to support the survival of embryonic chick ciliary ganglion neurons *in vitro* (Adler et al., 1979; Lin et al., 1989; Stöckli et al., 1989). Since then, its regenerative effect after injury on different subtypes of neurons, such as dopaminergic and motor neurons, has been reported (Sendtner et al., 1990; Hagg and Vern, 1993; Lee et al., 2008).

In development, CNTF is expressed at very low levels (Stockli et al., 1989; Sendtner et al., 1994). CNTF knock-out mice generated by the disruption of the CNTF gene show that at 4 weeks there were no detectable differences in motor neuron survival. However, there was a loss of neurons and associated muscle atrophy in the adult (Masu et al., 1993). This study suggests that CNTF may not be important developmentally as other members of the IL-6 family may compensate for its actions. The roles of CNTF in the adult centre on its role post-injury, for instance, by contributing to cell body development of sensory and motor neurons after sciatic nerve injury (Chen et al., 2010). However, although CNTF knockout (KO) mice develop relatively normally, mice in which CNTFR $\alpha$  is knocked out in all cells do not (DiChara et al., 1995). These KO mice are unable to feed, have reduced motor neuron numbers and usually die at birth. The authors argue that the paradoxical effect where CNTF is not expressed developmentally yet mice lacking its  $\alpha$  subunit die

prematurely means that there must be a CNTF-like ligand which may also use this subunit and may be more important developmentally. Although no CNTF-like molecule has been discovered to date, this explanation cannot be dismissed. An exquisite study by Lee and colleagues (2008) demonstrated the effect of CNTFR $\alpha$  in the adult exclusive of its effects developmentally. They show this by using a floxed CNTFR $\alpha$  mouse line and administered an adeno-associated virus vector to drive Cre recombinase expression to selectively delete the floxed genes in motor neurons. As a result, a greater loss of motor neurons was observed, an effect which was independent of developmental requirements (Lee et al., 2008). This adult gene disruption study enforces the idea that CNTF is required for the survival of neurons.

In MS, there is a relative failure for remyelination to occur although it has been shown that proliferating OPCs migrate and populate areas of demyelination (Redwine et al., 1998; Levine and Reynolds, 1999). CNTF's action on glial cells has been widely documented. Glial progenitors have been shown to differentiate into astrocytes after CNTF treatment (Hughes et al., 1988). Secretion of CNTF by astrocyte cultures has also been reported (Lillien et al., 1988; Rudge et al., 1992). CNTF administration into the rat neocortex resulted in an upregulation of genes associated with gliosis such as GFAP, vimentin and clusterin (Levison et al., 1996). In this study, astrocytes also underwent morphological changes where they became hypertrophic and the presence of microglia became apparent. However in another study by Winter et al. (1995), CNTF did not illicit a microglial response but the number of GFAP-positive cells increased. The increase in reactivity markers has also been demonstrated *in vitro* (Albrecht et al., 2000). CNTF was also detected in cerebrospinal fluid (CSF) of MS patients after a demyelination attack (Massaro et al. 1997). The above suggests that the glial reaction may be involved in repair and CNTF may be part of this protective mechanism.

The role of CNTF in repair and protection has raised questions as to whether genetic defects to the CNTF gene would contribute to neurological disease (Takahashi et al., 1994). Interestingly, CNTF-null MS patients have early disease onset and faster decline, although the incidence of CNTF null mutation is similar to that of the control population (Geiss et al., 2002). Hoffman and colleagues (2002) concur the findings regarding the incidence of null mutations amongst the normal population, but the authors argue that CNTF genotypes are not related to age of MS onset, course or severity of the disease. These studies demonstrate that CNTF may be involved in an immunoregulatory

mechanism; however, to what extent this could affect the disease outcome is not yet established.

As discussed previously (Section 1.4.2), astrocytes can be activated by CNTF to release factors which can promote oligodendrocyte survival and maturation as well as myelination (Albrecht et al., 2003; Albrecht et al., 2007; Williams et al., 2007). Astrocytes respond to CNTF by becoming 'activated' upregulating cytoskeletal molecules, increase in proliferation and the secretion of anti-inflammatory molecules (Liberto et al., 2004; John et al., 2005). Escartin et al. (2006) developed an *in vivo* model for astrocyte activation whereby they use a lentivirus-mediated CNTF overexpression in the rat striatum. They showed that CNTF overexpression resulted in the activation of astrocytes as measured by immunohistochemistry and Western blot of GFAP, nestin and vimentin. Interestingly, they also showed that intrastriatal injection of quinolinic acid, a dicarboxylic acid with a neurotoxic effect, resulted in improved handling of extracellular glutamate and increased energy supply. This study clearly demonstrates that astrocytes respond to CNTF in beneficial ways to regeneration.

#### **4.1.2 Aims of the Chapter**

As there is a strong background to CNTF's role in injury and activation of astrocytes, the main aim of this chapter is to investigate the effects of activating the astrocytes monolayer by using CNTF and to how this activation can affect myelination.

### **4.2 Results**

#### **4.2.1 Expression of O4 in Myelinating Cultures after CNTF Treatment**

CNTF was previously found to increase the level of myelinating fibres (Fig 3.6). To determine the optimal concentrations of CNTF for myelination, myelinating cultures were plated on a monolayer of neurosphere-derived astrocytes (PLL-astrocytes) and CNTF was added at 20 pg/ml, 200 pg/ml and 2 ng/ml. CNTF was added on day 12 onwards, and cultures were fixed and immunolabelled on day 26-28. The initial assessment of myelination was made using the oligodendroglial marker O4, marker of oligodendrocytes at most stages of development (Fig 1.2). The level of expression of the O4 antigen represents not only the myelin sheaths, but also non-myelinating oligodendrocytes. There

was a significant increase in O4 coverage with the addition of 200 pg/ml and 2 ng/ml of CNTF (Fig 4.1 C, D, E,  $p < 0.05$ ) compared with untreated controls (Fig 4.1 A) but not with 20 pg/ml (Fig 4.1 B,  $p > 0.05$ ). This initial observation led to a more diverse range of concentrations and a more detailed analysis of myelination and axonal ensheathment (see below).

#### **4.2.2 Concentration-Dependent Effect of CNTF**

Spinal cord cells were plated on top of PLL-astrocytes and CNTF was added directly into the culture dish from day 12 onwards. CNTF was added at concentrations ranging from 0.02 pg/ml to 20 ng/ml and the cultures were immunolabelled on day 26-28 for axonal density (%SMI31 immunoreactivity/total area) and axonal ensheathment with PLP myelin. At low concentrations (Fig 4.2 B-D), the percentage of axons covered in a myelin sheath was comparable to that found for untreated cultures (Fig 4.2 A). CNTF increased myelination in a dose-dependent manner. The optimal concentration was 2 ng/ml (Fig 4.2 E, G) and found to be significantly different to untreated control cultures ( $p < 0.005$ ). The promyelinating effect of CNTF at 20 ng/ml (Fig 4.2 F) was absent. Neurite density was comparable in all concentrations (Fig 4.2 H).

#### **4.2.3 CNTF does not have a Promyelinating Effect when Cultures are plated on a Monolayer of OECs**

It has previously been shown that olfactory ensheathing cells (OECs) support neurite survival and extension but not myelination (Sørensen et al., 2008). This observation was used to investigate whether CNTF was acting directly on the oligodendrocytes; spinal cord cells were plated on top of monolayers of PLL-astrocytes and OECs and some dishes were treated with CNTF (2 ng/ml) from day 12 onwards. CNTF treatment of myelinating cultures plated on OEC monolayers did not lead to an increase in the amount of myelination (Fig 4.3 E, G) compared to untreated OECs controls (Fig 4.3 E, G). As seen previously, there was an increase in myelination with CNTF treatment in cultures on PLL-astrocytes (Fig 4.3 A, B, G). Furthermore, there was no difference in neurite density between cultures plated on OECs and PLL-astrocytes with or without CNTF treatment (Fig 4.3 H).

Since myelination was less on OEC monolayers it was possible that OECs may be secreting an inhibitory factor that prevents myelination. To address this possibility

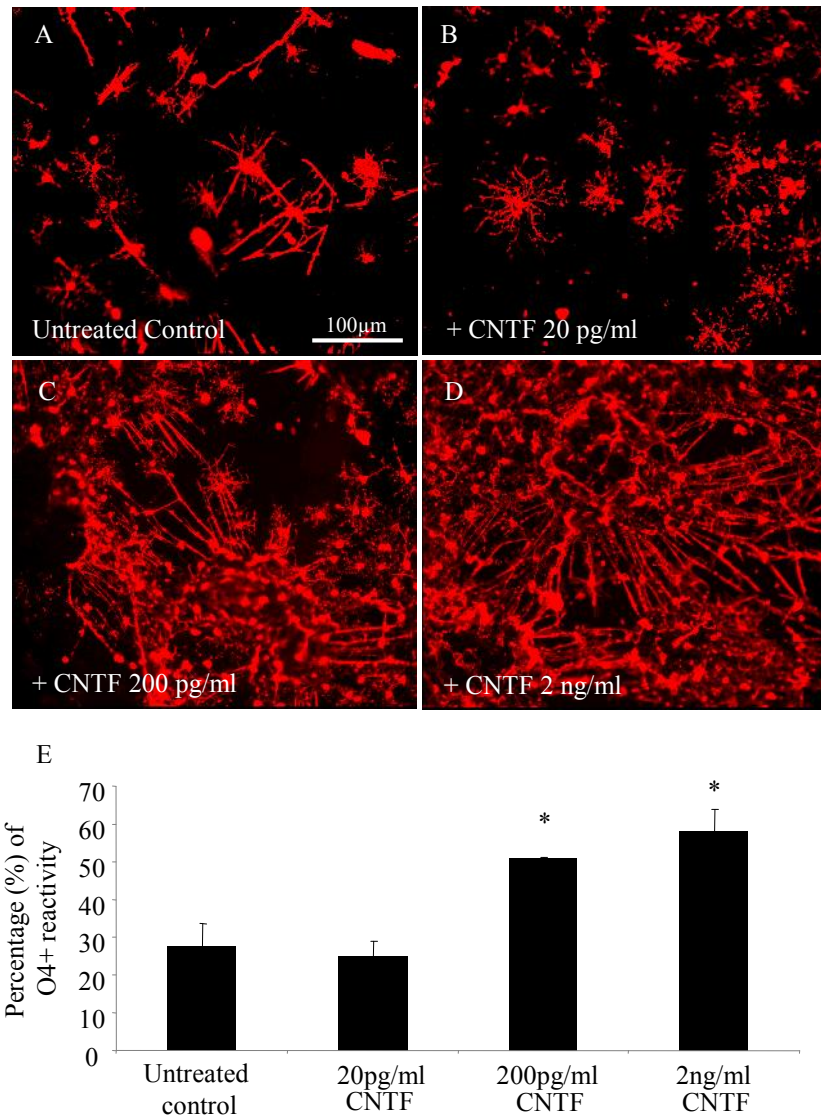


**Figure 4.1 CNTF Addition increases Expression of the O4 Ligand.** E15.5 mixed spinal cord cultures were plated onto a confluent monolayer of neurosphere-derived astrocytes on PLL (PLL-astrocytes) and cultured for 26-28 days. On day 12, cultures were either left untreated (A) or treated with CNTF at varying concentrations; 20 pg/ml (B) 200 pg/ml (C) or 2 ng/ml (D). Cultures were immunolabelled with an antibody which recognises the O4 ligand. There is a gradual increase in O4 expression with increasing concentration, which is significantly higher in 200 pg/ml and 2 ng/ml (E,  $p < 0.05$ ). Error bars indicate  $\pm$  SEM. Scale bar, 100 μm. Experiments were carried out in triplicates.

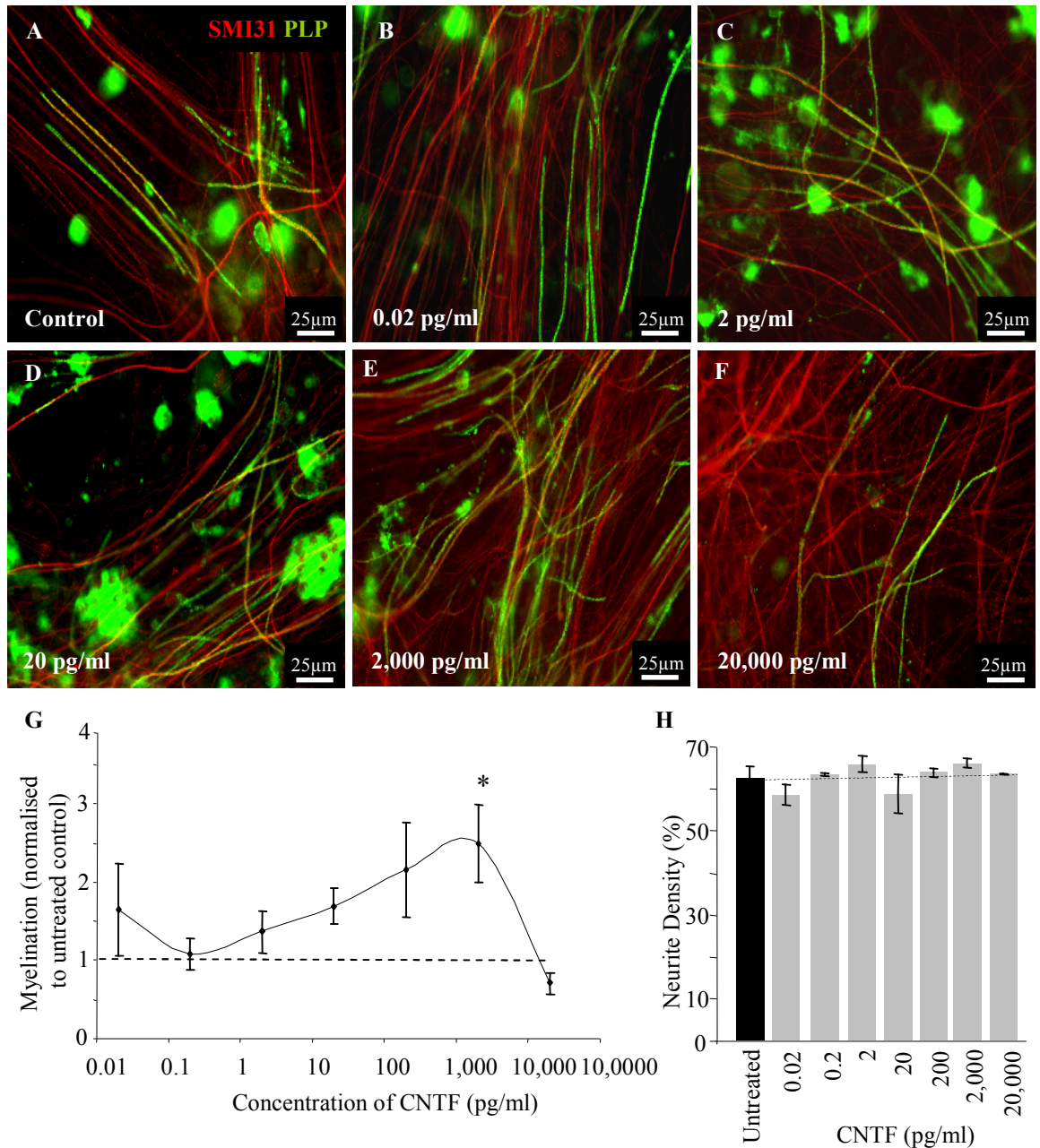


**Figure 4.2 Titration of CNTF Produced Variable Effects on Myelination.** E15.5 mixed spinal cord cultures were plated onto a confluent monolayer of neurosphere-derived astrocytes on PLL (PLL-astrocytes) and cultured for 26-28 days. On Day 12, cultures were either left untreated or treated with varying concentrations of CNTF (0.02 pg – 20 ng/ml). Treatment with low concentrations (B-D) and high concentration (F) of CNTF had no effect on myelination when compared to untreated controls (A). Conversely, treatment with 2000 pg/ml (E) had a significant increase in myelination when compared to control. Thus, addition of exogenous CNTF into myelination cultures leads a concentration dependent increase in myelination (G), where very low and very high concentration of CNTF do not have an effect dissimilar to untreated control. Myelination data was standardised to untreated control. Neurite density (assessed by SMI31 reactivity) was unchanged in all concentrations (E). Error bars indicate  $\pm$  SEM. Scale bar, 25  $\mu$ m. Experiments were carried out in triplicate.

myelinating cultures were plated on PLL-astrocytes which were continuously conditioned by two coverslips containing monolayers of OECs in the same Petri dish. OECs conditioned media increased myelination on cultures plated on PLL-astrocytes (Fig 4.3 C, G). Although this finding eliminates the possibility that OECs secrete inhibitory molecules, it does not rule out the likelihood of an inhibitory molecule/contact on OEC extracellular matrix which may be inhibiting oligodendrocyte differentiation. The presence of two monolayers of PLL-astrocytes in the same dish as a myelinating culture on OEC monolayer increased the level of myelination (Fig 4.3 F, G), confirming the idea that astrocytes secrete a promyelinating factor, corroborating data observed in Sørensen et al. (2008).

#### **4.2.4 CNTF does not Induce Oligodendrocyte Proliferation**

The addition of CNTF may be a mitogen for pre-myelinating oligodendrocytes, increasing the total number of oligodendrocytes capable of myelinating, and hence increasing the number of myelinated neurites observed with CNTF treatment. In order to assess this, cultures on PLL-astrocytes were treated with CNTF and bromodeoxyuridine (BrdU) on day 12. On day 13, the cultures were fixed and immunolabelled with the O4 antibody, anti BrdU (to visualise cells in S phase) and DAPI. Three experimental repeats were performed, taking 5 random images from each experiment and the number of positive cells counted. The average number of total cells counted per experiment (DAPI+) were  $1373 \pm 267$  and  $1528 \pm 227$  for control and CNTF-treatment, respectively. The average number of O4+ cells counted per experiment were  $124 \pm 13$  and  $146 \pm 25$ , and  $97 \pm 48$  and  $98 \pm 49$  for BrdU for control and CNTF-treatment, respectively. The mean number of O4+ cells per view was similar for both control and CNTF-treated cultures at day 12 (Fig 4.4,  $24 \pm 1.7$  and  $29 \pm 2.5$ , respectively,  $p > 0.05$ ). The total number of proliferating cells (BrdU+) was also similar between both conditions ( $19 \pm 3.7$  and  $19 \pm 5.1$ , respectively,  $p > 0.05$ ), suggesting that CNTF is not triggering the proliferation of other cell types, such as microglia. Crucially, the number of proliferating oligodendrocytes (both O4+ and BrdU+) was no different between control and CNTF treatment ( $1.6 \pm 0.4$  and  $1.0 \pm 0.3$ ,  $p > 0.05$ ). It can therefore be concluded that CNTF does not act as a mitogen for oligodendrocytes.

#### **4.2.5 CNTF and Oligodendrocyte Differentiation**

To examine whether the addition of CNTF subsequently leads to oligodendrocyte differentiation, cultures were treated on day 12, and fixed and immunolabelled after 24

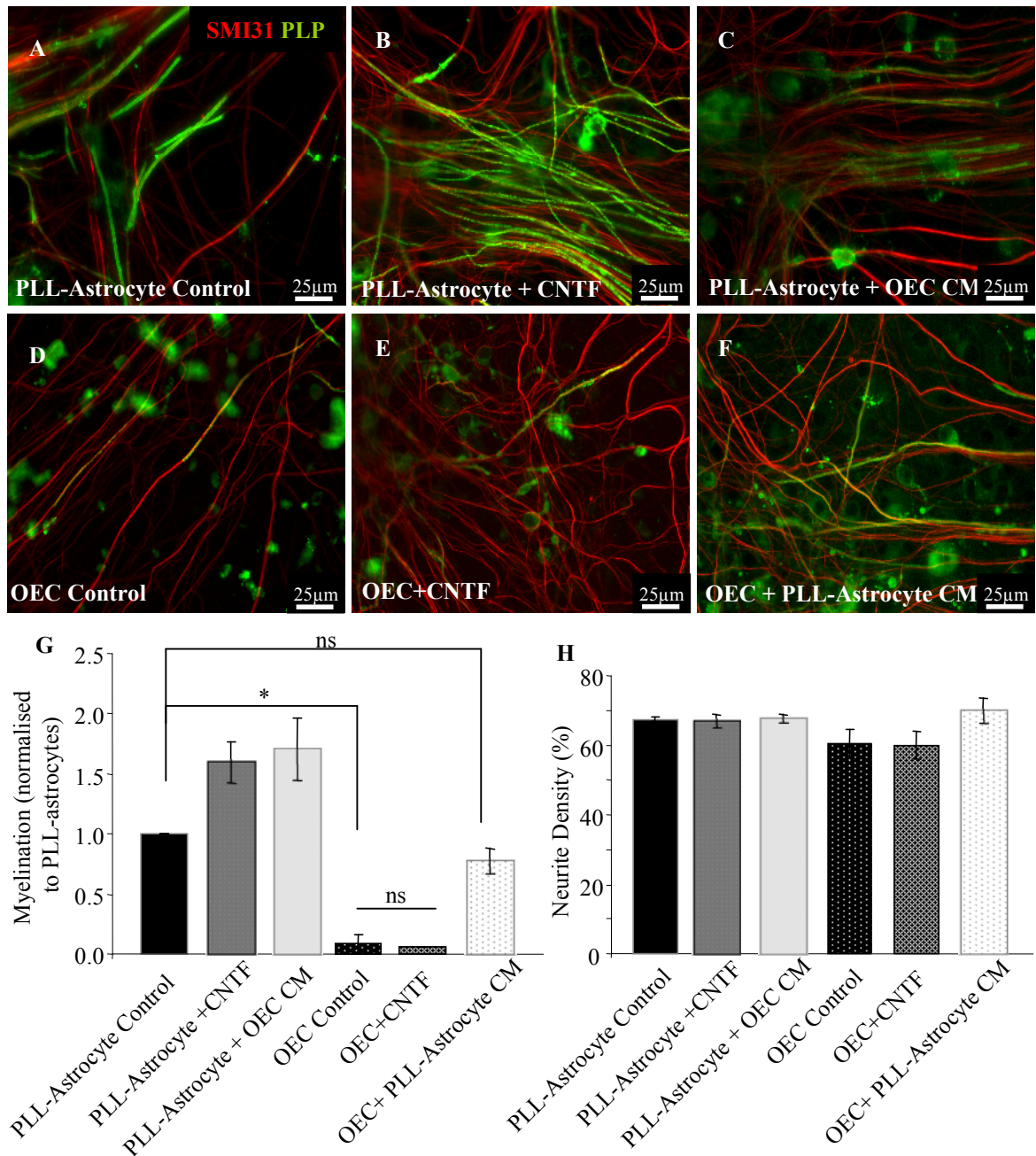


**Figure 4.3 CNTF does not have a Promyelinating Effect when Cultures are plated on a Monolayer of OECs.** Spinal cord cells were plated on neurosphere-derived astrocytes plated on PLL (PLL-astrocytes) (A, B and C) or OECs (E,F,G) and left untreated (A and D), treated with 2ng/ml CNTF (B and E). Further, cultures on PLL-astrocytes were placed in the same dish as two monolayers of OECs (C) and cultures on OECs were placed on the same dish as two PLL-astrocyte monolayers (F), therefore cultures were being continuously conditioned by monolayers. Myelination on cultures on OECs was poor and treatment CNTF does not lead to any further increase (D and E and H). OEC conditioned media (CM) is not inhibitory to myelination of PLL-astrocyte cultures but rather an increase in myelination is observed (C and G) compared to untreated PLL-astrocytes control cultures (A and G). The presence of PLL-astrocyte CM with cultures of OECs leads to an increase in myelination (F and G) as previously reported by Sørensen et al. (2008). The neurite density was similar in all conditions (H). Error bars indicate  $\pm$  SEM. Scale bar, 25 $\mu$ m. Experiments were carried out in triplicate.

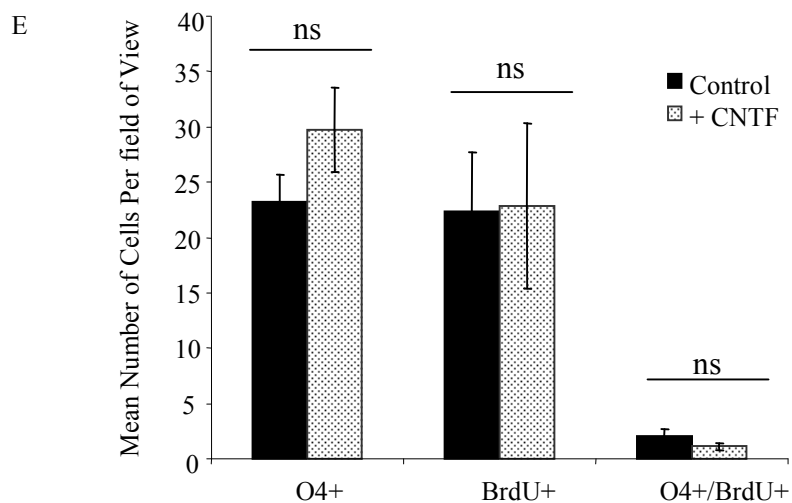
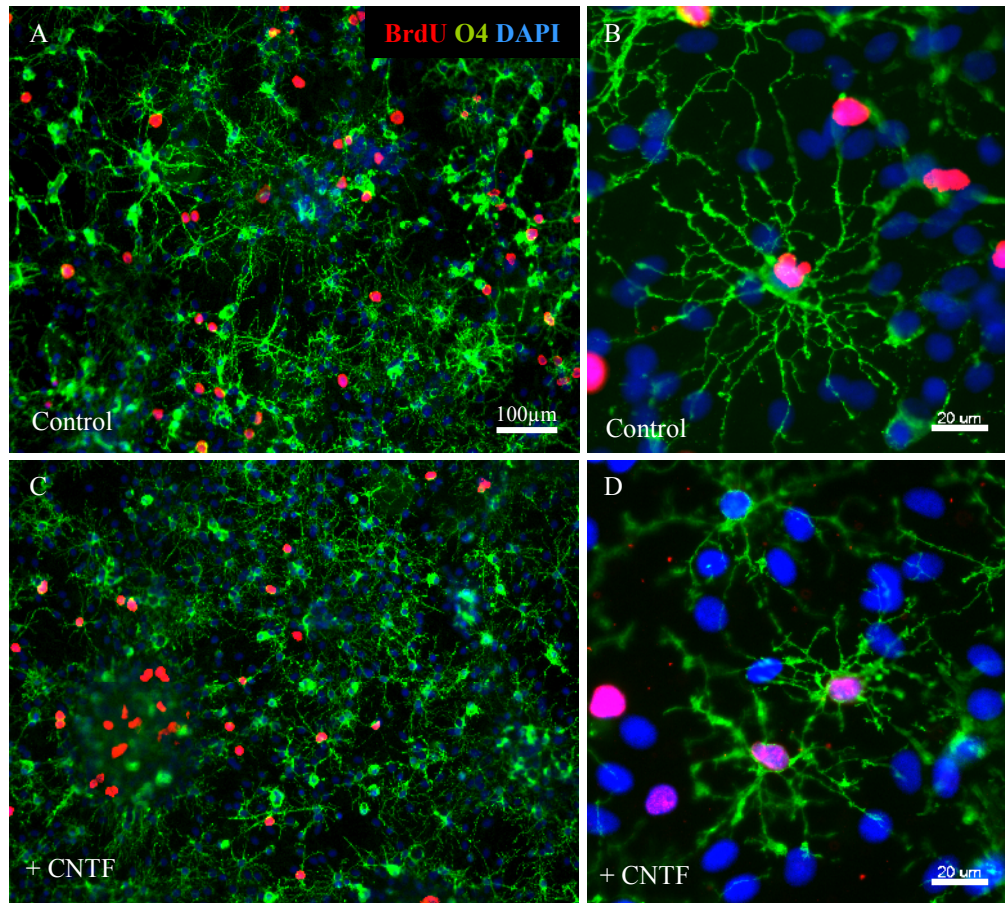


**Figure 4.4 CNTF Treatment does not lead to a increase in OPC Proliferation.** Spinal cord cells were plated on neurosphere-derived astrocytes on PLL (PLL-astrocytes) and either left untreated (A,B) or treated with 2ng/ml CNTF (C,D) on day 12. All cultures were also treated with BrdU on day 12. All cultures were fixed and immunolabelled with O4 and anti-BrdU. No difference in the number of proliferating O4+ cells between control and CNTF-treated cultures. Error bars indicate  $\pm$  SEM. Scale bar, 100 $\mu$ m for A and C, 25 $\mu$ m for B and D. Experiments were carried out in triplicate.

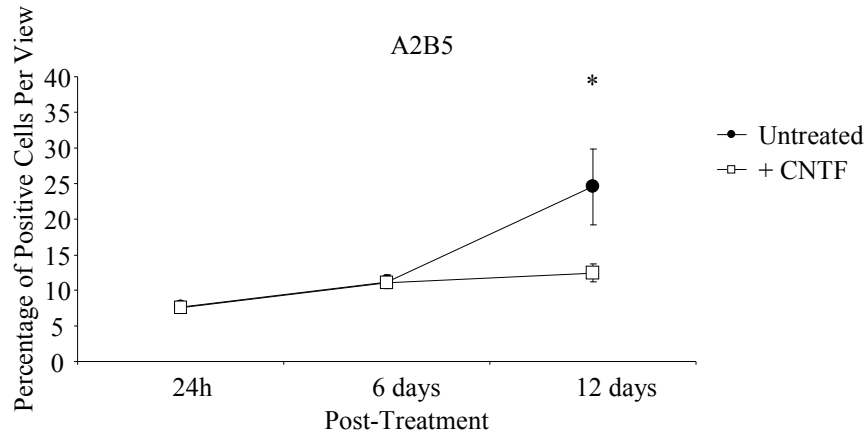
hours, 6 days and 12 days post-treatment (Fig 4.5). The panel of markers include A2B5, which labels OPCs, NG2, an early to middle progenitor and O4, a late progenitor to early myelinating oligodendrocytes (Fig 1.2).

At 24 hours and 6 days post treatment with CNTF (day 13 and 18 of entire culture period, respectively), no change in the number of A2B5+ cells was observed. However, a decrease in A2B5+ progenitors was observed 12 days post CNTF treatment (Fig 4.5 A,  $p < 0.05$ ). This may suggest that more progenitors differentiated into the myelinating phenotype after CNTF treatment. NG2+ late progenitors showed a similar pattern, whereby at 12 days post-treatment, there is a reduction in NG2+ progenitors in treated condition, which was statistically significant (Fig 4.5 B,  $p < 0.05$ ). However, at 6 days post-treatment, there is a transient increase in NG2+ cells in the treated condition. O4+ cell numbers show a similar pattern in control and the treated conditions (Fig 4.5 C) where there is a gradual increase in numbers over the culture period. There was no difference in the number of O4+ cells towards the end of the period in the CNTF treatment to the untreated controls. Thus, the increase in myelination may not be due to an increase in differentiated oligodendrocytes. However, as a more mature oligodendrocyte marker was not used, such as MOG, this can not be confirmed. It must be noted, however, that PLP was trialled and all cells were found to be PLP+ even at day 13. Thus, counting these cells did not truly represent the number of mature myelinating oligodendrocytes. CNTF treatment may create a more favourable environment for progenitor differentiation, leading to fewer progenitors present at later stages in the culture. However, as can be seen from Fig 4.5 B, the number of O4+ cells is unaffected 12 days post treatment.

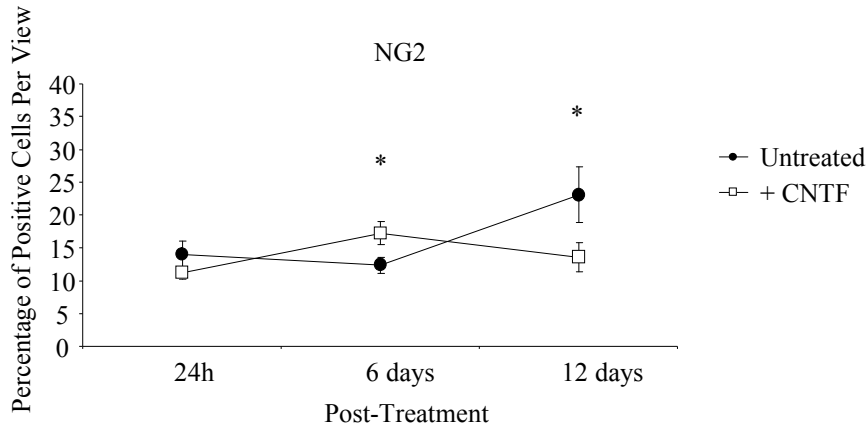
#### **4.2.6 CNTF and Microglial Activation**

The presence of microglia in the myelinating culture system introduces another variable to the targets of CNTF. In order to assess whether treatment with CNTF can increase the number of activated microglia, spinal cord cells were plated on PLL-astrocytes, and on day 12 onwards, some cultures were treated with CNTF. After 26-28 days, the cultures were fixed and immunolabelled with ED1, a marker for activated microglia (Slepko and Levi, 1996). Five images were taken from each condition, a mean total of  $1288 \pm 11$  and  $1450 \pm 116$  nuclei were counted for control and CNTF-treated conditions, respectively, for each experiment. There was no difference between the mean number of ED1+ cells of control and CNTF-treated cultures (Fig 4.6 A, B, C). However, when ED1+ cells were expressed as a percentage of the total DAPI count,  $0.12 \pm 0.01\%$  of total cells per view were

A



B



C

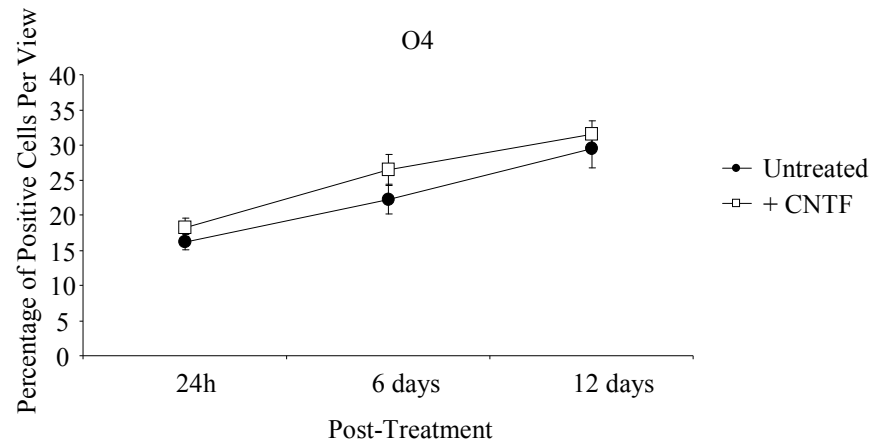


**Figure 4.5 Addition of CNTF does not lead to an increase in O4+ Oligodendrocytes.**

Embryonic spinal cord cells were plated on a confluent monolayer of neurosphere-derived astrocytes (PLL-astrocytes). On day 12, cultures were either left untreated or treated with CNTF (2ng/ml). The cultures were fixed and immunolabelled 24 hours, 6 or 12 days post the beginning or treatment with A2B5 (A), NG2 (B) or O4 (C). The number of positive cells were expressed as a percentage of the total cells were view (DAPI count) and the mean per view for each time-point is plotted. With treatment, there is a large decrease in A2B5+ cells at 12 days post treatment (A,  $p < 0.05$ ). NG2+ cell population increased at 6 days post treatment with CNTF ( $p < 0.05$ ) but decreased compared to untreated cultures ( $p < 0.05$ ). Finally, the O4+ cell population remains relatively consistent for untreated and CNTF-treated cultures. Error bars indicate standard error of the mean (SEM). Experiments were carried out in triplicate.

ED1+ in the untreated control conditions compared with  $0.09 \pm 0.01\%$  in the CNTF treatment (Fig 4.6 D,  $p < 0.05$ ). Thus, CNTF-treatment does not lead to an increase in ED1+ microglia, but possibility a slight decrease. What remains to be identified is the effect of CNTF treatment on microglial secretory profile.

#### **4.2.7 Effect of CNTF on Neurite Diameter**

Neurite diameter is related to whether an axon becomes myelinated or not (Duncan, 1935). In order to assess neurite thickness, a total of 50 images were taken per condition, per experiment. The measurements were made in Image J and arbitrary units were converted to  $\mu\text{m}$  using the image scale bar (Fig 4.7 B, C). There was no difference between neurite diameter in control and treated conditions (Fig 4.7A, C, D;  $1.6 \pm 0.16$  and  $1.98 \pm 0.14 \mu\text{m}$ ,  $p > 0.05$ ). Furthermore, no differences were found between myelinated and non-myelinated neurites in either condition (Fig 4.7 D). However, there is a trend for neurites in CNTF treatment to be slightly larger. When all values for every individual neurite were compared ( $n=150$ ), there was a significant increase in neurite diameter in cultures treated with CNTF whether they were myelinated or not. The number of myelinated neurites was compared to those that were non-myelinated. Of the neurites counted, 25% were myelinated compared to 43% with treatment (Fig 4.7 E). These data may indicate that CNTF treatment may increase the likelihood of a neurite to be myelinated due to its larger diameter, although, it cannot be assumed that CNTF does not make the neurites more 'responsive' to being myelinated.

#### **4.2.8 Effect of CNTF on Astrocyte Reactivity**

Astrocytes make up a larger number of the dissociated spinal cord cells as well as comprising the underlying monolayer. It can be assumed that CNTF may be acting on these astrocytes, changing their phenotype to one which may be more supportive to myelination. The biological properties of untreated and CNTF-treated astrocytes were compared. Astrocytes were plated onto PLL-coated coverslips, grown to confluency and treated with CNTF (2 ng/ml, Fig 4.8 A, B) for 24 hours or 48 hours. As reactive astrocytes undergo hypertrophy, their cell size was measured in Image J. A contour around the cell was drawn and the arbitrary units converted into  $\mu\text{m}^2$ . Astrocytes treated with CNTF were slightly smaller than controls (Fig 4.8 C,  $1041 \pm 122 \mu\text{m}^2$  and  $853 \pm 82 \mu\text{m}^2$ , respectively) although this was not statistically significant. Nuclear hypotrophy is also an indication of astrocyte reactivity (Levison et al., 1998) and was also measured. The straight line

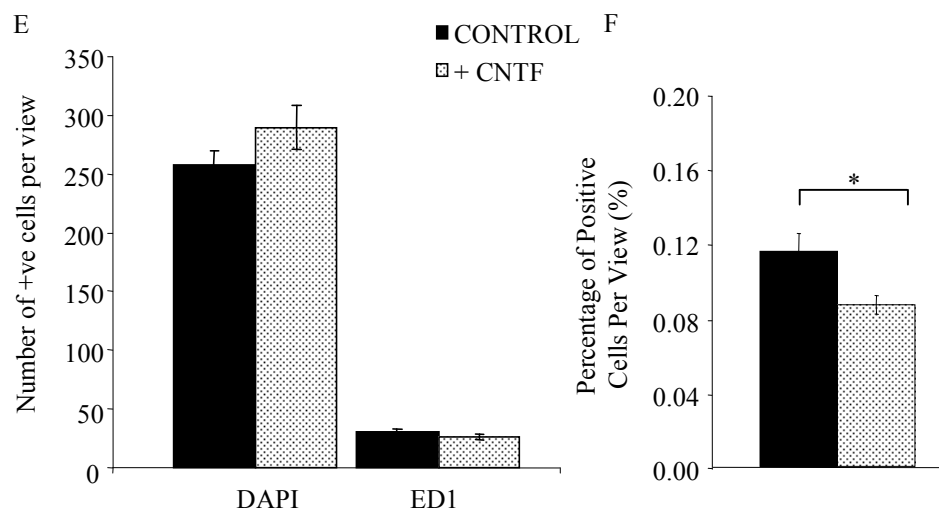
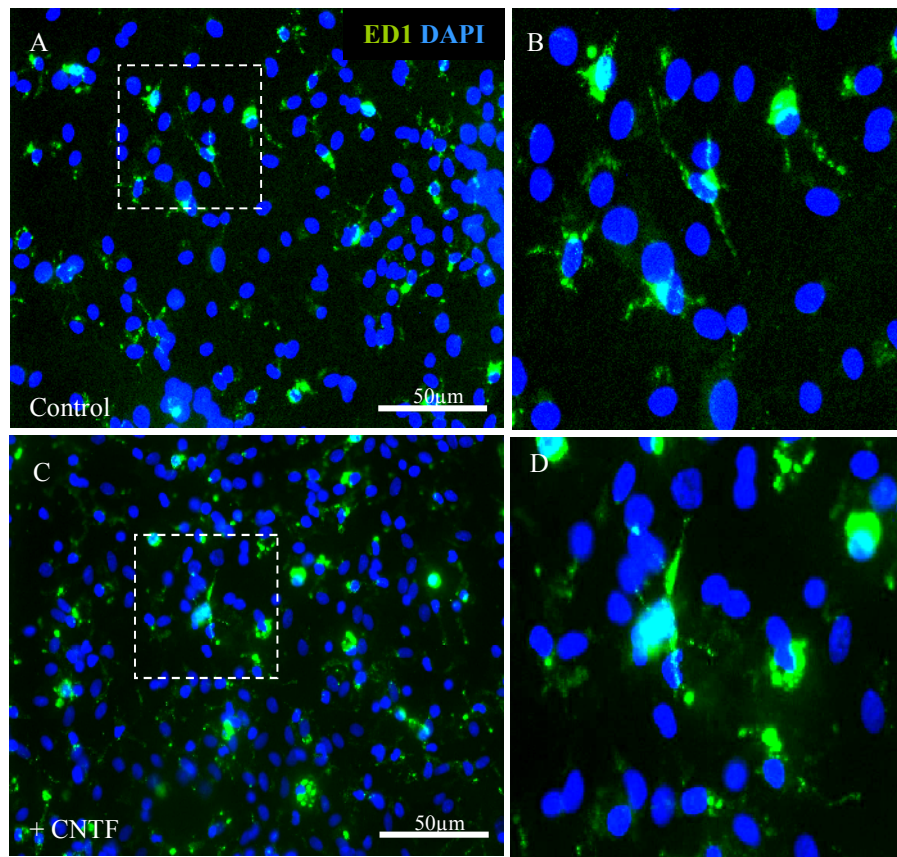


**Figure 4.6 anti-CNTF Slightly Increases the Number of Activated Microglia.** Embryonic spinal cord cells were plated on a confluent monolayer of neurosphere-derived astrocytes on PLL (PLL-astrocytes). On day 12, cultures were either left untreated (A, B) or treated with CNTF (C, D) on day 12 onwards. On day 26-28, cultures were fixed and immunolabelled with ED1, a marker for activated microglia and DAPI. The number of ED1+ cells per view were counted and represented as mean number of cells per view (E) and expressed as percentage of total cell number (F). There is no change in ED1+ or DAPI+ cells between untreated and treated cultures. However, a significant increase ( $p < 0.05$ ) is observed when cells are expressed as percentage of total cells per view (F). Experiments were performed in triplicate.

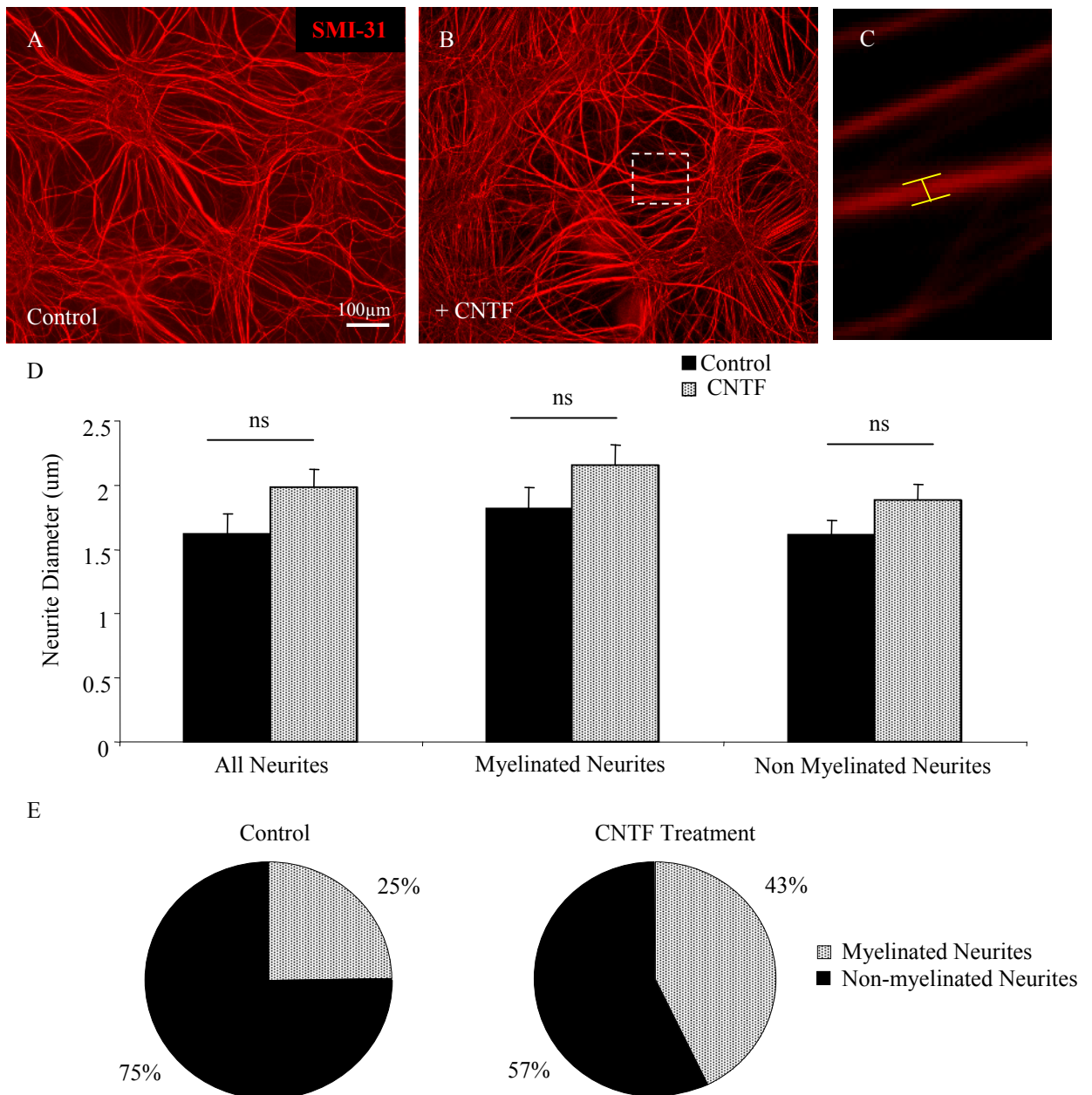


**Figure 4.7 Addition of CNTF does Increase Neurite Diameter.** Embryonic spinal cord cells were plated on a confluent monolayer of neurosphere-derived astrocytes (PLL-astrocytes). On day 12, cultures were either left untreated (A) or treated with CNTF (B) (2ng/ml). The cultures were fixed and immunolabelled on day 26-28 with SMI-31, and PLP. Using Image J, the diameter of the random neurites was measured (C) and it was noted whether the neurite was myelinated or not. Neurite diameter did not differ between untreated or CNTF treated cultures (D), although there is a slight increase in diameter with CNTF treatment. Many more unmyelinated axons were present in untreated conditions compared with CNTF-treatment (E). Experiments were performed in triplicate.

selection on Image J was used to draw across DAPI+ nuclei. There was no increase in nuclear size between control and CNTF treated astrocytes (Fig 4.8 D,  $13.71\pm 0.48$  and  $13.97\pm 0.38$ , respectively,  $p > 0.05$ ). The most documented observation of astrocyte reactivity is an increase in GFAP expression. Western blot analysis using anti-GFAP and cell lysates of astrocytes shows a slight increase in GFAP content after treatment with CNTF (Fig 4.8 E). Sister astrocyte monolayers were treated with CNTF for 24 hours, washed in PBS, and fresh media was added to collect astrocyte secretory products post CNTF treatment to assess if CNTF addition to astrocytes led to an increase in CNTF production. There was no difference between untreated and CNTF treated astrocytes in terms of further CNTF production ( $75.6\pm 21$  pg/ml in untreated vs.  $61.1\pm 9$  pg/ml in treated, Fig 2.8 F). Thus, CNTF-treatment of astrocytes does not alter the markers of reactivity reviewed here.

#### **4.2.9 Effect of CNTF Treatment on Astrocytic Expression of Nestin**

Nestin has been used as a marker of reactivity in injury and development (Clarke et al., 1994; Lin et al., 1995). Lipopolysaccharide (LPS) is frequently used *in vitro* experiments to induce a reactive phenotype in astrocytes (Pang et al., 2001; Gomez-Nicola et al., 2010; Lu et al., 2010). LPS treatment was used in these experiments to confirm a change in phenotype status with CNTF treatment, if indeed there is one. Astrocytes were grown to confluency and left untreated (Fig 4.9 A), treated with CNTF (2 ng/ml, Fig 4.9 B) or treated with LPS (1  $\mu$ g/ml, Fig 4.9 C) for 24 hours. Astrocytes were immunolabelled with GFAP and nestin. Sister monolayers were lysed and the proteins were run on a gel. Intensity of nestin (red) immunolabelling in the LPS treated condition is much stronger than control and CNTF conditions. This observation correlates with the literature suggesting that LPS is an activator of astrocytes. Visually, there is no striking difference between control and CNTF treatment. Protein levels were verified using Western blot (Fig 4.9 D). An insignificant increase in protein content was observed with CNTF and LPS treatment. The band intensity of 3 experimental repeats for CNTF and LPS treated astrocytes were verified and found to be no different to controls (Fig 4.9 E).

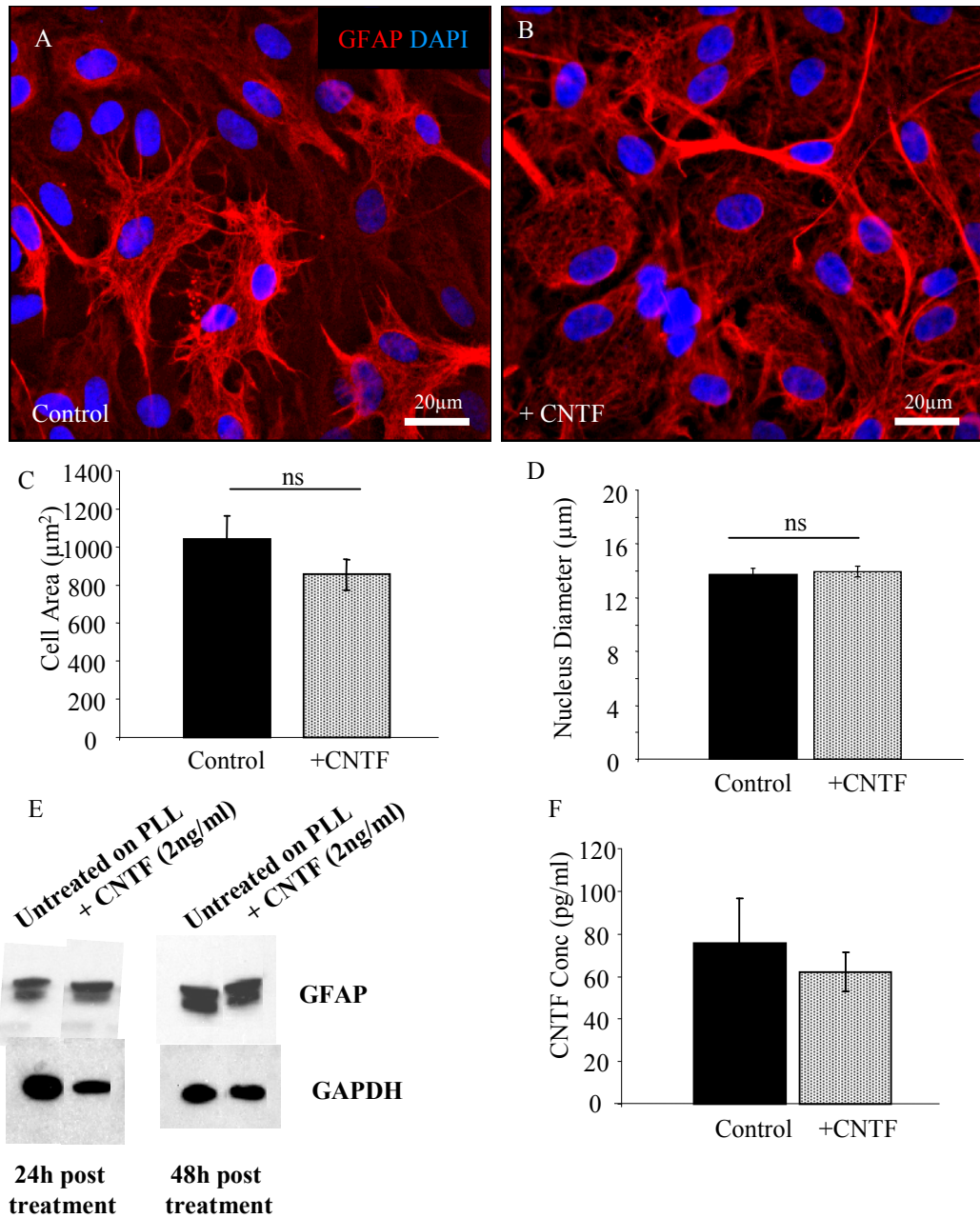


**Figure 4.8 Addition of CNTF does Increase Markers of Reactivity.** Neurosphere-derived astrocytes were plated on PLL (PLL-astrocytes) until confluency. On day 7, cultures were either left untreated (A) or treated with CNTF (2ng/ml, B). The cultures were fixed and immunolabelled with GFAP and DAPI. Using Image J, cell area and nuclear diameter were measured. No difference was observed between control astrocytes and CNTF-treated astrocytes for cell area (C) or nuclear diameter (D). Sister astrocyte monolayers were lysed 24 hours and 28 hours after treatment and western blot was performed to measure GFAP protein levels. No increase in GFAP content was observed at 24 hours or 48 hours post treatment (E). GAPDH was used as a loading control. In another set of sister astrocytes, some astrocytes were treated with CNTF for 24 hours and others left untreated. The CNTF-containing media was then removed and fresh media was added for a further 24 hours. This media was assayed for CNTF using ELISA (F). No increase in CNTF concentration was observed following CNTF treatment. All experiments were performed in triplicate.

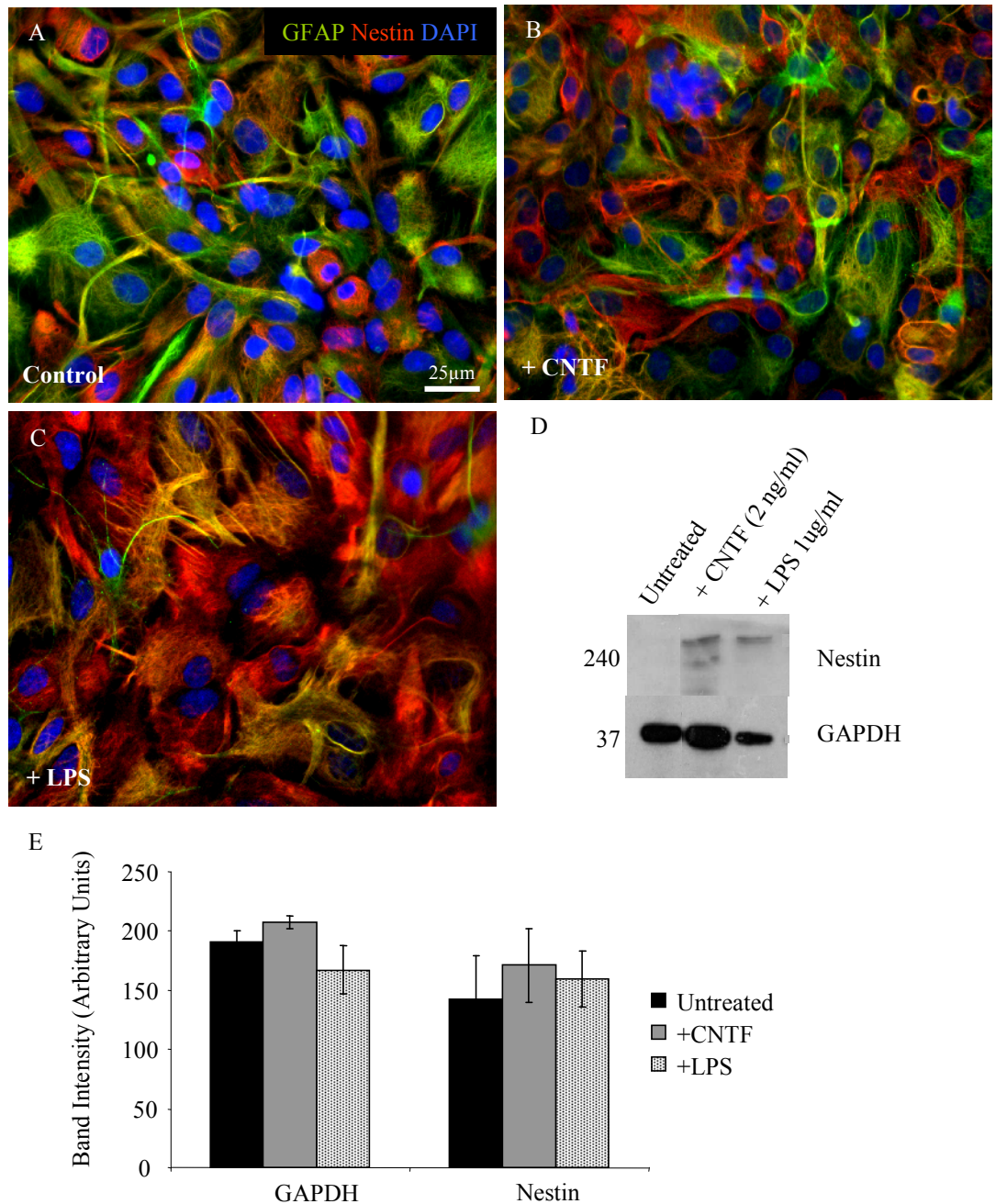


**Figure 4.9 Addition of CNTF does Increase Nestin Reactivity.** Neurosphere-derived astrocytes were plated on PLL (PLL-astrocytes) until confluency. On day 7, cultures were either left untreated (A) or treated with CNTF (2 ng/ml, B), or LPS (1 µg/ml, C) for 24 hours. The cultures were fixed and immunolabelled with GFAP, nestin and DAPI. Using Image J, cell area and nuclear diameter were measured. No difference was observed in immunoreactivity of nestin in CNTF treatment (B) whereas there was a visible increase in LPS treatment (C) compared to untreated control astrocytes (A). Western blot was performed to measure nestin protein levels. A slight increase in nestin protein content was observed (D). Densitometry of bands on was performed on experimental repeats and nestin content was similar in all conditions (E). Experiments were performed in triplicate.

### 4.3 Discussion

The experiments detailed in this chapter report that CNTF increases the percentage of myelinated fibres in a dose dependent manner in the myelinating cultures due to an activation of the astrocyte phenotype to one which is more supportive to myelin formation. CNTF addition did not increase neurite density or diameter but the responsiveness to myelination has not been investigated. CNTF was not a mitogen nor did it affect number of resident microglia in these cultures. When astrocytes alone were treated with CNTF, only a slight increase in activation markers was observed. This may be due to the requirement of the CNTFR $\alpha$  subunit of the signalling complex (see below).

The  $\alpha$  subunit of the CNTF receptor is critical for signalling but its expression is confined to neuronal cells in the rat adult brain (MacLennan et al. 1996; Kahn et al., 1997) suggesting that for CNTF to exert its actions, the  $\alpha$  subunit has to be ‘shed’ from neurons. Indeed, CNTF, in combination with the soluble form of the CNTFR $\alpha$  subunit, increased proliferation in a cell line (TF-1) not normally responsive to CNTF (Davis et al., 1993). TF-1 cell lines are responsive to LIF indicating the presence of gp130 and LIFR $\beta$ . Thus, this cell line had the ‘potential’ to be responsive to CNTF if the CNTFR $\alpha$  component were present. This could therefore explain the effects of CNTF in the culture system but not on astrocytes alone (Fig 4.2 and 4.4). In the cultures, the addition of CNTF leads an increase in the number of myelinated neurites. As it was hypothesised that this effect was due to an activation of astrocytes, an increase in activation markers such as GFAP and nestin were expected when astrocytes alone were treated with CNTF as previously shown *in vivo* (Kahn et al. 1997; Escartin et al., 2006). As no increase in these markers was observed, it can be concluded that this may be due to the lack of axons and the thus the presence of the CNTFR $\alpha$  subunit. Furthermore, astrocytes originating from the grey matter in the mouse were found to contain CNTFR $\alpha$  whereas ones from the white matter did not (Dallner et al., 2002). Neurosphere-derived astrocytes used here are originally harvested from the corpus striatum, a region of the brain rich with white matter. It is likely that the origin of the astrocytes used stems from a white matter origin and therefore may not express CNTFR $\alpha$ .

CNTF’s actions have become prominent in disease and injury. Astrocytes of a retinal origin induced CNTF expression post injury to the lens in adult rats (Müller et al., 2007), which later contributed to the regeneration of axotomised retinal ganglion cells. Furthermore, Rudge et al. (1994) have described how the CNTFR $\alpha$  subunit switches expression to astrocytes (from being predominantly neuronal) following injury and

therefore proposing that CNTF only forms a functional complex when required, in injury conditions. This observation suggests that CNTF-treated astrocytes in the myelinating cultures behave as though the exogenous CNTF is a 'damage signal' and alter their secretory profile and therefore release other promyelinating factors which then increase the myelinating capability of oligodendrocytes.

CNTF knockout mice experience a more severe form of EAE as well as early onset of disease, compared to wild type controls (Geiss et al., 2002; Linker et al., 2002) suggesting that an absence of CNTF impairs the activation mechanism of astrocytes and hence their pro-regenerative effects. The authors attribute the effects of lack of CNTF directly on the oligodendroglial lineage cells effecting their survival, maturation and myelin sheath maintenance. Although this may be the case, the fact that astrocytes are the main source of CNTF cannot be dismissed. It has been reported that CNTF acts directly on oligodendrocytes *in vitro*, to favour their final maturation (Stankoff et al., 2002). This is unlikely to be the case in the data presented as i) CNTF addition to myelinating cultures plated on OEC did not produce a promyelinating effect and ii) OEC conditioned media did not inhibit myelination and therefore the lack of myelination can not be attributed to a negative secretory factor. It has also been suggested that CNTF may be activating astrocytes indirectly, where OPCs *in vitro* were shown to proliferate after exposure to astrocyte conditioned media after exposure to CNTF (Albrecht et al., 2007). Although myelination was not investigated in the above study, the results shown here confirm that no increase in proliferation was observed after CNTF addition (Fig 4.4). From the literature above, astrocytes may release CNTF in injury conditions, to support surrounding neurons and oligodendrocytes, and to also act on their own receptors for further activation and additional release of trophic support.

Microglia make up less than 1% of the total cells within the myelinating culture system but they should not be overlooked as activated microglia have been shown to destroy developing OPCs via the secretion of Tumor necrosis factor alpha (TNF $\alpha$ ) (Miller et al., 2007; Pang et al., 2010). Activated microglia express the CNTFR $\alpha$  and can therefore be responsive to CNTF (Lin et al., 2009). However, conditioned media from CNTF-treated microglial cells have been shown to enhance the survival to spinal cord motor neurons (Krady et al., 2008). Interestingly, IL-6 conditioned media, despite being from the same family of cytokines, led to a reduction in the number of neurons after treatment with IL-6 conditioned media. No difference in the number or morphology of microglia was observed

in the cultures used here after CNTF treatment. However, as the secretory profile has not been evaluated, it can not be assumed that the promyelinating effect is solely due to the activation of astrocytes. For instance, CNTF can activate microglia to secrete a product which may make neurites more responsive to being ensheathed.

The treatment of astrocytes with CNTF does not lead to a further increase in CNTF secretion as shown by ELISA. This observation suggests that in response to CNTF treatment, further CNTF cannot be attributed to be the promyelinating factor released by astrocytes. Although CNTF may be released from astrocytes, work from other laboratories suggest that CNTF lacks a signaling peptide and more likely to be a cytosolic protein which is not available for conventional release methods (Lin et al., 1989; Stöckli et al., 1991). However, Kamiguchi et al., (1995) used an enzyme to cleave the glycosylphosphatidylinositol (GPI) linkage of the CNTFR $\alpha$  subunit of cultured astrocytes and demonstrated that astrocyte conditioned media contained up to 257.3 pg/ml of CNTF compared to less than 100pg/ml in non-treated astrocytes. This study suggests that cultured astrocytes do secrete CNTF but it is then trapped by surface receptors of the astrocytes and may possibly be acting via an autocrine loop.

There is still some controversy as to how CNTF acts on astrocytes and this depends on i) whether astrocytes possess the CNTFR $\alpha$  subunit or are situated in an environment where axonal shedding can take place, ii) whether an astrocyte needs to be damaged/activated to release the cytosolic protein and iii) whether the  $\alpha$  subunit of the astrocytic surface sequesters CNTF in an autocrine loop rather releasing it. On the whole however, CNTF's actions on astrocytes are well documented and it seems to be imperative that for this reaction to take place, the astrocyte needs to be in an environment that most resembles the *in vivo* situation, i.e. 3-dimensional milieu surrounded by other cell types.

## **Chapter 5**

# **Understanding the Role of CNTF and its Receptor**

# Understanding the role of CNTF and its Receptor

---

## 5.1 Introduction

### 5.1.1 Background

The effects of CNTF are mediated via its tripartite receptor complex, consisting one ligand-binding subunit, the CNTF receptor alpha (CNTFR $\alpha$ ), and two signal transducing proteins, LIF receptor  $\beta$  (LIFR $\beta$ ) and gp130. In order for CNTF to exert its actions, it first binds to CNTFR $\alpha$ . Once CNTF and CNTFR $\alpha$  are bound, the complex recruits gp130, which in turn recruits LIFR $\beta$ , leading to the activation of the Jak and Tyk kinases and STATs (Boulton et al., 1994; Stahl et al., 1994; Ip and Yancopoulos, 1996; Müller et al., 2007; Fig 5.1). The activation of gp130 alone is not sufficient for the activation of intracellular signalling substrates.

The CNTFR $\alpha$  subunit is a specialised receptor component which can either be soluble or membrane bound (Fig 5.2). This unique feature is due to a lack of a transmembrane domain for CNTF. Instead, the receptor is anchored to the cell surface via glycosyl phosphatidylinositol (GPI) linkage (Ip et al., 1993; Davis et al., 1991). The CNTFR $\alpha$  may also exist in soluble form. However, it has been suggested that the existence of the soluble form is only observed during injury in order to provide greater response from non-responding cells (Davis et al., 1993; Stahl and Yancopoulos, 1994).

Other members of the IL-6 family may use a combination of gp130 and LIFR $\beta$  to elicit their effects. For instance, IL-6 requires its own specialised ligand binding subunit IL-6R $\alpha$  (like CNTF) and two signal transducing gp130 components. LIF, however, requires gp130 and LIFR $\beta$  (Ip and Yancopoulos, 1996) with no ligand binding component required (Fig 5.3). Because members of the IL-6 family share many receptor components, it is likely to find overlapping signalling pathways (Ip et al., 1993; Patterson, 1992). For instance, both CNTF and LIF have trophic activity on neurons. In a study by Martinou et al. (1992), motor neuron survival was measured after treatment with, amongst others, CNTF and LIF. The authors report an almost identical increase in the number of motor neurons after treatment when compared to the untreated controls. Therefore, due to sharing some of the receptor components, members of the IL-6 family can have very similar roles. However, Davis et al. (1993) demonstrate that these effects highly depend on the types of cells used.

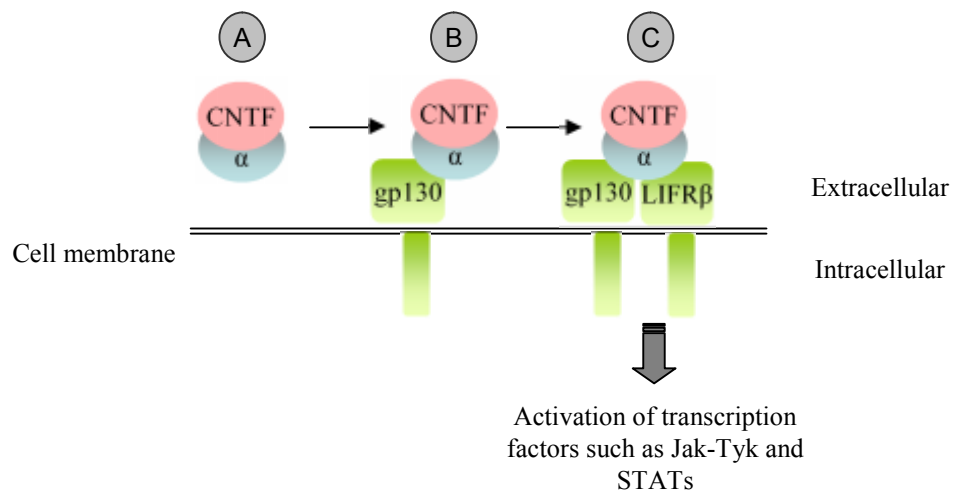


**Figure 5.1 An illustration of CNTF Binding and Signalling.** CNTF binds to its ligand binding subunit, CNTFR $\alpha$  (A), which recruits the membrane bound gp130 subunit (B) forming an inactive complex. The binding to gp130 recruits LIFR $\beta$  (C) which leads to signal transduction via Jak-Tyk and STATs.

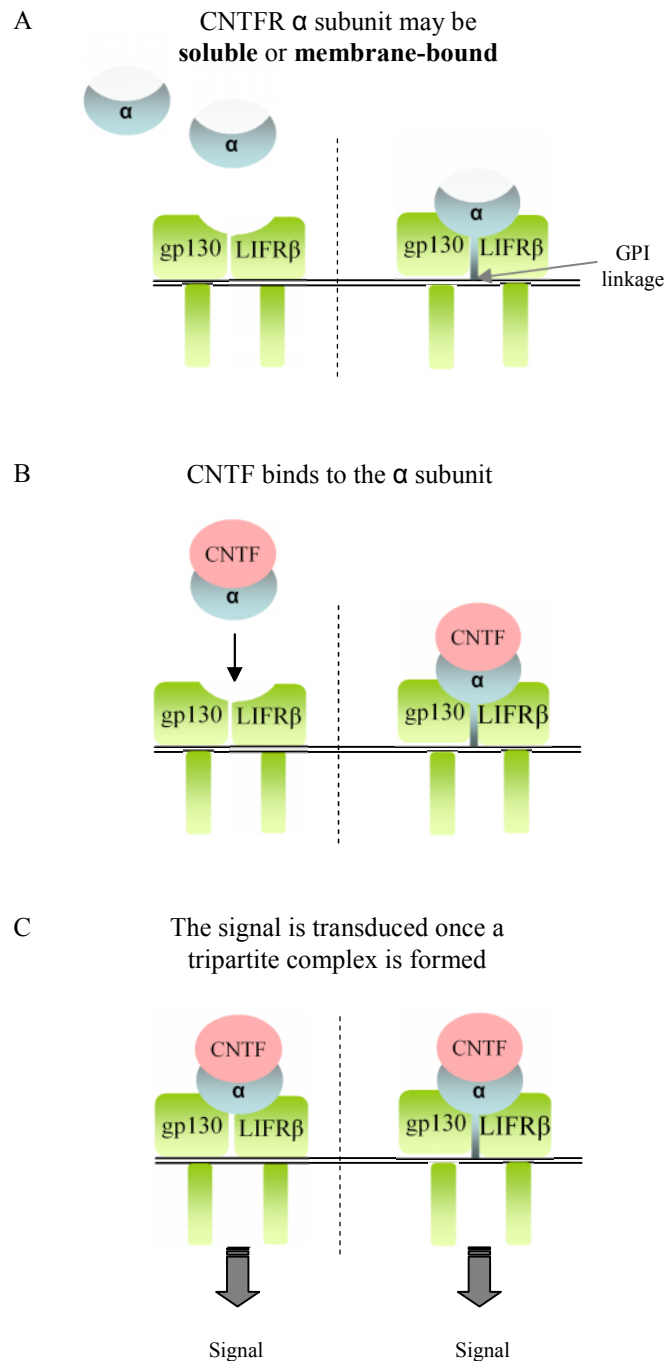


**Figure 5.2 CNTFR $\alpha$  can be Soluble or Membrane Bound.** CNTF receptor signalling is unique as the CNTFR $\alpha$  ligand-binding subunit is not a transmembrane component. Instead, CNTFR $\alpha$  is anchored to the cell membrane by glycosyl-phosphatidylinositol linkage (GPI, A). This GPI linkage allows the CNTFR $\alpha$  to be either be soluble or membrane bound (A). CNTF will bind to either the soluble form and then recruit the other two signal transducing membranes or CNTF can directly attach membrane bound subunit (B). Signal transduction is activated once a tripartite complex is formed (C).

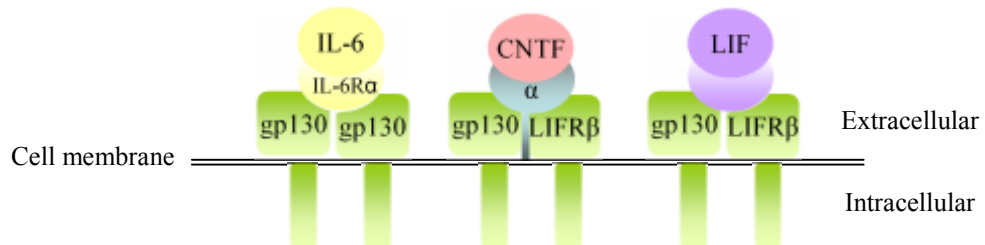


**Figure 5.3 Receptor Complexes of the IL-6 Cytokines.** Other members of the IL-6 cytokines share some of their receptor components. IL-6 does not require a LIFR $\beta$ , but instead utilises two gp130 components and its own ligand binding IL-6R $\alpha$  subunit. CNTF requires an CNTFR $\alpha$  as well as gp130 and LIFR $\beta$ . LIF, however, does not require a specialised ligand binding unit and only uses gp130 and LIFR $\beta$ .

For instance, they show that the addition of IL-6 and its ligand-binding subunit IL-6R $\alpha$  resulted in the phosphorylation of Jak-1 in EW-1 cells, Jak-2 in SK-MES cells and Jak-1, Jak-2 and Tyk-2 in U266 cells. Furthermore, addition of CNTF to EW-1 cells resulted in the phosphorylation of both Jak-1 and Jak-2. This study using cell lines demonstrates that not only can different cytokines of the IL-6 family elicit different kinase phosphorylation patterns in different cell lines but that cytokines also elicit different phosphorylation patterns depending on the cell type. Therefore, the IL-6 family of cytokines have shared and distinct patterns of regulation depending on the cells used. This may explain the wide range of actions that cytokines have in different tissues and cells.

### **5.1.2 Aims of the Chapter**

The aim of this chapter is to further investigate the roles of CNTF by using i) neutralising antibodies, ii) comparing the actions of other members of the IL-6 family and iii) study of its time-course of action.

## **5.2 Results**

### **5.2.1 Neutralising antibodies to CNTF lead to an Increase in Myelination**

In Chapter 4, the addition of CNTF to myelinating cultures resulted in an increase in myelination. To further confirm this promyelinating effect of CNTF, myelinating cultures were plated on neurosphere-derived astrocytes plated on PLL (PLL-astrocytes) and neutralising antibodies against CNTF were added from day 12 onwards. Two neutralising antibodies are commercially available, one that recognises CNTFR $\alpha$  and one that recognises CNTF itself. It was hypothesised that the addition of neutralising antibodies would inhibit the promyelinating effect seen with CNTF. Unexpectedly, antibodies against CNTF ligand (Fig 5.4 C, G) and against the CNTFR $\alpha$  receptor (Fig 5.4 D, G) both produced an increase in myelination, although only CNTF ligand antibody was significant ( $p < 0.05$ ) when compared to the untreated control cultures (Fig 5.4 A, G). The addition of both neutralising antibodies together also increased myelination (Fig 5.4 E, G,  $p < 0.05$ ) but not to the same extent as the CNTF ligand antibody alone. The addition of CNTF together with its neutralising ligand antibody did not affect myelination (Fig 5.4 F, H) presumably because CNTF and its antibody bound forming an inactive complex prior to

reaching the membrane bound or soluble  $\alpha$  subunit target necessary for CNTF signal transduction. Neurite density was similar in all conditions measured (Fig 5.4 H,  $p > 0.05$ ). These results indicate that the role of CNTF on astrocytes may be more complex than originally anticipated, where there may be a dual role which highly depends on control concentration. For instance, the endogenous levels of CNTF in the culture may be inhibitory to myelination and withdrawal of CNTF therefore leads to an increase in myelination. Considering that the exogenous addition of CNTF also increases myelination, likely via the activation of astrocytes, it can be hypothesised that astrocytes behave differently to different concentrations of CNTF. For instance, high levels of CNTF lead to an increase in myelination whereas its withdrawal also leads to an increase in myelination via either the same (bi-phasic response) or different pathways that secrete promyelinating factors.

### **5.2.2 Increase in Myelination with Neutralising Antibodies is only observed at 4 $\mu\text{g/ml}$**

In order to test whether there is a concentration dependent increase in myelination with the addition of neutralising CNTF ligand antibodies, concentrations ranging from 0.5-32  $\mu\text{g/ml}$  were added to cultures from day 12 onwards. Very low (0.5  $\mu\text{g/ml}$ , Fig 5.5 B, E) and very high concentrations (32  $\mu\text{g/ml}$ , Fig 5.5 D, E) had no affect on myelination compared to untreated control cultures (Fig 5.5 A). There is a significant increase in myelination at 4  $\mu\text{g/ml}$  (Fig 5.5 C, E,  $p < 0.05$ ) whilst the neurite density remains similar in all conditions (Fig 5.5 F). The data therefore suggests that the addition of 4  $\mu\text{g/ml}$  of anti CNTF may reduce the concentration of CNTF in the culture to a level which promotes myelination and thus aiding the concentration dependency hypothesis. Taken together with the results from the previous chapter (Fig 4.2), CNTF may act in a biphasic manner to increase myelination. However, it is not known whether the addition of neutralising CNTF antibodies actually reduce the amount of CNTF in the culture media.

### **5.2.3 There is a Slight Reduction in CNTF Concentration after Antibody Treatment**

To test whether CNTF levels were reduced when the neutralising ligand antibody was added, cultures were either left untreated or treated with varying concentrations of antibody (0.5-32  $\mu\text{g/ml}$ ). On day 28, media was collected from the cultures and levels of

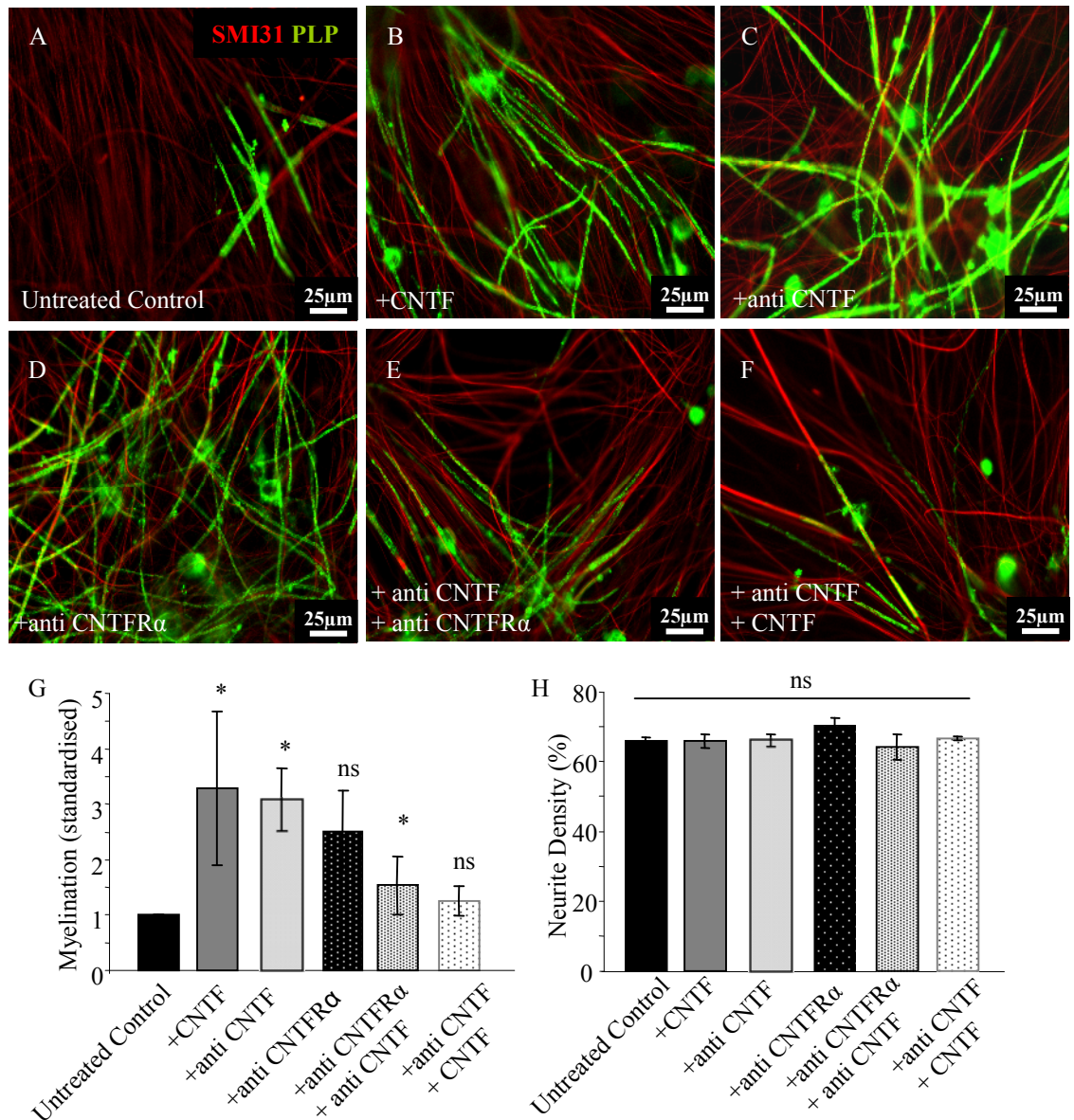


**Figure 5.4 Neutralising CNTF Leads to an Increase in Myelination.** Embryonic spinal cord cells were plated on confluent layer of astrocytes and cultured for 26-28 days. On day 12, cultures were either left untreated (A), treated with CNTF (2 ng/ml, B), treated with ligand neutralising CNTF antibody (4  $\mu$ g/ml, C),  $\alpha$  subunit neutralising antibody (0.2  $\mu$ g/ml, D), both neutralising antibodies at the same concentrations (E) and the CNTF with the ligand neutralising antibody (F). An increase in the amount of myelinated neurites was observed with the addition of CNTF, as previously documented. An unexpected increase in myelination was also observed upon the addition of CNTF neutralising antibodies, although only the ligand antibody was significant to untreated controls (G,  $p < 0.05$ ). Interestingly, the addition of both antibodies together also resulted in an increase in myelination, although not to the same extent as one antibody alone (G,  $p < 0.05$ ). Finally, the addition of both CNTF and its ligand neutralising antibody together results in no change from untreated controls (ns,  $p < 0.05$ ) possibly suggesting that an inactive complex is formed before reaching cell surface CNTFR $\alpha$  subunits. Experiments were performed in triplicates. Scale bar 25  $\mu$ m. Error bars indicate standard error of the mean.

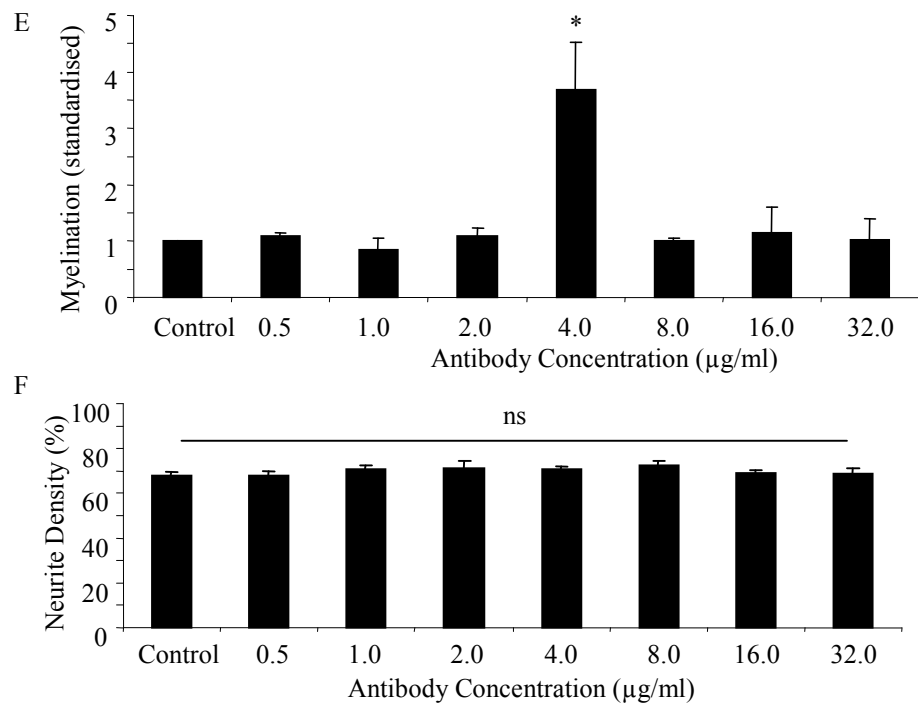
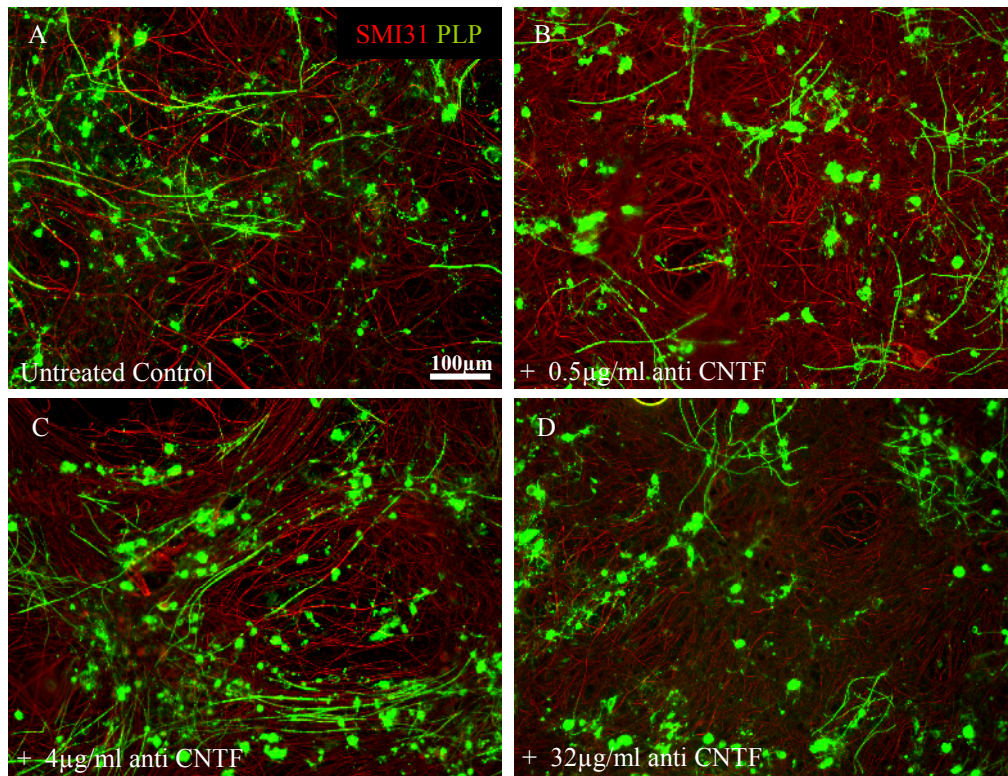


**Figure 5.5 Myelinating is only Increase at 4 µg/ml.** Embryonic spinal cord cells were plated on a confluent layer of astrocytes and cultured for 26-28 days. On day 12, cultures were either left untreated (A) or treated with a range of CNTF ligand neutralising antibody (0.5-32 µg/ml, B-D). An increase in myelination was only detected at 4 µg/ml (E,  $p < 0.05$ ) where all other concentrations had similar amounts of myelination to untreated control. The neurite density was unaffected by antibody treatment at all concentrations (F). Experiments were performed in triplicate. Error bars indicate standard error of the mean. Scale bar 100 µm.

CNTF assayed using an ELISA kit. There is a minor reduction (2-5 pg/ml) in the amount of CNTF within the cultures which have been treated with neutralising antibody compared to untreated controls (Fig 5.6). A few questions remain unanswered, including i) is the minor reduction in CNTF biologically relevant, ii) is the neutralising antibody functional since the reduction is so low and iii) since there is no information of CNTF values throughout the culture period, it is not known whether the cultures 'compensated' for the loss of CNTF via negative feedback mechanisms.

#### **5.2.4 CNTF and anti-CNTF May act via Different Pathways**

Although high concentrations of CNTF and treatment with the neutralising antibodies result in an increase in myelination when compared to untreated controls (Fig 4.2 and Fig 5.4) it is not known if they act via the same mechanisms. In order to clarify their mechanisms of action, treatments were started at either day 12 (internal control), 18 or 24. Treatments were given every 2-3 days until the end of the culture period. Experiments in which CNTF treatments began on day 12 and not at 18 or 24 produced the most myelinated axons (Fig 5.7, B-D, H). In experiments when the neutralising antibody was added at the various time points it was seen that maximal myelination was seen if treatment started on day 12 and 18, but not 24 (Fig 5.7 E-G, H), although only addition at day 12 was significant ( $p < 0.05$ ). The neurite density of all treatments at all time-points did not differ (Fig. 5.7 I). Although the mechanism of action for the growth factor and its neutralising antibody are yet to be identified, this data may suggest that there may be different mechanisms of action for CNTF and its neutralising antibody.

#### **5.2.5 Neutralising Antibodies and Oligodendrocyte Differentiation**

In order to examine whether the addition of neutralising antibodies to CNTF (anti-CNTF) lead to oligodendrocyte differentiation, cultures were treated on day 12, and fixed and immunolabelled at 24 hours, 6 and 12 days post-treatment (Fig 5.8). The panel of markers used included A2B5, perinatal oligodendrocyte progenitor cell, NG2, an early to middle progenitor marker and O4, a middle to late progenitor marker which is also expressed by myelinating oligodendrocytes (see Fig 1.2).

The percentage of A2B5+ cells in the culture at 24 hours and 6 days post anti-CNTF treatment were similar to the untreated condition (Fig 5.8 A). At 12 days post treatment,

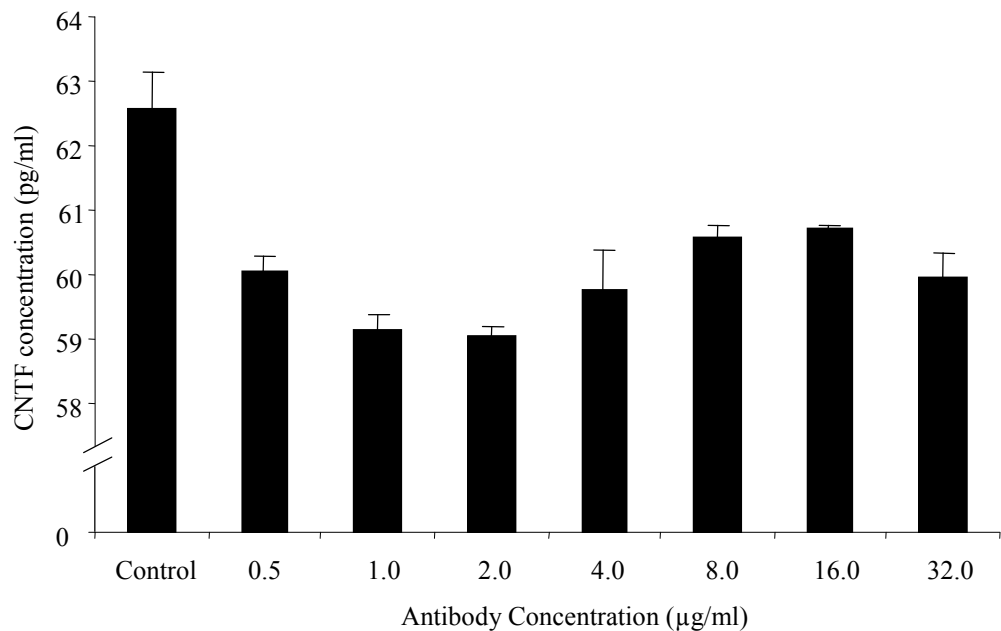


**Figure 5.6 Antibody Treatment Leads to Slight Reduction in CNTF in Media from Cultures.** Embryonic spinal cord cells were plated on a confluent layer of astrocytes and cultured for 26-28 days. On day 12, cultures were either left untreated or treated with a range of CNTF ligand neutralising antibody concentrations (0.5-32 µg/ml) throughout the culture period. On day 26, the media from cultures was collected and assayed for CNTF using a commercially available kit (R&D Systems). There is a slight reduction in the amount of CNTF in the media after antibody treatment (2-5pg-ml). Experiments was performed in duplicate. Error bars indicate standard errors of the mean.

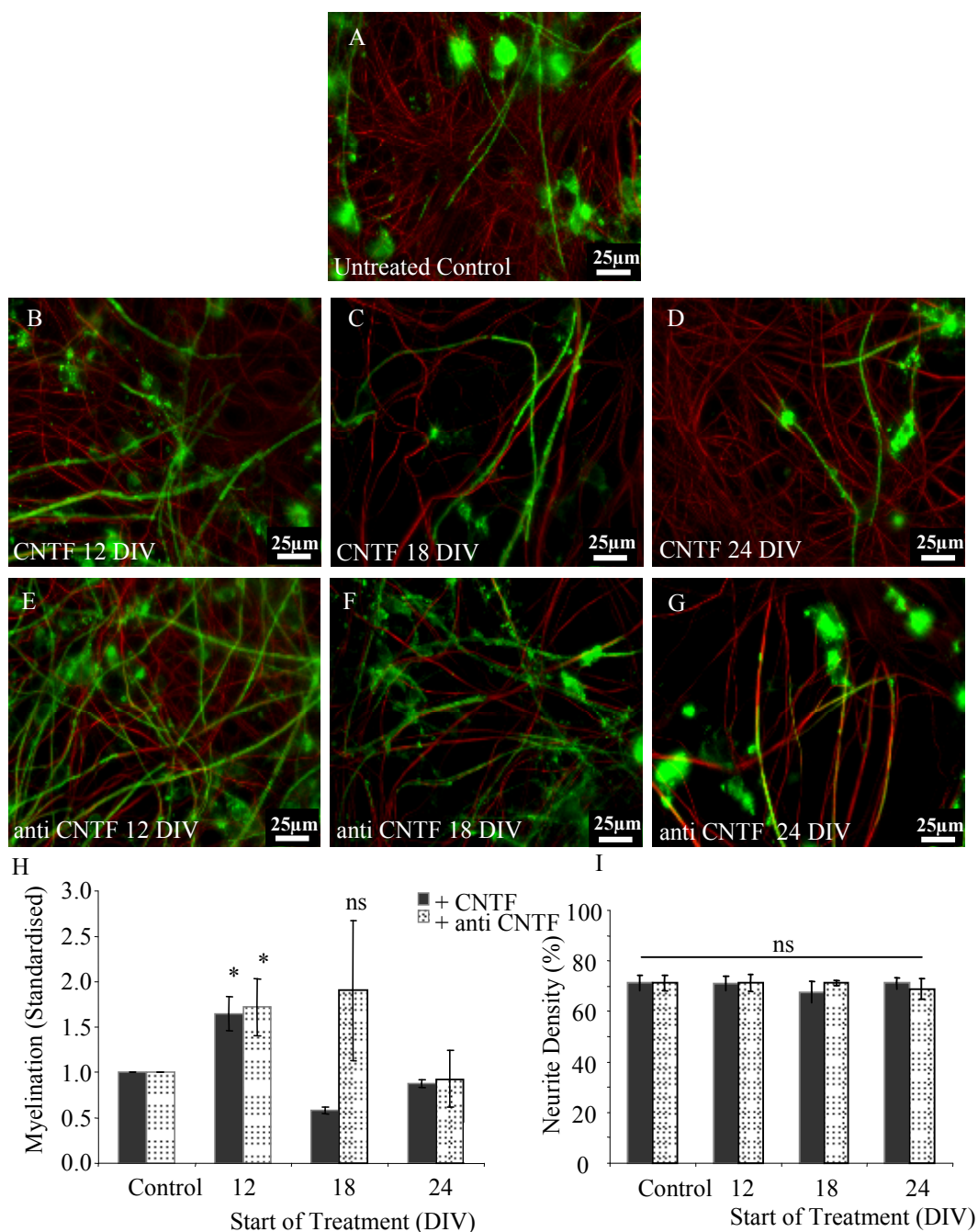


**Figure 5.7 Addition of CNTF and anti CNTF at Different Time Points Suggests that there may be Two Different Mechanisms for their Actions.**

Embryonic spinal cord cells were plated on confluent monolayer of astrocytes and left untreated (A) or treated CNTF (B-D) and anti CNTF (ligand neutralising antibody, E-G), beginning treatment on either Day 12 (B, E), 18 (C, F) or 24 (D, G), and continuing onwards until day 26-28. As previously observed, there was an increase in both CNTF and anti-CNTF when added on day 12 (H,  $p < 0.05$ ). For CNTF, no increase was observed when addition was on day 18 or 24 *in vitro* (DIV). However, the addition of anti-CNTF on day 18 resulted in an increase in myelination but this was not found to be statistically different (H, ns  $p < 0.05$ ). No change in myelination was observed when anti-CNTF was added on day 24. Neurite density was unchanged compared to untreated controls in the CNTF and anti CNTF treatments (I). Experiments were performed in triplicate. Error bars indicate the standard error of the mean.

there is a large reduction in the number of A2B5+ cells in the culture system with treatment (Fig 5.8 A,  $p < 0.05$ ). This data indicates that treatment with neutralising antibodies promoted the differentiation of A2B5+ cells into more mature cells. However, it can not be ruled out that treatment may also lead to the premature death of excess A2B5+ cells. NG2+ cells levels remain relatively consistent with a significant increase at 6 days post treatment (Fig 5.8 B,  $p < 0.05$ ). The percentage of NG2+ cells at 12 days post treatment is slightly higher in the untreated condition compared to that in treatment. These cells may represent the peak increase seen in A2B5 cell population at 12 days post treatment. Finally, the percentage of O4+ cells in the culture was consistent throughout the culture period (Fig 5.8 C), although there is an initial increase of O4+ in the treated condition (Fig 5.8 C,  $p < 0.05$ ). Although the data initially suggests that there is a reduction in the progenitor cell population and therefore a larger pool of differentiated cells able to myelination, this can not be the case as the O4+ percentages per view are similar in both treated and untreated conditions. It is hypothesised that oligodendrocytes in the treated condition are 'primed' for more efficient myelination, i.e. more myelinating processes per oligodendrocytes, explaining why there are similar numbers of O4+ labelled cells at the end of the culture.

### **5.2.6 Antibodies to CNTF do not lead to an Increase in Proliferation**

The withdrawal of CNTF from the culture system may be inducing the proliferation of oligodendrocytes and therefore increasing the number of cells capable of myelinating. Myelinating cultures were set up and neutralising antibodies were added on day 12 along with BrdU. Day 12 was chosen as it is the day CNTF is normally added to the cultures, which results in an increase in myelination. The cultures were then fixed and immunolabelled with the O4 antibody, anti BrdU and DAPI (Fig 5.9 A, B). Three experimental repeats were performed, taking 5 random images from each experiment and cells counted. The mean number of cells expressing the O4 antibody (O4+) cells was similar in both treated and non-treated conditions ( $29 \pm 3$  and  $24 \pm 1.7$ , respectively). Crucially, O4+ cells which were also BrdU+, the proliferating oligodendrocyte population, were slightly higher in numbers in the treatment compared to the controls ( $1.6 \pm 0.45$  and  $2.8 \pm 0.9$ , respectively, Fig 5.9 C), although this was not found to be statistically different ( $p > 0.05$ ).

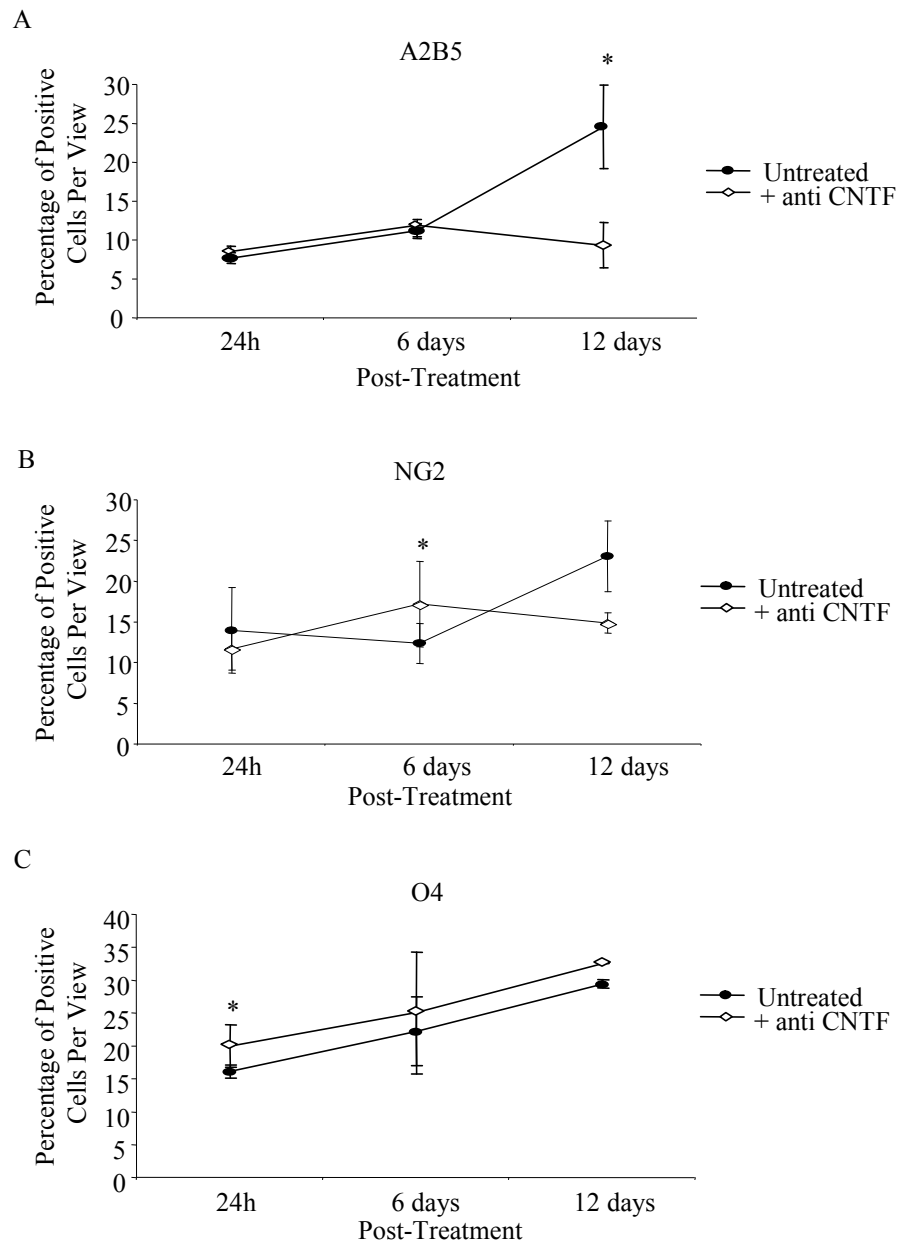


**Figure 5.8 Addition of anti-CNTF does not lead to an Increase in O4+ Oligodendrocytes.** Embryonic spinal cord cells were plated on a confluent monolayer of astrocytes. On day 12, cultures were either left untreated or treated with anti-CNTF. The cultures were fixed and immunolabelled 24 hours, 6 or 12 days post the beginning or treatment with A2B5 (A), NG2 (B) or O4 (C). The number of positive cells were expressed as a percentage of the total cells were view (DAPI count) and the mean per view for each time-point is plotted. With treatment, there is a large decrease in A2B5+ cells at 12 days post treatment (A,  $p < 0.05$ ). NG2+ cell population was relatively unchanged, but there was an increase in NG2+ cells on day 6 post treatment. Finally, the O4+ cell population peaks with anti-CNTF treatment at 24 hours post treatment ( $p < 0.05$ ) but then remains consistent between untreated and treated cultures. Experiments were performed in triplicate. Error bars indicate standard error of the mean.

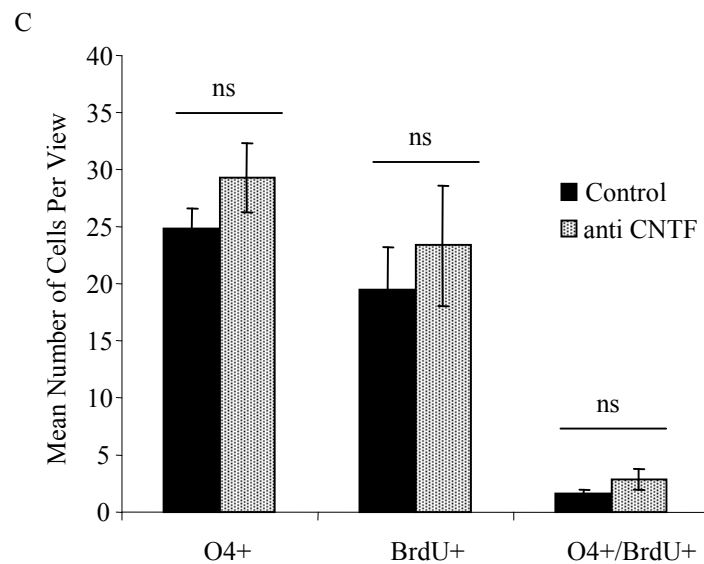
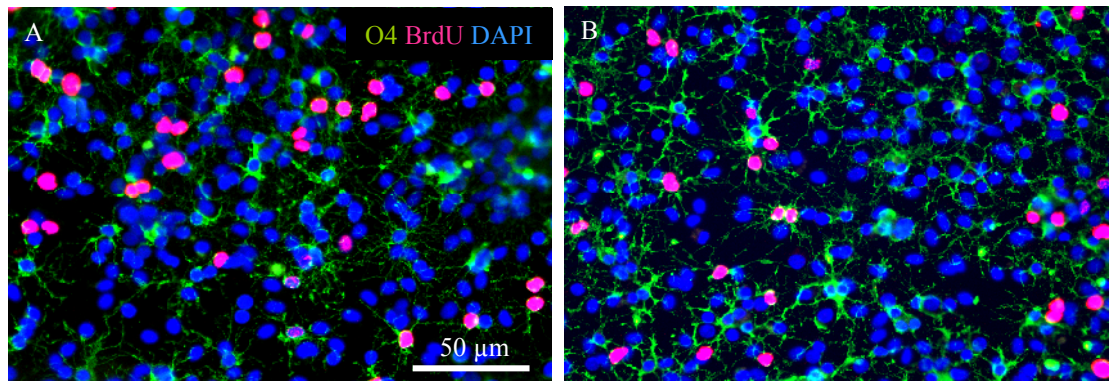


**Figure 5.9 Addition of anti-CNTF does not lead to the Proliferation of O4+ cells.** Embryonic spinal cord cells were plated on a confluent monolayer of astrocytes. One day 12, cultures were either left untreated (A) or treated with anti-CNTF (B) on day 12. BrdU was also added to both cultures on day 12. On day 13, the cultures were fixed and immunolabelled with O4 and anti-BrdU and counted and number were represented as mean number of cells per view. There was no difference between untreated control cultures and anti-CNTF treatment in the total number of O4 cells and BrdU+ cells (C,  $p > 0.05$ ). The numbers of proliferating oligodendrocytes (O4+/BrdU+) were also similar in both conditions (C,  $p > 0.05$ ). Scale bar 20  $\mu\text{m}$ . Experiments were performed in triplicates. Error bars indicate standard error of the mean.

#### **4.2.7 Neutralisation of CNTF may lead to a slight increase in Microglial Activation**

It has already been observed that the addition of exogenous CNTF does not lead to a change in numbers of activated microglia in the myelinating cultures (Fig 4.6). The next question is to investigate what happens when neutralising antibodies are added to the cultures. Myelinating cultures were treated with anti-CNTF from day 12 onwards. The cultures were then fixed and immunolabelled with ED1, a marker for activated microglia (Fig 5.10 A, B). There is an increase in both number of nuclei and in the number of ED1+ cells in the cultures with treatment (Fig 5.10 C,  $p < 0.05$ ). However, when the ED1+ population was expressed as the total number of DAPI+ cells, there was no difference to the untreated condition (Fig 5.10 D).

#### **5.2.8 LIF and anti-LIF Increase Myelination**

All IL-6 cytokine family members signal via gp130 and may therefore compensate for each other (Drögemüller et al., 2008). Therefore, it is possible that the neutralisation of CNTF could allow other members of the IL-6 family to act on the gp130/LIFR $\beta$  receptor complex. Leukemia inhibitory factor (LIF) is also known to be secreted by astrocytes (Ishibashi et al., 2006) and was thus chosen as a candidate to add to the myelinating cultures. Its addition (2 ng/ml) resulted in a slight increase in myelination and neurite density (Fig 5.11 B, F, G), although the increase in myelination was not significant. The increase in neurite density was not observed with CNTF or anti-CNTF. To examine whether its neutralising antibody (anti-LIF) leads to a similar increase in myelination as the CNTF antibody, it was added to the cultures alone and with anti-CNTF. Both treatments resulted in a significant increase in myelination (Fig 5.11 C, D, F) compared to untreated control (Fig 5.11 A,  $p < 0.05$ ), suggesting a similar mechanism of action to CNTF although the levels of myelination were less. There was no increase in myelination when both CNTF and LIF were added into the cultures (Fig 5.11, E, F). This observation is similar to the addition of CNTF at 20 ng/ml (Fig 4.2) suggesting that an excess of IL-6 cytokines does not promote myelination at such excessive concentrations. Other conditions did not affect the neurite density (Fig 5.11 G). Thus, members of the IL-6 family may have a bi-phasic mechanism of action where their addition at high (but not supra-maximal) levels as well as very low levels induced by their neutralisation leads to an increase in myelination.

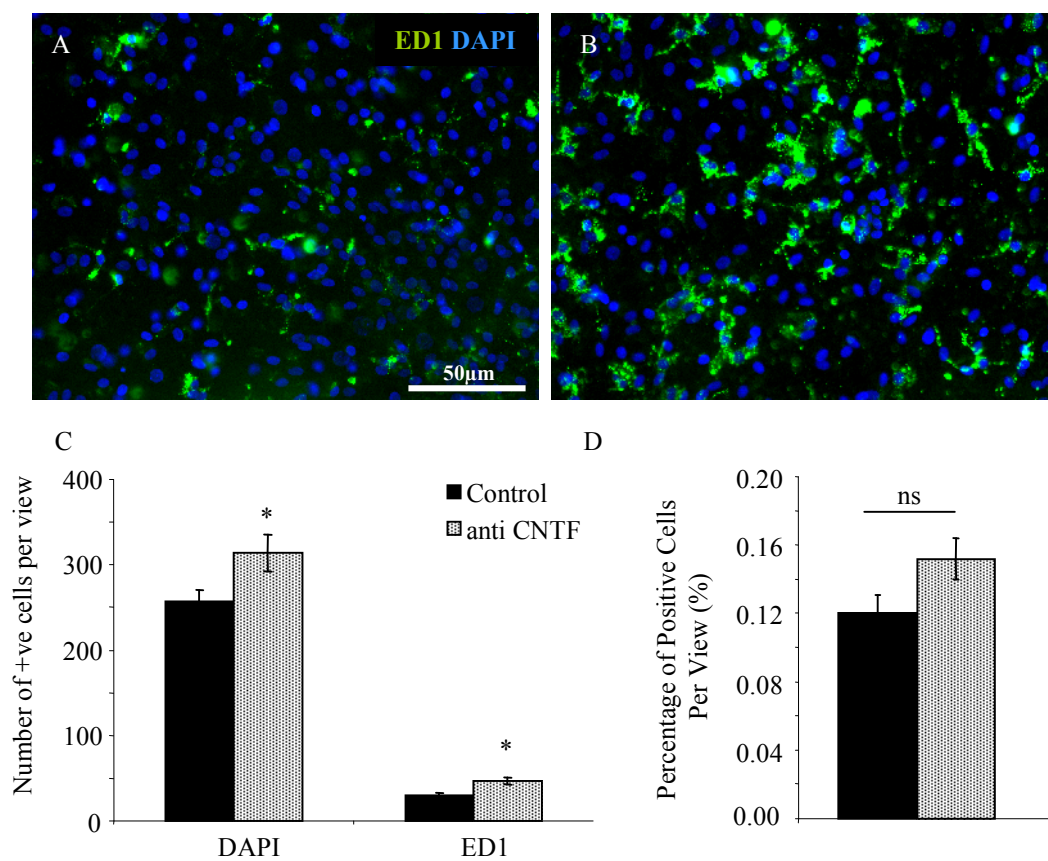


**Figure 5.10 anti-CNTF does not Increase the Number of Activated Microglia.** Embryonic spinal cord cells were plated on a confluent monolayer of astrocytes. On day 12, cultures were either left untreated (A) or treated with anti-CNTF (B) on day 12 onwards. On day 26-28, cultures were fixed and immunolabelled with ED1, a marker for activated oligodendrocytes and DAPI. The number of ED1+ cells per view were counted and represented as mean number of cells per view (C) and expressed as percentage of total cell number (D). There is an increase in both DAPI and ED1+ cells with treatment with anti-CNTF (C,  $p < 0.05$ ). However, when expressed as percentage of total cell number, there was no difference between conditions. Scale bar 50 μm. Experiments were performed in triplicate. Error bars indicate standard error of the mean.

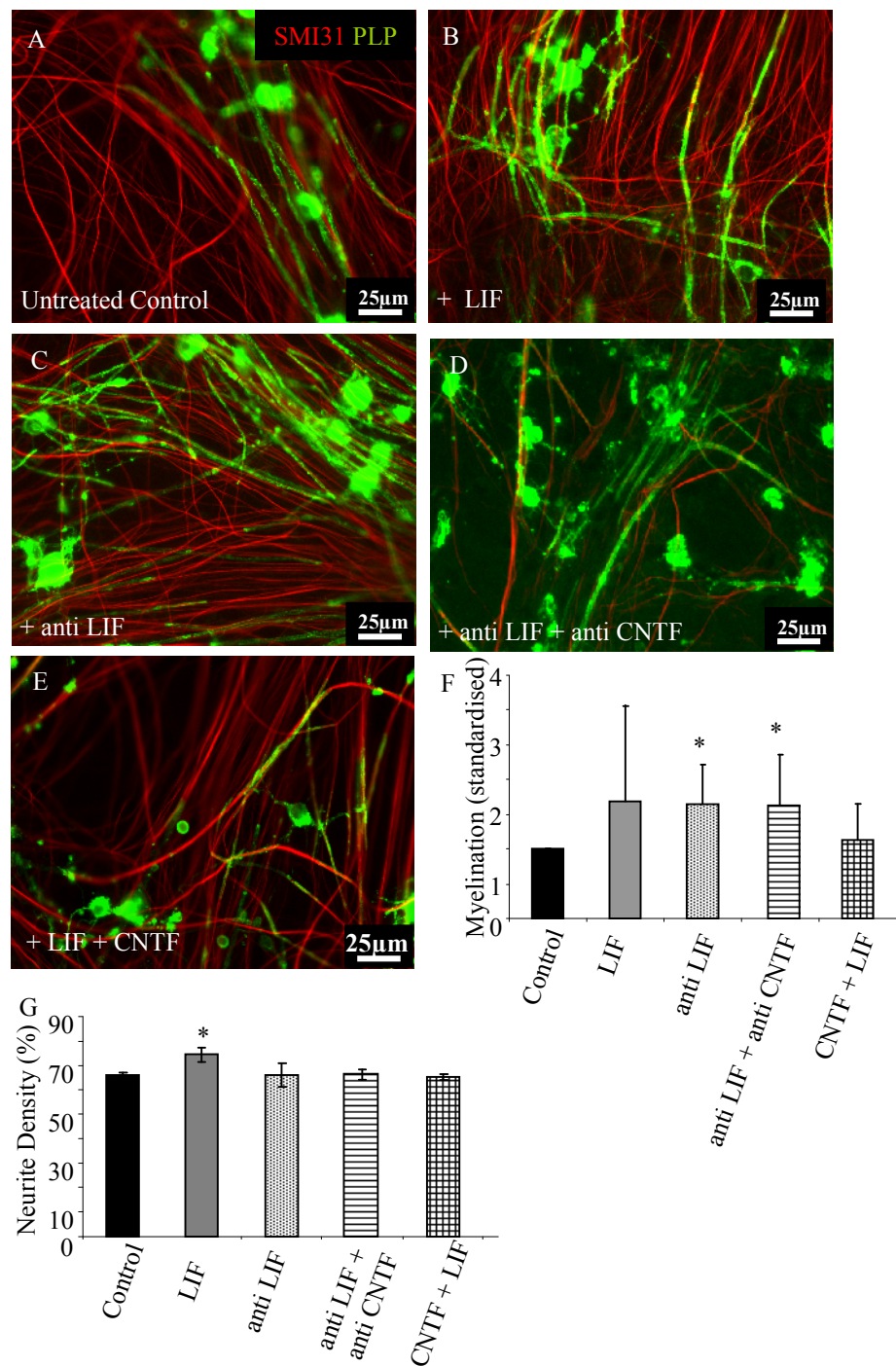


**Figure 5.11 anti-LIF addition leads to an Increase in Myelination.** Embryonic spinal cord cells were plated onto a confluent monolayer of astrocytes for 26-28 days. On Day 12, cultures were left untreated (A), treated LIF (2 ng/ml, B), LIF neutralising antibody (0.2  $\mu\text{g/ml}$ , C), anti-LIF and anti-CNTF (0.2  $\mu\text{g/ml}$  and 0.4  $\mu\text{g/ml}$ , respectively, D) or LIF and CNTF (both 2 ng/ml, E). Cultures were fixed and immunolabelled with SMI31 for axons and PLP for mature oligodendrocytes and myelin. Addition of LIF resulted in an increase in myelination, although this was not significant (D,  $p > 0.05$ ). Addition of anti-LIF alone and anti-LIF with anti-CNTF together led to an increase in myelination which was significant compared with untreated controls (G,  $p < 0.05$ ). The addition of both LIF and CNTF do not affect myelination (F). Neurite density was similar to untreated controls in all conditions except LIF, where there was a slight increase (G,  $p < 0.05$ ). Experiments were performed in triplicate. Error bars indicate standard error of the mean.

### 5.3 Discussion

CNTF's actions appear to operate in a biphasic fashion on astrocytes. The addition of CNTF increases myelination in a dose dependent manner. In this chapter, the effect of CNTF withdrawal was explored and it was found that the reduction of CNTF in the culture does not affect myelination until a certain amount is withdrawn. This paradigm is illustrated in Figure 5.12. It must be noted that at either end of the spectrum, myelination is not inhibited or reduced, but it is unaffected when compared to untreated cultures. This suggests that the actions of CNTF may only be necessary during injury or disease, where there is a need for secretion of pro-myelination factors, or rather, the reduction of myelin-inhibitory factors. It is not known whether this biphasic effect controls differing descending pathways.

The biphasic affect of CNTF has been previously observed on its actions on adrenergic cells from the neural crest (Sun and Maxwell, 1994). CNTF was added from 0.001 to 10 ng/ml where the increase in adrenergic cells was observed between 0.001-0.01 ng/ml. Unlike the data presented here, at high concentrations of CNTF (10 ng/ml), there was a reduction in number of adrenergic cells when compared to the untreated condition. In another study looking at the differentiation of late retinal progenitors, Bhattacharya et al. (2004) use RT-PCR to show that several genes increase with the addition of CNTF in a dose-dependent manner (10-50 ng/ml). At 0.1 ng/ml and 100 ng/ml (very low and very high), the expression of these genes remained unchanged. The concentration ranges between experiments that elicit responses are different possibly because the cell types used are not the same. This biphasic affect is further strengthened by the observation where the addition of CNTF and LIF together had no affect on myelination when compared to controls. It is therefore suggested that supra-maximal levels of one or a combination of IL-6 cytokines can withdraw their effect on astrocytes leading to the loss of the promyelinating effect.

As CNTF has been reported to activate astrocytes, Ishii et al. (2006) have hypothesised whether its neutralisation could result in an improved regeneration using a model of spinal cord injury. The authors demonstrated that the addition of anti-CNTF during the initial 2 week of injury resulted in a decrease in the number of GFAP+ astrocytes and an increase in number of oligodendrocytes. The authors argue that the neutralisation of CNTF reduces glial astrogliosis and therefore creating a more accommodating environment for regeneration. This is reasonable as the astrocytes within the spinal cord lesion are known

to be in a reactive state (Silver and Miller, 2004). However, untreated astrocytes in the cultures used here are presumed to be 'activated', due to the culture setting and the artificial environment (Section 1.4.6 and East et al., 2009). Thus, can endogenous CNTF be activating astrocytes at a level where they are unable to support myelination? This seems unlikely as the cultures support myelination without CNTF. However, to draw parallels between the study above and our data, it is hypothesised that the addition of CNTF at supra-maximal level ( $> 20$  ng/ml) will activate pathways which lead to the discontinued release of promyelinating factors, though this was not tested. This may make the astrocytes 'reactive' and direct comparison can be made with those seen within the glial scar.

An alternative hypothesis to explain the increase in myelination with CNTF withdrawal is the possible activation of other unknown descending pathways which lead to the secretion of other promyelinating factors. This is supported by a similar bifunctional, concentration-dependent effect which was reported for Schwann cell myelination after neuregulin 1 (Nrg1) treatment (Syed et al., 2010). In this study, the difference in myelination at high and low concentrations of Nrg1 was due to a concentration-dependent differential activation of its receptor. High concentrations activated Erk pathways but low concentrations activated the Akt pathways. A similar mechanism may explain our results with the range of CNTF treatments.

CNTF and anti-CNTF possibly act on different cell types or act at different periods during the development of the myelinating culture. This observation is supported by the varying time-courses of CNTF and anti-CNTF (Fig 5.7). Although CNTF clearly acts on the astrocyte monolayer (Chapter 4), anti-CNTF (withdrawal of CNTF) may be inducing another cell type to elicit an additional response which indirectly leads to the increase in myelination. This hypothesis was not investigated further. To further understand the differences between CNTF and anti-CNTF a more detailed, cell specific look into their signaling pathways is required.

The observation that LIF and its neutralising antibody show an increase in myelination in the myelinating cultures resembles that observed with CNTF and its neutralising antibody. As described previously, IL-6 family members share some receptor components. A theory arose where there may be competition between endogenous IL-6 family of cytokines within the culture for the same receptors (illustrated in Figure 5.13). The neutralising of one cytokine may make it more likely for another to bind. Some cytokines may have higher affinities to the receptor than the cytokines which were neutralised, leading to an

increase in response as a result. For instance, it is hypothesised that the neutralisation of CNTF may allow LIF to bind. As demonstrated, LIF does have promyelinating effects. Thus, the neutralisation of CNTF may lead to the increased activity of LIF, which shows similar increase in myelination when added to the cultures. Furthermore, since the inhibition of both CNTF and LIF also led to an increase in myelination, but not to the same extent as anti-LIF alone, it could be suggested that the neutralisation of two or more cytokines may lead to a 'dampening effect' where the neutralised cytokines may have been more potent.

Although the roles of CNTF in combination with its neutralising antibody and LIF have not been fully deciphered, it can be seen that their roles are complex, varying greatly from concentrations and differing cell types. Preliminary experiments were started using mice cultures to investigate whether CNTF has the same role on mouse cells. In fact, CNTF was found to have a much greater effect on mouse cultures. To further dissect the role of CNTF, transgenic mice which lack astrocyte specific gp130 expression (gp130<sup>-/-</sup>) can be used (Drögemüller et al., 2008). Astrocytes from these animals would be used as a monolayer for myelinating cultures which are then treated with CNTF. It is hypothesised that the pro-myelinating effect CNTF would be lost, as astrocytes would lack the expression of the CNTF receptor subunit gp130. Experiments are underway to investigate this.

### Possible Biphasic Role of CNTF

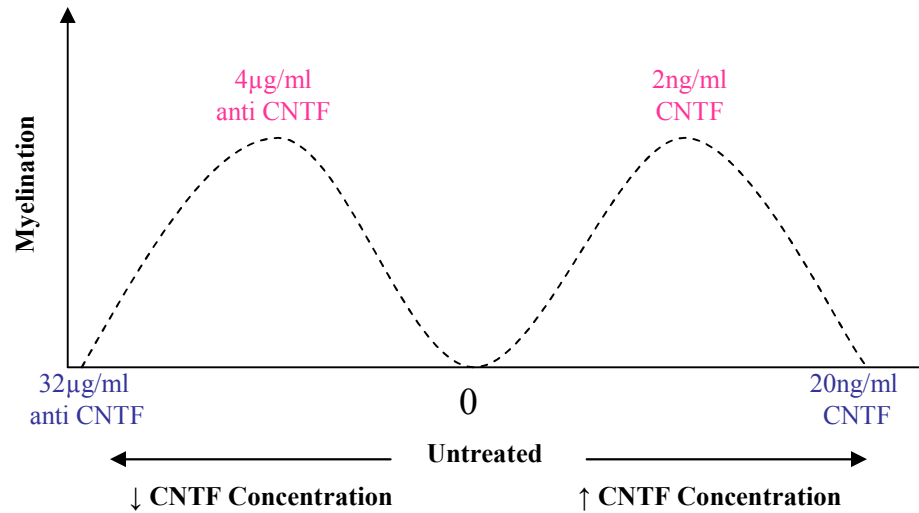


**Figure 5.12 Illustration of the Possible Biphasic Effect of CNTF.** From the data demonstrated here and in Chapter 4, CNTF exhibits a biphasic mechanism of action. The illustration demonstrates myelination (y axis) in relation to CNTF concentration (x axis) where the withdrawal of CNTF before 0 represents further CNTF release due to a negative feedback mechanism from cells in the culture. When very high concentrations of anti-CNTF are added to the cultures, myelination is not affected. However, when a certain amount was withdrawn (4 µg/ml of anti-CNTF) there is an increase in myelination. On the other side of the spectrum, low concentration of CNTF do not affect myelination, however, there is a dose-dependent increase reaching optimal levels when 2 ng/ml of CNTF is added to the cultures. Going beyond the optimal concentration, no increase in myelination is observed.

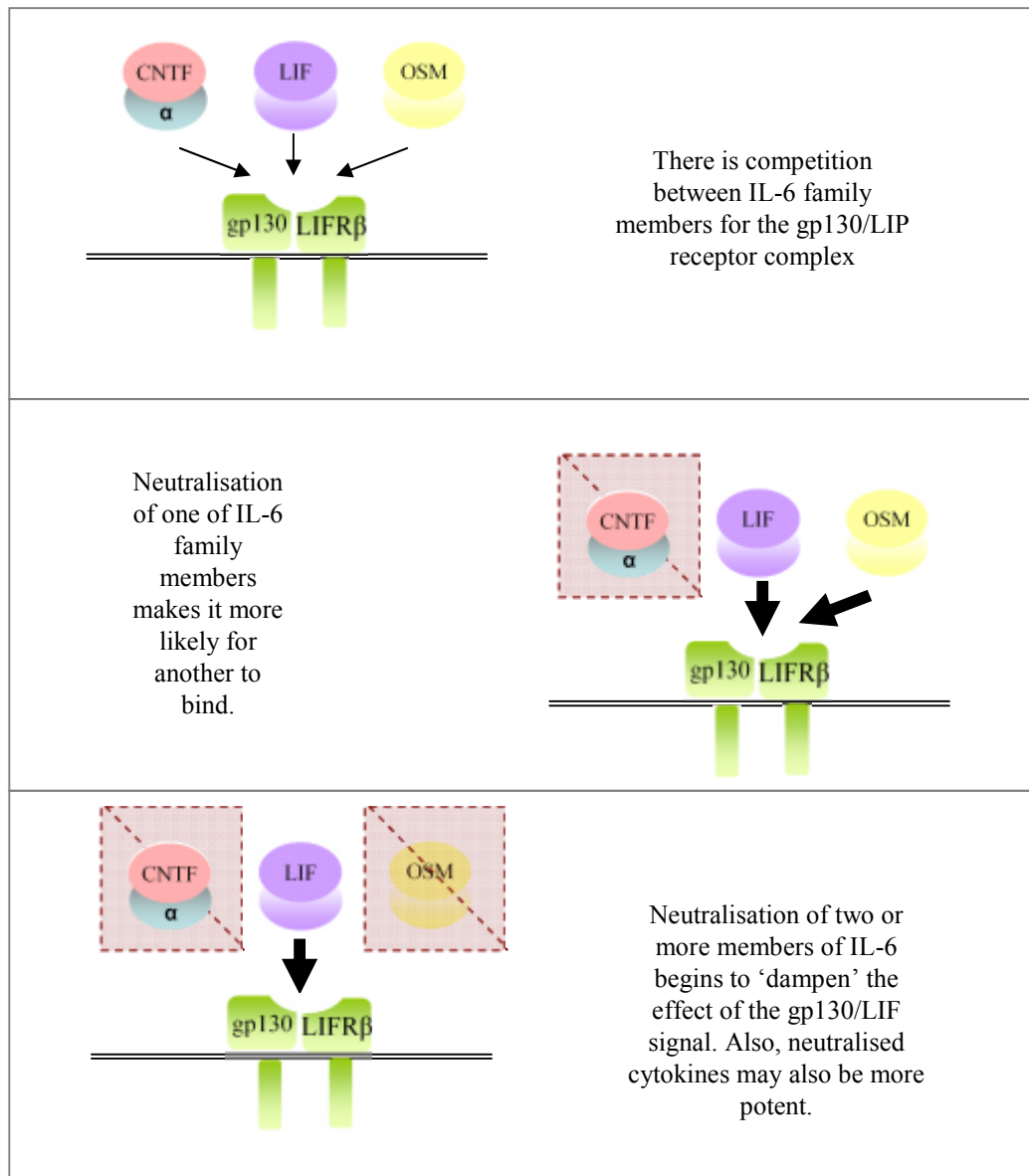


**Figure 5.13 Illustration of the Possible Competition between IL-6 Cytokines.** IL-6 cytokines share receptor components of gp130 and LIFR $\beta$ . Assuming all members are expressed and secreted in the culture, it is possible that there is competition between the cytokines for available receptor subunits. Upon the neutralisation of one cytokine, others cytokines, which may be more potent but have a lower affinity to the receptor are able to bind. For instance, when CNTF is neutralised, OSM or LIF can bind in its place and their actions may be more effective at activating signal transduction mechanisms. Finally, the neutralisation of one or more cytokines may lead to the 'dampening' effect where the neutralised antibodies were more potent and therefore a reduction in the original effect observed.

## **Chapter 6**

# **Changing the Phenotype of the Astrocyte and its Effect on Myelination**

# Changing the Phenotype of the Astrocyte and its Effect on Myelination

---

## 6.1 Introduction

### 6.1.1 Background

Although it has been shown that astrocytes can secrete pro-myelinating factors (previous chapter), it is not clear if in CNS pathology the astrocyte status/phenotype can affect myelination. In the normal CNS, astrocytes are often described as resting or quiescent (Eddleston and Mucke, 1993). In injury or disease, astrocytes respond to the surrounding inflammatory environment by upregulating their expression of cytoskeletal molecules, such as GFAP and nestin, and by secreting cytokines and extracellular matrix molecules (Silver and Miller, 2004; Williams et al., 2007; Sofroniew and Vinters, 2010). As previously described in Section 1.4, the degree of this response determines whether an astrocyte is supportive (activated) or non supportive (reactive) for repair/myelination.

To mimic quiescence, astrocytes were plated on a Tenascin-C substrate (TnC, TnC-astrocytes) in serum-free conditions (Holley et al., 2005). TnC is a highly conserved glycoprotein of the extracellular matrix and is expressed by astrocytes (Kruse et al., 1985; Faissner et al., 1988). During development, TnC expression is high in the cerebellar cortex and reduces over time (Bartsch et al., 1992; Czopka et al., 2009). Levels for TnC mRNA are relatively low in the adult CNS (Zhang et al., 1995; Ferhat et al., 1996) indicating that its role may be primarily developmental and/or pathological. Astrocytes plated on TnC expressed several characteristics of quiescence including a lower expression of molecules associated within the glial scar such as embryonic neural cell adhesion molecule (E-NCAM), epidermal growth factor receptor (EGFR), basic fibroblast growth factor (bFGF) and nestin, compared to astrocytes which are plated on PLL (Holley et al., 2005). Furthermore, the authors showed that TnC-astrocytes had a lower proliferation rate than those on PLL. These observations indicate that Holley et al. (2005) have successfully produced an *in vitro* astrocyte phenotype which resembles astrocytes in the normal CNS.

There have been many studies describing the association of TnC expression with neurite outgrowth and its role in regeneration post CNS injury. To investigate the expression of

TnC on astrocytes when in contact with neurites, Ard and Faissner (1991) cultured astrocytes from newborn rat cerebral cortex and used embryonic rat retina as a source of axonal outgrowth. They found that astrocytes downregulated their expression of TnC when in contact with axons, suggesting that astrocytes control the expression of TnC in order to allow axonal extension. As the expression of TnC is associated with the CNS injury (Niquet et al., 1995), it is interesting to investigate why astrocytes fail to downregulate TnC in these conditions. Indeed, another study has shown that a TnC substrate is inhibitory to axonal outgrowth (Treloar et al., 2009). The authors used a stripe assay, a method widely used to test the extension capability of neurites on different substrates, and use a TnC and poly-D-lysine (PDL) a control substrate. They showed that neurites extending from olfactory epithelium explant stopped extending when they reached the TnC substrate. This study clearly demonstrates neurite outgrowth is inhibited in the presence of TnC. In another study, using an *in vivo* model of reactive gliosis, in which a piece of nitrocellulose was implanted into the cortex of neonatal and adult animals, it was found that the expression of TnC correlated with the astrocytes most proximal to the glial scar, but only in adult animals (McKeon et al., 1991). Furthermore, the glial scar from the lesion of neonatal animals supported neurite outgrowth whereas the adult tissue did not, suggesting that the expression of TnC is highly associated with hindering axonal regeneration after injury. In the neonate, however, astrocytes may have more control over their expression of TnC.

TnC expression has also been implicated in oligodendrocyte survival and maturation. Czopka et al. (2009) demonstrated that when OPCs were grown on a residual ECM substrate taken from TnC-positive astrocytes they failed to differentiate into MBP-positive oligodendrocytes when compared to those grown on control substrate (poly-ornithine). Furthermore, the addition of residual matrix from TnC-negative astrocytes (astrocytes taken from TnC-null mice) was able to ‘rescue’ OPC differentiation, although not to the same extent as the control substrate. In another study, a TnC substrate was shown to be anti-adhesive and anti-migratory to primary rat OPCs (Keirnan et al., 1996).

The presence of TnC evidently has a role in OPC development and migration and axonal survival and extension. Holley et al. (2005) argue that astrocytes plated on TnC have a phenotype that resembles the ‘normal’ astrocyte in the adult CNS, whereas those on PLL are ‘activated/reactive’ and show a more similar profile to those within the glial scar. As outlined in Section 1.4.4, the glial scar is a major impediment for regeneration. The understanding how markers within a glial scar correlate to the phenotype of the astrocyte

and mechanisms by which this may alter processes such as axonal regeneration and oligodendrocyte differentiation may be of key importance in the treatment of CNS disease and injuries.

### **6.1.2 Aims of the Chapter**

The experiments below describe whether modulating the astrocyte phenotype *in vitro* can influence the myelinating capacity of endogenous oligodendrocytes and whether these effects can be reversed using cytokines and astrocyte conditioned media. The aim of this chapter is to assess whether astrocytes plated on TnC are truly ‘quiescent’ and how this phenotype will ultimately affect myelination in our myelinating culture system.

## **6.2 Results**

### **6.2.1 Myelination is Reduced on TnC-Astrocytes**

To assess if modulating the astrocyte phenotype could affect myelination, astrocytes were plated on either PLL (PLL-astrocytes, Fig 6.1 A) or TnC (TnC-astrocytes, Fig 6.1 B) to create an intact confluent monolayer of cells. Dissociated embryonic spinal cord cells were plated on top of these monolayers and myelination (axonal ensheathment) and neurite density was assessed at day 26-28. Neurite density was comparable on both types of astrocytes (Fig 6.1 E,  $p > 0.05$ ) suggesting that neurite extension was unaffected by the TnC substrate. Myelination on TnC-astrocytes (Fig 6.1 D, F) was reduced significantly, compared to myelination found on PLL-astrocytes (Fig 6.1 C, F;  $p < 0.05$ ). This data suggests that the phenotypic state of the astrocyte plays a major role in the capacity of oligodendrocyte to myelinate axons.

### **6.2.2 Astrocytes on PLL and TnC Show Similar Cellular Characteristics**

Since the astrocytes plated on TnC had such a dramatic effect on myelination, several classical astrocytic properties were compared. The purity, proliferation and antigenic characteristics of astrocytes on PLL and TnC substrates were assessed in order to identify differences which may contribute to their myelinating capacity, for instance, an inherently higher number of O4+ in the monolayer cells may contribute to the final number of

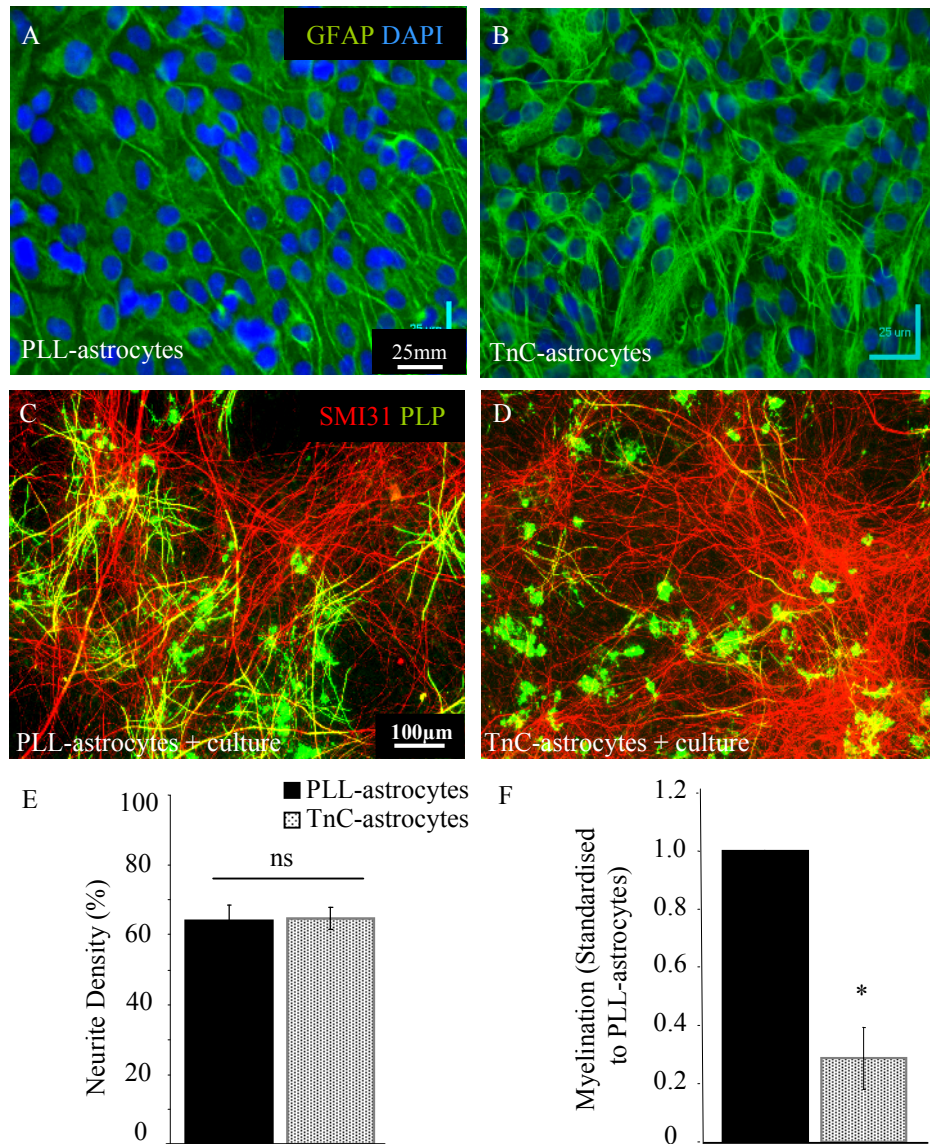


**Figure 6.1 Myelination was Reduced on Astrocytes plated on TnC.** Astrocytes were plated on top of coverslips which were either coated with poly-L-lysine (PLL-astrocytes, A, C) or TnC (TnC-astrocytes, B, D) in DMEM-FBS. Astrocytes were cultured for 7-10 days and some were fixed and immunolabeled with GFAP to check for confluency. When astrocytes were confluent, spinal cord cells (SCC) were plated on top and cultured for 26-28 days. Coverslips were then fixed and immunolabeled with SMI31 (axons, red) and PLP (myelin, green). Neurite density was similar in both conditions (E,  $p > 0.05$ ), whilst the number of myelinated axons was significantly higher on astrocytes plated on PLL compared to those plated on TnC (F,  $p < 0.05$ ). Scale bar 25  $\mu$ m for A and B, and 100  $\mu$ m for C and D. Experiments were performed in triplicate. Error bars indicate standard error of the mean.

myelinating oligodendrocytes. Five images were taken from astrocytes plated on each substrate were taken. An average of  $250 \pm 38$  cells were counted for each substrate, totalling up to an average of  $676 \pm 38$  cells per condition. The mean percentage for GFAP+ cells on PLL and TnC was  $78 \pm 3$  and  $78 \pm 2$  respectively (Fig 6.2 A, C, E). The percentage of O4+ pre-oligodendrocytes constituted  $10 \pm 2.5$  and  $9.59 \pm 2$  for PLL-astrocytes and TnC-astrocytes respectively. The percentage of O4/GFAP positive cells, which were previously described by Black et al. (1993) as astrocytes due to their stellate and process-bearing morphology were also counted;  $2 \pm 1.5$  and  $1.99 \pm 1.48$  for PLL-astrocytes and TnC-astrocytes respectively (Fig 6.2 A, C, E). Tuj1+ cells, a marker for neuron-specific class III beta-tubulin was also counted and found to be similar in both PLL and TnC astrocytes ( $5 \pm 0.7$  and  $8.6 \pm 1.4$ , respectively) (Fig 6.2 B, D, E). No differences in percentages (or number of cells per view, data not shown) were found between PLL-astrocytes and TnC-astrocytes for any of the markers immunolabelled ( $p > 0.05$ ). Tuj1 immunolabeling was for a sister coverslip to O4. The 'other' category represents DAPI nuclei without GFAP or O4 reactivity. The relative percentages of the 'other' category are strikingly similar to those of Tuj1 on the second coverslip ( $12.85 \pm 1.2$  and  $14.7 \pm 2$  for PLL and TnC respectively) suggesting that the majority of non-labelled nuclei on coverslips labelled with the O4 antibody could be Tuj1-positive cells. The O4+ cells counted in both conditions contained a morphologically heterogeneous population of cells including small branched pre-oligodendrocytes (Fig 6.2 F) and oligodendrocytes with a sheath-like appearance (Fig 6.2 G). Likewise, Tuj1 cells also exhibited different morphologies; simple bipolar-like cells (Fig 6.2 H) and highly branched cells (Fig 6.2 I).

### **6.2.3 Astrocytes on PLL Resemble the 'Activated' Phenotype**

In response to damage, CNS tissue will undergo some form of astrocytosis, whereby astrocyte morphology, size and secretory profile changes from that of a resting astrocyte to a reactive astrocyte. The characteristics of PLL-astrocytes and TnC-astrocytes were compared to assess essential differences in size, antigenic phenotype and proliferation. No change in proliferation was found between PLL-astrocytes and TnC-astrocytes (Fig 6.3 D), although PLL-astrocytes were larger than those plated on TnC (Fig 6.3 C,  $p < 0.05$ ). Furthermore, PLL-astrocytes had higher levels of nestin immunoreactivity ( $p < 0.05$ ) when compared to TnC-astrocytes. In addition, a greater number of astrocytes on PLL were nestin-positive compared to those plated on TnC (Fig 6.3 E,  $p < 0.05$ ). Nuclei diameter as assessed using DAPI staining was larger in PLL-astrocytes than TnC-astrocytes (Fig 6.3 G,  $p < 0.05$ ). An increase in size, nucleus diameter and nestin expression are characteristics typical an 'activated' astrocyte phenotype whilst the reduction of nestin

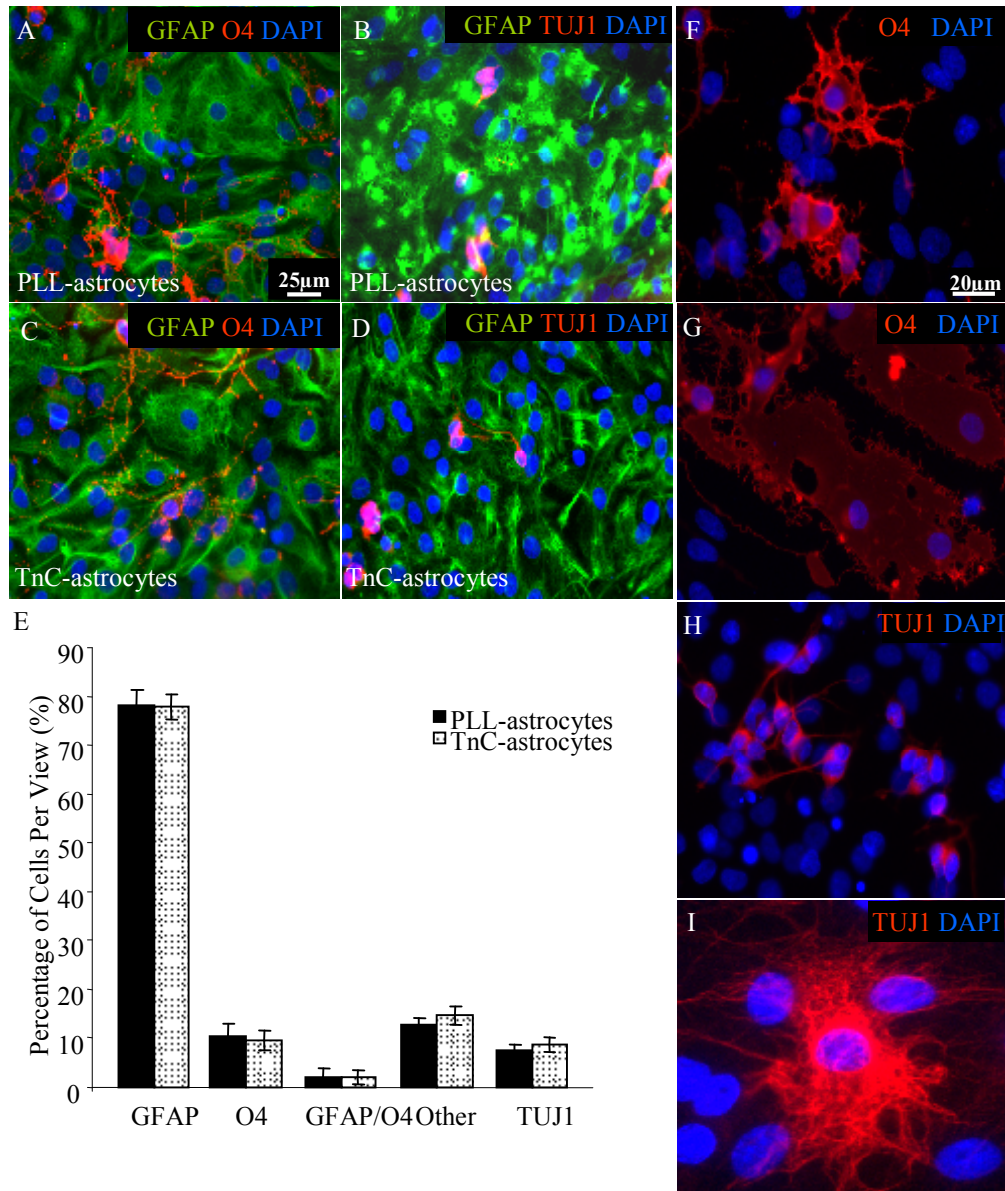


**Figure 6.2 Cellular Characteristics of Astrocytes on PLL or TnC are Similar.** Astrocytes were plated on top of coverslips which were either coated with poly-L-lysine (PLL-astrocytes, A, C) or TnC (TnC-astrocytes, B, D) in DMEM-FBS and cultured for 7-10 or until confluency. Coverslips were then immunolabelled with GFAP (intermediate filament for astrocytes, green), O4 (pre-myelinating oligodendrocyte, red) or TUJ1 (neuron-specific class III beta-tubulin, red). Images were taken for all markers and a positive cell for a particular marker was expressed as a percentage of the total DAPI count. There were no differences in the number of GFAP, O4, GFAP/O4 and TUJ1 cells between astrocytes plated on PLL and on TnC (E, paired t-test,  $p > 0.05$ ). Heterogeneous populations of O4 and TUJ1 cells were observed on both substrates (F-I, all images from PLL substrate). Scale bar 25  $\mu\text{m}$  for A-D and 20  $\mu\text{m}$  for F-I. Experiments were performed in triplicate. Error bars indicate standard error of the mean.

observed in TnC-astrocytes is typical of ‘quiescent’ in accordance with observations by Holley et al. (2005).

#### **6.2.4 TnC-Astrocytes as a Substrate for Myelinating Cultures; Can TnC Directly Influence Oligodendrocyte Differentiation?**

As TnC has been shown to inhibit oligodendrocyte differentiation (Czopka et al., 2009), it is not known whether or not the TnC substrate for astrocytes is exposed to developing OPCs present in the myelinating culture and therefore limiting their differentiation. In order to assess true confluency, phalloidin, a toxin which binds to F-actin, the filamentous protein in the cytoskeleton, was used to visualise the extent of confluency in astrocytes on PLL and TnC. It can be seen from Figure 6.4 that GFAP grossly underestimates the size of the cell. Using phalloidin to visualise astrocytes, it can be seen that astrocytes cover more space than when using GFAP (Fig 6.4 A-F arrows) on both PLL and TnC substrates. However, due to the nano-scale nature of such molecules, it can not be assumed that TnC can not still penetrate through the F-actin filaments.

#### **6.2.5 Expression of TnC is Comparable on PLL-Astrocytes and TnC-Astrocytes**

It is possible that astrocytes ‘take-up’ the TnC substrate and re-express it on their surface, which could result in an inhibition of oligodendrocyte differentiation leading to a lower level of myelination. TnC surface expression was similar in both PLL and TnC astrocytes by immunohistochemistry (Fig 6.5 A, B). Comparison of TnC levels by Western blot of astrocytes plated on PLL and TnC show that there is no difference in TnC expression (Fig 6.5 E, F). Arbitrary units of the bands (Fig 6.5 F) were measured in Image J from 3 separate experimental blots. As TnC has been described as an inhibitory molecule to neurite outgrowth (McKeon et al., 1991), SMI31-reactivity was confirmed to be similar on astrocytes plated on either substrate, as a dense expanse of SMI31 positive neurites can be seen (Fig 6.5 A, D and Fig 6.1 C, D). TnC-astrocytes are therefore not inhibitory to neurite outgrowth. Rather, astrocytes grown on TnC compared to PLL may differ in their expressional and/or secretory profile.

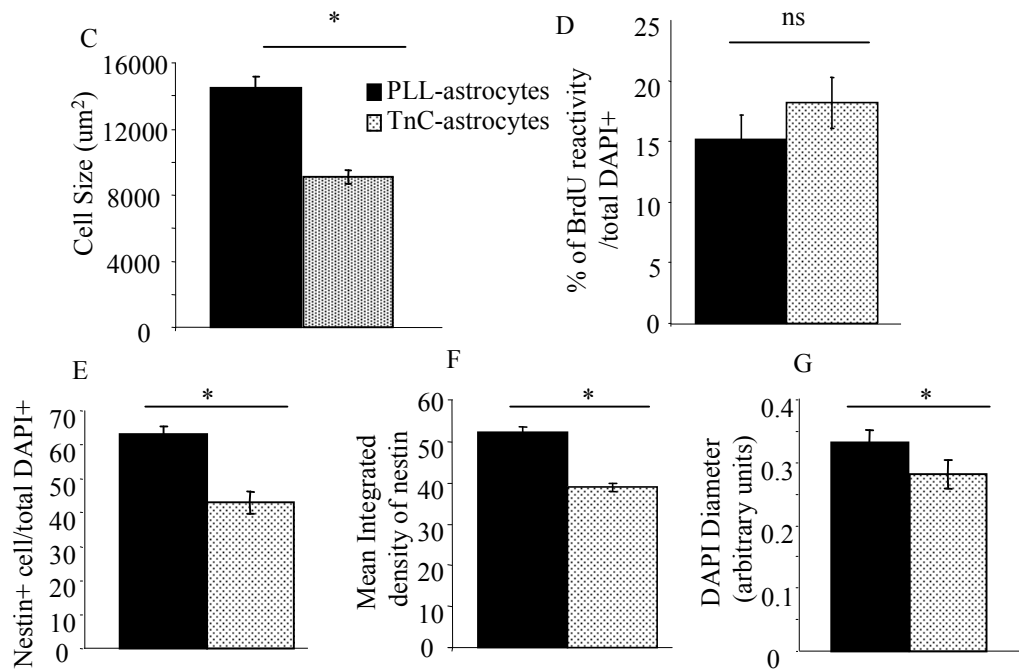
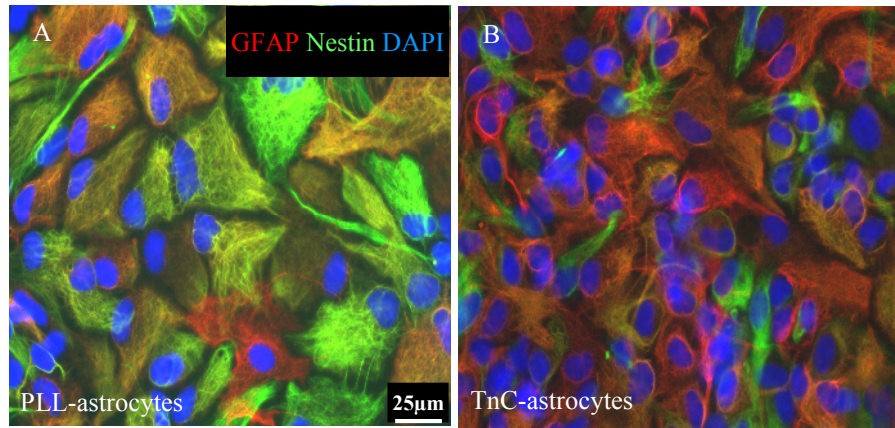


**Figure 6.3 Astrocytes plated on PLL Exhibit an ‘Activated’ Phenotype whilst those on TnC Exhibit a ‘Quiescent’ Phenotype.** Astrocytes were plated on top of PLL (A) or TnC (B) coated coverslips. Bromodeoxyuridine (BrdU) was added to coverslips for 18-24 hours, then fixed and immunolabelled with anti-BrdU. Sister coverslips were directly fixed and stained for GFAP and nestin expression. The numbers of positive cells per marker were counted as percentage of total DAPI count. Cell size, DAPI size and integrated density were measured. Astrocytes on PLL have a significantly larger area and DAPI diameter to those on TnC (C, G). Astrocytes on PLL also had a greater number of nestin positive cells and a larger nestin integrated density than astrocytes on TnC (E, F). There was no difference in rate of proliferation between PLL-astrocytes and TnC-astrocytes (D). Scale bar 25 µm for A and B. Experiments were carried out in triplicate. Error bars indicate standard error of the mean.

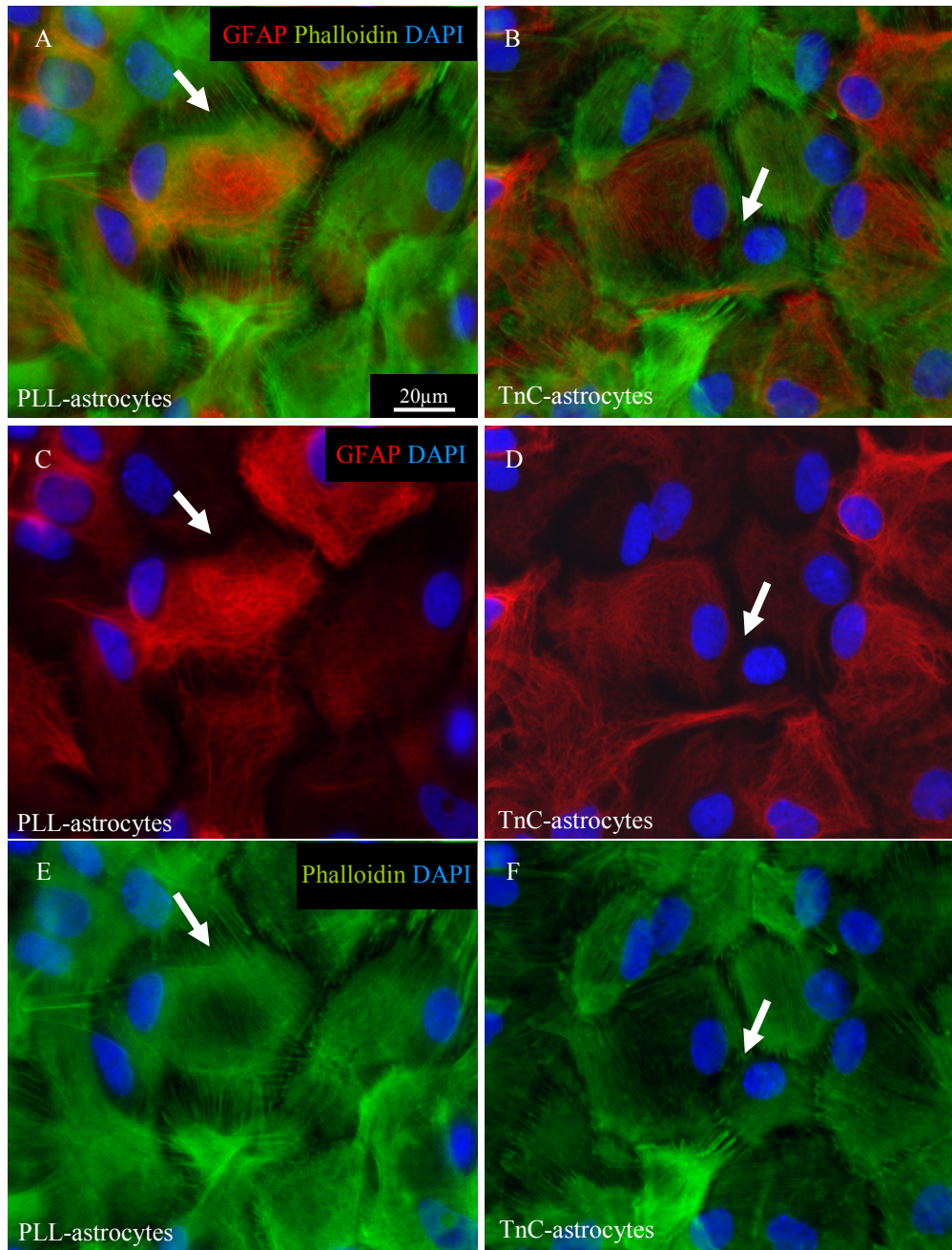


**Figure 6.4 Confluency is Achieved when Astrocytes are plated on PLL or TnC.** Astrocytes were plated on top of coverslips which were either coated with poly-L-lysine (A, C, E) or TnC (B, D, F) in DMEM-FBS and cultured for 7-10 or until reaching confluency. Cells were fixed and immunolabelled with GFAP and phalloidin. Astrocytes visualised with Phalloidin cover more space than GFAP (A-F arrows) on both PLL and TnC conditions. Scale bar for A-F 20  $\mu\text{m}$ .

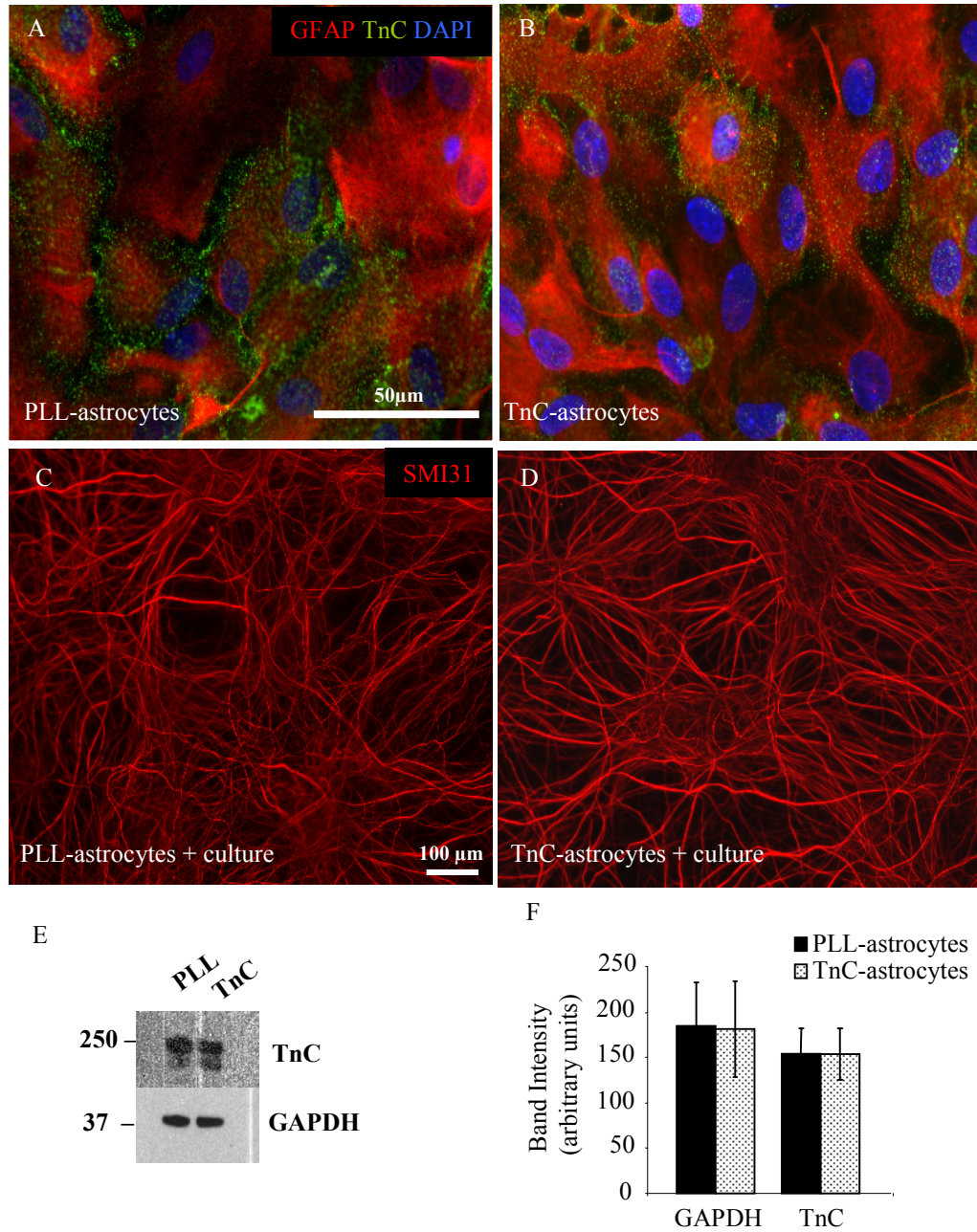


**Figure 6.5 Plating Astrocyte on a TnC Substrate Does Not Affect Neurite Extension or Expression of TnC on Astrocytic Surface.** Astrocytes were plated on coverslips which were either treated with PLL (A) or TnC (B) in DMEM-FBS. The cells were fixed and immunostained with GFAP and TnC. Spinal cord cultures were added to PLL or TnC monolayers and cultured for 26-28 days and then fixed and stained for SMI31 (C, D respectively). Sister astrocyte monolayers were lysed and immunoblotted for TnC and GAPDH expression (E) and the intensity of blots was quantified from 3 experiments (F). Astrocytes did not express higher levels of TnC when plated on a TnC substrate (A, B). Axonal extension was unaffected by either substrate. Scale bar 50  $\mu\text{m}$  for A-D and 100  $\mu\text{m}$  for E and F.

### **6.2.6 Quiescent Astrocyte Phenotype can be Overcome by Activated Astrocyte Conditioned Media or CNTF**

To assess if the quiescent ‘status’ of the astrocytes could be overcome, cultures were treated in several ways. Two groups of cultures were set up: i) classical myelinating cultures placed on PLL-astrocytes and ii) myelinating cultures placed on TnC-astrocytes. Each group contained control non treated cultures (Fig 6.6 A, D); addition of 2 ng/ml CNTF (images not shown); addition of a monolayer of astrocytes plated on the opposite monolayer than its grouping, i.e. TnC-astrocytes were used to condition a myelinating culture on PLL-astrocytes (and vice versa); and lastly PLL-astrocytes which were pre-treated with CNTF (2 ng/ml) for 24-28 hours and washed with PBS before being placed in the same Petri dish as myelinating cultures (see Methods Section 2.1.4). It can be seen that CNTF alone or after pretreating astrocytes led to an increase in myelination in both groups (Fig 6.6 G). TnC-astrocytes allowed to condition a typical myelinating culture (culture on PLL-astrocytes) did not affect the resulting levels of myelination (Fig 6.6 B, G) but PLL-astrocytes allowed to condition a myelinating culture plated on TnC-astrocytes increased the level of myelination (Fig 6.6 E, G) possibly by secreting CNTF (Chang et al., 2003). Thus, astrocytes plated on TnC appear to inhibit myelination which could then be overcome by CNTF treatment. The effect appears to be via the expression of a molecule rather than a secretory factor, as conditioning a culture on PLL with TnC conditioned media does not lead to a reduction in myelination. The axonal density of all groups and conditions was similar (Fig 6.6 H). It is therefore suggested that if astrocytes on TnC can be termed ‘quiescent’ then myelination is affected by this astrocyte phenotype.

### **6.3 Discussion**

Astrocytes on TnC show characteristics of quiescence and this has been shown to be inhibitory to myelination, *in vitro*. No differences were found in monolayer composition between those quiescent (TnC-astrocytes) and activated astrocytes (PLL-astrocytes). The reduced level of axonal ensheathment by oligodendrocytes on quiescent astrocytes is reversible upon the addition of activated-astrocytes conditioned media or by the cytokine CNTF.

Holley et al. (2005) achieved quiescence not only by plating astrocytes on a TnC substrate but also by serum deprivation. It has also been demonstrated that Bone Morphogenetic

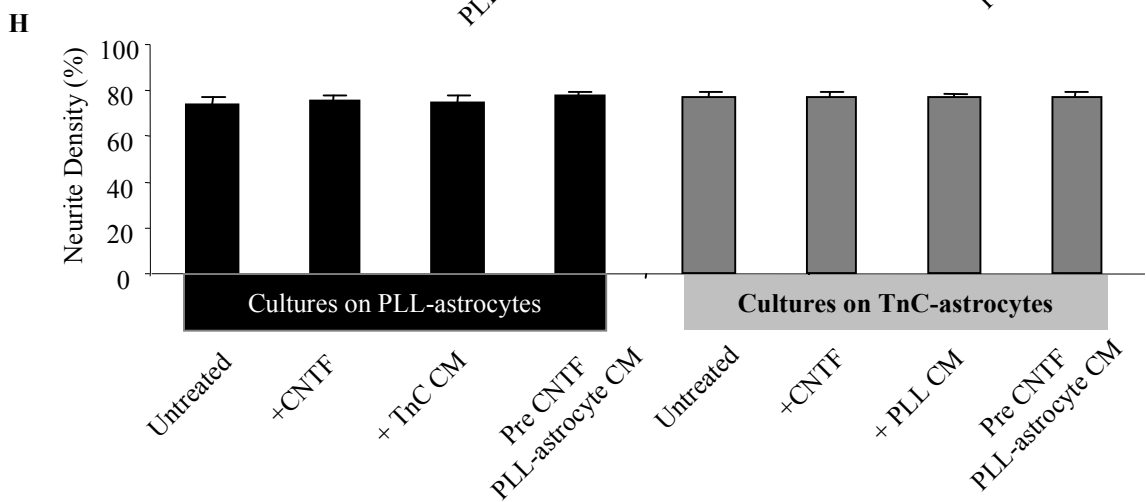
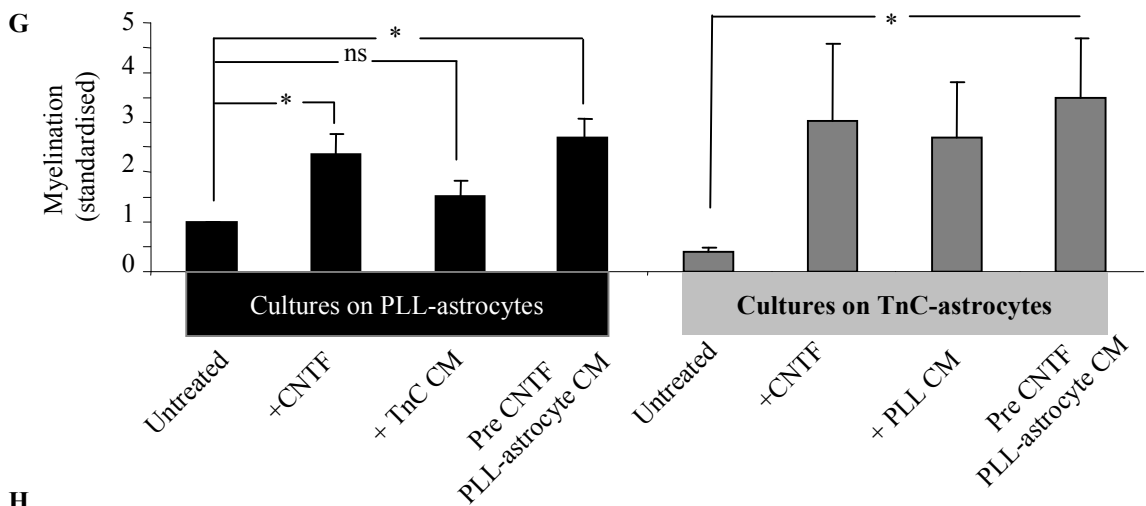
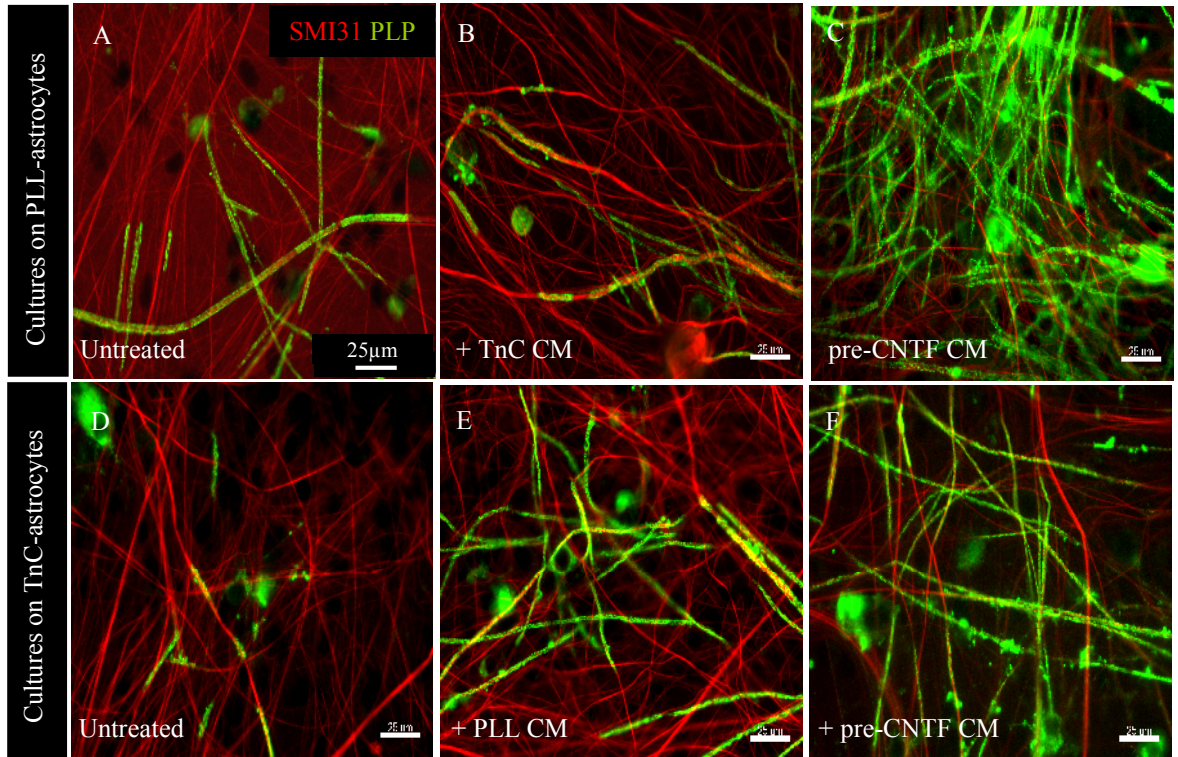


**Figure 6.6** Please see overleaf for figure legend.

**Figure 6.6 Myelinating Cultures Conditioned with Astrocytes Pre-treated with CNTF Increased Myelination and this effect was Dominant to the Reduction in Myelination by Quiescent Astrocytes.** E15.5 mixed spinal cord cultures were plated onto a confluent monolayer of astrocytes on PLL (A-C) or TnC (D- F). Myelinating cultures were left untreated (A, D), or treated with CNTF (not shown). Myelinating cultures plated on PLL-astrocytes were conditioned by coverslips of TnC-astrocytes, whilst myelinating cultures plated on TnC-astrocytes were conditioned by coverslips of PLL-astrocytes (B, E respectively). Myelinating cultures on PLL and TnC were conditioned with PLL-astrocytes pre-treated with CNTF for 24-48 hours. (C, F). PLL cultures were unaffected by TnC CM (B, G). Myelination was increased on TnC cultures conditioned with PLL CM (E, G). CNTF-treated CM increased myelination on both PLL and TnC cultures (C, F respectively, and G). Neurite density was unaffected in any of the conditions (H). Scale bar 100  $\mu$ m. *CM conditioned media*. Experiments were performed in triplicate. Error bars indicate standard error of the mean.

Protein-like factors (BMPs) in serum can induce astrocyte differentiation (Obayashi et al., 2009). It has long been proposed the astrocytes in cultures display an ‘activated’ phenotype and resemble the activated astrocyte, especially since most astrocyte preparations are exposed to serum whereas astrocytes in the normal brain are not (Espinosa de los Monteros et al., 1993; Loo et al., 1995). As astrocytes in these experiments, including TnC-astrocytes, are grown in serum the extent to which our TnC-astrocytes can be termed ‘quiescent’ is yet to be fully established. In this study, it is reported that TnC-astrocytes can not support myelination to the same extent to those grown on PLL. We and others hypothesise that activated astrocytes (PLL-astrocytes) have a secretory profile which is favourable to myelination, whereas quiescent astrocytes do not. For instance, in response to electrical stimulation, LIF, a member of the IL-6 family, was secreted by astrocytes in response to ATP being liberated from firing axons (Ishibashi et al., 2006). The authors also demonstrate that the exogenous addition of LIF onto co-cultures comprising of DRG neurons and OPCs, lead to a concentration dependent increase in the number of myelinated fibres. Thus, LIF-secretion by electrically stimulated astrocytes results in enhanced oligodendrocyte differentiation. However, it can also be speculated that activated astrocytes may suppress an inhibitory factor for myelination and quiescent ones do not. For instance, TNF $\alpha$ , member of the tumour necrosis family, is secreted at low levels by astrocytes in culture but strongly amplified when induced by pro-inflammatory agents, such as Interferon- $\gamma$  (IFN- $\gamma$ ) and Interleukin-1 $\beta$  (IL-1 $\beta$ ) (Chung and Benveniste, 1990). TNF $\alpha$  has been reported to induce both myelin and oligodendrocyte damage *in vitro* (Selmaj and Raine, 1988; Cammer and Zhang, 1999; Deng et al., 2010) and its expression in MS plaques from patients is positively correlated with the extent of demyelination (Bitsch et al., 2000). Thus, it is not known whether activated astrocytes secrete factors that promote myelination or factors which inhibit other molecules from hindering myelination. Taken together these data suggest that quiescent astrocytes do not support myelination. Although they have the opposite expression profile to reactive astrocytes, reported in the glial scar, both types display properties which are inhibitory to myelination.

Due to the inhibitory nature of TnC on OPC differentiation, it is reasonable to question if the reduction in myelination on TnC-astrocytes is simply due to expression of TnC from the substrate or by upregulation on the astrocyte surface. To address the above questions, the levels of TnC on PLL-astrocytes and TnC-astrocytes was compared. TnC-astrocytes expressed comparable levels of TnC compared to PLL-astrocytes (Fig 6.5). This therefore suggests that the TnC substrate does not lead to the re-expression of TnC on the astrocytes.

Although the astrocyte monolayer is fully confluent (as shown by F-actin, Fig 6.4), it can not be assumed that the TnC substrate is not exposed to developing OPCs.

Neurite outgrowth on TnC-astrocytes was unaffected, as SMI31-positive neurites can be seen covering the coverslip (Fig 4.5 A, D and Fig 4.1 C, D). TnC is multi-domain molecule, comprising of a cysteine-rich amino terminal domain, 14.5 EGF-type repeats (mouse), 8 fibronectin type III homologous repeats and fibrinogen  $\beta$  and  $\gamma$  homologous domain at the carboxyl-terminal end (Husmann et al., 1992). Work by Lochter et al. (1991) demonstrates that TnC can have dual effect on neurite outgrowth. The authors found neurites extended processes 40% longer on TnC than on control substrate (poly-ornithine) whereas the addition of soluble TnC largely inhibited neurite outgrowth. The domain identified to be responsible for neurite outgrowth is flanked by the 10<sup>th</sup> and 11<sup>th</sup> fibronectin type III homologous repeats. The domains between 3<sup>rd</sup> and 5<sup>th</sup> fibronectin type III homologous repeats have been shown to positively influence migration of rat cerebellar neurons (Husmann et al., 1992). Andrews et al. (2009) have shown that  $\alpha 9\beta 1$  integrin, which was previously shown to bind to the fibronectin type III domain (Yokosaki et al., 1998), expressed in neurons can overcome the inhibitory function of TnC both *in vitro* and in the injured CNS. The study demonstrates that cell types with the ‘appropriate’ receptor repertoire are able to overcome the inhibitory nature of TnC. Therefore, it is critical to identify the inhibitory domains to specific injuries or the pro-regenerative cell receptors which may overcome it, in order to develop antibody targeted therapy and/or transgenic cell transplantation to prevail over the glial scar.

It was shown in previous chapters (Chapters 4 and 5) that CNTF is most likely to act on the astrocyte by increasing its state of activation. There is a great deal of research undertaken regarding the activation of astrocytes, which was previously discussed (Section 1.4.2). It was found that cultures on TnC-astrocytes can be ‘rescued’ to increase the number of myelinated neurites by the addition of CNTF. In addition, the characteristics of TnC astrocytes shown here bear a resemblance to those described as quiescent in the literature. Thus, it is hypothesised that CNTF addition to cultures on quiescent TnC astrocytes reverses their state to one which is more activated. Astrocyte re-activation has been previously described in Holley et al. (2005) where the quiescence of TnC-astrocytes in serum-free media was partially reversed by addition of serum. This was shown to increase both nestin and basic fibroblast growth factor expression, suggesting the phenotype had reverted back to an activated one. In another study, lipopolysaccharide-induced activation of astrocytes reduces the expression of iNOS, TNF $\alpha$  and IL-1 $\beta$  by the addition of sodium

benzoate, a sodium salt of benzoic acid (Bramachari et al., 2009) and lovastatin, a drug used as a hypolipidemic agent (Pehan et al., 1997). Furthermore, morphological change of astrocytes from stellate to flat is a characteristic of astrogliosis and can be induced by thrombins, which are serine proteases (Pindon et al., 1998). The authors show that this morphologically-induced change by thrombin can be blocked by a serine/threonine-kinase inhibitor, H7. The phenotype of astrocytes, defined their expression of 'reactive' markers and their morphology, can therefore be reversed via numerous ways. This is of significant value as understanding the possible reversal of astrocytes within the glial scar may lead to a combinational treatment for CNS conditions which involve reactive gliosis.

The activated astrocyte (PLL-astrocytes) can support myelination and can be cytokine-induced to a higher level of activation which can further support myelination. Quiescent astrocytes (TnC-astrocytes) do not support myelination but this can be overcome by activated astrocyte conditioned media or the addition of CNTF. Tenascin-C is upregulated in astrocytes after injury (McKeon et al., 1991; Laywell et al., 1992) and is also identified as a component of the glial scar (Gutowski et al., 1999) suggesting an inhibitory role for growth and repair. Thus, an astrocyte in a reactive state, like in an MS glial scar and one which is in a quiescent state, like those on TnC, both do not support myelination to the same extent as an activated astrocyte (see Figure 1.8). These data demonstrate the dual role of astrocytes and the remarkable effect this has on the myelinating capability of the oligodendrocytes. The identification of these pro-myelinating factors is crucial in establishing the secretory profile of an activated astrocyte and in the understanding of myelination biology. In MS, these factors can be manipulated to ameliorate the environment in which remyelination can resume successfully.

## **Chapter 7**

# **Identification of Molecules Secreted by Activated and Quiescent Astrocytes**

# Identification of Molecules by Activated and Quiescent Astrocytes

---

## 7.1.1 Introduction

The function of astrocytes, especially in disease, is highly dependent on their environment. The molecular changes that occur during the changes in their environment are key in understanding astrocyte biology and whether or not they maintain the support they provide to surrounding cells. The term phenotype is used to represent the characteristic of the astrocytes in terms of morphological and physiological properties. In this study, two astrocyte phenotypes have been identified; astrocytes plated on PLL (PLL-astrocytes) which support myelination are classified as ‘activated’ whereas those on TnC (TnC-astrocytes) which do not support myelination to the same to the same extent, and have been termed in the literature as ‘quiescent’. A highly activated astrocyte by cytokine activation (addition of CNTF) is more supportive for myelination,. Thus, the reactive status of astrocytes determines their capability to support myelination. In order to further understand the molecular changes between these astrocyte phenotypes, a more detailed investigation into the genetic profiles is required.

A microarray uses a platform with tens of thousands of known genes and it a method to measure gene expression profile changes in cells grown under different conditions. A microarray study yields an enormous amount of data, which is then analysed and sorted by fold change differences and statistical significance.

Although microarray gene expression profile studies provide a vast amount of information, the validation of these genes in a feasible model is also necessary. Target genes can be identified, but they are of little use if their functions are not confirmed using a reliable biological system. Zhang et al. (2006) used a microarray analysis approach of cytokine treated astrocyte and identified IL-11, a member of the IL-6 family of cytokines, to be produced by astrocytes and important in oligodendrocyte protection and myelin formation. In this study, the authors treated human fetal astrocytes with IL-1 $\beta$  or TGF $\beta$ 1, cytokines known to be upregulated in MS (Baranzini et al., 2000). They identified IL-11 to be highly upregulated in cytokine treated astrocytes when compared to untreated astrocytes. IL-11 was then validated in a myelinating culture model using dorsal root ganglion (DRG) neurons and purified oligodendrocytes. They found a concentration dependent increase in

the number of myelin segments per field of view with IL-11 treatment. Zhang and colleagues illustrate the usefulness of gene identification studies by testing target genes on a model system to show a functional effect.

The myelinating cultures used in our study provides an excellent platform for microarray analysis. These cultures contain multiple cell types which develop from embryonic cells to mature differentiated cells over 28 days. Validation of gene function by addition of proteins or/and neutralising antibodies into the myelinating cultures at defined time points allows specific questions regarding how differentiation can be affected. For instance, adding a protein once myelination is complete would probe whether the exogenous addition of this protein has the potential to demyelinate myelinated axons and addition factors during myelin ensheathment may compromise the end stages of myelination.

### **7.1.2 Aims**

The aim of this chapter is to identify novel genes which are associated with changes in the supportive nature of astrocytes, correlating this with its reactivity status and validate these genes using myelinating cultures.

## **7.2 Results**

Many of the figures in this chapter are Venn diagrams which represent genes which are shared between two conditions. Tables are also used to list all genes within a category. However, only genes with relevance to the work presented in this thesis (marked by asterisks adjacent to the results tables) will be discussed.

### **7.2.1 Schematic of Experimental Design and Analysis of Microarray**

Neurosphere derived astrocytes were harvested and grown in DMEM-FBS on either PLL or TnC coated coverslips (Fig 7.1). When confluent, the media was changed to differentiation media, as used in the myelinating cultures, for 5 days. Some of the PLL-astrocytes received 2 ng/ml of CNTF. RNA was extracted at 4 hours and 24 hours post-treatment, but only at 4 hours for TnC-astrocytes. RNA was converted to cRNA and hybridized using an Illumina BeadArray Reader platform and analysed using Beadstudio (see Section 2.10.4 for more details). Significance was determined using the False

Discovery Rates (FDR) multiple testing correction method (Benjamini and Hochberg, 1995), with a FDR cut-off of 5%. Venn diagrams were used to look for consistent differences between time points and conditions.

## **7.2.2 Gene Expression Changes over Time in Untreated and CNTF Treated PLL-Astrocytes**

In order to assess differences over time with and without CNTF treatment, PLL-astrocytes were left untreated (Fig 7.2 A) or treated with CNTF (Fig 7.2 B) and compared after 4 hours and 24 hours. Genes which were changed over time in both untreated and CNTF-treated PLL-astrocytes (Fig 7.2 AB) were also included. The expression of 30 genes changed over time in untreated PLL-astrocytes. It would be of interest to keep astrocytes for a longer time and assess whether the age of astrocytes affects the support they provide the process of myelination and whether there are genes associated with older/younger astrocytes which do/do not support myelination. However, although extremely relevant, these experiments were beyond the scope of this thesis.

There were 60 genes that changed over time from 4 hours to 24 hours in CNTF-treated astrocytes (Fig 7.2 B). This group represents the genes which may influence the increase in myelination we have found with CNTF treatment in the myelinating cultures. Furthermore, there were 47 genes which were upregulated in both PLL-astrocytes untreated and treated with CNTF over time (Fig 7.2 AB). Group AB represents genes changes which are changed over time in both PLL-astrocytes and PLL-astrocytes treated with CNTF.

Table 7.1, 7.2 and 7.3 represents gene groups shown in Figure 7.2. A disintegrin and metalloproteinase with thrombospondin motifs 1 (ADAMTS1) was down regulated in both PLL-astrocytes untreated and treated with CNTF over time (-1.6657 for untreated and -1.5781 for CNTF treatment, Table 7.3, both FDR < 0.05). ADAMTS1 belongs to a group of protease enzymes play a role in degradation of chondroitin sulphate proteoglycans. Haddock et al. (2006) have shown that ADAMTS1 expression is reduced in MS tissue compared with normal tissue using qRT-PCR. However, when investigating protein levels, ADAMTS1 levels in MS tissue are similar to normal tissue. In fact, there is a slight increase in chronically inactive lesions. These observations suggest that the presence of ADAMTS1 is associated with extracellular matrix modulation in MS and may contribute to the overall inhibitory environment around the cells involved in myelin formation.

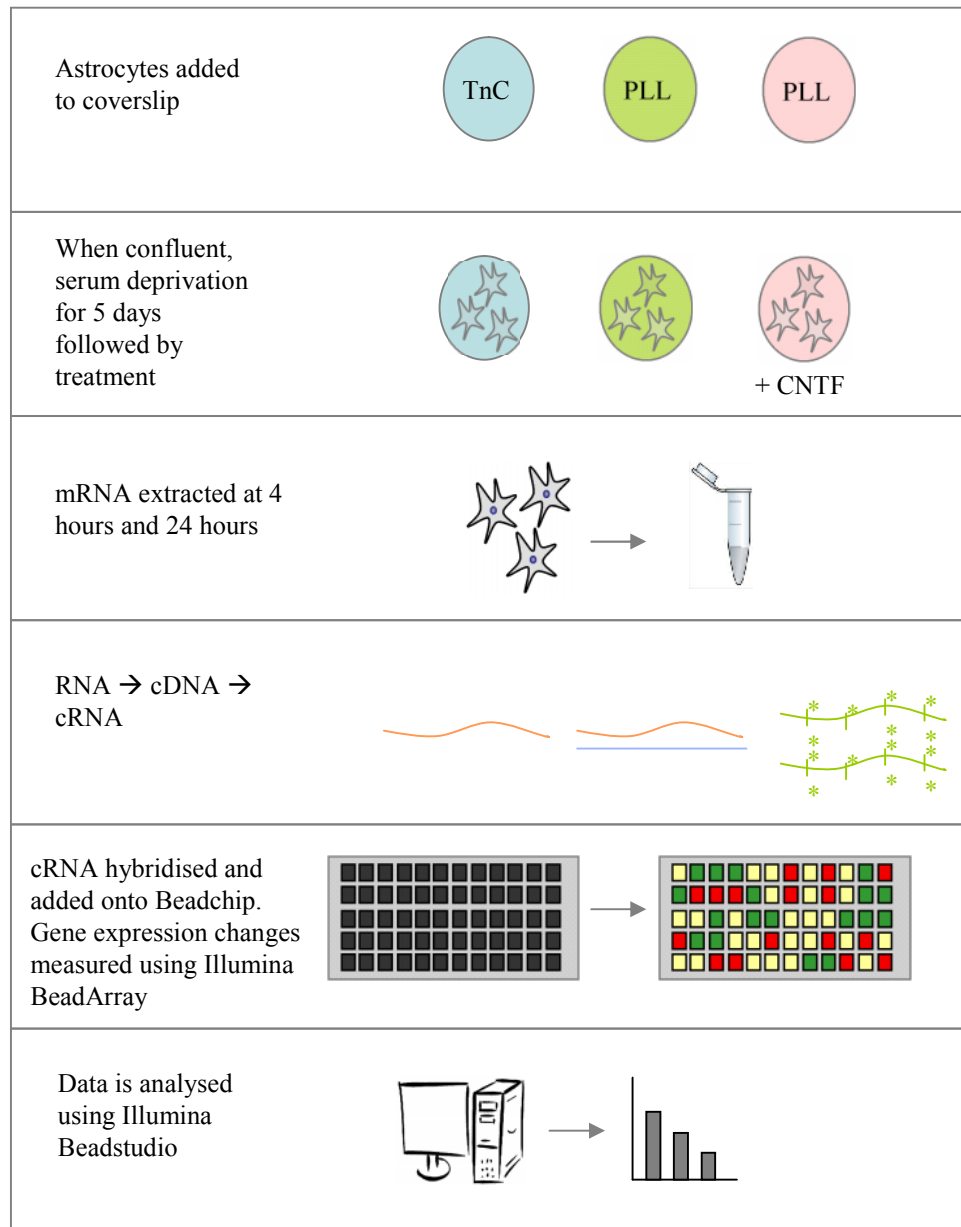


**Figure 7.1 Schematic Diagram Representing the Experimental Plan and Step Wise Process of a Microarray Study.** Neurosphere-derived astrocytes are plated on to PLL or TnC-coated coverslips. Upon confluency, astrocytes were serum deprived so as to resemble the culture conditions for a myelinating culture. After 5 days some PLL-astrocytes were treated with 2 ng/ml CNTF. RNA was extracted from TnC-astrocytes at 4 hours, PLL-astrocytes and PLL-astrocyte treated with CNTF at 4 hours and 24 hours. RNA was then reverse transcribed to cDNA and then using an *In Vitro* Transcription, cDNA was converted to cRNA. Following several washing and blocking steps, cDNA was hybridised to the Illumina Beadchip and changes in gene expression were recorded using Illumina Beadarray Reader. The recorded data was then analysed using Illumina Beadtudio where it was sorted by fold changes and significance using a False Detection Rate of cut off of 5%.

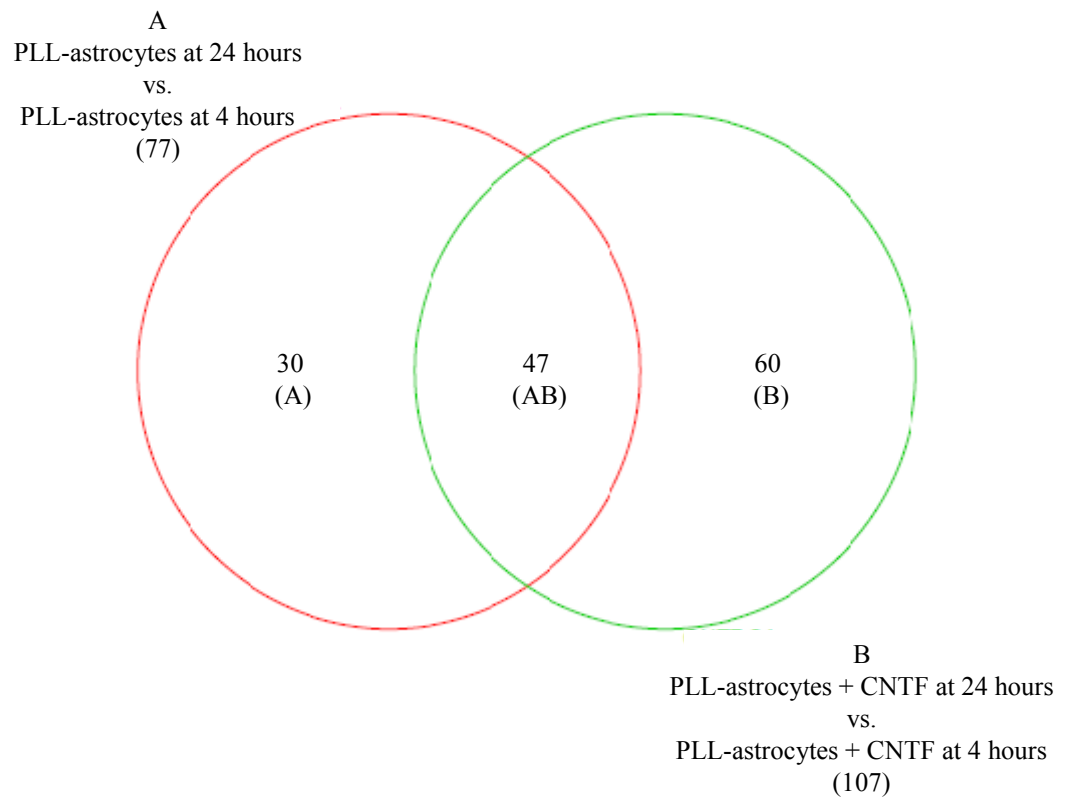


**Figure 7.2 Venn diagram Representing Transcript Distribution over time in PLL-astrocytes with and without CNTF Treatment.** Section A represents the number of genes with changed expression between untreated PLL-astrocytes after 4 hours and 24 hours. Section B represents the number of genes with changed expression between PLL-astrocytes treated with CNTF (2 ng/ml) after 24 hours and 4 hours. Section AB represents the number of genes changed between untreated and CNTF-treated PLL-astrocytes over time. Numbers represent the number of genes having significantly different expression between conditions (FDR > 0.05, n=3).

A.only			
		CON24 - CON4	
PROBE_ID	ILMN_GENE	FDR	FC
ILMN_1371619	KBTBD9_PREDICTED	0.0114	-1.9734
ILMN_1367475	ALDH1A1	0.0340	-1.7993
ILMN_1365068	S100A3	0.0365	-1.7578
ILMN_1530390	TMEM140	0.0340	-1.7456
ILMN_1367962	LOC310395	0.0340	-1.7425
ILMN_1349829	MAFK	0.0430	-1.7166
ILMN_1366331	HABP4_PREDICTED	0.0447	-1.7061
ILMN_1361905	RGD1309930	0.0469	-1.6657
ILMN_1374837	RGD1308967_PREDICTED	0.0398	-1.6558
ILMN_1350901	KCND3	0.0340	-1.6293
ILMN_1358334	LOC501407	0.0340	-1.6291
ILMN_1359646	SOX11	0.0447	-1.5592
ILMN_1349555	COQ10B	0.0469	-1.5507
ILMN_1357848	SLC35D1_PREDICTED	0.0470	1.4978
ILMN_1368643	THRSP	0.0399	1.5201
ILMN_1371109	RGD1561135_PREDICTED	0.0397	1.5338
ILMN_1650251	RGD1309427_PREDICTED	0.0396	1.5347
ILMN_1351683	RILP_PREDICTED	0.0362	1.5512
ILMN_1369914	RASD1	0.0353	1.5561
ILMN_1358490	CDC2	0.0364	1.5606
ILMN_1360216	ID3	0.0399	1.5655
ILMN_2039396	NQO1	0.0470	1.5890
ILMN_1348939	CD93	0.0469	1.5898
ILMN_1350709	NDOR1_PREDICTED	0.0398	1.6155
ILMN_1354279	MMP11	0.0399	1.6167
ILMN_1354198	UAP1L1_PREDICTED	0.0340	1.6184
ILMN_1360039	PAFAH1B3	0.0251	1.6198
ILMN_1355084	RGD1562952_PREDICTED	0.0190	1.6365
ILMN_1368826	RTP4_PREDICTED	0.0353	1.6382
ILMN_1368089	RRM2	0.0190	1.6748

**Table 7.1 Genes identified by Microarray Expression Profiling between PLL-Astrocytes at 4 and 24 hours (Section A of Figure 7.2).** The table shows the 30 probes significantly different (FDR < 0.05) in PLL-astrocytes untreated after 4 hours and 24 hours. These correspond in Figure 7.2 Section A of the Venn diagram. Shown here are false discovery rates (FDR) and fold changes (FC).

B.only			
		CNTF24 - CNTF4	
PROBE ID	ILMN_GENE	FDR	FC
ILMN_1376630	MAP6	0.0113	-2.0664
ILMN_1367985	NRP1	0.0082	-2.0364
ILMN_1373357	SPHK1	0.0169	-1.9606
ILMN_1363074	AREG	0.0099	-1.9275
ILMN_1373253	PNLIP	0.0077	-1.8890
ILMN_1370665	ZFAND2A	0.0298	-1.8107
* ILMN_1364335	CXCL10	0.0164	-1.8091
ILMN_1368793	CDR2	0.0303	-1.7976
ILMN_1365343	BAIAP2	0.0186	-1.7908
ILMN_1351883	CHRM3	0.0186	-1.7519
ILMN_1358241	ADAMTS9_PREDICTED	0.0196	-1.7492
ILMN_1367508	EEF1A2	0.0241	-1.7426
ILMN_1349804	ATP2B1	0.0297	-1.7245
ILMN_1364257	KCNK3	0.0253	-1.7231
ILMN_1353549	RRAS2	0.0446	-1.6957
ILMN_1375224	PRICKLE1	0.0420	-1.6951
ILMN_1349890	SLC30A1	0.0490	-1.6782
ILMN_1360331	HIST1H2BN_PREDICTED	0.0340	-1.6749
ILMN_1364908	TMEPAI_PREDICTED	0.0282	-1.6571
ILMN_1354679	ADAMTS7_PREDICTED	0.0455	-1.6477
ILMN_1350369	FLRT3_PREDICTED	0.0303	-1.6360
ILMN_1359095	MAT2A	0.0225	-1.6351
ILMN_1369446	OLR757	0.0420	-1.6081
ILMN_1376823	LOX	0.0449	-1.6047
ILMN_1651066	RGD1310975_PREDICTED	0.0292	-1.5906
ILMN_1362230	NGFB_MAPPED	0.0443	-1.5902
ILMN_1357070	RNPC1_PREDICTED	0.0295	-1.5881
ILMN_1366621	RGD1306235_PREDICTED	0.0417	-1.5821
ILMN_1367486	DUSP1	0.0303	-1.5790
ILMN_1349946	EIF1B_PREDICTED	0.0420	-1.5788
ILMN_1354409	NGEF_PREDICTED	0.0422	-1.5744
ILMN_1376851	RND3	0.0443	-1.5623
ILMN_1354516	KCNS3	0.0443	-1.5610
* ILMN_1350042	THBS4	0.0343	-1.5470
ILMN_1361968	RGD1560523_PREDICTED	0.0476	-1.5468
ILMN_1352105	CRY1	0.0482	-1.5453
ILMN_1371209	SECTM1	0.0360	-1.5440
ILMN_1360404	STC1	0.0493	-1.5423
ILMN_1356203	ADM	0.0443	-1.5415
* ILMN_1649910	CXCR4	0.0417	-1.5243
ILMN_1650382	RGD1560542_PREDICTED	0.0443	-1.5029
ILMN_1363836	EPHB6	0.0482	1.4512
ILMN_1357297	STAT6_PREDICTED	0.0451	1.4564
ILMN_1365818	LOC503241	0.0432	1.4628
ILMN_1366631	MVP	0.0429	1.4659

**Table 7.2** Please see overleaf for continuation of table and figure legend.

B.only			
		CNTF24 - CNTF4	
		FDR	FC
ILMN_1368121	OGFRL1	0.0444	1.4681
ILMN_1362982	C1GALT1	0.0432	1.4697
ILMN_1351782	RGD1305779_PREDICTED	0.0417	1.4774
ILMN_1350274	EFNA4_PREDICTED	0.0443	1.5013
ILMN_1355240	PNOC	0.0335	1.5054
ILMN_1357041	PCP4	0.0298	1.5198
ILMN_1370145	MTERFD3	0.0251	1.5390
ILMN_1376411	PPP1R3C	0.0417	1.5428
ILMN_1376818	TUBB3	0.0443	1.5494
ILMN_1376479	GSTP1	0.0169	1.5665
ILMN_1356454	FGFRL1	0.0340	1.5963
ILMN_1375078	RGD1561154_PREDICTED	0.0082	1.6565
ILMN_1358030	CLDN10_PREDICTED	0.0090	1.6929
ILMN_1360780	UGT1A6	0.0170	1.6931
ILMN_1368809	BTG2	0.0169	1.6936

**Table 7.2 Genes Identified by Microarray Expression Profiling between PLL-Astrocytes Treated with CNTF at 4 and 24 hours (Section B of Figure 7.2).** The table shows the 60 probes significantly different (FDR < 0.05) in PLL-astrocytes treated with CNTF after 4 hours and 24 hours. These correspond in Figure 7.2 Section B of the Venn diagram. Shown here are false discovery rates (FDR) and fold changes (FC).

AB.					
		CON24 - CON4		CNTF24 - CNTF4	
PROBE ID	ILMN_GENE	FDR	FC	FDR	FC
ILMN_1650285	HMOX1	0.0000	-3.4716	0.0009	-4.2928
ILMN_1367740	MT1A	0.0000	-2.9376	0.0009	-2.9539
ILMN_2040557	SERPINE1	0.0055	-2.2778	0.0041	-2.8045
ILMN_1355237	CXCL1	0.0053	-2.2499	0.0009	-2.7131
ILMN_1371618	PHLDA1	0.0081	-2.1644	0.0036	-2.5620
ILMN_1364192	RGD1560523_PREDICTED	0.0072	-2.1526	0.0036	-2.5534
ILMN_1364747	JUB	0.0072	-2.0911	0.0041	-2.4653
ILMN_1372919	CYR61	0.0081	-2.0687	0.0041	-2.4503
ILMN_1350180	EMPI	0.0083	-2.0520	0.0041	-2.4424
ILMN_1376417	SERPINE1	0.0084	-2.0306	0.0041	-2.2579
ILMN_1365610	RGD1565319_PREDICTED	0.0083	-2.0218	0.0074	-2.1306
ILMN_1364149	RGD1560587_PREDICTED	0.0101	-1.9952	0.0041	-2.1240
ILMN_1372925	LOC498208	0.0104	-1.9902	0.0077	-2.0965
ILMN_1359516	GCLC	0.0084	-1.9775	0.0077	-2.0901
ILMN_1364863	HIST1H2AO_PREDICTED	0.0114	-1.9730	0.0077	-2.0508
ILMN_1357783	HBEGF	0.0084	-1.9416	0.0073	-2.0427
ILMN_1351237	TXNRD1	0.0149	-1.9098	0.0123	-2.0417
ILMN_1364005	RND1	0.0163	-1.8933	0.0082	-2.0243
ILMN_1375922	NR4A3	0.0114	-1.8929	0.0098	-1.9909
ILMN_1353747	FST	0.0114	-1.8913	0.0169	-1.9192
ILMN_1373609	TNFRSF12A	0.0114	-1.8794	0.0154	-1.8585
* ILMN_1364113	CTGF	0.0141	-1.8304	0.0275	-1.8495
ILMN_1361302	KLF5	0.0281	-1.7926	0.0152	-1.8395
* ILMN_1351674	GDF15	0.0340	-1.7895	0.0100	-1.8377
ILMN_1354748	OSGIN1	0.0341	-1.7894	0.0100	-1.7897
ILMN_1354070	ISG12(B)	0.0359	-1.7759	0.0335	-1.7768
ILMN_1370948	CREG_PREDICTED	0.0359	-1.7752	0.0164	-1.7622
ILMN_1356516	RGD1563344_PREDICTED	0.0362	-1.7718	0.0404	-1.7309
ILMN_1363449	OCIL	0.0353	-1.7312	0.0186	-1.7091
ILMN_1362353	LOC683385	0.0413	-1.7226	0.0169	-1.6901
ILMN_1371943	RUNX1	0.0447	-1.7095	0.0171	-1.6839
ILMN_1369511	BCAR3_PREDICTED	0.0362	-1.6979	0.0340	-1.6746
ILMN_1353590	GADD45B	0.0398	-1.6970	0.0304	-1.6298
ILMN_1363245	CSF1	0.0353	-1.6849	0.0320	-1.6208
ILMN_1650105	UGT8	0.0469	-1.6704	0.0360	-1.5987
* ILMN_1367103	ADAMTS1	0.0321	-1.6657	0.0420	-1.5781
ILMN_1352067	CITED2	0.0398	-1.6172	0.0491	-1.5659
ILMN_1371786	CPEB4_PREDICTED	0.0353	-1.6151	0.0449	-1.5519
ILMN_1371772	PVR	0.0398	-1.5793	0.0447	-1.5011
ILMN_1354540	PDCD4	0.0447	1.6022	0.0404	1.4837
ILMN_1358464	PDE9A	0.0203	1.6407	0.0292	1.5364
ILMN_1374191	SCD1	0.0081	1.7531	0.0443	1.5481
ILMN_1366138	LOC306428	0.0083	1.8256	0.0169	1.5705
ILMN_1366294	GSTP2	0.0082	1.8464	0.0169	1.5812
ILMN_1370454	AOX1	0.0014	2.0586	0.0090	1.6352
ILMN_1350091	G0S2	0.0012	2.0619	0.0100	1.6660
ILMN_1359696	TXNIP	0.0015	2.0803	0.0077	1.8669

**Table 7.3 Genes identified by Microarray Expression Profiling between PLL-Astrocytes Untreated and Treated with CNTF after 4 and 24 hours (Section AB of Figure 7.2).** The table shows the 47 probes significantly different (FDR < 0.05) in PLL-astrocytes untreated and treated with CNTF after 4 hours and 24 hours. These correspond in Figure 6.2 Section AB of the Venn diagram. Shown here are false discovery rates (FDR) and fold changes (FC).

Furthermore, Cross et al. (2006) show that there is an increase in ADAMST1 following focal cerebral ischaemia, suggesting that extracellular matrix breakdown is observed following injury. Data presented here suggests that this gene is downregulated over time in astrocytes which are supportive for myelination which is consistent with data in the literature, and supports the view that ADAMST1 expression contributes to an environment which is non-supportive for myelination.

### **7.2.3 Very few genes are changed in Untreated PLL-astrocytes compared to those Treated with CNTF**

In order to investigate the genes which are responsible for the increase in myelination and how these differ from the untreated cultures, PLL-astrocytes treated with CNTF at 4 hours were compared to those untreated at 4 hours (Fig 7.3 A). Surprisingly, no genes were identified in this category. When PLL-astrocytes treated for 24 hours with CNTF were compared to those untreated at 24 hours, only 2 genes were identified (Fig 7.3 B). Consequently, no genes were upregulated in both categories (Fig 7.3 AB). This result was unexpected and may be due to the fact that both astrocytes support myelination and therefore genes which are attributable to this are common to both conditions. Other possible reasons for this observation are further investigated in the discussion.

The two genes which were down-regulated in PLL-astrocyte treated with CNTF for 24 hours compared to untreated PLL-astrocytes for 24 hours are represented in Table 7.4. Growth differentiation factor 15 (GDF15) was downregulated by -1.7955 folds (FDR < 0.0455). GDF15 is a protein belonging to the transforming growth factor  $\beta$  superfamily. It is expressed in the CNS including the choroid plexus as well as various brain regions e.g. such as the cortex, and striatum. GDF15 is also expressed in cultured astrocytes, oligodendrocytes and dorsal root ganglia cells (Böttner et al., 1999; Strelau et al., 2000). Cluster of Differentiation 93 (CD93) was also down regulated in CNTF-treated astrocytes at 24 hours by -1.7056 (FDR > 0.0277). CD93 is a transmembrane receptor which is expressed by monocytes and macrophages and has been shown to play a role in the regulation of phagocytosis and cell adhesion (Nepomuceno et al., 1999; Ikewaki et al., 2000). The expression of CD93 is not associated with astrocytes, but instead other cells types including myeloid cells, microglia and endothelial cells (Jeon et al., 2010). This suggests that the downregulation of CD93 in CNTF-treated astrocytes may be due to a contaminating cell type.

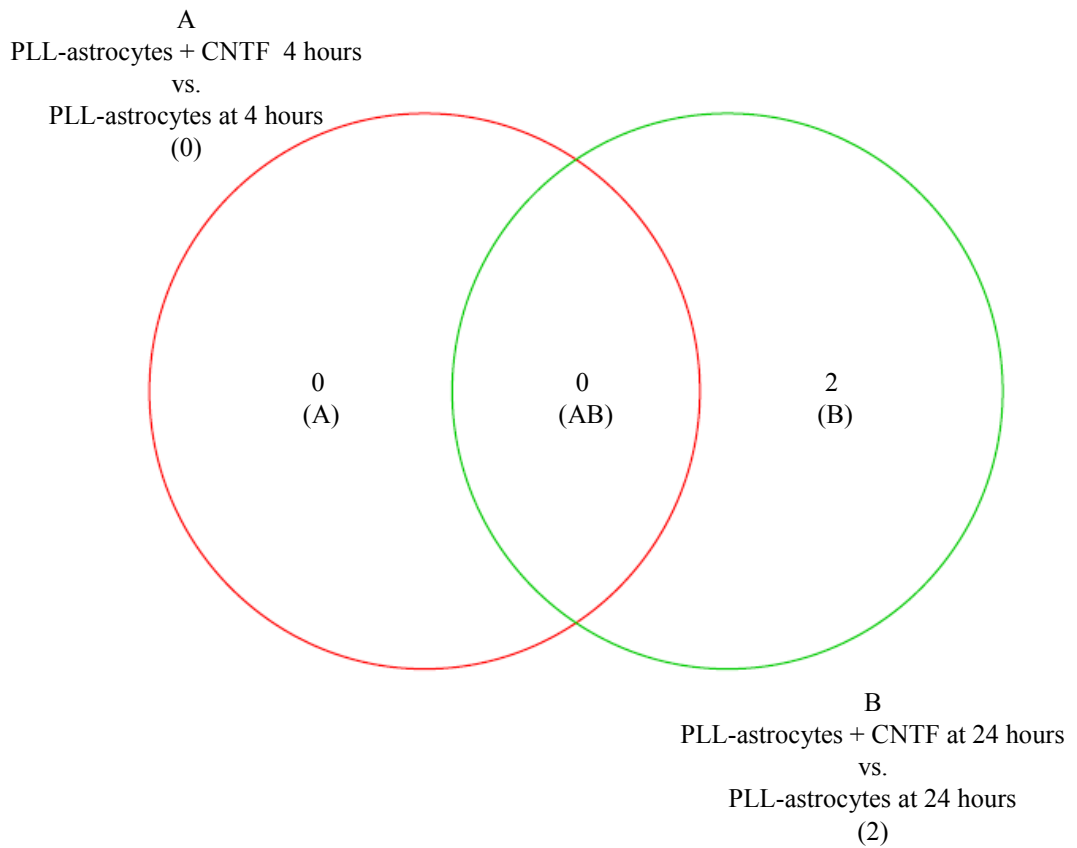


**Figure 7.3 Venn diagram Representing Transcript Distribution between PLL-astrocytes Untreated and Treated with CNTF after 4 hours and 24 hours.** Section A represents the number of genes with changed expression in untreated PLL-astrocytes when compared to CNTF-treated astrocytes after 4 hours. Section B represents the number of genes with changed expression between CNTF-treated astrocytes and untreated astrocytes at 24 hours. Section AB represents the number of genes which are changed in both astrocyte conditions at 4 and 24 hours. Numbers represents the number of genes having significantly different expression between conditions (FDR > 0.05, n=3).

A. Only			
		CNTF4 - CON4	
PROBE_ID	ILMN_GENE	FDR	FC
B. only			
		CNTF24 - CON24	
PROBE_ID	ILMN_GENE	FDR	FC
* ILMN_1351674	GDF15	0.0455	-1.7955
* ILMN_1348939	CD93	0.0227	-1.7056

**Table 7.4 Genes identified by Microarray Expression Profiling between PLL-Astrocytes Untreated and Treated with CNTF after 24 hours (Figure 7.3).** The table shows the 2 probes significantly different (FDR < 0.05) in PLL-astrocytes untreated and treated with CNTF after 24 hours. Note that there were no probes identified when comparing the same conditions after 4 hours. These correspond to Figure 7.3. Shown here are false discovery rates (FDR) and fold changes (FC).

## 7.2.4 Numerous Genes are identified when TnC-astrocytes were compared to untreated and CNTF-Treated PLL-Astrocytes at 4 hours and 24 hours

TnC-astrocytes were compared to both PLL-astrocytes untreated and treated with CNTF at 4 hours. Ten and 30 genes were changed in PLL-astrocytes untreated and PLL-astrocytes treated with CNTF when compared to TnC-astrocytes (Fig 7.4 A and B, respectively). Interestingly, when comparing TnC-astrocytes to both CNTF-treated and untreated astrocytes, 22 genes were changed (Fig 7.4 AB).

Table 7.5 represents all the genes within the categories A and B, whereas Table 7.6 represents AB from Figure 7.4. These includes pleiotrophin, Transgelin, Tenascin-R, and Insulin-like growth factor binding protein.

Pleiotrophin (PTN), also known as heparin-binding growth-associated molecule (HB-GAM), is a protein that has a diverse array of functions including neurite outgrowth and oligodendrocyte differentiation (Deuel et al., 2002). The expression of PTN is downregulated in TnC-astrocytes compared with untreated PLL-astrocytes by -2.0740 (Table 7.5, A only, FDR < 0.0269).

Trangelin, a gene associated with changes in cell shape (Shapland et al., 1988), where it binds to actin changing its loose distribution to one which is more aggregated and tousel. Transgelin is upregulated in TnC-astrocytes by 1.8136 (Table 7.5, FDR < 0.473), which is interesting as morphological changes are associated with different astrocyte phenotypes.

Expression of tenascin-R (TNR) is down regulated -1.8005 (FDR < 0.0099) in TnC-astrocytes when compared to untreated astrocytes at 4 hours (Table 7.5, A only). TNR is an extracellular glycoprotein which is part of the Tenascin family and its expression is associated with enhanced oligodendroglial differentiation and adhesion (Pesheva et al., 1997). It has been shown that TNR enhanced cell adhesion and expression of myelin proteins when pre-myelinating oligodendrocytes were plated on a TNR substrate.

The expression of Insulin-like growth factor binding protein (IGFBP2, Table 7.6, AB) was found to be downregulated in TnC-astrocytes when compared to untreated PLL-astrocytes by -2.1250 (FDR < 0.0442) and in CNTF treated PLL-astrocytes by -2.5403 (FDR <

0.0190). IGFBP2 is a polypeptide known to be secreted by astrocytes and involved in tightly regulating the actions of Insulin Growth Factors (IGFs) which in turn control the survival and differentiation of oligodendrocytes (Liu et al., 1994; Chesik et al., 2008). The downregulation of IGFBP2 may contribute to an astrocyte phenotype which is unsupportive to myelination. Interestingly, the comparison of TnC-astrocytes to both PLL-astrocytes untreated and PLL-astrocytes treated with CNTF after 24 hours also shows a downregulation of IGF gene expression (Table 7.9 AB, fold change of -1.6064 and -1.5895, respectively) further supporting a role for IGF and IGFBP in the support of myelination.

The comparison of TnC-astrocytes at 4 hours and PLL-astrocytes untreated and treated with CNTF at 24 hours exemplifies the spectrum of astrocyte support for myelination. These comparisons look into genes which are changed at either end of the spectrum; TnC-astrocyte, being the least supportive, and PLL-astrocyte treated with CNTF, being the most supportive. Figure 7.5 represents genes which were changed between TnC-astrocytes and PLL-astrocytes untreated (Fig 7.5 A), PLL-astrocytes treated with CNTF (Fig. 7.5 B) and the genes which were changed in both PLL-astrocytes untreated and treated with CNTF (Fig 7.5 AB).

Of the genes which were changed in both PLL-astrocyte conditions (untreated and treated with CNTF after 24 hours) compared to TnC-astrocytes after 4 hours is connective tissue growth factor (CTGF, Table 7.9 AB, fold change of 4.3210 when compared with untreated PLL-astrocytes and 4.1239 for PLL-astrocytes treated with CNTF, both FDR < 0.05). Thus, the expression of CTGF was high in TnC-astrocytes when compared to the other conditions. CTGF is an astrocyte-derived extracellular matrix molecule associated with astrocytosis (Kondo et al., 1999; Conrad et al., 2005).

Expression of the extracellular matrix glycoprotein Thrombospondin-4 (THBS4), was upregulated in TnC-astrocytes by 3.2528 compared to PLL-astrocytes and 3.3336 compared to PLL-astrocytes treated with CNTF (Table 7.9 AB, both FDR < 0.05). The function of THBS4 in the CNS is not known and its expression in the normal CNS is relatively low (Lawler et al., 1993). However, astrocyte-derived THSB1, a member of the same family as THSB4, has been reported to be involved in the regulation of oligodendrocyte precursor migration (Scott-Drew and French-Constant, 1997). This suggests that THSB4 may also have an effect on myelination.

The expression of C-X-C motif chemokine 10 (CXCL10), also known as IFN-gamma-inducible protein-10 (IP-10), was found to be upregulated in TnC-astrocytes by 3.3695 compared to PLL-astrocytes and by 3.6146 when compared to PLL-astrocytes treated with CNTF (Table 7.9 AB, both FDR < 0.05). CXCL10 binds to the receptor CXCR3, and is implicated in the recruitment of leukocytes into the CNS. The inhibition of CXCL10 using neutralising antibodies is associated with reduced EAE progression (Fife et al., 2001). Moreover, it is also downregulated in PLL-astrocytes treated with CNTF over time (Table 7.2).

Interestingly, the expression of CTGF, THBS4 and CXCL10 is also increased in TnC-astrocytes at 4 hours when compared to PLL-astrocytes at 4 hours. (Table 7.6). The molecules upregulated in TnC-astrocytes demonstrate the array of factors which may contribute to an astrocyte phenotype which is non-supportive for myelination. These observations reveal a startling resemblance between quiescent astrocytes (TnC-astrocytes) and reactive astrocytes found within the glial scar, as it has been suggested that the presence of reactive astrocytes may contribute to the remyelination failure (Fawcett and Asher, 1999).

### **7.2.5 Validation of CXCL10 by qRT-PCR in TnC-Astrocytes**

The microarray analysis identified numerous potential genes which are altered in the various astrocyte phenotypes, some of which may either be supportive or non-supportive to oligodendrocyte growth, differentiation and myelination. In order to verify these candidate genes, qRT-PCR was performed on the original RNA samples used for the microarray. cDNA was synthesised from RNA samples and qRT-PCR was performed using GAPDH as an internal control.

The results for the qRT-PCR can be seen in Fig 7.6. The two polarized forms of astrocyte phenotypes were compared (TnC-astrocytes and PLL-astrocytes + CNTF). The expression of CXCL10 was significantly increased ( $p < 0.05$ ). CTGF was also confirmed to be expressed in higher levels on TnC-astrocytes, although this was not found to be statistically significant. GDF15 and IGF2 were also investigated and found not to be significantly different but their expression followed the same direction as the expression seen in the microarray analysis. Expression of THBS4, however, was upregulated in the microarray in TnC-astrocytes but this was found to be unchanged when expression levels were compared to PLL-astrocyte treated with CNTF after qRT-PCR. The lack of significance within the qRT-PCR data samples will be discussed later.

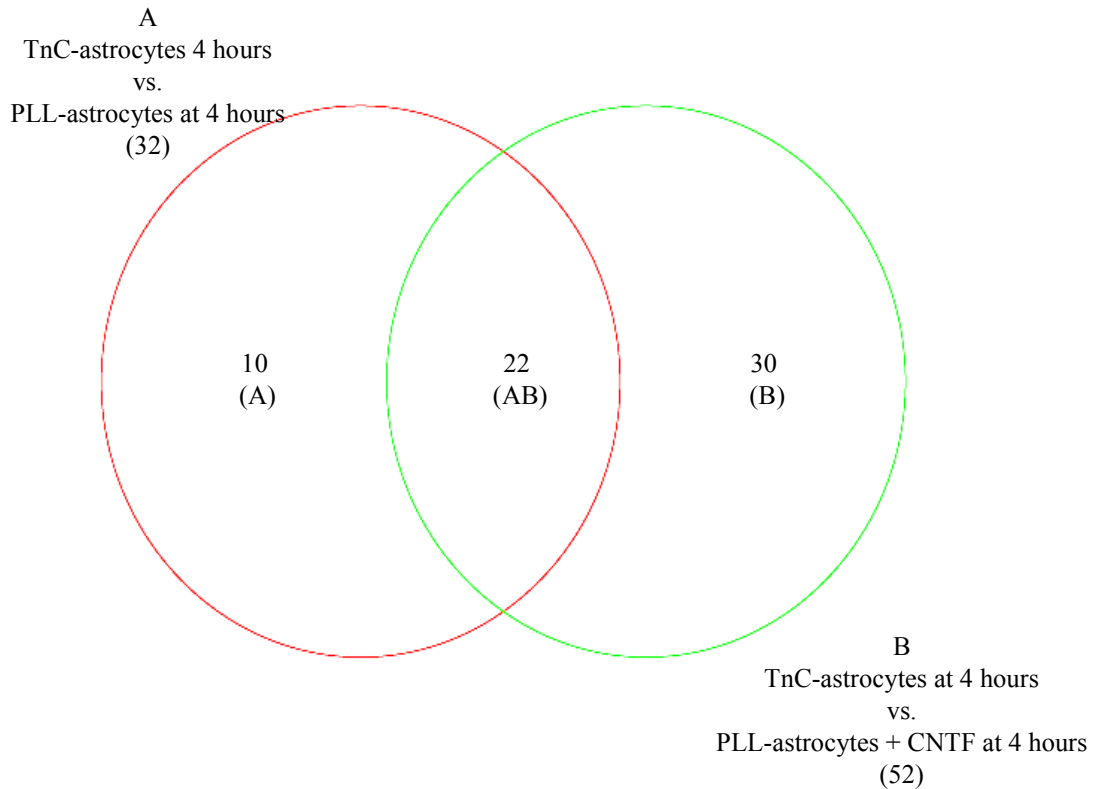


**Figure 7.4 Venn diagram Representing Transcript Distribution between TnC-astrocytes compared to PLL-astrocytes untreated and treated with CNTF after 4 hours.** Section A represents the number of genes with changed expression in TnC-astrocytes after 4 hours compared to PLL-astrocytes after 4 hours. Section B represents the number of genes with changed expression in TnC-astrocytes when compared to PLL-astrocyte + CNTF also at 4 hours. Section AB represents the number of genes with changed expression in TnC-astrocytes when comparing PLL-astrocytes untreated and treated with CNTF. Numbers represents the number of genes having significantly different expression between conditions (FDR > 0.05, n=3).

A. only			
		TNC4 - CON4	
PROBE_ID	ILMN_GENE	FDR	FC
* ILMN_1365825	PTN	0.0269	-2.0740
ILMN_1367475	ALDH1A1	0.0157	-1.8723
* ILMN_1353848	TNR	0.0099	-1.8005
ILMN_1354799	KCNN2	0.0258	-1.6854
ILMN_1366046	LOC298120	0.0428	-1.6485
ILMN_1530180	ASRGL1	0.0445	-1.6260
ILMN_1363608	CYP1A1	0.0473	1.6327
ILMN_1357368	LOC497841	0.0428	1.7687
* ILMN_1376842	TAGLN	0.0473	1.8136
ILMN_1361708	FBLN5	0.0269	1.9776
B. only			
		TNC4 - CNTF4	
PROBE_ID	ILMN_GENE	FDR	FC
ILMN_1353118	CALN1_PREDICTED	0.0358	-2.1498
ILMN_1372909	LSAMP	0.0358	-2.1325
ILMN_1367450	DBX2	0.0365	-2.0063
ILMN_1349449	HTRA1	0.0487	-1.9084
ILMN_1353247	ELOVL2_PREDICTED	0.0365	-1.5716
ILMN_1358241	ADAMTS9_PREDICTED	0.0432	-1.5340
ILMN_1366515	TJP2	0.0408	-1.4863
ILMN_1367519	ID11	0.0358	-1.4833
ILMN_2040770	RGD1560826_PREDICTED	0.0358	-1.4809
ILMN_1361968	RGD1560523_PREDICTED	0.0408	-1.4613
ILMN_1351240	HSPA5	0.0487	1.4996
ILMN_1367697	GALP	0.0388	1.5376
ILMN_1374720	ITGB4	0.0365	1.5542
ILMN_1376615	EFEMP1	0.0358	1.5734
ILMN_1530551	RN.23597	0.0405	1.5824
ILMN_1363601	RGD1560020_PREDICTED	0.0253	1.6136
ILMN_1352410	PENK1	0.0365	1.6380
ILMN_1368826	RTP4_PREDICTED	0.0190	1.6520
ILMN_1351851	LOC499513	0.0432	1.6789
ILMN_1356945	DYNLRB2_PREDICTED	0.0190	1.6975
ILMN_1352469	IRF7	0.0408	1.6996
ILMN_1373796	RGD1561932_PREDICTED	0.0378	1.7258
ILMN_1349672	RGD1310052_PREDICTED	0.0358	1.7574
ILMN_1352762	IFITM3	0.0487	1.7846
ILMN_1376635	CYP1B1	0.0379	1.8704
ILMN_1365965	PCDH8	0.0418	1.9188
ILMN_1363449	OCIL	0.0190	1.9311
ILMN_1359696	TXNIP	0.0186	1.9699
ILMN_2040297	NDRG1	0.0190	1.9860
ILMN_1353876	SULT1A1	0.0225	2.1284

**Table 7.5 Genes identified by Microarray Expression Profiling between TnC-Astrocytes and PLL-Astrocytes untreated (A) and treated with CNTF (B) after 4 hours (Figure 7.4, A and B).** Results of the microarray experiment for the 10 probes significantly different (FDR < 0.05) in comparing TnC-astrocytes compared with PLL-astrocytes at 4 hours (A only). The table also shows the 30 probes different in TnC-astrocytes compared to PLL-astrocytes treated with CNTF at 4 hours (B only). These correspond to Section A and B in Figure 7.4. Shown here are false discovery rates (FDR) and fold changes (FC).

AB.					
		TNC4 – CON4		TNC4 - CNTF4	
PROBE ID	ILMN GENE	FDR	FC	FDR	FC
* ILMN 1352040	SLC22A3	0.0090	-2.2266	0.0171	-2.7262
* ILMN 1360048	IGFBP2	0.0442	-2.1250	0.0190	-2.5403
ILMN 1352018	RGS16	0.0445	-2.0783	0.0171	-2.3598
ILMN 1369130	PCDH17 PREDICTED	0.0457	-2.0653	0.0340	-2.1265
ILMN 1371157	LOC360435	0.0057	-2.0234	0.0492	-1.7746
ILMN 1367577	SLC4A4	0.0445	-1.6211	0.0405	-1.4621
ILMN 1363947	HMGCS2	0.0457	1.6399	0.0358	1.5742
ILMN 1351562	CASP12	0.0445	1.8401	0.0171	1.7511
ILMN 1356949	COL6A1 PREDICTED	0.0457	1.9627	0.0309	1.7974
ILMN 1350896	GSTM2	0.0269	1.9684	0.0271	1.8117
ILMN 1349973	CHRDL1	0.0269	1.9759	0.0171	1.8120
ILMN 1365298	MFAP5 PREDICTED	0.0258	2.0044	0.0190	1.9362
ILMN 1352014	OGN PREDICTED	0.0375	2.0476	0.0358	1.9857
ILMN 1354048	NUPR1	0.0087	2.0630	0.0131	1.9893
* ILMN 1364335	CXCL10	0.0090	2.1209	0.0171	2.0031
ILMN 1361636	MLF1 PREDICTED	0.0036	2.3218	0.0171	2.0492
* ILMN 1364113	CTGF	0.0122	2.3439	0.0171	2.1884
ILMN 1348956	FN1	0.0099	2.4481	0.0171	2.1933
* ILMN 1350042	THBS4	0.0086	2.4851	0.0084	2.2384
ILMN 1375112	OMD	0.0060	2.7953	0.0036	2.4431
ILMN 1361640	LTBP2	0.0036	2.8963	0.0032	2.7241
ILMN 1373199	KRT19	0.0009	5.3350	0.0009	3.7854

**Table 7.6 Genes identified by Microarray Expression Profiling between TnC-Astrocytes and both PLL-Astrocytes untreated and treated with CNTF at 4 hours (Figure 7.4, Section AB).** The table shows the 22 probes significantly different (FDR < 0.05) in TnC-astrocytes compared to both PLL-astrocytes treated and untreated with CNTF at 4 hours (Fig 7.4, AB). These correspond to Section AB in Figure 7.4. Shown here are false discovery rates (FDR) and fold changes (FC).

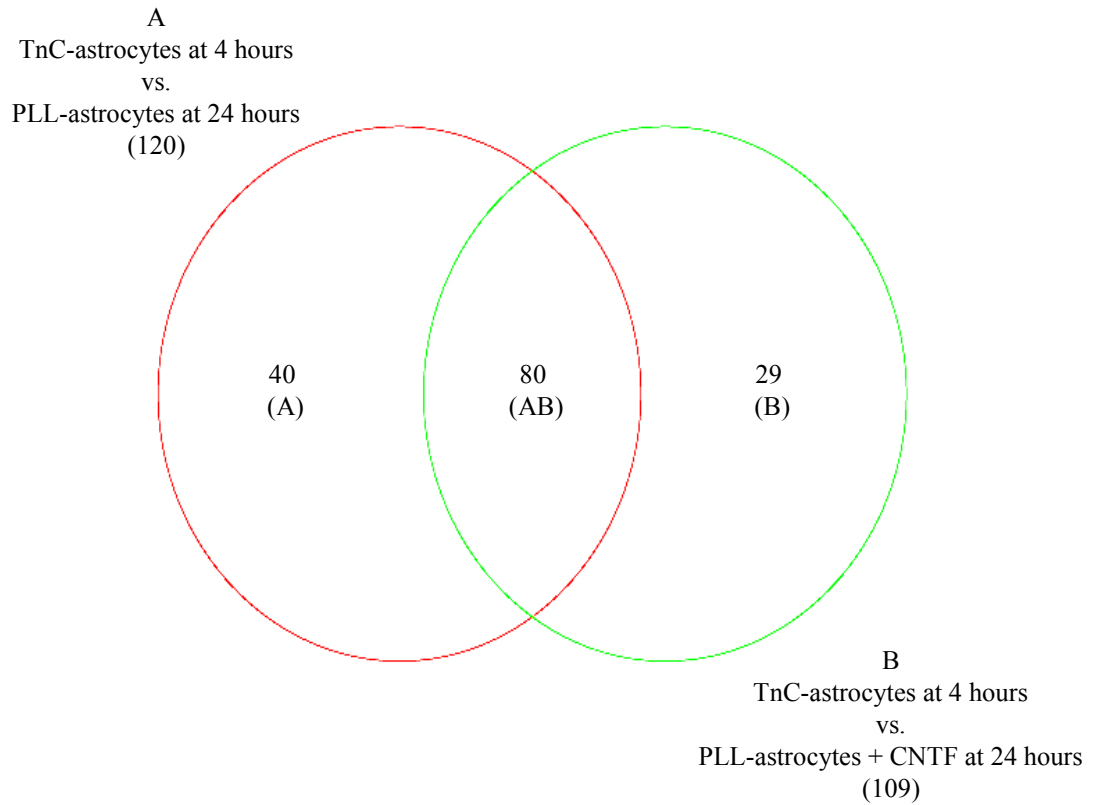


**Figure 7.5 Venn diagram Representing Transcript Distribution between TnC-astrocytes at 4 hours compared to PLL-astrocytes untreated and treated with CNTF at 24 hours.** Section A represents the number of genes with changed expression in TnC-astrocytes at 4 hours compared to PLL-astrocytes at 24 hours. Section B represents the number of genes with changed expression in TnC-astrocytes compared to PLL-astrocyte treated with CNTF also at 24 hours. Section AB represents the number of genes with changed expression in TnC-astrocytes when compared to PLL-astrocytes untreated and treated with CNTF. Numbers represents the number of genes significantly different between conditions (FDR > 0.05, n=3).

A. only			
		TNC4 - CON24	
PROBE_ID	ILMN_GENE	FDR	FC
ILMN_1366294	GSTP2	0.0132	-2.3734
* ILMN_1365825	PTN	0.0242	-2.2467
ILMN_1352040	SLC22A3	0.0277	-2.1563
ILMN_1370454	AOX1	0.0342	-2.0466
ILMN_1353118	CALN1_PREDICTED	0.0375	-2.0177
ILMN_1350723	RAB3B	0.0375	-1.9685
ILMN_1376725	CSPG5	0.0405	-1.9173
ILMN_1369295	BHLHB5_PREDICTED	0.0411	-1.9008
ILMN_1365134	DBC1	0.0411	-1.8882
ILMN_1371675	RGS8	0.0417	-1.8676
ILMN_2039308	NPPB	0.0454	-1.8437
ILMN_1359461	LIX1_PREDICTED	0.0466	-1.7691
ILMN_1371639	GUCY1B3	0.0262	-1.7136
ILMN_1373210	ENTPD5	0.0282	-1.6270
ILMN_1650251	RGD1309427_PREDICTED	0.0284	-1.6115
ILMN_1363531	LOC498427	0.0325	-1.5676
ILMN_1362982	C1GALT1	0.0342	-1.5552
ILMN_1364149	RGD1560587_PREDICTED	0.0466	1.6869
ILMN_1357783	HBEGF	0.0454	1.6938
ILMN_1364257	KCNK3	0.0411	1.7335
ILMN_1366621	RGD1306235_PREDICTED	0.0411	1.7355
ILMN_1361672	TM4SF1_PREDICTED	0.0492	1.7504
ILMN_1361214	NCOR2_PREDICTED	0.0407	1.7671
ILMN_1366331	HABP4_PREDICTED	0.0446	1.7758
ILMN_1373796	RGD1561932_PREDICTED	0.0284	1.8660
ILMN_1650120	CLDN11	0.0284	1.8758
ILMN_1365343	BAIAP2	0.0284	1.8835
ILMN_1371299	RGD1308329_PREDICTED	0.0409	1.8882
ILMN_1372919	CYR61	0.0277	1.9157
ILMN_1351851	LOC499513	0.0466	1.9488
ILMN_1362278	SLC5A3	0.0345	1.9545
ILMN_1357413	LOC360443	0.0256	1.9818
ILMN_1372782	SERPINA3N	0.0422	2.0018
ILMN_1367643	OLFML3_PREDICTED	0.0405	2.0319
ILMN_1350480	S100A6	0.0311	2.0608
ILMN_1360121	FLNC_PREDICTED	0.0375	2.0720
ILMN_1359282	GPRC5A	0.0298	2.0729
ILMN_1354048	NUPR1	0.0208	2.2669
ILMN_1357368	LOC497841	0.0198	2.3348
ILMN_1348956	FN1	0.0089	2.4422

**Table 7.7 Genes identified by Microarray Expression Profiling between TnC-Astrocytes at 4 hours and PLL-Astrocytes at 24 hours (Figure 7.5, Section A).** The table shows the 40 probes significantly different (FDR < 0.05) in TnC-astrocytes at 4 hours compared to PLL-astrocytes at 24 hours. These correspond to Section A in Figure 7.5. Shown here are false discovery rates (FDR) and fold changes (FC).

B only			
		TNC4 - CNTF24	
PROBE_ID	ILMN_GENE	FDR	FC
ILMN_1360425	ANK2	0.0282	-1.9326
ILMN_1356454	FGFRL1	0.0236	-1.8987
ILMN_1530180	ASRGL1	0.0489	-1.8403
ILMN_1376479	GSTP1	0.0269	-1.8221
ILMN_1356032	MMD2	0.0349	-1.8155
ILMN_1371346	LOC685529	0.0359	-1.8072
ILMN_1371895	RGD1561849_PREDICTED	0.0317	-1.8014
ILMN_1353247	ELOVL2_PREDICTED	0.0389	-1.7356
ILMN_1366515	TJP2	0.0334	-1.6876
ILMN_1365159	RGD1564459_PREDICTED	0.0397	-1.5523
ILMN_1352067	CITED2	0.0401	1.7388
ILMN_1650537	GPC4	0.0434	1.7722
ILMN_1362820	SSG1	0.0418	1.7742
ILMN_1364414	VGF	0.0406	1.7916
ILMN_1356140	LOC501170	0.0312	1.8253
ILMN_1352762	IFITM3	0.0312	1.8268
ILMN_1351367	RNF7_PREDICTED	0.0358	1.8308
ILMN_1349809	METTL7A	0.0312	1.8394
ILMN_1355920	MX2	0.0359	1.8402
ILMN_1353833	ACOT1	0.0330	1.8872
ILMN_1353540	CYP4B1	0.0269	1.9237
ILMN_1360556	RGD1559432_PREDICTED	0.0286	1.9289
ILMN_1351562	CASP12	0.0408	1.9394
ILMN_1367697	GALP	0.0406	1.9410
ILMN_1371943	RUNX1	0.0361	1.9673
ILMN_1370948	CREG_PREDICTED	0.0240	1.9729
ILMN_1352477	LRRK1_PREDICTED	0.0334	1.9988
ILMN_1355237	CXCL1	0.0266	2.1258
* ILMN_1351674	GDF15	0.0062	2.8475

**Table 7.8 Genes identified by Microarray Expression Profiling between TnC-Astrocytes after 4 hours and PLL-Astrocytes Treated with CNTF after 24 hours (Figure 7.5, Section B).** The table shows the 29 probes significantly different (FDR < 0.05) in TnC-astrocytes at 4 hours compared to PLL-astrocytes treated with CNTF at 24 hours. These correspond to Section B in Figure 7.5. Shown here are false discovery rates (FDR) and fold changes (FC).

AB.					
		TNC4 - CON24		TNC4 - CNTF24	
PROBE_ID	ILMN_GENE	FDR	FC	FDR	FC
ILMN_1367450	DBX2	0.0034	-3.0915	0.0031	-2.9256
ILMN_1369130	PCDH17_PREDICTED	0.0136	-2.6927	0.0050	-2.6069
ILMN_1354799	KCNN2	0.0102	-2.5139	0.0153	-2.4251
ILMN_1366607	TRH	0.0242	-2.2849	0.0133	-2.2205
ILMN_1371157	LOC360435	0.0220	-2.2561	0.0137	-2.2122
ILMN_1372909	LSAMP	0.0256	-2.1968	0.0152	-2.1154
ILMN_1368199	SEZ6	0.0194	-2.1573	0.0047	-2.0644
ILMN_1350091	G0S2	0.0284	-2.1356	0.0149	-1.9979
ILMN_1352018	RGS16	0.0284	-2.1129	0.0074	-1.9873
ILMN_1370876	ANK2	0.0305	-2.0611	0.0269	-1.9786
ILMN_1358464	PDE9A	0.0411	-1.9831	0.0149	-1.9084
ILMN_1366138	LOC306428	0.0436	-1.9739	0.0312	-1.9084
ILMN_1374191	SCD1	0.0375	-1.9708	0.0282	-1.8997
ILMN_1351871	PTPRR	0.0375	-1.9487	0.0449	-1.8548
ILMN_1364348	CAR2	0.0281	-1.8993	0.0347	-1.8169
ILMN_1359367	RGD1310117_PREDICTED	0.0284	-1.8217	0.0389	-1.7892
ILMN_1367246	CAMK2B	0.0492	-1.7899	0.0418	-1.7712
ILMN_1530410	TM7SF2	0.0496	-1.7894	0.0171	-1.6912
ILMN_1360838	DMPK_PREDICTED	0.0284	-1.7850	0.0492	-1.6825
ILMN_1370437	GPNMB	0.0396	-1.7478	0.0240	-1.6403
ILMN_1358030	CLDN10_PREDICTED	0.0277	-1.6430	0.0269	-1.6183
* ILMN_1359301	IGF2	0.0288	-1.6064	0.0312	-1.5895
ILMN_1376258	DDIT4L	0.0321	-1.5725	0.0359	-1.5610
* ILMN_1353848	TNR	0.0469	-1.4937	0.0416	-1.5488
ILMN_1371618	PHLDA1	0.0417	1.7761	0.0416	1.7273
ILMN_1353747	FST	0.0360	1.7845	0.0416	1.7308
ILMN_1371491	METRNL	0.0344	1.7881	0.0359	1.7586
ILMN_1354516	KCNS3	0.0342	1.8002	0.0416	1.7811
ILMN_1369511	BCAR3_PREDICTED	0.0289	1.8535	0.0337	1.7885
ILMN_1373820	GLDN	0.0288	1.8642	0.0406	1.7944
ILMN_1364744	LOC294942	0.0466	1.8754	0.0336	1.8679
ILMN_1364984	AZIN1	0.0321	1.8822	0.0279	1.8762
ILMN_1361708	FBLN5	0.0430	1.9033	0.0320	1.8892
ILMN_1376851	RND3	0.0411	1.9286	0.0279	1.8902
ILMN_1359095	MAT2A	0.0259	1.9608	0.0317	1.8954
ILMN_1350369	FLRT3_PREDICTED	0.0388	1.9738	0.0312	1.9014
ILMN_1356313	KCNK1	0.0423	1.9930	0.0312	1.9031
ILMN_1360331	HIST1H2BN_PREDICTED	0.0286	2.0000	0.0312	1.9095
ILMN_1650285	HMOX1	0.0242	2.0112	0.0312	1.9110
ILMN_1361968	RGD1560523_PREDICTED	0.0242	2.0147	0.0442	1.9131
ILMN_1364192	RGD1560523_PREDICTED	0.0282	2.0234	0.0358	1.9708
ILMN_1370795	IFITM1_PREDICTED	0.0411	2.0275	0.0275	1.9842
ILMN_1367752	PRSS23	0.0242	2.0282	0.0239	1.9906
ILMN_1376823	LOX	0.0311	2.0325	0.0277	2.0156

**Table 7.9 Please see overleaf for continuation of table and figure legend**

AB continued.						
PROBE ID	ILMN GENE	FDR	FC	FDR	FC	
		TNC-CON24		TNC-CNTF24		
	ILMN 1373357	SPHK1	0.0277	2.0470	0.0227	2.0172
	ILMN 1364863	HIST1H2AO PREDICTED	0.0327	2.0503	0.0269	2.0180
	ILMN 2040297	NDRG1	0.0305	2.0663	0.0237	2.0367
*	ILMN 1376842	TAGLN	0.0289	2.0878	0.0317	2.0419
	ILMN 1650153	THBS2	0.0284	2.1029	0.0236	2.0424
	ILMN 1354409	NGEF PREDICTED	0.0254	2.1058	0.0227	2.0539
	ILMN 1370339	RARRES2	0.0325	2.1191	0.0312	2.0630
	ILMN 1349829	MAFK	0.0284	2.1285	0.0310	2.0860
	ILMN 1359626	LOC311772	0.0277	2.1642	0.0176	2.0942
	ILMN 1363431	LTBP1	0.0298	2.2010	0.0279	2.1034
	ILMN 1361905	RGD1309930	0.0271	2.2192	0.0279	2.1236
	ILMN 1372925	LOC498208	0.0262	2.2327	0.0155	2.1410
	ILMN 1365610	RGD1565319 PREDICTED	0.0183	2.2628	0.0149	2.1542
	ILMN 1353876	SULT1A1	0.0281	2.2887	0.0236	2.2123
	ILMN 1352014	OGN PREDICTED	0.0256	2.3879	0.0149	2.2149
	ILMN 1364747	JUB	0.0242	2.4005	0.0116	2.2253
	ILMN 1349973	CHRD1	0.0220	2.4798	0.0149	2.2272
	ILMN 1361636	MLF1 PREDICTED	0.0119	2.5049	0.0227	2.2382
	ILMN 1350896	GSTM2	0.0158	2.5249	0.0227	2.2398
	ILMN 1373609	TNFRSF12A	0.0135	2.6316	0.0062	2.3543
	ILMN 1376635	CYP1B1	0.0184	2.6348	0.0074	2.3992
	ILMN 1376417	SERPINE1	0.0108	2.7266	0.0051	2.4563
	ILMN 1356949	COL6A1 PREDICTED	0.0083	2.8252	0.0062	2.4676
	ILMN 1365298	MFAP5 PREDICTED	0.0089	2.9099	0.0137	2.4993
	ILMN 1371619	KBTBD9 PREDICTED	0.0089	2.9264	0.0051	2.9561
	ILMN 1354712	COL1A2	0.0084	3.1408	0.0050	2.9580
	ILMN 1375112	OMD	0.0069	3.1696	0.0058	3.0105
	ILMN 1363449	OCIL	0.0080	3.2439	0.0050	3.2762
*	ILMN 1350042	THBS4	0.0069	3.2528	0.0047	3.3336
*	ILMN 1364335	CXCL10	0.0058	3.3695	0.0041	3.6146
	ILMN 1373199	KRT19	0.0058	3.4419	0.0036	3.6239
	ILMN 1361640	LTBP2	0.0058	3.5159	0.0031	3.7369
	ILMN 1367740	MT1A	0.0020	3.8202	0.0031	3.7382
	ILMN 2040557	SERPINE1	0.0020	3.9793	0.0033	3.7769
	ILMN 1350180	EMP1	0.0020	4.2599	0.0031	3.8603
*	ILMN 1364113	CTGF	0.0018	4.3210	0.0027	4.1239

**Table 7.9 Genes identified by Microarray Expression Profiling between TnC-Astrocytes after 4 hours and PLL-Astrocytes Untreated and Treated with CNTF after 24 hours (Figure 7.5, Section AB).** The table shows the 80 probes significantly different (FDR < 0.05) in TnC-astrocytes after 4 hours compared to both PLL-astrocytes untreated and treated with CNTF after 24 hours. These correspond to Section AB in Figure 7.5. Shown here are false discovery rates (FDR) and fold changes (FC).

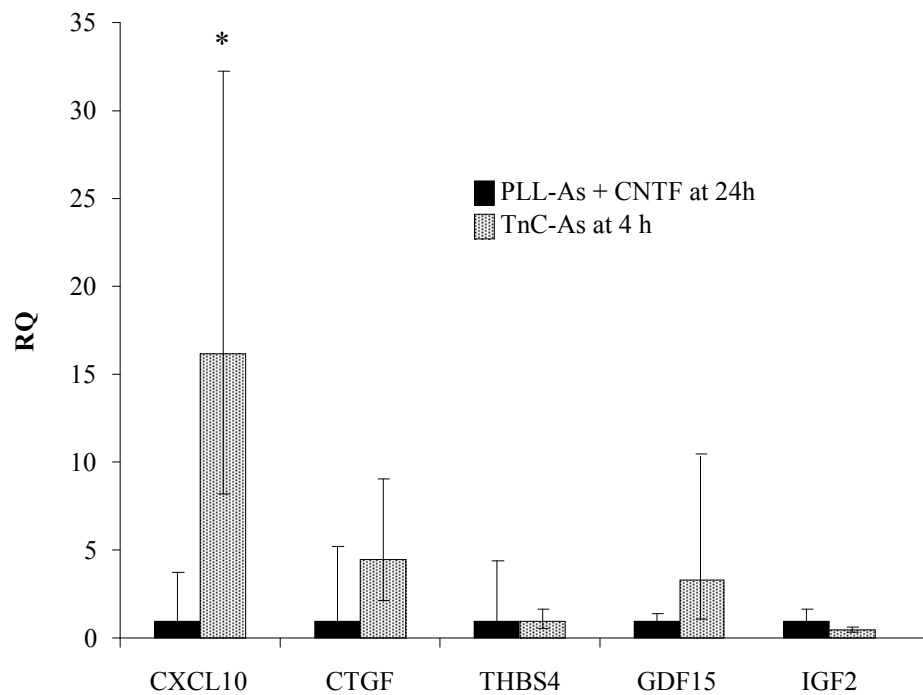


**Figure 7.6 Validation of CXCL10 in TnC-Astrocytes.** Relative quantification (RQ) for CXCL10, CTGF and THBS4 mRNA. Neurosphere derived astrocytes were plated on PLL (PLL-astrocytes) until confluency and treated with CNTF (2 ng/ml) for 24 hours were compared with astrocytes plated on TnC (TnC-astrocytes) after 4 hours. CXCL10 mRNA was significantly increased in TnC-astrocytes when compared to PLL-astrocytes treated with CNTF ( $p < 0.05$ ,  $n=3$ ).

## 7.2.6 CXCL10 Antibodies Increase Myelination in TnC-Astrocytes Cultures

To determine if CXCL10 can actually reduce myelination on TnC-astrocytes, the neutralising antibody to CXCL10 was added to myelinating cultures plated on PLL-astrocytes (Fig 7.7 B, D, F, G) and TnC-astrocytes (Fig 7.7 A, C, E, G) at concentrations from 0.2-20  $\mu\text{g/ml}$ , added on day 12. As shown previously, cultures on TnC-astrocytes have reduced levels of myelination compared to cultures on PLL-astrocytes (Fig 6.1,  $p < 0.05$ ). The addition of neutralising antibodies, at all concentrations, resulted in an increase in the percentage of myelinated fibres (Fig 7.7 C, E, G and Fig 7.8 A), although this was not significant ( $p > 0.05$ ). Conversely, the addition of CXCL10 neutralising antibodies resulted in a slight reduction in myelinated fibres (Fig 7.7 D, F, H and Fig 7.8 A), although this was not statistically significant. The neurite density for all conditions was similar (Fig 7.8 B). These observations suggest that the inhibition of CXCL10, which is highly expressed in TnC astrocytes, results in an increase in myelination.

Since antibodies to cytokines can be notoriously difficult to modulate function in culture, a more reliable method to examine the effects CXCL10 would be to use recombinant protein. CXCL10 was added to myelinating cultures plated in PLL-astrocytes from day 12 onwards and also on myelinating cultures at day 28 where it was added for a further 5 days (Fig 7.9). The addition of CXCL10 on day 12 resulted in a decrease in myelination which was found to be statistically different to untreated cultures on PLL-astrocytes (Fig 7.9 A, B, D,  $p < 0.05$ ). The addition of CXCL10 on day 28 lead to a slight reduction in myelination, but this was not significant (Fig 7.9 C, D). Therefore, this data supports the trend seen for the addition of neutralising antibodies on myelination in cultures on TnC-astrocytes, and shows a significant effect of CXCL10 protein to decrease myelination on PLL-astrocytes.

To assess if CXCL10 can reduce myelination in cultures plated on TnC-astrocytes, myelinating cultures plated on TnC-astrocytes were treated with CXCL10 from day 12 onwards (Fig 7.10). The addition of CXCL10 did not result in a further decrease in myelination (Fig 7.10 A-C). No change in neurite density was observed (Fig 7.10 D).

### **6.2.7 CNTF may Regulate the Expression of CXCL10**

As shown previously, the addition of CNTF to myelinating cultures plated on TnC-astrocytes lead to an increase in myelination when compared to untreated myelinating control cultures (Fig 6.6). The next logical step was to investigate whether CNTF is able to modulate the expression of CXCL10. It was hypothesised that the addition of CNTF to cultures on TnC-astrocytes would downregulate the expression of CXCL10 and thus lead to an increase in myelination. To test this hypothesis, myelinating cultures plated on PLL-astrocytes and TnC-astrocytes, where some were left untreated and others treated with CNTF (2 ng/ml). After 24 hours of treatment, cultures were lysed, RNA was extracted, cDNA was synthesised and qRT-PCR was performed. Myelinating cultures on TnC-astrocytes show a reduction in CXCL10 expression after CNTF treatment, although this was not statistically significant (Fig 6.11,  $p > 0.05$ ). Interestingly, untreated myelinating cultures plated on PLL-astrocytes and TnC-astrocytes had similar levels of CXCL10 expression, which was surprising, as it was presumed that myelinating cultures plated on TnC-astrocytes were expected to have a higher expression of CXCL10. There are two possible explanations for this. Firstly, CXCL10 was not upregulated in the TnC-astrocytes in this particular experiment or alternatively, other cells in myelinating cultures on PLL-astrocytes might also express CXCL10, for example, microglia, which mask the expression of CXCL10 in astrocytes.

### **7.3 Discussion**

The identification of genes which contribute to a particular astrocyte phenotype is central to understanding astrocyte behavior in health and in disease. As astrocytes make up the largest population of cells in the CNS, they are heavily involved in much of its function. For example, astrocytes are involved in the regulation of minute changes in the pH of the tissue environment as well as taking on extreme morphological and metabolic changes in disease states. In this study, microarray analysis identified an increase in mRNA expression of CXCL10 in TnC-astrocytes. The role of CXCL10 in myelination was validated using myelinating cultures. The addition of neutralising antibodies to CXCL10 to myelinating cultures plated on TnC-astrocytes resulted in a trend in increase in myelination whereas the addition of CXCL10 to myelinating cultures on PLL-astrocytes resulted in a decrease in myelination. These observations demonstrate the efficiency of microarray data collection, their validation in a working culture system as well as the importance of gene selection for future therapeutics in MS.

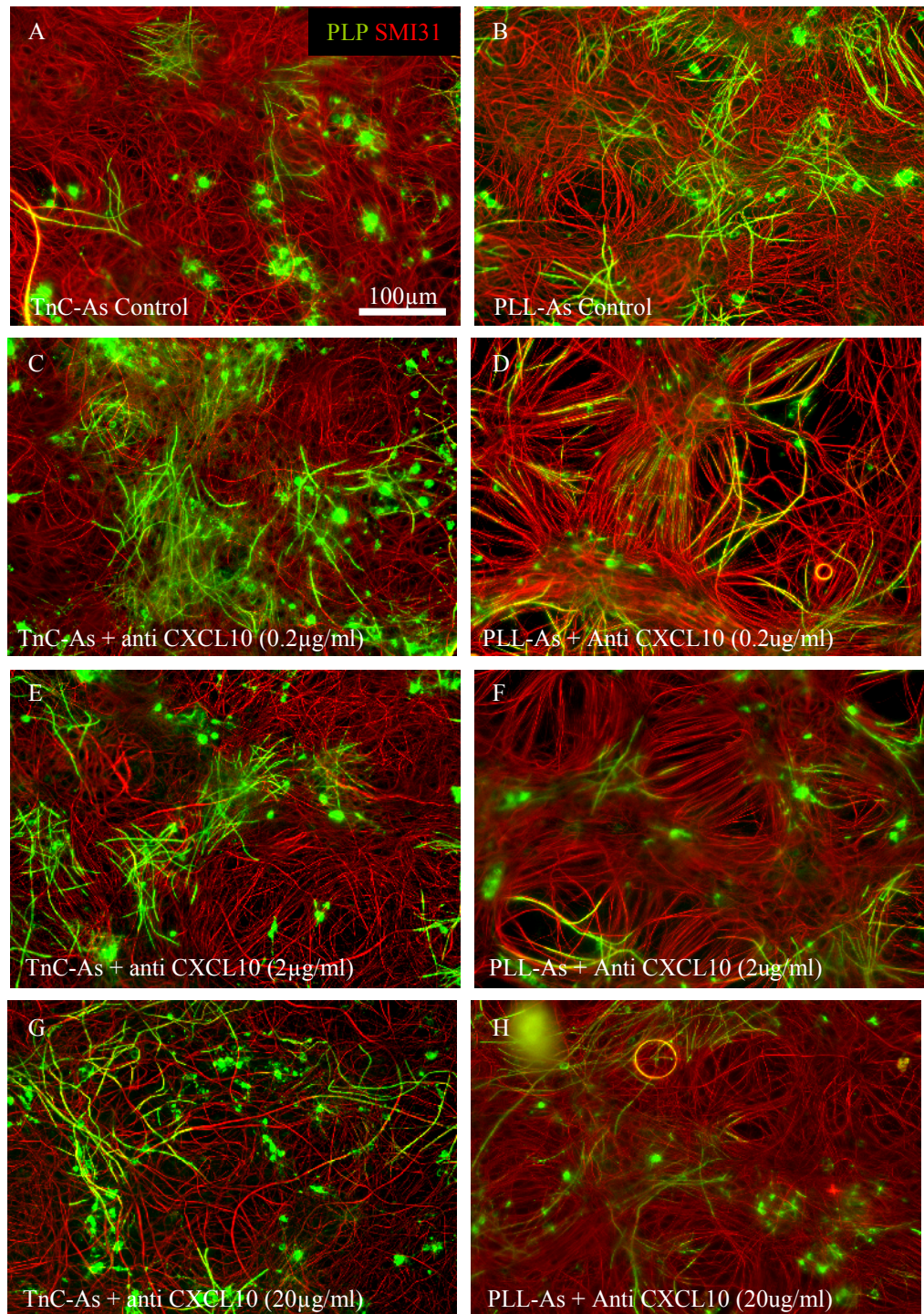


**Figure 7.7 CXCL10 Neutralising Antibodies increase Myelination in TnC-Astrocytes.** Myelinating cultures were plated onto TnC-astrocytes (A, C, E, G) or PLL-astrocytes (B, D, F, H). Cultures were either left untreated (A-B) or treated with neutralising antibodies to CXCL10 at 0.2 µg/ml (C-D), 2 µg/ml (E-F) and 20 µg/ml (G-H). Myelination and neurite density was calculated by immunofluorescence using SMI31 antibody (red) for neurites and anti-PLP (green) for mature myelin using Image J and Adobe Photoshop. Treatment with neutralising antibodies to CXCL10 resulted in an increase in myelination in TnC-astrocytes compared to control cultures. Treatment with antibodies resulted in a slight decrease in myelination in PLL-astrocytes. Scale bar 100 µm. Experiments were performed in triplicates.

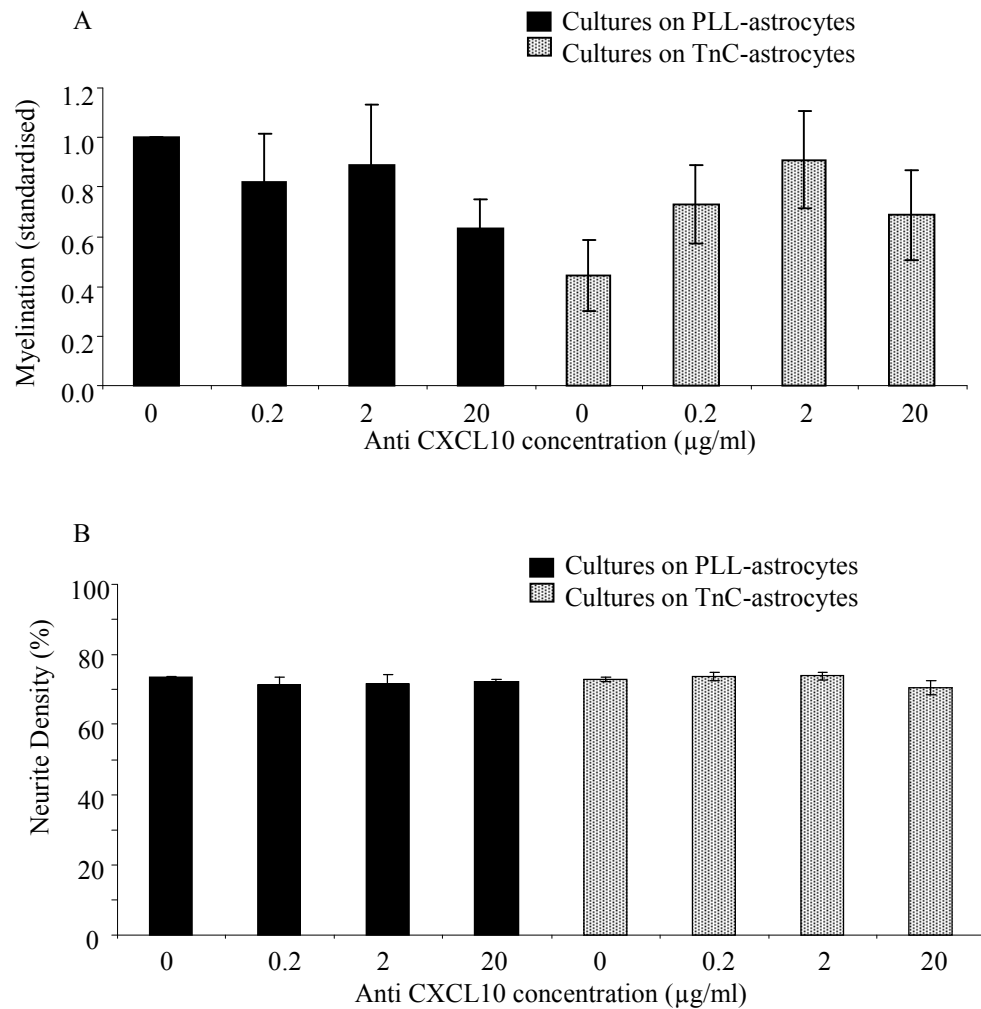


**Figure 7.8 CXCL10 Neutralising Antibodies increase Myelination in TnC-Astrocytes with no effect on Neurite Density.** Myelinating cultures were plated onto PLL-astrocytes or TnC-astrocytes. Bar chart represents quantification from Figure 6.7. Cultures were either left untreated or treated with neutralising antibodies to CXCL10 at 0.2-20 µg/ml. Myelination and neurite density was calculated by immunofluorescence using SMI31 antibody (red) for neurites and anti-PLP (green) for mature myelin using Image J and Adobe Photoshop. Treatment with neutralising antibodies to CXCL10 resulted in an increase in myelination in cultures on TnC-astrocytes compared to cultures on PLL-astrocytes, although this was not significant (A). Treatment with antibodies resulted in a slight decrease in myelination in PLL-astrocytes, which was not significant (A). The neurite density was unaffected by treatment across all conditions (B). Experiments were performed in triplicates. Error bars indicate standard error of the mean.

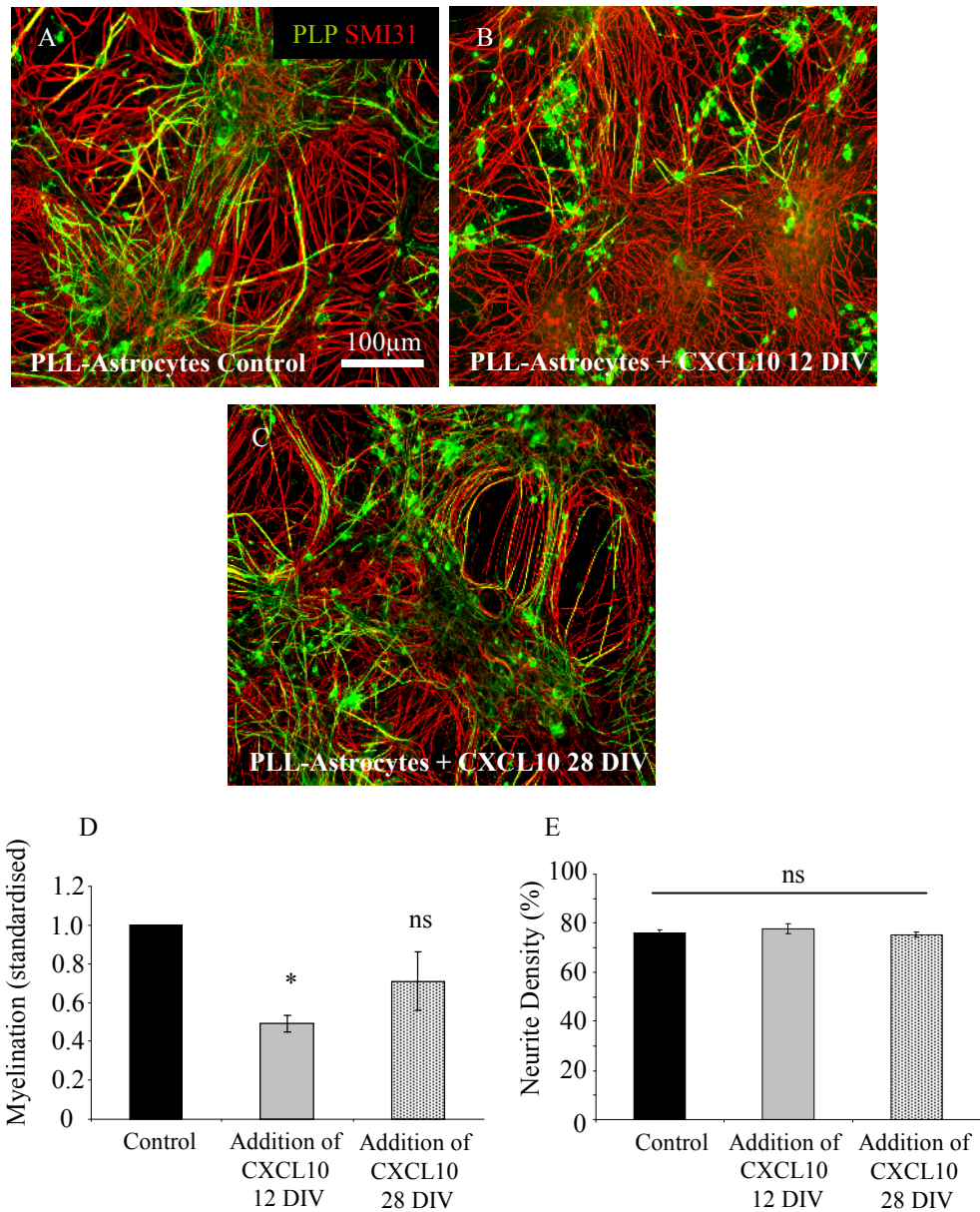


**Figure 7.9 The Addition of CXCL10 to Myelinating Cultures on PLL-Astrocytes Resulted in a decrease in Myelination.** Myelinating cultures were plated onto PLL-astrocytes. Cultures were either left untreated (A) or treated with CXCL10 on day 12 (B) or 28 (C). Myelination and neurite density was calculated by immunofluorescence using SMI31 antibody (red) for neurites and anti-PLP (green) for mature myelin using Image J and Adobe Photoshop. Treatment with CXCL10 on day 12 resulted in a significant decrease in myelination (D,  $p < 0.05$ ). The addition of CXCL10 on day 28 had no affect on myelination (D). The neurite density was unaffected by treatment across all conditions. Scale bar 100 μm. Experiments were carried out in triplicates. Error bars indicate standard error of the mean.

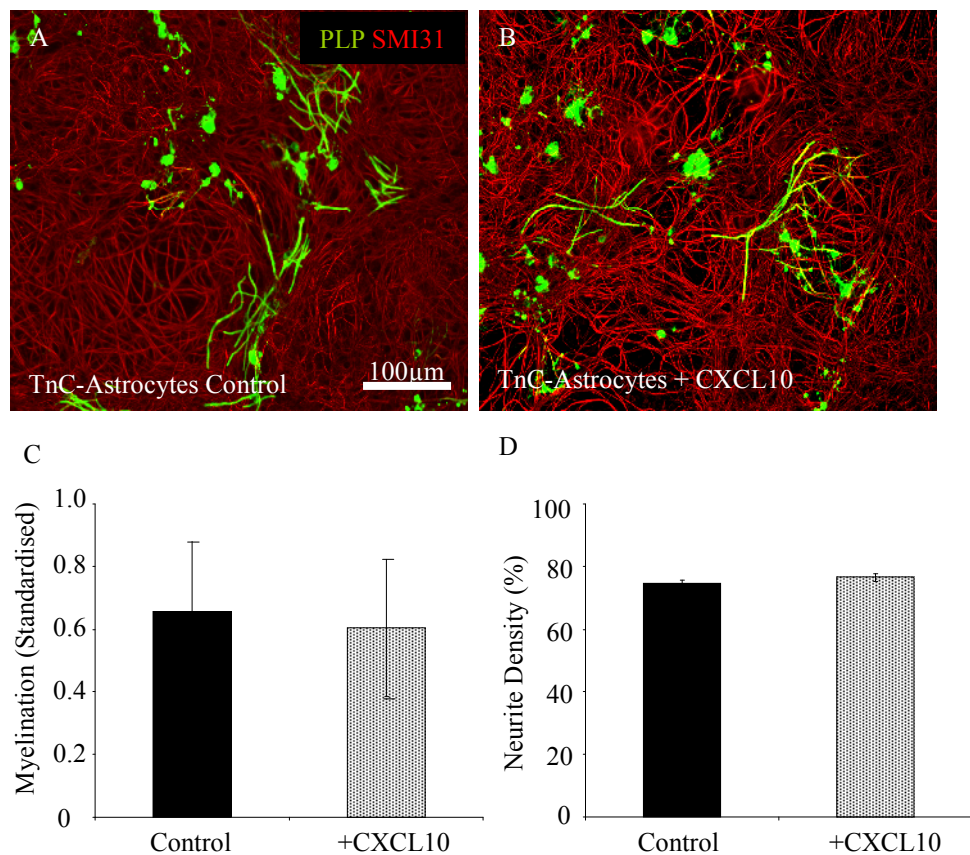


**Figure 7.10 The Addition of CXCL10 to Myelinating Cultures on TnC-Astrocytes does not affect Myelination.** Myelinating cultures were plated onto TnC-astrocytes. Cultures were either left untreated (A) or treated with CXCL10 on day 12 onwards (B). Myelination and neurite density was calculated by immunofluorescence using SMI31 antibody (red) for neurites and anti-PLP (green) for mature myelin using Image J and Adobe Photoshop. Myelination was quantified and it can be seen that treatment with CXCL10 did not affect myelination levels compared to untreated cultures on TnC-astrocytes (C). The neurite density was calculated and found to be unaffected by treatment (D). Experiments were performed in triplicates. Scale bar 100  $\mu$ m. Error bars indicate the standard error of the mean.

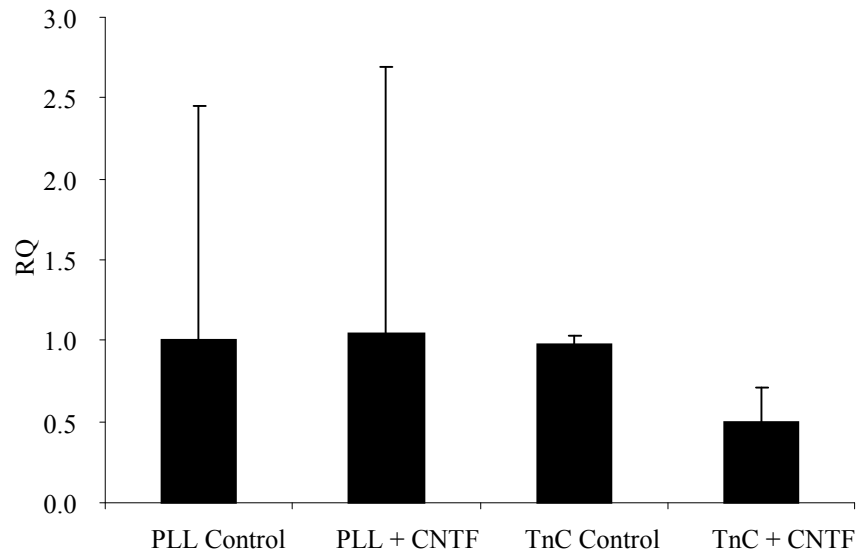


**Figure 7.11 CXCL10 is slightly reduced in Myelinating Cultures plated on TnC-Astrocytes Treated with CNTF as Measured by qRT-PCR.** Myelinating cultures were plated on PLL-astrocytes and TnC-astrocytes; on day 12 some cultures were left untreated and others treated with CNTF (2 ng/ml). After 24 hours, the cultures were lysed, RNA was extracted and cDNA synthesised. qRT-PCR was performed using primers for CXCL10 and GAPDH (house keeping gene). Bar chart represents the relative quantification (RQ) results for CXCL10 mRNA after CNTF treatment in myelinating cultures plated on PLL-astrocytes and TnC-astrocytes. Myelinating cultures on TnC-astrocytes had a slight reduction in CXCL10 expression after CNTF treatment, although not significant. CNTF treatment of myelinating cultures plated on PLL astrocytes had no effect on CXCL10 expression. Experiments were performed in triplicate. Error bars indicate the standard error of the mean.

The expression of genes which change when comparison is made between TnC-astrocytes at 4 hours and PLL-astrocyte untreated or treated with CNTF at 24 hours correlate with the phenotype of the astrocyte (TnC-astrocyte being least supportive and PLL-astrocyte treated with CNTF being the most supportive). In hindsight, a more appropriate comparison should have been with the gene expression changes in TnC-astrocytes after 24 hours. The original decision not to include this time frame was made because astrocytes plated on TnC do not receive any particular treatment, and timing starts with media change at 4 hours as carried out for untreated PLL-astrocytes. Thus, one time point was chosen. However, analysis of mRNA expression in TnC-astrocytes after 24 hours is still expected to obtain changes in the expression of other genes of interest. Nonetheless, the comparison between TnC-astrocytes at 4 hours and those on PLL-astrocytes at 24 hours in culture did yield many key genes which can be further investigated in myelinating cultures.

The Illumina BeadArray Reader and Beadstudio programs used in the microarray have rigorous methods of analysis using the FDR as well as fold changes. The experimental astrocyte samples were derived from different groups of pups, each from a different outbred female, and therefore have a wide range of genetic variability which is translated into noise in the resulting data sets. The analytical methods performed using Illumina Beadstudio filtered out the noise in the data and thus presenting a sound and statistically significant product. The same RNA samples used for the microarray were used for the qRT-PCR analysis. No noise filtering took place when quantifying the qRT-PCT data which may explain the lack of significance for genes which were identified as significant in the microarray.

Many reports have demonstrated the pro-regenerative properties of cytokine-activated astrocytes although the exact factor(s) secreted and targets are still unknown (Ridet et al., 1997; Liberto et al., 2004; Williams et al, 2007). Using the microarray gene expression profiling of the various treated astrocyte monolayers, only the change in expression of 2 genes were observed when comparison was made between untreated PLL-astrocytes and those treated with CNTF. This may be because analysis was carried out on pure astrocyte monolayers lacking myelinating cultures plated on their surface. Without the mixed cell population from the myelinating cultures we may be eliminating any cross talk between the various cell types (oligodendrocyte, microglia, stem cells etc.). For example, CNTF treatment may promote the secretion of an astrocyte factor which in turn affects oligodendrocyte lineage cells to secrete a factor that either directly or indirectly (via the

astrocyte) influences myelination. It is also possible that CNTF could not activate astrocytes due to the lack of one of the components of its receptor. CNTF effects are mediated by a tripartite receptor complex consisting of the CNTF receptor  $\alpha$ , LIFR $\beta$  receptor and gp130 (Lee et al., 1997; Sleeman et al., 2000; Fig 5.1). Signal transduction by CNTF requires the binding of CNTF to CNTFR  $\alpha$ , permitting the recruitment of gp130 and LIFR $\beta$  which leads to heterodimerization of the receptor subunits and tyrosine phosphorylation. As it has been shown that neurons shed the CNTFR  $\alpha$  subunit (Sleeman et al., 2000), it is possible to speculate that the lack genes obtained from the microarray study may be due to the absence of one of its receptor component and thus their inability to form the tripartite complex required for signalling.

The downregulation of GDF15 in PLL-astrocytes treated with CNTF for 24 hours compared to control PLL-astrocytes as well as its upregulation in TnC-astrocytes is interesting as GDF15 has previously been associated with neuroprotection and injury states. For instance, Strelau et al. (2000) show the neuroprotective actions of GDF15 in the 6-hydroxydopamine (6-OHDA) model of Parkinson's disease. 6-OHDA was injected into the rat brain and resulted in loss of dopaminergic nigrostriatal neurons. Intravenous administration of GDF15 into the medial forebrain bundle prior to the 6-OHDA injection resulted in a significant increase of neuronal survival. The authors argue that the neuroprotective effect observed is not due to astrocytes as no change in their proliferation or maturation after GDF15 treatment was observed. However, it is not necessary for astroglial numbers to change in order for them to respond to a particular treatment as astrocytes more distal to a lesion, although termed activated, do not show a proliferative profile (Sonfroniew and Vinters, 2010). In our study, TnC-astrocytes which do not support myelination show an increase in GDF15 whilst PLL-astrocytes treated with CNTF which do support myelination show a decrease in GDF15. As CNTF leads to an increase in myelination when added to the myelinating cultures, it was surprising that the expression of GDF15 expression in these astrocyte cultures is in contrast to that reported in the literature. It is a possibility that GDF15 has multiple roles, including novel roles not yet identified, and that GDF15 may act differently *in vivo* and *in vitro*. GDF15's role remains unresolved and will need further investigation.

The changes in TnC-astrocytes compared to untreated and CNTF-treated PLL-astrocytes at 4 and 24 hours will now be discussed. This comparison represents the 'extremes' in astrocyte support for myelination. TnC-astrocytes are the least supportive, whereas PLL-

astrocytes at a later time-point are most supportive, especially with CNTF treatment. A number of relevant genes were identified with a change in expression after treatment, including PTN, Transgelin, TNR, IGFBP2, IGF1, CXCL10, CTGF and THSB4. The relevance of each will be discussed in turn.

PTN was downregulated in TnC-astrocytes. PTN is associated with the syndecan family, which is a subtype of heparan sulfate proteoglycans (HSPGs) which can bind to PTN. Syndecan expression is associated with reactive astrocytes, therefore suggesting that PTN may be associated with the glial scar and may have possible roles post injury (Iseki et al., 2002). In a model of spinal cord injury, an increase in the expression of PTN correlated with reactive astrocytes as well as oligodendrocytes and neurons, suggesting a wider role after injury (Wang et al., 2004). The authors attribute the expression of PTN as supportive, although they show no evidence of this in their work. The presence of PTN could equally hinder regeneration attempts. The downregulation of PTN in TnC-astrocytes is not yet fully understood as the role of PTN in injury is not fully known. If PTN is indeed supportive to regeneration, then its downregulation in TnC-astrocytes could contribute to the non-supportive phenotype of astrocytes and hence the reduction in myelination observed when myelinating cultures are plated on TnC-astrocytes.

Astrocyte size and shape have widely been associated with their reactivity status. Olk et al., (2010) show that the knock down of the connexin Cx43 (using RNAi) resulted in a decrease in astrocyte size, which was associated with an increase in Transgelin. Similarly, TnC-astrocytes used in this study are smaller (Fig 6.3) and upregulated Transgelin. Although Transgelin may not have an active and direct role to play in lack of support for myelination, its increased expression in TnC-astrocytes contributes to the overall astrocyte phenotype and thereby contributing indirectly to an environment which does not support myelination.

TNR is expressed in oligodendrocytes (Pesheva et al., 1997; Zhao et al., 2009) and its presence is either due to contaminating oligodendrocytes progenitors or its presence in astrocytes. If the latter is true this will be a novel finding. It is likely to be the former and indeed Czopka et al. (2009) have shown that pre-oligodendrocytes from TNR null mice grow normally but have reduced MBP expression on a control substrate (P-Orn) and can be rescued if plated on the TNR substrate. Therefore the expression of TNR on

oligodendrocytes is required for the differentiation of oligodendrocyte precursors. Since TnC-astrocytes in our study have a reduced TNR expression compared to PLL-astrocytes, it suggests that although the progenitors are present, they do not differentiate. However, it must be noted that this observation implies that progenitors are also present on PLL-astrocytes which are not inhibited from differentiating. This observation also suggests that progenitor cells on top of the astrocyte monolayer contribute to the myelinating oligodendrocyte population in the myelinating cultures.

Liu et al. (1994) have shown that the expression of IGFBP2 and IGF1 in astrocytes in EAE animals correlated with the expression of IGF1 receptor in oligodendrocytes. These data suggest that the presence of IGFBP2 on astrocytes contributes to the remyelination process. Furthermore, Yao et al. (1995) used a cryogenic model of spinal cord injury to induce neuronal loss and demyelination and found that IGFBP2-expressing astrocytes were in proximity to regenerating neurons and remyelination. TnC-astrocytes downregulate the expression of this molecule further supporting the fact that these molecules contribute to a phenotype of astrocytes which is not supportive for myelination.

The increased expression of CTGF in TnC-astrocytes unquestionably requires further investigation. There is a strong association of the overexpression of CTGF with astrocytes which form the glial scar (Kondo et al., 1999; Hertel et al., 2000; Conrad et al., 2005). In addition, Stritt et al. (2009) demonstrated that the adenovirus-mediated expression of CTGF in mice resulted in reduced number of mature oligodendrocytes *in vivo*. They further investigate the mechanism of this reduction in an *in vitro* set up. Oligodendrocytes normally increase in number in the presence of IGF whereas the addition of IGF with CTGF inhibited this increase in oligodendrocytes. These observations, along with the downregulation of IGF in TnC-astrocytes (Table 6.9 AB) strongly suggest an imperative role for CTGF in astrocyte/oligodendrocyte interaction as well as the regulation of myelination.

Reactive astrocytes have also been shown to secrete CXCL10 (Ransohoff et al., 1993). This is a small molecule belonging to the CXC chemokine family and shares its CXCR3 receptor with CXCL9 and CXCL11. Interestingly, CXCL10 has been shown to be expressed by reactive astrocytes surrounding active MS lesions (Omari et al., 2005; Carter et al., 2007). Since oligodendrocytes express the CXCR3 receptor they may be the target for CXCL10. Furthermore, CXCL10 mRNA was shown to be significantly increased

during peak disease and reduced during the recovery phases in animal models of MS including MOG-induced EAE (Godiska et al., 1995; Glabinski, et al., 1997; Fife et al., 2001). It has been shown, that CXCL10<sup>-/-</sup> and CXCR3<sup>-/-</sup> mice provoked more severe clinical and histological symptoms and earlier onset in MS disease models compared to wild type controls (Klein et al., 2004; Liu et al., 2006; Muller et al., 2007). However, in a viral model of MS, neutralising antibodies to CXCL10 lead to a reduction in disease progression and suppressed ongoing demyelination (Liu et al., 2001). This conflicting evidence for the effects of CXCL10 suggests possible multiple functions on CNS pathologies. In the data presented here, the addition of CXCL10 to cultures on PLL-astrocytes resulted in a decrease in myelination and the addition of neutralising antibodies to cultures on TnC-astrocytes shows a trend where there is an increase in myelination. The validation of this gene in the myelinating culture system demonstrates an obvious inhibitory role played by astrocyte-derived CXCL10.

These findings are the first show that polarization of astrocyte phenotypes can affect myelination; quiescent (TnC-astrocytes) do not support myelination whereas activated (PLL-astrocytes treated with CNTF) do to a high degree. Untreated PLL-astrocytes also support myelination, suggesting that when astrocytes are plated *in vitro* they become activated (as discussed in Section 1.4.6). The quiescent phenotype, which was defined as a phenotype resembling that of a resting astrocyte in the normal brain (Holley et al., 2005), does not appear to be a passive phenotype as it prevents myelination by the secretion of CXCL10, a factor reported to be expressed by reactive astrocytes (Ransohoff et al., 1993; Tani et al., 1996). These data suggest that astrocytes are, to some extent, activated *in vitro* and can promote myelination. This degree of activation can be further induced by cytokines, such as CNTF. Furthermore, CNTF can also reverse the quiescent phenotype to a more activated one, possibly by downregulating expression of CXCL10. While CXCL10 evidently plays a role in myelination it should be noted that other possible candidates were identified in the microarray analysis and it is possible they all contribute to the effects observed. The identification of other molecules that are associated with the varied astrocyte phenotypes will shed light on the complex and multifaceted environment of astrocytosis and may lead to therapeutic avenues for the treatment of MS.

## **Chapter 8**

### **General Discussion**

## General Discussion

---

### 8.1 Cross-talk Between Astrocytes and Neurons

In this thesis I have demonstrated the important role for astrocytes in regulating aspects of myelination. From the literature and what has been described in this thesis, it is apparent that astrocytes can exist in different ‘states’. These ‘states’ determine their functional outcome and for this reason this topic needs further investigation. In this thesis, two astrocyte phenotypes were described, namely, the ‘activated’ astrocyte and the ‘quiescent’ astrocyte. Activated astrocytes used as a monolayer for myelinating cultures supported myelination whereas quiescent astrocytes did not. CXCL10 was identified as an quiescent astrocyte-derived molecule which inhibited myelination and its neutralisation resulted in an increase in myelination. CNTF was used to activate astrocytes and its addition to myelinating cultures resulted in an increase in myelination. However, comparing microarray data from untreated and CNTF treated astrocytes did not identify any genes which could be attributable to the increase in myelination. A likely explanation for this observation is the required cross-talk between astrocytes and other cell types. Indeed, cross-talk between astrocytes and neurons has previously been described by Wang et al. (2009) regarding neuropathic pain. The authors show data demonstrating that astrocytic activation enhances neuronal activation, and therefore strengthening the idea of cross-talk between cells in order to achieve their function. As previously discussed in Chapter 5, CNTF requires the  $\alpha$  subunit of its receptor complex in order to activate signaling pathways, which may be shed from neurites (Kahn et al., 1997). Furthermore, astrocytes may require signals from other cells types in order to secrete promyelinating factors. In order to investigate this hypothesis, a microarray study needs to be conducted on whole myelinating cultures, rather than astrocyte monolayers alone. A comparison between myelinating cultures left untreated and treated with CNTF on activated and quiescent astrocytes will undoubtedly identify more genes associated with the phenotypic state of the astrocytes. However, as the myelinating cultures comprise many different cell types, and genes which will be identified may not necessary be astrocyte-specific ones. To resolve this, genes identified should be tested in the myelinating cultures and their effects on astrocytes in particular can be verified via Western blotting, immunohistochemistry or qRT-PCR.

## 8.2 Mechanisms of Action

In terms of modes of action, the role of CXCL10 was not fully investigated. It is hypothesised that CXCL10 secretion from astrocytes acts directly on the oligodendrocyte precursor cells (OPCs). There are several experiments that should next be carried out in order to verify this hypothesis. For instance, CXCL10 can be directly added to purified OPCs and cell death, proliferation and ability to differentiate into mature myelin forming oligodendrocytes can be investigated. Furthermore, the descending pathways which lead to these effects would also need to be investigated. For instance, could CXCL10 be affecting oligodendrocyte differentiation via the upregulation of Hes5, which ultimately leads to blockage of oligodendrocyte maturation (John et al., 2002)? Alternatively, CXCL10 could be inducing apoptotic and/or necrotic cell death via the activation of Caspase 3 (Casaccia-Bonofil, 2000).

Upstream signaling pathways of CXCL10 also need to be investigated to understand the triggers which lead to its expression. NF- $\kappa$ B is a protein complex and its descending canonical pathway can act as a ‘master switch’ for many inflammatory mechanisms (Schmid et al., 2006). Indeed, the activation of NF- $\kappa$ B has been demonstrated using inflammatory cytokines such as IL-1 $\beta$ , IFN- $\gamma$  and TNF- $\gamma$  and interestingly, resulted in the upregulation of CXCL10 message and protein in endothelial cells (Yeruva et al., 2008; Lombardi et al., 2001). Whether this is the same case in astrocytes, remains to be elucidated. Interestingly, the deactivation of astroglial-NF- $\kappa$ B in transgenic mice resulted in improved functional recovery, increased white matter preservation, reduced expression of chondroitin sulfate proteoglycans and reduced expression of inflammatory cytokines including CXCL10, 8 weeks after spinal cord injury (Brambilla et al., 2005). Although the exact mechanisms are not clear, it is apparent that CXCL10 regulates the inflammatory response of astrocytes, which in turn affects oligodendrocyte maturation and/or survival (Fig 8.1). It would be extremely interesting to investigate whether NF- $\kappa$ B is responsible for the effects observed in quiescent astrocytes.

## 8.3 Astrocyte Phenotype and Control of Myelination

The definitions of astrocytes as reactive, activated and quiescent are still quite nebulous. Quiescent astrocytes have been described as ‘passive’ and this may be the incorrect definition of these cells. In fact they actively regulate the process of myelination. It is hypothesised that quiescent astrocytes express CXCL10 in order to ‘control’ myelination.

Indeed, myelination occurs in early life and usually ends in adolescence (Buffo et al., 2010) and CXCL10 is not expressed in normal adult tissue (John et al., 2002). Therefore, it could be hypothesised that astrocytes secrete CXCL10 in late adolescence in order to stop myelination and once it is stopped, the expression of CXCL10 would no longer be required. It would be interesting to find out whether tissue from the developing rodent corresponds to this hypothesis. Undoubtedly, other astrocyte-specific molecules may also regulate myelination during development. To what extent the expression of these molecules can be 're-activated' or 'de-activated' to induce myelination during disease is yet to be investigated.

## **8.4 Astrocyte Heterogeneity**

A complexity in understanding astrocyte behavior in disease is their heterogeneity which depends on their morphology and location (Zhang and Barres, 2010). Astrocytes in different locations of the brain may respond differently to particular injuries and consequently treatments. Yeh et al. (2009) used a microarray gene analysis study to investigate and compare the heterogeneity of astrocytes from the neocortex, cerebellum, brainstem and optic nerve. They found that the astrocytes fell into individual groups with both similarities and distinctions in gene profiles suggesting that astrocytes may have overlapping and distinct functions depending on their location. Interestingly, Hochstim et al. (2008) have confirmed the presence of three positionally distinct astrocyte subtypes. By using loss and gain of function experiments, the authors were able to demonstrate the three subtypes based on their expression of Reelin and Slit1, which are guidance molecules. The data from these studies propose that not only do astrocytes from anatomically distinct regions vary in heterogeneity, but also that there are subtypes within these regions. It would be interesting to develop these studies further and investigate how these astrocyte subtypes react to inflammatory agents and/or physical injury as well as how their support and/or communication with other cells, like neurons and oligodendrocytes, is altered. It seems that astrocyte heterogeneity is much more complex than originally anticipated. This could therefore explain the variety in astrocytic response depending on treatment agent, type of injury and location in the CNS. To what extent these heterogeneous astrocyte subtypes correspond to the continuum of astrocyte reactivity is undeniably a very important question and in need of further investigation.

## 8.5 Astrocytes Phenotypes *In Vivo*

The identification of astrocyte phenotypes *in vivo* is fundamental in understanding astrocyte biology; where the identification of particular molecules is associated with specific astrocyte phenotype. It is likely that future therapies will identify specific astrocyte phenotypes and target secretory or expressional molecules to reverse or change from one phenotype to another *in vivo*. A method to directly target a specific gene, or a number of genes, is the use of conditional knockout animals. However, knockout animals may consequently be affected by the lack of particular proteins developmentally and may not answer the specific questions about disease states in the adult. Therefore, RNA interference (RNAi) may be used to target specific genes in the adult without developmental interference. RNAi is also known as post transcriptional gene silencing in plants and quelling in fungi (Zeringue and Constantine-Paton, 2004), is where double stranded RNA is delivered to the cell leading the degradation of transcripts with complementary sequences. This approach will aid in understanding the cellular and molecular basis of particular proteins and how these in turn affect the animal *in vivo*. Once more is understood about particular sets of genes attributable to a particular phenotype, these can then be targeted and switched on or off in order to reverse the phenotype. For instance, CXCL10 can be switched off in astrocytes within the glial scar whilst CNTF can be switched on in astrocytes distal to the scar. Although these changes may not ‘cure’ MS, they may create a more favorable environment in which re-myelination can take place and therefore providing some functional recovery. The treatment for MS is largely symptomatic and usually to control the inflammation. These drugs can inhibit, to some extent, the inflammatory component of MS but they do not suppress the progressive clinical disability. Furthermore, immunosuppressive agents can usually also disturb immunoregulatory mechanisms and cause adverse effects (Condarri et al., 2010). Mangas et al. (2010) argue that MS should not be viewed only as an inflammatory disease and other aspects of MS should be incorporated into drug manufacturing including oxidative stress, demyelination and neuronal death. It has also been argued that therapies should focus on strategies which promote remyelination via promoting the division, recruitment, and differentiation of OPCs (Casaccia-Bonnel, 2000). Thus, MS will greatly benefit if researchers and drug manufacturers were to be more innovative and resourceful using a combinatorial approach to treat MS.

## **8.6 Cytokines and Models of Multiple Sclerosis**

It is extremely difficult to investigate the role of cytokines in MS due to its multifaceted nature. The use of preclinical models of MS requires much more investigation before their translation into human work. Firstly, the induction of MS in these models is artificial and although similar characteristics are observed, they are not a true representation of the disease. As a result, the treatments used for these models do not translate well into human research. Secondly, data using cytokines in MS models are often oversimplified (Codarri et al., 2010). The models do not translate well in human trials because cytokine-related effects are likely to be indirect and involving many cells. Therefore, until the etiology of MS is resolved, it will remain difficult to interpret the data obtained from animal models of MS and their potential use of cytokines in treatment.

Takuya et al. (2000) discuss several methods whereby cytokines could be incorporated into future experimentation and disease conditions. Firstly, they discussed the potential of neutralising IL-6 using a cocktail of neutralising antibodies or using a constructed fusion protein of mutated IL-6 and its soluble subunit (sIL-6R) which are covalently bound and act as effective antagonists without inducing dimerization (Renne et al., 1998; Beck et al., 1994; Wendling et al., 1996). Secondly, some cytokines have both anti-inflammatory and pro-inflammatory effects and addressing the balance in these may provide therapeutic advantages when combined with other treatments. Finally, the 'receptor conversion model' is whereby a cytokine is coupled with its soluble receptor linked by a flexible peptide chain (Fischer et al., 1996) could be used. These joint molecules have been shown to illicit actions on cells non responsive to the particular cytokine thereby increasing the receptor repertoire. Furthermore, they have also been found to activate slightly differing descending pathways. These attributes could be balanced in order to provide therapeutic strategies for many cytokine-related diseases. Thus, when the activity of cytokines is finely tuned, it is likely that they will greatly contribute to the therapeutic outcome of many inflammatory diseases.

## **8.7 Future Experiments**

The results from this thesis shed some light on the existence of astrocyte-specific molecules which influence myelination. However, there are a vast number of questions left

unanswered. Firstly, the effects of CNTF on astrocytes are not fully understood in the myelinating culture context. Although CNTF's action on neurite diameter, microglial numbers and oligodendrocyte proliferation and maturation have been ruled out, the direct action on astrocytes has not been fully established. For instance, the levels of GFAP, nestin and other astrocyte molecules which have been attributed to astrocyte reactivity could have been measured within the myelinating cultures with and without CNTF treatment. Secondly, a microarray experiment comparing CNTF treated cultures to untreated could also reveal how CNTF is activating astrocytes and the resulting effects this has on other cells types. The microarray experiments will reveal the importance of cross-talk between astrocytes and other cell types in the myelinating cultures. Thirdly, the use of astrocyte-specific gp130<sup>-/-</sup> mice will establish whether CNTF is acting via the astrocyte monolayer. However, the results of this experiment must be interpreted with care as gp130 is a shared receptor component of other members of the IL-6 family, in which CNTF belongs. Therefore, the effects observed might be a wider effect of IL-6 family members rather than CNTF specific effects. Finally, it was discussed that CNTF requires the  $\alpha$  subunit to mediate its effects. The soluble  $\alpha$  subunit can be purchased and added alongside CNTF in order to activate astrocyte monolayers to test whether this hypothesis is true.

A microarray to comparing quiescent and activated astrocytes in culture should also be investigated with and without CNTF. This will explore whether CNTF can modulate the astrocytic phenotype from quiescent to a more activated one and therefore relating this to the astrocytes' ability to support myelination.

It was found that the astrocyte-derived CXCL10 lead to the reduction of myelination. In terms of mechanisms of action, the ability of CXCL10 to inhibit myelination has not been fully assessed. It is known, however, that CXCL10 does not induce demyelination as its addition to mature myelinating cultures does not lead to a reduction in myelination. What requires further investigation is how CXCL10 affects OPCs, i.e. inhibiting proliferation and/or differentiation or their ability to extend processes and ensheath axons. These experiments are straight forward and will answer many questions about CXCL10 biology. Although the myelinating cultures provide a functional model for myelination, they can also be used to investigate descending pathways. The cultures can be lysed and particular downstream pathways could be investigated.

In terms of *in vivo* experimentation, animals with experimental autoimmune encephalomyelitis (EAE) or spinal cord injuries could be used to further investigate

astrocyte-related molecules. For instance, astrocyte-specific RNAi could target glial scarring by downregulating the expression of chondroitin sulphate proteoglycans and particular cytokines and chemokines, such as CXCL10. This method should be used a combinatorial approach with other astrocyte-related molecules and systemic drugs which ameliorate the inhibitory environment. Immunohistochemical studies would reveal the extent of scarring after treatment compared to control animals. Furthermore, behavioural analysis could be used to assess functional recovery after treatment therefore providing a true indication of how efficacious the treatment is.

## **8.8 Conclusions of Thesis**

Many laboratories are now recognising astrocytes as more than an obstacle to regeneration. It is believed that astrocytes may hold therapeutic potential if they were triggered via the correct methods (Buffo et al., 2010; Hamby and Sofroniew, 2010). As astrocytes make up a large majority of the cells in the CNS, as well as contributing to numerous functions, it is not surprising that they respond dynamically to injury. Although reactive gliosis is a characteristic feature of MS, it is also manifested in numerous neurodegenerative diseases, including Alzheimer's disease, and Huntington disease (Norton et al., 1992; Mucke and Eddelston, 1993). Therefore, any efforts to further our understanding of astrocytes and how they respond to disease and injury will benefit a wide range of patients with varying diseases. The future of astrocyte biology holds promising potential therapies. Astrocyte biology and relating phenotype is an emerging field in neuroscience and is finally beginning to get the attention it deserves.



# References

## References

---

- Abbott NJ, Rönnbäck L, Hansson E (2006) Astrocyte-endothelial interactions at the blood-brain barrier. *Nat Rev Neurosci.* 7(1):41-53
- Alder R, Landa KB, Manthorpe M, Varon S (1979) Cholinergic neuronotrophic factors: intraocular distribution of soluble trophic activity of ciliary neurons. *Science* 204, 1434-1436
- Albrecht P J, Murtie JC, Ness JK, Redwine JM, Enterline JR, Armstrong RC, Levison SW (2003). Astrocytes produce CNTF during the remyelination phase of viral-induced spinal cord demyelination to stimulate FGF-2 production. *Neurobiol. Dis.* 13, 89–101
- Albrecht PJ, Dahl JP, Stoltzfus OK, Levenson R, Levison SW (2000) Ciliary neurotrophic factor activates spinal cord astrocytes, stimulating their production and release of fibroblast growth factor-2, to increase motor neuron survival. *Exp Neurol.* 173(1):46-62
- Albrecht PJ, Enterline JC, Cromer J, Levison, SW (2007) CNTF-activated astrocytes release a soluble trophic activity for oligodendrocyte progenitors. *Neurochem Res.* 32(2), pp. 263-271
- Alexander WS (1949) Progressive fibrinoid degeneration of fibrillary astrocyte associated with mental retardation in a hydrocephalic infant. *Brain* 72:373-81
- Alexander CL, Fitzgerald UF, Barnett SC (2002) Identification of growth factors that promote long-term proliferation of olfactory ensheathing cells and modulate their antigenic phenotype. *Glia.* 37(4):349-64
- Aloisi F, Rosa S, Testa U, Bonsi P, Russo G, Peschle C, Levi G (1994) Regulation of leukemia inhibitory factor synthesis in cultured human astrocytes. *J Immunol.* 152(10):5022-31
- Allaman I, Gavillet M, Bélanger M, Laroche T, Viertl D, Lashuel HA, Magistretti PJ (2010) Amyloid-beta aggregates cause alterations of astrocytic metabolic phenotype: impact on neuronal viability. *J Neurosci.* 30(9):3326-38
- Anderson JM, Hampton DW, Patani R, Pryce G, Crowther RA, Reynolds R, Franklin RJ, Giovannoni G, Compston DA, Baker D, Spillantini MG, Chandran S. (2008) Abnormally phosphorylated tau is associated with neuronal and axonal loss in experimental autoimmune encephalomyelitis and multiple sclerosis. *Brain* 131(Pt 7):1736-48
- Andrews MR, Czvitkovich S, Dassie E, Vogelaar CF, Faissner A, Blits B, Gage FH, French-Constant C, Fawcett JW (2009) Alpha9 integrin promotes neurite outgrowth on tenascin-C and enhances sensory axon regeneration. *J Neurosci.* 29(17):5546-57

- Arai K, Lo EH (2010) Astrocytes protect oligodendrocyte precursor cells via MEK/ERK and PI3K/Akt signalling. *J Neurosci Res.* 88(4):758-63
- Arakawa, Y, Sendtner, M, and Thoenen, H (1990) Survival effect of ciliary neurotrophic factor (CNTF) on chick embryonic motoneurons in culture: comparison with other neurotrophic factors and cytokines. *J Neurosci.* 10(11):3507-15
- Araque A, Martín ED, Perea G, Arellano JI, Buño W (2002) Synaptically released acetylcholine evokes Ca<sup>2+</sup> elevations in astrocytes in hippocampal slices. *J Neurosci.* 22(7):2443-50
- Ard MD, Faissner A (1991) Components of astrocytic extracellular matrix are regulated by contact with axons. *Ann N Y Acad Sci.* 633:566-9
- Auron PE (1998) The interleukin 1 receptor: ligand interactions and signal transduction. *Cytokine Growth Factor Rev.* 9(3-4):221-37
- Badaut J, Ashwal S, Adami A, Tone B, Recker R, Spagnoli D, Ternon B, Obenaus A (2010) Brain water mobility decreases after astrocytic aquaporin-4 inhibition using RNA interference. *J Cereb Blood Flow Metab.* [Epub ahead of print]
- Baranzini SE, Elfstrom C, Chang SY, Butunoi C, Murray R, Higuchi R, Oksenberg JR (2000) Transcriptional analysis of multiple sclerosis brain lesions reveals a complex pattern of cytokine expression. *J Immunol.* 165(11):6576-82
- Barres BA, Hart IK, Coles HS, Burne JF, Voyvodic JT, Richardson WD, Raff MC. (1992) Cell death and control of cell survival in the oligodendrocyte lineage. *Cell* 70(1):31-46
- Barres BA (2010) The mystery and magic of glia: a perspective on their roles in health and disease. *Neuron.*60(3):430-40
- Barrett CP, Donati EJ, Guth L (1984) Differences between adult and neonatal rats in their astroglial response to spinal injury. *Exp Neurol.* 84(2):374-85
- Bartsch S, Bartsch U, Dörries U, Faissner A, Weller A, Ekblom P, Schachner M (1992) Expression of tenascin in the developing and adult cerebellar cortex. *J Neurosci.* 12(3):736-49
- Bauer NG, Richter-Landsberg C, French-Constant C (2009) Role of the oligodendrocyte cytoskeleton in differentiation and myelination. *Glia* 57, 1790-1801
- Beck JT, Hsu SM, Wijdenes J, Bataille R, Klein B, Vesole D, Hayden K, Jagannath S, Barlogie B. (1993) Brief report: alleviation of systemic manifestations of Castleman's disease by monoclonal anti-interleukin-6 antibody. *N Engl J Med.*330(9):602-5

- Benjamini Y, Hochberg Y (1995) Controlling the False Discovery Rate – a practical and powerful approach to multiple testing. *JRSS-B* 57:289-300
- Bergles DE, Diamond JS, Jahr CE (1999) Clearance of glutamate inside the synapse and beyond. *Curr Opin Neurobiol.* 9(3):293-8
- Berthold CH, Nilsson I, Rydmark M (1983) Axon diameter and myelin sheath thickness in nerve fibres of the ventral spinal root of the seventh lumbar nerve of the adult and developing cat. *J Anat.* 136(Pt 3):483-508
- Bhattacharya S, Dooley C, Soto F, Madson J, Das AV, Ahmad I (2004) Involvement of Ath3 in CNTF-mediated differentiation of the late retinal progenitors. *Mol Cell Neurosci.* 27(1):32-43
- Bitsch A, Kulmann T, Da Costa Bunkowski S, Polak T, Bruck W (2000) Tumour necrosis factor alpha mRNA expression in early multiple sclerosis lesions: correlation with demyelinating activity and oligodendrocyte pathology. *123(6):1174-83*
- Black JA, Sontheimer H, Waxman SG (1993) Spinal cord astrocytes in vitro: phenotypic diversity and sodium channel immunoreactivity. *Glia.* 7(4):272-85
- Blakemore WF (1982) Ethidium bromide induced demyelination in the spinal cord of the cat. *Neuropathol Appl Neurobiol.* 8(5):365-75
- Blakemore WK (1984) The response of oligodendrocytes to chemical injury. *Acta Neurol Scand Suppl* 100, 33-38
- Blondel O, Collin C, McCarran WJ, Zhu S, Zamostiano R, Gozes I, Brenneman DE, McKay RD (2000) A glia-derived signal regulating neuronal differentiation. *J Neurosci.* (21):8012-20
- Boomkamp SD, Riehle MO, Olson MF, Barnett SC (2010) A novel in vitro model of Spinal Cord Injury S.D. (*Submitted to Nature Methods*)
- Bottenstein JE, Sato GH (1979) Growth of a rat neuroblastoma cell line in serum-free supplemented medium. *Proc Natl Acad Sci U S A.* 76(1):514-7
- Böttner M, Suter-Crazzolara C, Schober A, Unsicker K (1999) Expression of a novel member of the TGF-beta superfamily, growth/differentiation factor-15/macrophage-inhibiting cytokine-1 (GDF-15/MIC-1) in adult rat tissues. *Cell Tissue Res.* 297(1):103-10
- Boulton TG, Stahl N, Yancopoulos GD (1994) Ciliary neurotrophic factor/leukemia inhibitory factor/interleukin 6/oncostatin M family of cytokines induces tyrosine phosphorylation of a common set of proteins overlapping those induced by other cytokines and growth factors. *J Biol Chem.* 269(15):11648-55

- Bowman T, Garcia R, Turkson J, Jove R (2000) STATs in oncogenesis. *Oncogene*. 19(21):2474-88
- Bradl M, Linington C (1996) Animal models of demyelination. *Brain Pathol*. 6(3):303-11
- Bradl M, Lassmann H (2010) Oligodendrocytes: biology and pathology. *Acta Neuropathol*. 119(1):37-53
- Brahmachari S, Jana A, Pahan K (2009) Sodium benzoate, a metabolite of cinnamon and a food additive, reduces microglial and astroglial inflammatory responses. *J Immunol*. 183(9):5917-27
- Brambilla R, Hurtado A, Persaud T, Esham K, Pearse DD, Oudega M, Bethea JR (2009) Transgenic inhibition of astroglial NF-kappa B leads to increased axonal sparing and sprouting following spinal cord injury. *J Neurochem*. 110(2):765-78
- Bray GM, Villegas-Pérez MP, Vidal-Sanz M, Carter DA, Aguayo AJ (1991) Neuronal and nonneuronal influences on retinal ganglion cell survival, axonal regrowth, and connectivity after axotomy. *Ann N Y Acad Sci*. 633:214-28
- Breitling R, Herzyk P (2005) Rank-based methods as a non-parametric alternative of the t-statistic for the analysis of biological microarray data. *J Bioinform Comput Biol* 3:1171-1189
- Brenner M, Johnson AB, Boespflug-Tanguy O, Rodriguez D, Goldman JE, Messing A (2001) Mutations in GFAP, encoding glial fibrillary acidic protein, are associated with Alexander disease. *Nature Genetics* 27 117-120
- Brenneman DE, Neale EA, Foster GA, d'Autremont SW, Westbrook GL (1987) Nonneuronal cells mediate neurotrophic action of vasoactive intestinal peptide. *J Cell Biol*. 104(6):1603-10
- Brinkmann BG, Agarwal A, Sereda MW, Garratt AN, Müller T, Wende H, Stassart RM, Nawaz S, Humml C, Velanac V, Radyushkin K, Goebbels S, Fischer TM, Franklin RJ, Lai C, Ehrenreich H, Birchmeier C, Schwab MH, Nave KA. (2008) Neuregulin-1/ErbB signaling serves distinct functions in myelination of the peripheral and central nervous system. *Neuron*.59(4):581-95
- Brown AM, Ransom BR (2007) Astrocyte glycogen and brain energy metabolism. *Glia* 55(12):1263-71
- Brück W, Porada P, Poser S, Rieckmann P, Hanefeld F, Kretzschmar HA, Lassmann H (1995) Monocyte/macrophage differentiation in early multiple sclerosis lesions. *Ann Neurol*. 38(5):788-96
- Buffo A, Rite I, Tripathi P, Lepier A, Colak D, Horn AP, Mori T, Götz M (2008) Origin and progeny of reactive gliosis: A source of multipotent cells in the injured brain. *Proc Natl Acad Sci U S A*. 105(9):3581-6
- Buffo A, Rolando C, Ceruti S (2010) Astrocytes in the damaged brain: molecular and cellular insights into their reactive response and healing potential. *Biochem Pharmacol*.79(2):77-89

- Bugga L, Gadiant RA, Kwan K, Stewart CL, Patterson PH (1998) Analysis of neuronal and glial phenotypes in brains of mice deficient in leukemia inhibitory factor. *J Neurobiol.* 36(4):509-24
- Bunge RP, Wood P (1973) Studies on the transplantation of spinal cord tissue in the rat. I. The development of a culture system for hemisections of embryonic spinal cord. *Brain Res.* 1973 Jul 27;57(2):261-76
- Bush TG, Puvanachandra N, Horner CH, Polito A, Ostenfeld T, Svendsen CN, Mucke L, Johnson MH, Sofroniew MV (1999) Leukocyte infiltration, neuronal degeneration, and neurite outgrowth after ablation of scar-forming, reactive astrocytes in adult transgenic mice. *Neuron* 23(2):297-308
- Butzkueven H, Zhang JG, Soilu-Hanninen M, Hochrein H, Chionh F, Shipham KA, Emery B, Turnley AM, Petratos S, Ernst M, Bartlett PF, Kilpatrick TJ (2002) LIF receptor signaling limits immune-mediated demyelination by enhancing oligodendrocyte survival. *Nat Med.* 8(6):613-9
- Cammer W, Zhang H (1999) Maturation of oligodendrocytes is more sensitive to TNF alpha than is survival of precursors and immature oligodendrocytes. *J Neuroimmunol* 97(1-2):37-42
- Canning DR, Höke A, Malemud CJ, Silver J (1996) A potent inhibitor of neurite outgrowth that predominates in the extracellular matrix of reactive astrocytes. *Int J Dev Neurosci.* 14(3):153-75
- Canoll PD, Musacchio JM, Hardy R, Reynolds R, Marchionni MA and Salzer JL (1996) GGF/neuregulin is a neuronal signal that promotes the proliferation and survival and inhibits the differentiation of oligodendrocyte progenitors. *Neuron* 17(2), pp 229-243
- Carter SL, Muller M, Manders P, Campbell IL (2007) Induction of the genes for Cxcl9 and Cxcl10 is dependent on IFN $\gamma$  but shows differential cellular expression in experimental autoimmune encephalomyelitis and by astrocytes and microglia in vitro. *Glia* 55:1728-1739
- Casaccia-Bonnel P (2000) Cell death in the oligodendrocyte lineage: a molecular perspective of life/death decisions in development and disease. *Glia.* 29(2):124-35.
- Cataldo AM, Broadwell RD (1986) Cytochemical identification of cerebral glycogen and glucose-6-phosphatase activity under normal and experimental conditions. II. Choroid plexus and ependymal epithelia, endothelia and pericytes. *J Neurocytol.* 15(4):511-24
- Cenci di Bello I, Dawson MRL, Levine JM, Reynolds R (1999) Generation of oligodendroglial progenitors in acute inflammatory demyelinating lesions of the rat brain stem is stimulated by demyelination rather than inflammation. *J. Neurocytol.* 28, 366–381
- Chan JR, Watkins TA, Cosgaya JM, Zhang C, Chen L, Reichardt LF, Shooter EM, Barres BA (2004) NGF controls axonal receptivity to myelination by Schwann cells or oligodendrocytes. *Neuron* 43(2):183-91

- Chang MY, Son H, Lee YS, Lee SH (2003) Neurons and astrocytes secrete factors that cause stem cells to differentiate into neurons and astrocytes, respectively. *Mol Cell Neurosci.* 23(3):414-26
- Charcot, JM (1868) Histologie de la Sclérose en plaque. *Gaz Hop de Paris* 41:554-556, 558
- Chen J, Chu YF, Chen JM, Li BC (2010) Synergistic effects of NGF, CNTF and GDNF on functional recovery following sciatic nerve injury in rats. *Adv Med Sci.* 2010 Jun;55(1):32-42
- Chesik D, De Keyser J, Wilczak N (2008) Insulin-like growth factor system regulates oligodendroglial cell behavior: therapeutic potential in CNS. *J Mol Neurosci.* 35(1):81-90
- Chung IY, Benveniste EN (1990) Tumour necrosis factor-alpha production by astrocytes. Induction by lipopolysaccharide, IFN-gamma, and IL-1 beta. *J Immunol* 144(8):2999-3007
- Clarke SR, Shetty AK, Bradley JL, Turner DA (1994) Reactive astrocytes express the embryonic intermediate neurofilament nestin. *Neuroreport.* 5(15):1885-8
- Codarri L, Fontana A, Becher B (2010) Cytokine networks in multiple sclerosis: lost in translation. *Curr Opin Neurol.* 23(3):205-11.
- Colello RJ, Pott U, Schwab ME. (1994) The role of oligodendrocytes and myelin on axon maturation in the developing rat retinofugal pathway. *J Neurosci.* 14(5 Pt 1):2594-605
- Compston A, Coles A (2008) Multiple sclerosis. *Lancet.* 372(9648):1502-17
- Conrad S, Schluesener HJ, Adibzahdeh M, Schwab JM (2005) Spinal cord injury induction of lesional expression of profibrotic and angiogenic connective tissue growth factor confined to reactive astrocytes, invading fibroblasts and endothelial cells. *J Neurosurg Spine.* 2(3):319-26
- Cross AK, Haddock G, Stock CJ, Allan S, Surr J, Bunning RA, Buttle DJ, Woodroffe MN (2006) ADAMTS-1 and -4 are up-regulated following transient middle cerebral artery occlusion in the rat and their expression is modulated by TNF in cultured astrocytes. *Brain Res.* 1088(1):19-30
- Cui QL, Almazan G (2007) IGF-I-induced oligodendrocyte progenitor proliferation requires PI3K/Akt, MEK/ERK, and Src-like tyrosine kinases. *J Neurochem.* 100(6):1480-93
- Czopka T, Von Holst A, Schmidt G, French-Constant C, Faissner A (2009) Tenascin C and tenascin R similarly prevent the formation of myelin membranes in a RhoA-dependent manner, but antagonistically regulate the expression of myelin basic protein via a separate pathway. *Glia.* 57(16):1790-801
- Daginakatte GC, Gadzinski A, Emmett RJ, Stark JL, Gonzales ER, Yan P, Lee JM, Cross AH, Gutmann DH (2008) Expression profiling identifies a molecular signature of reactive astrocytes stimulated by cyclic AMP or proinflammatory cytokines. *Exp Neurol.* 210(1): 261-267

- Dallner C, Woods AG, Deller T, Kirsch M, Hofmann HD (2002) CNTF and CNTF receptor alpha are constitutively expressed by astrocytes in the mouse brain. *Glia* 37(4):374-8
- Darsalia V, Allison SJ, Cusulin C, Monni E, Kuzdas D, Kallur T, Lindvall O, Kokaia Z (2010) Cell number and timing of transplantation determine survival of human neural stem cell grafts in stroke-damaged rat brain. *J Cereb Blood Flow Metab.* [Epub ahead of print]
- Davis S, Aldrich TH, Velnzuela DM, Wong VV, Furth Me, Squinto SP, Yancopoulos GD (1991) The receptor of ciliary neurotrophic factor. *Science* 253(5015):59-63
- Davis S, Aldrich TH, Ip NY, Stahl N, Scherer S, Farruggella T, DiStefano PS, Curtis R, Panayotatos N, Gascan H, Chevalier S, Yancopoulos GD (1993) Released form of CNTF receptor alpha component as a soluble mediator of CNTF responses. *Science* 259(5102):1736-9
- Dawson MR, Polito A, Levine JM, Reynolds R (2003) NG2-expressing glial progenitor cells: an abundant and widespread population of cycling cells in the adult rat CNS. *Mol Cell Neurosci.* 24(2):476-88
- DeChiara TM, Vejsada R, Poueymirou WT, Acheson A, Suri C, Conover JC, Friedman B, McClain J, Pan L, Stahl N, Ip NY, Yancopoulos GD (1995) Mice lacking the CNTF receptor, unlike mice lacking CNTF, exhibit profound motor neuron deficits at birth. *Cell.* 83(2):313-22
- Defaux A, Zurich MG, Honegger P, Monnet-Tschudi F (2010) Inflammatory responses in aggregating rat brain cell cultures subjected to different demyelinating conditions. *Brain Res* 1353:213-24
- Derfuss T, Linington C, Hohlfeld R, Meinl E (2010) Axo-glial antigens as targets in multiple sclerosis: implications for axonal and grey matter injury. *J Mol Med.* 88(8):753-61
- Deng YY, Lu J, Ling EA, Kaur C (2010) Microglia-derived macrophage colony stimulating factor promotes generation of proinflammatory cytokines by astrocytes in the periventricular white matter in the hypoxic neonatal brain. *Brain Pathol* 5(4):e10240
- Deuel TF, Zhang N, Yeh HJ, Silos-Santiago I, Wang ZY (2002) Pleiotrophin: a cytokine with diverse functions and a novel signaling pathway. *Arch Biochem Biophys.* 397(2):162-71
- Dietrich J, Lacagnina M, Gass D, Richfield E, Mayer-Pröschel M, Noble M, Torres C, Pröschel C (2005) EIF2B5 mutations compromise GFAP+ astrocyte generation in vanishing white matter leukodystrophy. *Nat Med.* 11(3):277-83
- Dietrich J, Imitola J, Kesari S (2008) Mechanisms of Disease: the role of stem cells in the biology and treatment of gliomas. *Nat Clin Pract Oncol.* 5(7):393-404
- Doetsch F, Caillé I, Lim DA, García-Verdugo JM, Alvarez-Buylla A (1999) Subventricular zone astrocytes are neural stem cells in the adult mammalian brain. *Cell.* 97(6):703-16

- Dougherty KD, Dreyfus CF, Black IB (2000) Brain-derived neurotrophic factor in astrocytes, oligodendrocytes, and microglia/macrophages after spinal cord injury. *Neurobiol Dis.* 7(6 Pt B):574-85
- Drögemüller K, Helmuth U, Brunn A, Sakowicz-Burkiewicz M, Gutmann DH, Mueller W, Deckert M, Schlüter D (2008) Astrocyte gp130 expression is critical for the control of *Toxoplasma* encephalitis. *J Immunol.* 181(4):2683-93
- Dubois-Dalcq M, Behar T, Hudson L, Lazzarini RA (1986) Emergence of three myelin proteins in oligodendrocytes cultured without neurons. *J Cell Biol.* 102(2):384-92
- Duncan, D (1935) A relation between axon diameter and myelination determined by measurement of myelinated spinal root fibers. *J.Comp. Neur.*, 60: 437-472
- Dziewulska D, Jamrozik Z, Podlecka A, Rafałowska J (1999) Do astrocytes participate in rat spinal cord myelination? *Folia Neuropathol.* 37(2):81-6
- East E, Golding JP, Phillips JB (2009) A versatile 3D culture model facilitates monitoring of astrocytes undergoing reactive gliosis. *J Tissue Eng Regen Med* 3, 634-46
- Eckenhoff MF, Rakic P (1991) A quantitative analysis of synaptogenesis in the molecular layer of the dentate gyrus in the rhesus monkey. *Brain Res Dev Brain Res.* 64(1-2):129-35
- Eddleston M, Mucke L (1993) Molecular profile of reactive astrocytes- implications for their role in neurologic disease. *Neurosci* 54:15-36
- Emsley JG, Arlotta P, Macklis JD (2004) Star-cross'd neurons: astroglial effects on neural repair in the adult mammalian CNS. *Trends Neurosci.* 27(5):238-40
- Eng LF, Vanderhaeghen JJ, Bignami A, Gerstl B (1971) An acidic protein isolated from fibrous astrocytes. *Brain Res* 28, 351-354
- Eng LF (1985) Glial fibrillary acidic protein (GFAP): the major protein of glial intermediate filaments in differentiated astrocytes. *J Neuroimmunol.* 8(4-6):203-14
- Escartin C, Brouillet E, Gubellini P, Trioulier Y, Jacquard C, Smadja C, Knott GW, Kerkerian-Le Goff L, Déglon N, Hantraye P, Bonvento G. (2006) Ciliary neurotrophic factor activates astrocytes, redistributes their glutamate transporters GLAST and GLT-1 to raft microdomains, and improves glutamate handling in vivo. *J Neurosci.* 26(22):5978-89
- Espinosa de los Monteros A, Zhang M, De Vellis J (1993) O2A progenitor cells transplanted into the neonatal rat brain develop into oligodendrocytes but not astrocytes. *Proc Natl Acad Sci U S A.* 90(1):50-4

- Faissner A, Kruse J, Chiquet-Ehrismann R, Mackie E (1988) The high-molecular-weight J1 glycoproteins are immunochemically related to tenascin. *Differentiation*. 37(2):104-14
- Faulkner JR, Herrmann JE, Woo MJ, Tansey KE, Doan NB, Sofroniew MV (2004). Reactive astrocytes protect tissue and preserve function after spinal cord injury. *J Neurosci* 24:2143–2155
- Fawcett JW, Asher RA (1999) The glial scar and central nervous system repair. *Brain Res Bull*. 1999 Aug;49(6):377-91
- Fedoroff S, McAuley W.E, Houle JD and Devon RM (1984) Astrocyte cell lineage. V. Similarity of astrocytes that form in the presence of dBcAMP in cultures to reactive astrocytes *in vivo*, *J. Neurosci. Res* 12:14–27
- Ferhat L, Chevassus au Louis N, Jorquera I, Niquet J, Khrestchatisky M, Ben-Ari Y, Represa A (1996) Transient increase of tenascin-C in immature hippocampus: astroglial and neuronal expression. *J Neurocytol*. 25(1):53-66
- Ferguson B, Matyszak MK, Esiri MM, Perry VH (1997) Axonal damage in acute multiple sclerosis lesions. *Brain*.120 ( Pt 3):393-9
- Fife BT, Kennedy KJ, Paniagua MC, Lukacs NW, Kunkel SL, Luster AD, Karpus WJ (2001) CXCL10 (IFN-gamma-inducible protein-10) control of encephalitogenic CD4+ T cell accumulation in the central nervous system during experimental autoimmune encephalomyelitis. *J Immunol*. 166(12):7617-24
- Filous AR, Miller JH, Coulson-Thomas YM, Horn KP, Alilain WJ, Silver J (2010) Immature astrocytes promote CNS axonal regeneration when combined with chondroitinase ABC. *Dev Neurobiol*. 70(12):826-41
- Finkbeiner S (1992) Calcium waves in astrocytes-filling in the gaps. *Neuron*. 1992 Jun;8(6):1101-8.
- Fischer M, Goldschmitt J, Peschel C, Brakenhoff JP, Kallen KJ, Wollmer A, Grötzinger J, Rose-John S. (1997) I. A bioactive designer cytokine for human hematopoietic progenitor cell expansion. *Nat Biotechnol*. 15(2):142-5
- Fitch MT, Silver J (2008) CNS injury, glial scars, and inflammation: Inhibitory extracellular matrices and regeneration failure. *Exp Neurol*. 209(2):294-301
- Fogarty M, Richardson WD, Kessaris N (2005) A subset of oligodendrocytes generated from radial glia in the dorsal spinal cord. *Development* 132:1951–1959
- Francis A, Raabe TD, Wen D, DeVries GH (1999) Neuregulins and ErbB receptors in cultured neonatal astrocytes. *J Neurosci Res* 57(4):487-494

- Franklin RJ, Crang AJ, Blakemore WF (1991) Transplanted type-1 astrocytes facilitate repair of demyelinating lesions by host oligodendrocytes in adult rat spinal cord. *J Neurocytol* 20:420–430
- Friede RL (1972) Control of myelin formation by axon caliber (with a model of the control mechanism). *J Comp Neurol*. 144(2):233-52
- Fujimoto Y, Yamasaki T, Tanaka N, Mochizuki Y, Kajihara H, Ikuta Y, Ochi M (2006) Differential activation of astrocytes and microglia after spinal cord injury in the fetal rat. *Eur Spine J*. 15(2):223-33
- Gähwiler BH, Capogna M, Debanne D, McKinney RA, Thompson SM (1997) Organotypic slice cultures: a technique has come of age. *Trends Neurosci*. 20(10):471-7
- Gard AL, Pfeiffer SE (1993) Glial cell mitogens bGFG and PDGF differentially regulate development of O4+GalC- oligodendrocyte progenitors. *Dev Biol* 155(2):618-30
- Gard AL, Burrell MR, Pfeiffer SE, Rudge JS, Williams WC (1995) Astroglial control of oligodendrocyte survival mediated by PDGF and Leukemia Inhibitory Factor-like protein. *Development* 121, 2187-2197
- Gehrmann J, Matsumoto Y, Kreutzberg GW (1995) Microglia: intrinsic immuneffector cell of the brain. *Brain Res Brain Res Rev*. 20(3):269-87
- Giess R, Mäurer M, Linker R, Gold R, Warmuth-Metz M, Toyka KV, Sendtner M, Rieckmann P. (2002) Association of a null mutation in the CNTF gene with early onset of multiple sclerosis. *Arch Neurol* 59:407-409
- Glabinski AR, Tani M, Strieter RM, Tuohy VK, Ransohoff RM (1997) Synchronous synthesis of alpha- and beta-chemokines by cells of diverse lineage in the central nervous system of mice with relapses of chronic experimental autoimmune encephalomyelitis. *Am J Pathol* 150:617– 630
- Godiska R, Chantry D, Dietsch GN, Gray PW (1995) Chemokine expression in murine experimental allergic encephalomyelitis. *J Neuroimmunol* 58:167-76
- Goetzl EJ, Voice JK, Shen S, Dorsam G, Kong Y, West KM, Morrison CF, Harmor AJ (2001) Enhanced delayed-type hypersensitivity and diminished immediate-type hypersensitivity in mice lacking the inducible VPAC2 receptor for vasoactive intestinal peptide. *Proc Natl Acad Sci USA* 98(24):13854-9
- Gomez-Nicola D, Pallas-Bazarra N, Valle-Argos B, Nieto-Sampedro M (2010) CCR7 is expressed in astrocytes and upregulated after an inflammatory injury. *J Neuroimmunol*. 2010 Jul 15. [Epub ahead of print]
- Gozes I, Bassan M, Zamostiano R, Pinhasov A, Davidson A, Giladi E, Perl O, Glazner GW, Brenneman DE (1999) A novel signaling molecule for neuropeptide action: activity-dependent neuroprotective protein. *Ann. NY Acad. Sci.* 897, 125–135

- Graça and Blakemore (1986) Delayed remyelination in rat spinal cord following ethidium bromide injection. *Neuropathol Appl Neurobiol* 12, 595-605
- Guillemin GJ, Brew BJ (2004) Microglia, macrophages, perivascular macrophages, and pericytes: a review of function and identification. *J Leukoc Biol.* 75(3):388-97
- Gutowski NJ, Newcombe J, Cuzner ML (1999) Tenascin-R and C in multiple sclerosis lesions: relevance to extracellular matrix remodelling. *Neuropathol Appl Neurobiol.* 25(3):207-14
- Haddock G, Cross AK, Plumb J, Surr J, Buttle DJ, Bunning RA, Woodroffe MN (2006) Expression of ADAMTS-1, -4, -5 and TIMP-3 in normal and multiple sclerosis CNS white matter. *Mult Scler.* 12(4):386-96
- Hagg T, Varon S. Ciliary neurotrophic factor prevents degeneration of adult rat substantia nigra dopaminergic neurons in vivo. *Proc Nat Acad Sci USA* 1993; 90:6315-6319
- Halassa MM, Fellin T, Haydon PG (2007) The tripartite synapse: roles for gliotransmission in health and disease. *Trends Mol Med.* 13(2):54-63
- Hamby ME, Sofroniew MV (2010) Reactive astrocytes as therapeutic targets for CNS disorders. *Neurotherapeutics.* 7(4):494-506
- Hansen-Pupp I, Harling S, Berg AC, Cilio C, Hellström-Westas L, Ley D (2005) Circulating interferon-gamma and white matter brain damage in preterm infants. *Pediatr Res.* 58(5):946-52
- Hassinger TD, Atkinson PB, Strecker GJ, Whalen LR, Dudek FE, Kossel AH, Kater SB (1995) Evidence for glutamate-mediated activation of hippocampal neurons by glial calcium waves. *J Neurobiol.* 28(2):159-70
- Helgren ME, Squinto SP, Davis HL, Parry DJ, Boulton TG, Heck CG, Zhu Y, Yancopoulos GD, Lindsay RM, DiStefano PS (1994) Trophic effect of ciliary neurotrophic factor on denervated skeletal muscle. *Cell* 76(11):493-504
- Hertel M, Tretter Y, Alzheimer C, Werner S (2000) Connective tissue growth factor: a novel player in tissue reorganization after brain injury? *Eur J Neurosci.* 12(1):376-80
- Herx LM, Rivest S, Yong VW (2000) Central nervous system-initiated inflammation and neurotrophism in trauma IL-1beta is required for the production of ciliary neurotrophic factor. *J Immunol* 165(4):2232-9
- Herx LM, Yong VW (2001) Interleukin-1b is required for the early evolution of reactive astrogliosis following CNS lesion. *J Neuropathol Exp Neurol* 60(10):961-71
- Higginson JR, Barnett SC (2010) The culture of olfactory ensheathing cells (OECs)-a distinct glial cell type. *Exp Neurol.* 2010 Sep 15. [Epub ahead of print]

- Hini M, Murakami M, Saito M, Hirano T, Taga T, Kishimoto T (1990) Molecular cloning and expression of an IL-6 signal transducer, gp130. *Cell* 63(6):1149-57
- Hochstim C, Deneen B, Lukaszewicz A, Zhou Q, Anderson DJ (2008) Identification of positionally distinct astrocyte subtypes whose identities are specified by a homeodomain code. *Cell*. 133(3):510-22
- Hoffmann V, Pöhlau D, Przuntek H, Epplen JT, Hardt C (2002) A null mutation within the ciliary neurotrophic factor (CNTF)-gene: implications for susceptibility and disease severity in patients with multiple sclerosis. *Genes Immun*. 3(1):53-5
- Holley JE, Gveric D, Whatmore JL, Gutowski NJ (2005) Tenascin C induces a quiescent phenotype in cultured adult human astrocytes. *Glia*. 2005 Oct;52(1):53-8
- Hughes SM, Lillien LE, Raff MC, Rohrer H, Sendtner M (1988) Ciliary neurotrophic factor induces type-2 astrocyte differentiation in culture. *Nature* 335(6185):70-3
- Hunanyan AS, García-Alías G, Alessi V, Levine JM, Fawcett JW, Mendell LM, Arvanian VL (2010) Role of Chondroitin Sulfate Proteoglycans in Axonal Conduction in Mammalian Spinal Cord. *J Neurosci* 30(23):7761-9
- Husmann K, Faissner A, Schachner M (1992) Tenascin promotes cerebellar granule cell migration and neurite outgrowth by different domains in the fibronectin type III repeats. *J Cell Biol*. 116(6):1475-86
- Ikewaki N, Tamauchi F, Yamada A, Mori N, Yamao H, Inoue H, Inoko H (2000) A unique monoclonal antibody mNI-11 rapidly enhances spread formation in human umbilical vein endothelial cells. *J. Clin. Immunol*. 20: 317–324
- Ip NY, McClain J, Barrezueta NX, Aldrich TH, Pan L, Li Y, Wiegand SJ, Friedman B, Davis S, Yancopoulos GD (1993) The alpha component of the CNTF receptor is required for signaling and defines potential CNTF targets in the adult and during development. *Neuron* 10(1):89-102
- Ip NY, Yancopoulos GD (1996) The neurotrophins and CNTF: two families of collaborative neurotrophic factors. *Annu Rev Neurosci*. 1996;19:491-515
- Iseki K, Hagino S, Mori T, Zhang Y, Yokoya S, Takaki H, Tase C, Murakawa M, Wanaka A (2002) Increased syndecan expression by pleiotrophin and FGF receptor-expressing astrocytes in injured brain tissue. *Glia*. 39(1):1-9
- Ishibashi T, Dakin KA, Stevens B, Lee PR, Kozlov SV, Stewart CL, Fields RD (2006) Astrocytes promote myelination in response to electrical impulses. *Neuron* 49, 823–832

- Ishii K, Nakamura M, Dai H, Finn TP, Okano H, Toyama Y, Bregman BS (2006) Neutralization of ciliary neurotrophic factor reduces astrocyte production from transplanted neural stem cells and promotes regeneration of corticospinal tract fibers in spinal cord injury. *J Neurosci Res.* 84(8):1669-81
- Janzer RC, Raff MC (1987) Astrocytes induce blood-brain barrier properties in endothelial cells. *Nature* 325(6101):253-7
- Jayakumar AR, Norenberg MD. (2010) The Na-K-Cl Co-transporter in astrocyte swelling. *Metab Brain Dis.* 25(1):31-8
- Jeon JW, Jung JG, Shin EC, Choi HI, Kim HY, Cho ML, Kim SW, Jang YS, Sohn MH, Moon JH, Cho YH, Hoe KL, Seo YS, Park YW (2010) Soluble CD93 Induces Differentiation of Monocytes and Enhances TLR Responses. *J Immunol.* 185(8):4921-7
- John GR, Shankar SL, Shafit-Zagardo B, Massimi A, Lee SC, Raine CS, Brosnan CF (2002) Multiple sclerosis: re-expression of a developmental pathway that restricts oligodendrocyte maturation. *Nat Med.* 8(10):1115-21
- John GR, Lee SC, Brosnan CF (2003) Cytokines: powerful regulators of glial cell activation. *Neuroscientist* 9, 10-22
- John GR, Lee SC, Song X, Riviaccio M, Brosnan CF (2005) IL-1-regulated responses in astrocytes: relevance to injury and recovery. *Glia.* 49(2):161-76
- Kahn MA, De Vellis J (1994) Regulation of an oligodendrocyte progenitor cell line by the interleukin-6 family of cytokines. *Glia.* 12(2):87-98
- Kahn MA, Ellison JA, Chang RP, Speight GJ, de Vellis J (1997) CNTF induces GFAP in a S-100 alpha brain cell population: the pattern of CNTF-alpha R suggests an indirect mode of action. *Brain Res Dev Brain Res.* 98(2):221-33
- Kamiguchi H, Yoshida K, Sagoh M, Sasaki H, Inaba M, Wakamoto H, Otani M, Toya S (1995) Release of ciliary neurotrophic factor from cultured astrocytes and its modulation by cytokines. *Neurochem Res.* 20(10):1187-93
- Karim SA, Barrie JA, McCulloch MC, Montague P, Edgar JM, Kirkham D, Anderson TJ, Nave KA, Griffiths IR, McLaughlin M. (2007) PLP overexpression perturbs myelin protein composition and myelination in a mouse model of Pelizaeus-Merzbacher disease. *Glia* 55(4):341-51
- Kaur C, Hao AJ, Wu CH, Ling EA (2001) Origin of microglia. *Microsc Res Tech.* 54(1):2-9
- Keirstead HS, Levine JM, Blakemore WF (1998) Response of the oligodendrocyte progenitor cell population (defined by NG2 labelling) to demyelination of the adult spinal cord. *Glia.* 22(2):161-70

- Kahn MA, De Vellis J (1994) Regulation of an oligodendrocyte progenitor cell line by the interleukin-6 family of cytokines. *Glia* 12(2):87-98
- Kiernan BW, Götz B, Faissner A, French-Constant C (1996) Tenascin-C inhibits oligodendrocyte precursor cell migration by both adhesion-dependent and adhesion-independent mechanisms. *Mol Cell Neurosci.* 7(4):322-35
- Kinouchi R, Takeda M, Yang L, Wilhelmsson U, Lundkvist A, Pekny M, Chen DF (2003) Robust neural integration from retinal transplants in mice deficient in GFAP and vimentin. *Nat Neurosci.* 6(8):863-8
- Kirby BB, Takada N, Latimer AJ, Shin J, Carney TJ, Kelsh RN, Appel B (2006) In vivo time-lapse imaging shows dynamic oligodendrocyte progenitor behavior during zebrafish development. *Nat Neurosci.* 9(12):1506-11
- Klein RS, Izikson L, Means T, Gibson HD, Lin E, Sobel RA, Weiner HL, Luster AD (2004) IFN-inducible protein 10/CXC chemokine ligand 10-independent induction of experimental autoimmune encephalomyelitis. *J Immunol* 172, :550-559
- Kondo T, Raff M (2000) Oligodendrocyte precursor cells reprogrammed to become multipotential CNS stem cells. *Science.* 289(5485):1754-7
- Kondo Y, Nakanishi T, Takigawa M, Ogawa N (1999) Immunohistochemical localization of connective tissue growth factor in the rat central nervous system. *Brain Res.* 834(1-2):146-51
- Krady JK, Lin HW, Liberto CM, Basu A, Kremlev SG, Levison SW (2008) Ciliary neurotrophic factor and interleukin-6 differentially activate microglia. *J Neurosci Res.* 86(7):1538-47
- Krum JM, Rosenstein JM (1998) VEGF mRNA and its receptor flt-1 are expressed in reactive astrocytes following neural grafting and tumor cell implantation in the adult CNS. *Exp Neurol* 154(1):57-65
- Kruse J, Keilhauer G, Faissner A, Timpl R, Schachner M (1985) The J1 glycoprotein--a novel nervous system cell adhesion molecule of the L2/HNK-1 family. *Nature* 316(6024):146-8
- LaFerla FM, Sugarman MC, Lane TE, Leissring MA (2000) Regional hypomyelination and dysplasia in transgenic mice with astrocyte-directed expression of interferon-gamma. *J Mol Neurosci.* 15(1):45-59
- Lai C, Feng L (2004) Implication of gamma-secretase in neuregulin-induced maturation of oligodendrocytes. *Biochem Biophys Res Commun.* 314(2):535-42
- Larner AJ, Johnson AR, Keynes RJ (1995) Regeneration in the vertebrate central nervous system: phylogeny, ontogeny, and mechanisms. *Biol Rev* 70: 597-619

- Lawler J, Duquette M, Whittaker CA, Adams JC, McHenry K, DeSimone DW (1993) Identification and characterization of thrombospondin-4, a new member of the thrombospondin gene family. *J Cell Biol.* 1993 Feb;120(4):1059-67
- Laywell ED, Dörries U, Bartsch U, Faissner A, Schachner M, Steindler DA (1992) Enhanced expression of the developmentally regulated extracellular matrix molecule tenascin following adult brain injury. *Proc Natl Acad Sci U S A.* 89(7):2634-8
- Lee MY, Deller T, Kirsch M, Frotscher M, Hoffmann HD (1997) Differential regulation of ciliary neurotrophic factor (CNTF) and CNTF receptor alpha expression in astrocytes and neurons of the fascia dentate after entorhinal cortex lesion. *J Neurosci* 17:1137-1146
- Lee N, Robitz R, Zurbrugg RJ, Karpman AM, Mahler AM, Cronier SA, Vesey R, Spearry RP, Zolotukhin S, MacLennan AJ. (2008) Conditional, genetic disruption of ciliary neurotrophic factor receptors reveals a role in adult motor neuron survival. *Eur J Neurosci.* 27(11):2830-7
- Lennon VA, Kryzer TJ, Pittock SJ, Verkman AS, Hinson SR (2005) IgG marker of optic-spinal multiple sclerosis binds to the aquaporin-4 water channel. *J Exp Med* 202:473– 477
- Levine JM, Reynolds R (1991) Activation and proliferation of endogenous oligodendrocytes precursor cells during ethidium bromide demyelination. *Exp Neurol* 160(2):333-47
- Levine JM, Reynolds R (1999) Activation and proliferation of endogenous oligodendrocyte precursor cells during ethidium bromide-induced demyelination. *Exp Neurol.* 160(2):333-47
- Levison SW, Ducceschi MH, Young GM, Wood TL (1996) Acute exposure to CNTF in vivo induces multiple components of reactive gliosis. *Exp Neurol* 141(2):256-68
- Levison SW, Hudgins SN, Crawford JL (1998) Ciliary neurotrophic factor stimulates nuclear hypertrophy and increases the GFAP content of cultured astrocytes. *Brain Res.* 803(1-2):189-93
- Li A, Guo H, Luo X, Sheng J, Yang S, Yin Y, Zhou J, Zhou J (2006) Apomorphine-induced activation of dopamine receptors modulates FGF-2 expression in astrocytic cultures and promotes survival of dopaminergic neurons. *FASEB J.* 20(8):1263-5
- Li H, Mei Y, Wang Y, Xu L (2006) Vasoactive Intestinal Polypeptide Suppressed Experimental Autoimmune Encephalomyelitis by Inhibiting T Helper 1 Responses. *J Clin Immunol* 26(5):430-7
- Li R, Messing A, Goldman JE, Brenner M (2002) GFAP mutations in Alexander disease. *Int J Dev Neurosci* 20 259-68
- Liberto CM, Albrecht PJ, Herx LM, Yong VW, Levison SW (2004) Pro-regenerative properties of cytokine-activated astrocytes. *J Neurochem* 89(5):1092-100

- Liedtke W, Edelmann W, Bieri PL, Chiu FC, Cowan NJ, Kucheriapatie, Raine CS (1996) GFAP is necessary for the integrity of CNS white matter architecture and long-term maintenance of myelination. *Neuron* 17(4):607-15
- Lillien LE, Sendtner M, Rohrer H, Hughes SM, Raff MC (1988) Type-2 astrocyte development in rat brain cultures is initiated by a CNTF-like protein produced by type-1 astrocytes. *Neuron* 1(6):485-94
- Lin HW, Jain MR, Li H, Levison SW (2009) Ciliary neurotrophic factor (CNTF) plus soluble CNTF receptor alpha increases cyclooxygenase-2 expression, PGE2 release and interferon-gamma-induced CD40 in murine microglia. *J Neuroinflammation* 6:7
- Lin LF, Mismar D, Lile JD, Armes LG, 3<sup>rd</sup> Butler ET, Vannice JL, Collins F (1989) Purification, cloning and expression of ciliary neurotrophic factor. *Science* 246(4933):1023-5
- Lin RC, Matesic DF, Marvin M, McKay RD, Brüstle O (1995) Re-expression of the intermediate filament nestin in reactive astrocytes. *Neurobiol Dis.* 2(2):79-85
- Lin W, Kemper A, Dupree JL, Harding HP, Ron D, Popko B (2006) Interferon-gamma inhibits central nervous system remyelination through a process modulated by endoplasmic reticulum stress. *Brain.* 129(Pt 5):1306-18
- Linker RA, Mäurer M, Gaupp S, Martini R, Holtmann B, Giess R, Rieckmann P, Lassmann H, Toyka KV, Sendtner M, Gold R (2002) CNTF is a major protective factor in demyelinating CNS disease: a neurotrophic cytokine as modulator in neuroinflammation. *Nat Med.* 8(6):620-4
- Liu L, Huang D, Matsui M, He TT, Hu T, Demartino J, Lu B, Gerard C, Ransohoff RM (2006) Chemokine CXCL10 promotes atherogenesis by modulating the local balance of effector and regulatory T cells (2006) *J Immuno* 176(7):4399-409
- Liu MT, Keirstead HS, Lane TE (2001) Neutralization of the chemokine CXCL10 reduces inflammatory cell invasion and demyelination and improves neurological function in a viral induced model of multiple sclerosis. *J Immunol* 167(7):4091-7
- Liu X, Yao DL, Bondy CA, Brenner M, Hudson LD, Zhou J, Webster HD (1994) Astrocytes express insulin-like growth factor-I (IGF-I) and its binding protein, IGFBP-2, during demyelination induced by experimental autoimmune encephalomyelitis. *Mol Cell Neurosci.* 5(5):418-30
- Liu Y, Rao MS (2004) Glial progenitors in the CNS and possible lineage relationships among them. *Biol Cell.* 96(4):279-90
- Livak KJ, Schmittgen TD (2001) Analysis of relative gene expression data using real-time quantitative PCR and the 2<sup>-</sup>(Delta Delta C(T)) Method. *Methods.* 25(4):402-8

- Lochter A, Vaughan L, Kaplony A, Prochiantz A, Schachner M, Faissner A (1991) J1/tenascin in substrate-bound and soluble form displays contrary effects on neurite outgrowth. *J Cell Biol.* 113(5):1159-71
- Lombardi A, Cantini G, Piscitelli E, Gelmini S, Francalanci M, Mello T, Ceni E, Varano G, Forti G, Rotondi M, Galli A, Serio M, Luconi M (2001) A new mechanism involving ERK contributes to rosiglitazone inhibition of tumor necrosis factor-alpha and interferon-gamma inflammatory effects in human endothelial cells. *Arterioscler Thromb Vasc Biol.* 28(4):718-24
- Loo DT, Althoen MC, Cotman CW (1995) Differentiation of serum-free mouse embryo cells into astrocytes is accompanied by induction of glutamine synthetase activity. *J Neurosci Res.* 42(2):184-91
- Lu X, Ma L, Ruan L, Kong Y, Mou H, Zhang Z, Wang Z, Wang JM, Le Y (2010) Resveratrol differentially modulates inflammatory responses of microglia and astrocytes. *J Neuroinflammation.* 7(1):46
- Lubetzki C, Demerens C, Anglade P, Villarroya H, Frankfurter A, Lee VM, Zalc B (1993) Even in culture, oligodendrocytes myelinate solely axons. *Proc Natl Acad Sci U S A.* 90(14):6820-4
- Lutz SE, Zhao Y, Gulinello M, Lee SC, Raine CS, Brosnan CF (2009) Deletion of astrocyte connexins 43 and 30 leads to a dysmyelinating phenotype and hippocampal CA1 vacuolation. *J Neurosci.* 29(24):7743-52
- Maciaczyk J, Singec I, Maciaczyk D, Klein A, Nikkhah G (2009) Restricted spontaneous in vitro differentiation and region-specific migration of long-term expanded fetal human neural precursor cells after transplantation into the adult rat brain. *Stem Cells Dev.* 18(7):1043-58
- MacLennan AJ, Vinson EN, Marks L, McLaurin DL, Pfeifer M, Lee N (1996) Immunohistochemical localization of ciliary neurotrophic factor receptor alpha in the rat nervous system *J Neurosci* 16(2):621-30
- Magistretti PJ, Manthorpe M, Bloom FE, Varon S (1983) Functional receptors for vasoactive intestinal polypeptide in cultured astroglia from neonatal rat brain. *Regul Pept* 6(1):71-80
- Malhotra and Shintka (2002) Diversity in Reactive Astrocytes. In *Neuroglia of the aging brain* by Jean De Vellis. New Jersey: Humana Press Inc 17-33
- Mangas A, Coveñas R, Geffard M (2010) New drug therapies for multiple sclerosis. *Curr Opin Neurol.* 223(3):287-92
- Marshall CA, Goldman JE (2002) Subpallial dlx2-expressing cells give rise to astrocytes and oligodendrocytes in the cerebral cortex and white matter. *J Neurosci.* 22(22):9821-30
- Martinou JC, Martinou I, Kato AC (1992) Cholinergic differentiation factor (CDF/LIF) promotes survival of isolated rat embryonic motoneurons in vitro. *Neuron.* 8(4):737-44

- Marz P, Heese K, Dimitriadis-Schmutz B, Rose-John S, Otten U (1999) Role of interleukin-6 and soluble IL-6 receptor in region-specific induction of astrocytic differentiation and neurotrophin expression. *Glia* 26, 191-2000
- Mason JL, Suzuki K, Chaplin DD, Matsushima GK (2001) Interleukin-1beta promotes repair of the CNS. *J Neurosci* 21, 7046-7052
- Massaro AR, Soranzo C, Carnevale A (1997) Cerebrospinal-fluid ciliary neurotrophic factor in neurological patients. *Eur Neurol.* 37(4):243-6
- Masu Y, Wolf E, Holtmann B, Sendtner M, Brem G, Thoenen H (1993) Disruption of the CNTF gene results in motor neuron degeneration. *Nature* 365(6441):27-32
- Mathey EK, Derfuss T, Storch MK, Williams KR, Hales K, Woolley DR, Al-Hayani A, Davies SN, Rasband MN, Olsson T, Moldenhauer A, Velhin S, Hohlfeld R, Meinl E, Lington C (2007) Neurofascin as a novel target for autoantibody-mediated axonal injury. *J Exp Med.* 204(10):2363-72
- Matyash V, Kettenmann H (2010) Heterogeneity in astrocyte morphology and physiology. *Brain Res Rev.* 63(1-2):2-10
- Mayer M, Bhakoo K, Noble M (1994) Ciliary neurotrophic factor and leukemia inhibitory factor promote the generation, maturation and survival of oligodendrocytes in vitro. *Development.* 120(1):143-53
- McKeon RJ, Schreiber RC, Rudge JS, Silver J (1991) Reduction of neurite outgrowth in a model of glial scarring following CNS injury is correlated with the expression of inhibitory molecules on reactive astrocytes. *J Neurosci.* 11(11):3398-411
- McTigue DM, Horner PJ, Stokes BT, Gage FH (1998) Neurotrophin-3 and brain-derived neurotrophic factor induce oligodendrocyte proliferation and myelination of regenerating axons in the contused adult rat spinal cord. *J Neurosci* 18(14):5354-5365
- Meeuwse S, Persoon-Deen C, Bsibsi M, Ravid R, van Noort JM (2003) Cytokine, chemokine and growth factor gene profiling of cultured human astrocytes after exposure to proinflammatory stimuli. *Glia.* 43(3):243-53
- Messersmith DJ, Murtie JC, Le TQ, Frost EE, Armstrong RC (2000) Fibroblast Growth Factor 2 (FGF2) and FGF receptor expression in an experimental demyelinating disease with extensive remyelination. *J Neurosci Res* 62:241-256
- Michailov GV, Sereda MW, Brinkmann BG, Fischer TM, Haug B, Birchmeier C, Role L, Lai C, Schwab MH, Nave KA (2004) Axonal neuregulin-1 regulates myelin sheath thickness. *Science* 304(5671):700-3

- Miller RH, David S, Patel R, Abney ER, Raff MC (1985) A quantitative immunohistochemical study of macroglial cell development in the rat optic nerve: in vivo evidence for two distinct astrocyte lineages. *Dev Biol.* 111(1):35-41
- Miller BA, Crum JM, Tovar CA, Ferguson AR, Bresnahan JC, Beattie MS (2007) Developmental stage of oligodendrocytes determines their response to activated microglia in vitro. *J Neuroinflammation* 4:28
- Miller RH, Raff MC (1984) Fibrous and protoplasmic astrocytes are biochemically and developmentally distinct. *J Neurosci.* 4(2):585-92
- Minagar A, Jy W, Jimenez JJ, Sheremata WA, Mauro, LM, Mao, WW, Horstman LL, and Ahn YS (2001) Elevated plasma endothelial microparticles in multiple sclerosis *Neurology* 56:1319-1324
- Minagar A, Alexander JS (2003) Blood-brain barrier disruption in multiple sclerosis. *Mult Scler.* 9(6):540-9
- Mirshafiey A, Mohsenzadegan M (2009) TGF-beta as a promising option in the treatment of multiple sclerosis. *Neuropharmacology.* 56(6-7):929-36
- Mucke L, Eddleston M (1993) Astrocytes in infectious and immune-mediated diseases of the central nervous system. *FASEB J.* 7(13):1226-32
- Müller A, Hauk TG, Fischer D (2007) Astrocyte-derived CNTF switches mature RGCs to a regenerative state following inflammatory stimulation. *Brain* 130(Pt 12):3308-20
- Muller M, Carer SL, Hofer MJ, Manders P, Getts DR, Getts MT, Dreykluft A, Lu B, Gerard C, King NJC (2007) CXCR3 signalling reduces the severity of experimental autoimmune encephalomyelitis by controlling the parenchymal distribution of effector and regulatory T cells in the central nervous system. *J Immuno* 178(12) 8175-82
- Murakami M, Hibi M, Nakagawa N, Nakagawa T, Yasukawa K, Yamanishi K, Taga T, Kishimoto T (1993) IL-6 induced homodimerization of gp130 and associated activation of tyrosine kinase. *Science* 260(5115):1808-10
- Nair A, Frederick TJ, Miller SD (2008) Astrocytes in multiple sclerosis: A product of their environment. *Cell Mol Life Sci* 65, 2702-2720
- Nägler K, Mauch DH, Pfrieger FW (2001) Glia-derived signals induce synapse formation in neurones of the rat central nervous system. *J Physiol.* 533(Pt 3):665-79
- Nagy JI, Rash JE (2003) Astrocyte and oligodendrocyte connexins of the glial syncytium in relation to astrocyte anatomical domains and spatial buffering. *Cell Commun Adhes.* 10(4-6):401-6

- Nepomuceno RR, Ruiz S, Park M, Tenner AJ (1999) C1qRP is a heavily O-glycosylated cell surface protein involved in the regulation of phagocytic activity. *J Immunol.* 162(6):3583-9
- Neumann H, Kotter MR, Franklin RJ (2009) Debris clearance by microglia: an essential link between degeneration and regeneration. *Brain.* 132(Pt 2):288-95
- Newman EA (2003) New roles for astrocytes: regulation of synaptic function. *Trends Neurosci.* 26(10):536-42
- Nielsen S, Nagelhus EA, Amiry-Moghaddam M, Bourque C, Agre P, Ottersen OP (1997) Specialized membrane domains for water transport in glial cells: high-resolution immunogold cytochemistry of aquaporin-4 in rat brain. *J Neurosci.* 17(1):171-80
- Niquet J, Jorquera I, Faissner A, Ben-Ari Y, Represa A (1995) Gliosis and axonal sprouting in the hippocampus of epileptic rats are associated with an increase of tenascin-C immunoreactivity. *J Neurocytol.* 24(8):611-24
- Noble M, Murray K (1984) Purified astrocytes promote the in vitro division of a bipotential glial progenitor cell. *EMBO J* 3, 2243-2247
- Norton WT, Aquino DA, Hozumi I, Chiu FC, Brosnan CF (1992) Quantitative aspects of reactive gliosis: a review. *Neurochem Res.* 17(9):877-85
- Noseworthy JH, Lucchinetti C, Rodriguez M, Weinshenker BG (2000) Multiple sclerosis *N Engl J Med* 343: 938–52
- Notterpek LM, Bullock PN, Malek-Hedayat S, Fisher R, Rome LH (1993) Myelination in cerebellar slice cultures: development of a system amenable to biochemical analysis. *J Neurosci Res.* 36(6):621-34
- Obara M, Szeliga M, Albrecht J (2008) Regulation of pH in the mammalian central nervous system under normal and pathological conditions: facts and hypotheses. *Neurochem Int* 52:905–919
- Obayashi S, Tabunoki H, Kim SU, Satoh J (2009) Gene expression profiling of human neural progenitor cells following the serum-induced astrocyte differentiation. *Cell Mol Neurobiol.* 29(3):423-38
- Ohtani T, Ishihara K, Atsumi T, Yoshida Y, Nishida K, Narimatsu K, Shirogane T, Hibi M, Hirano T (2000) gp130-mediated signalling as a therapeutic target. *Expert Opinion on Therapeutic Targets* 4:4: 459-479
- Olk S, Turchinovich A, Grzendowski M, Stühler K, Meyer HE, Zoidl G, Dermietzel R (2010) Proteomic analysis of astroglial connexin43 silencing uncovers a cytoskeletal platform involved in process formation and migration. *Glia.* 58(4):494-505

- Omari KM, John GR, Sealton SC, Raine CS (2005) CXC chemokine receptors on human oligodendrocytes: implications for multiple sclerosis. *Brain* 128:1003-1015
- Pahan K, Sheikh FG, Namboodiri AM, Singh I (1997) Lovastatin and phenylacetate inhibit the induction of nitric oxide synthase and cytokines in rat primary astrocytes, microglia, and macrophages. *J Clin Invest* 100(11):2671-9
- Pang Y, Cai Z, Rhodes PG (2001) Analysis of genes differentially expressed in astrocytes stimulated with lipopolysaccharide using cDNA arrays. *Brain Res.* 2001 Sep 28;914(1-2):15-22
- Pang Y, Campbell L, Zheng B, Fan L, Cai Z, Rhodes P (2010) Lipopolysaccharide-activated microglia induce death of oligodendrocyte progenitor cells and impede their development. *Neuroscience* 166(2):464-75
- Parenti R, Cicirata F, Zappalà A, Catania A, La Delia F, Cicirata V, Tress O, Willecke K (2010) Dynamic expression of Cx47 in mouse brain development and in the cuprizone model of myelin plasticity. *Glia* 58(13):1594-609
- Park SK, Miller R, Krane I, Vartanian T (2001) The erbB2 gene is required for the development of terminally differentiated spinal cord oligodendrocytes. *J Cell Biol.* 154(6):1245-58
- Parpura V, Basarsky TA, Liu F, Jefinija K, Jefinija S, Haydon PG (1994) Glutamate-mediated astrocyte-neuron signalling. *Nature.* 369(6483):744-7
- Patterson PH (1992) The emerging neuropoietic cytokine family: first CDF/LIF, CNTF and IL-6; next ONC, MGF, GCSF? *Curr Opin Neurobiol.* 2(1):94-7
- Pedraza L, Huang JK, Colman DR. (2001) Organizing principles of the axoglial apparatus. *Neuron* 30, 335-344
- Peles E, Nativ M, Lustig M, Grumet M, Schilling J, Martinez R, Plowman GD, Schlessinger J. (1997) Identification of a novel contactin-associated transmembrane receptor with multiple domains implicated in protein-protein interactions. *EMBO J.* 16(5):978-88
- Pellerin L (2005) How astrocytes feed hungry neurons. *Mol Neurobiol* 32(1):59-72
- Pesheva P, Gloor S, Schachner M, Probstmeier R (1997) Tenascin-R is an intrinsic autocrine factor for oligodendrocyte differentiation and promotes cell adhesion by a sulfatide-mediated mechanism. *J Neurosci.* 17(12):4642-51
- Peters A, SL Palay, and H de F Webster (1976) *The Fine Structure of the Nervous System: The Neurons and Supporting Cells*, pp. 242-244, W. B. Saunders Co., Philadelphia

- Pfeiffer SE, Warrington AE, Bansal R (1993) The oligodendrocyte and its many cellular processes. *Trends Cell Biol.* 3(6):191-7
- Pfriefer FW, Barres BA (1997) Synaptic efficacy enhanced by glial cells in vitro. *Science* 277(5332):1684-7
- Piccio L, Buonsanti C, Mariani M, Cella M, Gilfillan S, Cross AH, Colonna M, Panina-Bordignon P (2007) Blockade of TREM-2 exacerbates experimental autoimmune encephalomyelitis. *Eur J Immunol.* 37(5):1290-301
- Pillai R, Scintu F, Scorciapino L, Carta M, Murru L, Biggio G, Cabras S, Reali C, Sogos V (2006) Human astrocytes can be induced to differentiate into cells with neuronal phenotype. *Exp Cell Res* 312(12):2336-46
- Pindon A, Festoff BW, Hantaï D (1988) Thrombin-induced reversal of astrocyte stellation is mediated by activation of protein kinase C beta-1. *Eur J Biochem.* 255(3):766-74
- Raff MC, Abney ER, Cohen J, Lindsay R, Noble M (1983a) Two types of astrocytes in cultures of developing rat white matter: differences in morphology, surface gangliosides, and growth characteristics. *J Neurosci.* 3(6):1289-1300
- Raff MC, Miller RH, Noble M (1983b) A glial progenitor cell that develops in vitro into an astrocyte or an oligodendrocyte depending on culture medium. *Nature.* 03(5916):390-6
- Raff MC, Lillien LE, Richardson WD, Burne JF, Noble MD (1988) Platelet-derived growth factor from astrocytes drives the clock that times oligodendrocyte development in culture. *Nature.* 333(6173):562-5
- Raine CS, Wu E (1993) Multiple Sclerosis: remyelination in acute lesions. *J Neuropathol Exp Neurol* 52(3):199-204
- Ramagopalan SV, Dobson R, Meier UC, Giovannoni G (2010) Multiple sclerosis: risk factors, prodromes, and potential causal pathways. *Lancet Neurol.* 9(7):727-39
- Ransohoff RM, Hamilton TA, Tani M, Stoler MH, Shick HE, Major JA, Estes ML, Thomas DM, Tuohy VK, (1993). Astrocyte expression of mRNA encoding cytokines IP-10 and JE/MCP-1 in experimental autoimmune encephalomyelitis. *FASEB J* 7, 592– 600
- Ransom B, Behar T, Nedergaard M (2003) New roles for astrocytes (stars at last). *Trends Neurosci.* 26(10):520-2
- Rao MS, Tyrrell S, Landis SC, Patterson PH (1992) Effects of ciliary neurotrophic factor (CNTF) and depolarization on neuropeptide expression in cultured sympathetic neurons. *Dev Biol.* 150(2):281-93

- Rasband MN, Trimmer JS (2001) Developmental clustering of ion channels at and near the node of Ranvier. *Dev Biol.* 236(1):5-16
- Redwine, JM, Armstrong, RC (1998) In vivo proliferation of oligodendrocyte progenitors expressing PDGF- $\alpha$ R during early remyelination, *J Neurobiol* 37, pp. 413–428
- Renné C, Kallen KJ, Müllberg J, Jostock T, Grötzinger J, Rose-John S (1998) A new type of cytokine receptor antagonist directly targeting gp130. *J Biol Chem.* 273(42):27213-9
- Reynolds BA, Weiss S (1996) Clonal and population analyses demonstrate that an EGF-responsive mammalian embryonic CNS precursor is a stem cell. *Dev Biol* 175:1–13
- Reynolds R, Hardy R (1997) Oligodendroglial progenitors labeled with the O4 antibody persist in the adult rat cerebral cortex in vivo. *J Neurosci Res.* 47(5):455-70
- Ridet JL, Malhotra SK, Privat A, Gage FH (1997) Reactive astrocytes: cellular and molecular cue to biological function. *Trends Neurosci* 20:570-577
- Ritch PS, Carroll SL, Sontheimer H (2005) Neuregulin-1 enhances survival of human astrocytic glioma cells. *Glia.* 51(3):217-28
- Roessmann U, Gambetti P (1986) Pathological reaction of astrocytes in perinatal brain injury. Immunohistochemical study. *Acta Neuropathol.* 70(3-4):302-7
- Rosenberg PA (1991a) Accumulation of extracellular glutamate and neuronal death in astrocyte-poor cortical cultures exposed to glutamine. *Glia* 4(1):91-100
- Rosenberg PA, Amin S, Leitner M (1991b) Glutamate uptake disguises neurotoxic potency of glutamate agonists in cerebral cortex in dissociated cell culture. *J Neurosci* 12(1): 56-61
- Rosenberg SS, Kelland EE, Tokar E, De la Torre AR, Chan JR (2008) The geometric and spatial constraints of the microenvironment induce oligodendrocyte differentiation. *Proc Natl Acad Sci U S A.* 105(38):14662-7
- Rowitch DH (2004) Glial specification in the vertebrate neural tube. *Nat Rev Neurosci.* 5(5):409-19
- Rudge JS, Silver J (1990) Inhibition of neurite outgrowth on astroglial scars in vitro. *J. Neurosci.* 10:3594 – 3603
- Rudge JS, Alderson RF, Pasnikowski E, McClain J, Ip NY, Lindsay RM (1992) Expression of Ciliary Neurotrophic Factor and the Neurotrophins-Nerve Growth Factor, Brain-Derived Neurotrophic Factor and Neurotrophin 3-in Cultured Rat Hippocampal Astrocytes *Eur J Neurosci.* 4(6):459-471

- Rudge JS, Li Y, Pasnikowski EM, Mattsson K, Pan L, Yancopoulos GD, Wiegand SJ, Lindsay RM, Ip NY (1994) Neurotrophic factor receptors and their signal transduction capabilities in rat astrocytes. *Eur j Neurosci* 6(5):693-705
- Salmaj KW, Raine CS (1988) Tumour necrosis factor mediates myelin and oligodendrocyte damage in vitro. *Ann Neurol* 23(4):339-46
- Salzer JL (2003) Polarized domains of myelinated axons. *Neuron*. 40(2):297-318
- Satoh J, Tabunoki H, Yamamura T, Arima K, Konno H (2007) Human astrocytes express aquaporin-1 and aquaporin-4 in vitro and in vivo. *Neuropathology* 27(3):245-56
- Schmid H, Boucherot A, Yasuda Y, Henger A, Brunner B, Eichinger F, Nitsche A, Kiss E, Bleich M, Gröne HJ, Nelson PJ, Schlöndorff D, Cohen CD, Kretzler M; European Renal cDNA Bank (ERCB) Consortium (2006) Modular activation of nuclear factor-kappaB transcriptional programs in human diabetic nephropathy. *Diabetes*. 55(11):2993-3003
- Scott-Drew S, French-Constant C. (1997) Expression and function of thrombospondin-1 in myelinating glial cells of the central nervous system. *J Neurosci Res* 50:202-214
- Siegel GJ, Agranoff BW, Albers RW (1999) in *Basic Neurochemistry: Molecular, Cellular and Medical Aspects*. 6th edition. Philadelphia: Lippincott-Raven
- Seil FJ (1977): Tissue culture studies of demyelinating disease: A critical review. *Ann Neurol* 2:345-355
- Selmaj KW, Raine CS (1988) Tumor necrosis factor mediates myelin and oligodendrocyte damage in vitro. *Ann Neurol*. 23(4):339-46
- Selmaj K, Raine CS, Cannella B, Brosnan CF (1991) Identification of lymphotoxin and tumor necrosis factor in multiple sclerosis lesions. *J Clin Invest*. 87(3):949-54
- Sendtner M, Kreutzberg GM, Thoenen H (1990): Ciliary neurotrophic factor prevents the degeneration of motor neurons after axotomy. *Nature* 345:440-441
- Sendtner M, Carroll P, Holtmann B, Hughes RA, Thoenen H. (1994) Ciliary neurotrophic factor. *J Neurobiol*. 25(11):1436-53
- Silver J, Miller JH (2004) Regeneration beyond the glial scar. *Nat Rev Neurosci* 5, 146–156
- Simard M, Nedergaard M (2004) The neurobiology of glia in the context of water and ion homeostasis. *Neuroscience*. 129(4):877-96

- Shapland C, Hsuan JJ, Totty NF, Lawson D (1988) Purification and properties of transgelin: a transformation and shape change sensitive actin-gelling protein. *J Cell Biol.* 121(5):1065-73
- Sherman DL, Brophy PJ (2005) Mechanisms of axon ensheathment and myelin growth. *Nat Rev Neurosci* 6(9):683-90
- Skaper SD (2007) The brain as a target for inflammatory processes and neuroprotective strategies. *Ann N Y Acad Sci.* 1122:23-34
- Skoff RP (1990) Gliogenesis in rat optic nerve: astrocytes are generated in a single wave before oligodendrocytes. *Dev Biol.* 139(1):149-68
- Sleeman MW, Anderson KD, Lambert PD, Yancopoulos GD, Wiegand SJ (2000) CNTF and its receptors. *Pharm Acta Helv* 74:265-72
- Slepko N, Levi G (1996) Progressive activation of adult microglial cells in vitro. *Glia.* 16(3):241-46
- Slezak M, Pfrieger FW (2003) New roles for astrocytes: regulation of CNS synaptogenesis. *Trends Neurosci.* 26(10):531-5
- Sofroniew MW, Vinters HV (2010) Astrocytes; biology and pathology *Acta Neuropathol* 119:7-35
- Song H, Stevens CF, Gage FH (2002) Astroglia induce neurogenesis from adult neural stem cells. *Nature.* 417(6884):39-44
- Sørensen A, Moffat K, Thomson CE, Barnett SC (2008) Astrocytes but not olfactory ensheathing cells, promote myelination of CNS axons in vitro. *Glia* 56:750-63
- Stahl N, Boulton TG, Farruggella T, Ip NY, Davis S, Witthuhn BA, Quelle FW, Silvennoinen O, Barbieri G, Pellefrini S, Ihle JN, Yancopoulos GD (1994) Association and activation of Jak-Tyk kinases by CNTF-LIF-OSM-IL-6 beta receptor components. *Science* 263(5143):92-5
- Stahl N, Yancopoulos GD (1994) The tripartite CNTF receptor complex: activation and signalling involves components shared with other cytokines. *J neurobiol* 25(11):1454-66
- Stankoff B, Aigrot MS, Noël F, Wattilliaux A, Zalc B, Lubetzki C (2002) Ciliary neurotrophic factor (CNTF) enhances myelin formation: a novel role for CNTF and CNTF-related molecules. *J Neurosci* 22:9221-9927
- Stariha RL, Kim SU (2001) Protein kinase C and mitogen-activated protein kinase signalling in oligodendrocytes. *Microsc Res Tech.* 52(6):680-8

- Stein I, Neeman M, Shweiki D, Itin A, Keshet E (1995) Stabilization of vascular endothelial growth factor mRNA by hypoxia and hypoglycemia and coregulation with other ischemia-induced genes. *Mol Cell Biol.* 15(10):5363-8
- Steinman L (1996) Multiple sclerosis: a coordinated immunological attack against myelin in the central nervous system. *Cell.* 85(3):299–302
- Stöckli KA, Lottspeich F, Sendtner M, Masiakowski P, Carroll P, Gotz R, Lindholm D, Thoenen H (1989) Molecular cloning, expression and regional distribution of rat ciliary neurotrophic factor. *Nature* 342(6252):920-3
- Stöckli KA, Lillien LE, Näher-Noé M, Breitfeld G, Hughes RA, Raff MC, Thoenen H, Sendtner M (1991) Regional distribution, developmental changes, and cellular localization of CNTF-mRNA and protein in the rat brain. *J Cell Biol.* 115(2):447-59
- Strelau J, Sullivan A, Böttner M, Lingor P, Falkenstein E, Suter-Crazzolara C, Galter D, Jaszai J, Kriegstein K, Unsicker K (2000) Growth/differentiation factor-15/macrophage inhibitory cytokine-1 is a novel trophic factor for midbrain dopaminergic neurons in vivo. *J Neurosci.* 20(23):8597-603
- Stritt C, Stern S, Harting K, Manke T, Sinske D, Schwarz H, Vingron M, Nordheim A, Knöll B (2009) Paracrine control of oligodendrocyte differentiation by SRF-directed neuronal gene expression. *Nat Neurosci.* 12(4):418-27
- Sun T, Pringle NP, Hardy AP, Richardson WD, Smith HK (1998) Pax6 influences the time and site of origin of glial precursors in the ventral neural tube. *Mol Cell Neurosci* 12:228–239
- Sun Y, Maxwell GD. (1994) Ciliary neurotrophic factor (CNTF) has a dose-dependent biphasic effect on the number of adrenergic cells which develop in avian trunk neural crest cultures. *Neurosci Lett.* 165(1-2):1-4
- Susuki K, Rasband MN (2008) Molecular mechanisms of node of Ranvier formation. *Curr Opin Cell Biol.* 20(6):616-23
- Svendsen CN (2002) The amazing astrocyte. *Nature.* 417(6884):29-32
- Swingler RJ, Compston D (1986) The distribution of multiple sclerosis in the United Kingdom. *J Neurol Neurosurg Psychiatry.* 49(10):1115-24
- Syed N, Reddy K, Yang DP, Taveggia C, Salzer JL, Maurel P, Kim HA (2010) Soluble neuregulin-1 has bifunctional, concentration-dependent effects on Schwann cell myelination. *J Neurosci.* 2010 Apr 28;30(17):6122-31

- Tait S, Gunn-Moore F, Collinson JM, Huang J, Lubetzki C, Pedraza L, Sherman DL, Colman DR, Brophy PJ (2000) An oligodendrocyte cell adhesion molecule at the site of assembly of the paranodal axo-glial junction. *J Cell Biol.* 150(3):657-66
- Takahashi K, Prinz M, Stagi M, Chechneva O, Neumann H (2007) TREM2- transduced myeloid precursors mediate nervous tissue debris clearance and facilitate recovery in an animal model of multiple sclerosis. *PLoS Med* 2007; 4: e124.
- Takahashi R, Yokoji H, Misawa H, Hayashi M, Hu J, Deguchi T (1994) A null mutation in the human CNTF gene is not causally related to neurological diseases. *Nat Genet.* 7(1):79-84
- Talbot JF, Loy DN, Liu Y, Qiu MS, Bunge MB, Rao MS, Whitemore SR (2005) Endogenous Nkx2.2+/Olig2+ oligodendrocytes precursors cells fail to remyelinate the demyelinated adult rat spinal cord in the absence of astrocytes. *Exp Neurol* 192:11-24
- Tani M, Glabinski AR, Tuohy VK, Stoler MH, Estes ML, Ransohoff RM (1996) In situ hybridization analysis of glial fibrillary acidic protein mRNA reveals evidence of biphasic astrocyte activation during acute experimental autoimmune encephalomyelitis. *Am J Pathol* 148:889– 896
- Tao-Cheng JH, Nagy Z, Brightman MW (1987) Tight junctions of brain endothelium in vitro are enhanced by astroglia. *J Neurosci.* 7(10):3293-9
- Tasukada N, Miyagi K, Matsuda M, Yanagisawa N, Yone K (1991) Tumour necrosis factor and interleukin-1 in the CSF and sera of patients with multiple sclerosis. *J Neurol Sci* 104(2):230-4
- Taveggia C, Zanazzi G, Petrylak A, Yano H, Rosenbluth J, Einheber S, Xu X, Esper RM, Loeb JA, Shrager P, Chao MV, Falls DL, Role L, Salzer JL (2005) Neuregulin-1 type III determines the ensheathment fate of axons. *Neuron* 47(5), pp. 681-694
- Taveggia C, Thaker P, Petrylak A, Caporaso GL, Toews A, Falls DL, Einheber S, Salzer JL (2008) Type III neuregulin-1 promotes oligodendrocyte myelination. *Glia.* 56(3):284-93
- Their, M, März P, Otten U, Weis J, Rose-John S (1999) Interleukin-6 (IL-6) and its soluble receptor support survival of sensory neurons. *J Neurosci Res* 55:411–422
- Thomson CE, Hunter AM, Griffiths IR, Edgar JM, McCulloch MC (2006) Murine spinal cord explants: a model for evaluating axonal growth and myelination in vitro. *J Neurosci Res.* 84(8):1703-15
- Thomson CE, McCulloch M, Sorenson A, Barnett SC, Seed BV, Griffiths IR, McLaughlin M (2008) Myelinated, synapsing cultures of murine spinal cord--validation as an in vitro model of the central nervous system. *Eur J Neurosci.* 28(8):1518-35

- Tian GF, Azmi H, Takano T, Xu Q, Peng W, Lin J, Oberheim N, Lou N, Wang X, Zielke HR, Kang J, Nedergaard M (2005) An astrocytic basis of epilepsy. *Nat Med.* 11(9):973-81
- Trapp BD, Nishiyama A, Cheng D, Macklin W (1997) Differentiation and death of premyelinating oligodendrocytes in developing rodent brain. *J Cell Biol.* 137(2):459-68
- Traugott U, Lebon P (1988) Interferon-gamma and Ia antigen are present on astrocytes in active chronic multiple sclerosis lesions. *J Neurol Sci.* 84(2-3):257-64
- Treloar HB, Ray A, Dinglasan LA, Schachner M, Greer CA (2009) Tenascin-C is an inhibitory boundary molecule in the developing olfactory bulb. *J Neurosci.* 29(30):9405-16
- Tsukada N, Miyagi K, Matsuda M, Yanagisawa N, Yone K (1991) Tumor necrosis factor and interleukin-1 in the CSF and sera of patients with multiple sclerosis. *J Neurol Sci.* 104(2):230-4
- Tumani H, Hartung HP, Hemmer B, Teunissen C, Deisenhammer F, Giovannoni G, Zettl UK (2007) Cerebrospinal fluid biomarkers in multiple sclerosis. *Neurobiology of Disease* 35:117–127
- Ullian EM, Christopherson KS, Barres BA (2004) Role for glia in synaptogenesis. *Glia* 47(3):209-16
- Uzawa A, Mori M, Arai K, Sato Y, Hayakawa S, Masuda S, Taniguchi J, Kuwabara S (2010) Cytokine and chemokine profiles in neuromyelitis optica: significance of interleukin-6. *Mult Scler.* 2010 Aug 25. [Epub ahead of print]
- Vartanian T, Fischbach G, Miller R (1999) Failure of spinal cord oligodendrocyte development in mice lacking neuregulin. *Proc Natl Acad Sci U S A.* 96(2):731-5
- Vereyken EJ, Fluitsma DM, Bolijn MJ, Dijkstra CD, Teunissen CE (2009) An in vitro model for de- and remyelination using lysophosphatidyl choline in rodent whole brain spheroid cultures. *57(12):1326-40*
- Verkhatsky A, Parpura V (2010) Recent advances in (patho)physiology of astroglia. *Acta Pharmacol Sin.* 31(9):1044-54
- Villarroya H, Violleau K, Ben Younes-Chennoufi A, Beaumann N (1996) Myelin-induced experimental allergic encephalomyelitis in Lewis rats: tumour necrosis factor levels in serum and cerebrospinal fluid immunohistochemical expression in glial cells and macrophages of optic nerve and spinal cord. *J Neuroimmunol* 64(1):55-61
- Voskuhl RR, Peterson RS, Song B, Ao Y, Morales LB, Tiwari-Woodruff S, Sofroniew MV (2009) Reactive astrocytes form scar-like perivascular barriers to leukocytes during adaptive immune inflammation of the CNS. *J Neurosci.* 29(37):11511-22

- Wakins TA, Emery B, Mulinyawe S, Barres BA (2008) Distinct stages of myelination regulated by gamma-secretase and astrocytes in a rapidly myelination CNS coculture system. *Neuron* 60(4):555-69
- Wang C, Rougon G, Kiss JZ (1994) Requirement of polysialic acid for the migration of the O-2A glial progenitor cell from neurohypophyseal explants. *J Neurosci.* 14(7):4446-57
- Wang W, Wang W, Mei X, Huang J, Wei Y, Wang Y, Wu S, Li Y. (2009) Crosstalk between spinal astrocytes and neurons in nerve injury-induced neuropathic pain. *PLoS One.* 4(9):e6973
- Wang YT, Han S, Zhang KH, Jin Y, Xu XM, Lu PH (2004) Upregulation of heparin-binding growth-associated molecule after spinal cord injury in adult rats. *Acta Pharmacol Sin.* 25(5):611-6
- Wang Z, Colognato H, French-Constant C (2007) Contrasting effects of mitogenic growth factors on myelination in neuron-oligodendrocyte co-cultures. *Glia.* 55(5):537-45
- Wendling D, Racadot E, Wijdenes J. (1993) Treatment of severe rheumatoid arthritis by anti-interleukin 6 monoclonal antibody. *J Rheumatol.* 20(2):259-62
- White RE, Jakeman LB (2008) Don't fence me in: Harnessing the beneficial roles of astrocytes for spinal cord repair. *Restor Neurol Neurosci* 26, 197-214
- Wiemelt AP, Lehtinen M, McMorris FA (2001) Agonists calcitonin, corticotropin-releasing hormone, and vasoactive intestinal peptide, but not prostaglandins or b-Adrenergic agonists, elevate cyclic adenosine monophosphate levels in oligodendroglial cells. *J Neurosci Res* 65(2)165-72
- Williams A, Piaton G, Lubetzki C (2007) Astrocytes-friends or foes in multiple sclerosis. *Glia* 55:1300-1312
- Williams BP, Price J (1992) What have tissue culture studies told us about the development of oligodendrocytes? *Bioessays.* 14(10):693-8
- Wilkin GP, Marriott DR, Cholewinski AJ. (1990) Astrocyte heterogeneity. *Trends Neurosci.* 13(2):43-6
- Winter CG, Saotome Y, Levison SW, Hirsh D (1995) A role for ciliary neurotrophic factor as an inducer of reactive gliosis, the glial response to central nervous system injury. *Proc Natl Acad Sci U S A.* 92(13):5865-9
- Wolswijk G, Noble M (1989) Identification of an adult-specific glial progenitor cell. *Development* 105(2):387-400
- Woodward WF, Nishi R, Meshul CK, Williams TE, Coulombe M, Eckenstein FP (1992) Nuclear and Cytoplasmic Localization of Basic Fibroblast Growth Factor in Astrocytes and CA2 Hippocampal Neurons. *J Neurosci* 12(1): 142-152

- Wu E, Raine CS (1992) Multiple sclerosis. Interactions between oligodendrocytes and hypertrophic astrocytes and their occurrence in other, nondemyelinating conditions. *Lab Invest.* 67(1):88-99
- Yamamuro A, Ago Y, Takuma K, Maeda S, Sakai Y, Baba A, Matsuda T (2003) Possible involvement of astrocytes in neuroprotection by the cognitive enhancer T-588. *Neurochem Res.* 28(12):1779-83
- Yao DL, West NR, Bondy CA, Brenner M, Hudson LD, Zhou J, Collins GH, Webster HD. (1995) Cryogenic spinal cord injury induces astrocytic gene expression of insulin-like growth factor I and insulin-like growth factor binding protein 2 during myelin regeneration. *J Neurosci Res.* 40(5):647-59
- Yeh TH, Lee da Y, Gianino SM, Gutmann DH (2009) Microarray analyses reveal regional astrocyte heterogeneity with implications for neurofibromatosis type 1 (NF1)-regulated glial proliferation. *Glia.* 57(11):1239-49
- Yeruva S, Ramadori G, Raddatz D (2008) NF-kappaB-dependent synergistic regulation of CXCL10 gene expression by IL-1beta and IFN-gamma in human intestinal epithelial cell lines. *Int J Colorectal Dis.* 23(3):305-17
- Yiu G, He Z (2006) Glial inhibition of CNS axon regeneration. *Nat Rev Neurosci.* (8):617-27
- Yokosaki Y, Matsuura N, Higashiyama S, Murakami I, Obara M, Yamakido M, Shigeto N, Chen J, Sheppard D. (1998) Identification of the ligand binding site for the integrin alpha9 beta1 in the third fibronectin type III repeat of tenascin-C. *J Biol Chem.* 273(19):11423-8
- Yong VW, Moundjian R, Yong FP, Ruijs TC, Freedman MS, Cashman N, Antel JP (1991) Gamma-interferon promotes proliferation of adult human astrocytes in vitro and reactive gliosis in the adult mouse brain in vivo. *Proc Natl Acad Sci U S A.* 88(16):7016-20
- Yoo YM, Kim YJ, Lee U (2003) Expression of mRNAs for BDNF and NT-3 in Reactive Astrocytes. *J Korean Neurosurg Soc* 33(6):572-575
- Yoshida M, Saito H, Katsuki H (1995) Neurotrophic effects of conditioned media of astrocytes isolated from different brain regions on hippocampal and cortical neurons. *Experientia.* 51(2):133-6
- Zeringue HC, Constantine-Paton M (2004) Post-transcriptional gene silencing in neurons. *Curr Opin Neurobiol.* 14(5):654-9
- Zhang SC, Lundberg C, Lipsitz D, O'Connor LT, Duncan ID (1998) Generation of oligodendroglial progenitors from neural stem cells. *J Neurocytol* 27:475-489
- Zhang SC (2001) Defining glial cells during CNS development. *Nat Rev Neurosci.* 2(11):840-3

- Zhang Y, Anderson PN, Campbell G, Mohajeri H, Schachner M, Lieberman AR (1995) Tenascin-C expression by neurons and glial cells in the rat spinal cord: changes during postnatal development and after dorsal root or sciatic nerve injury. *J Neurocytol.* 24(8):585-601
- Zhang Y, Taveggia C, Melendez C, Einheber D, Raine CS, Salzer JL, Brosnan CF, John GR (2006) Interleukin-11 potentiates oligodendrocyte survival and maturation, and myelin formation. *J Neurosci* 26(47):12174-85
- Zhang Y, Barres BA (2010) Astrocyte heterogeneity: an underappreciated topic in neurobiology. *Curr Opin Neurobiol.* 20(5):588-94
- Zhao C, Fancy SP, Franklin RJ, French-Constant C (2009) Up-regulation of oligodendrocyte precursor cell alphaV integrin and its extracellular ligands during central nervous system remyelination. *J Neurosci Res.* 87(15):3447-55
- Zhu ZH, Yang R, Fu X, Wang YQ, Wu GC (2006) Astrocyte-conditioned medium protecting hippocampal neurons in primary cultures against corticosterone-induced damages via PI3-K/Akt signal pathway. *Brain Res.* 1114(1):1-10

# Appendix

## Myelin Macro

---

```
//set the thresholds here
thresh_red = 33;
thresh_green = 85;
thresh_blue = 128;

//get the name of the open image, and the folder it came from
iTtitle=getTtitle;
imageDirectory = getDirectory("image");
print (imageDirectory);
print ("Image name,Red Black,Red White,Green Black,Green White,Blue
Black,Blue White")

//build a list of all images in the folder
fList=getFileList(imageDirectory);
selectWindow(iTtitle);
run("Close");

//start the loop to open files
for (i=0; i<fList.length; i++){
    //check that file is a valid image
    if (endsWith(fList[i],"tif")) {
        //if it is valid, open it
        open(imageDirectory + fList[i]);

        //build names of color component images
        iTtitle=getTtitle;
        iTtitleRed=iTtitle + " (red)";
        iTtitleGreen=iTtitle + " (green)";
        iTtitleBlue=iTtitle + " (blue)";

        //split image into colour components
        run("RGB Split");

        //get red and blue areas and threshold

        string="image1=["+iTtitleGreen + "] operation=AND image2=[" +
iTtitleBlue+"] create";
        run("Image Calculator...", string);
        iTtitleAND = getTtitle;
        setThreshold(thresh_blue, 255);
        run("Threshold", "thresholded remaining black");
        run("Invert");

        //measure areas
        getStatistics(area, mean, min, max, std, histogram);
        n_blue_black=histogram[0];
        n_blue_white=histogram[255];

        //close windows
        selectWindow(iTtitleAND);
        run("Close");
        selectWindow(iTtitleBlue);
        run("Close");

        //get red threshold
        selectWindow(iTtitleRed);
        setThreshold(thresh_red, 255);
        run("Threshold", "thresholded remaining black");
        run("Invert");
```

```

//measure areas
getStatistics(area, mean, min, max, std, histogram);
n_red_black=histogram[0];
n_red_white=histogram[255];

selectWindow(iTitleRed);
run("Close");

//get green threshold
selectWindow(iTitleGreen);
setThreshold(thresh_green, 255);
run("Threshold", "thresholded remaining black");
run("Invert");

//measure areas
getStatistics(area, mean, min, max, std, histogram);
n_green_black=histogram[0];
n_green_white=histogram[255];

selectWindow(iTitleGreen);
run("Close");

//display results
print
(iTitle+", "+n_red_black+", "+n_red_white+", "+n_green_black+", "+n_green_whi
te+", "+n_blue_black+", "+n_blue_white);
}
}

```